POLITECNICO DI TORINO

Collegio di Ingegneria Chimica e dei Materiali

Corso di Laurea Magistrale
in Ingegneria dei Materiali

Tesi di Laurea Magistrale

DLP – 3D Printing of Poly (Ionic Liquid)s for VOCs' Absorption

Relatori

prof. Andrea Lamberti
dott.ssa Annalisa Chiappone

Candidato

Giulia Zanut

Luglio 2021

Contents

Riassunto in Italiano .... *I*

I. Obiettivi .... **I**

II. Liquidi Ionici e *Poly(Ionic Liquid)s* .... **I**

III. Fotopolimerizzazione radicalica .... **III**

IV. Stampa 3D: Digital Light Processing .... **IV**

V. Materiali e Metodi .... **V**

VI. Risultati .... **VII**

VI.I Foto-Reologia VII

VI.II Stampa 3D VII

VI.III Spettroscopia IR IX

VI.IV Osservazione al SEM e Microscopio Ottico X

VI.V DSC e DMTA XIII

VI.VI Prove di Assorbimento e di Desorbimento di VOCs XIV

VII. Conclusioni .... **XXI**

Aim of the Work *1*

Chapter 1: Introduction *2*

1.1 Volatile Organic Compounds (VOCs) **2**

1.1.1 Direct Exposure to VOCs 3

1.1.2 Secondary Effects of VOCs: Impact on the Atmosphere 4

1.2 VOCs Removal: Existing Methods **7**

1.2.1 Destruction of VOCs 7

1.2.2 Recovery of VOCs 9

1.2.3 Recent Developments 11

1.3 References **13**

Chapter 2: Ionic Liquids *16*

2.1 Definition and Nomenclature **16**

2.2 Classification of ILs **18**

2.3 General properties of ILs **20**

2.3.1 Thermal properties 20

2.3.2 Density 20

2.3.3 Volatility and Nonflammability 21

2.3.4 Viscosity 21

2.3.5 Polarity 22

2.3.6 Solubility..23
2.3.7 Electrical Conductivity..23
2.4 Applications..24
2.5 Polymerized Ionic Liquids or Poly(Ionic Liquid)s (PILs)..26
2.5.1 Classification and synthesis..27
2.5.2 Properties and Applications of PILs..29
2.6 References..34
Chapter 3: Photopolymerization and 3D Printing..38
3.1 Photopolymerization..38
3.1.1 Reaction Mechanisms..39
3.1.2 Radical Photoinitiators..42
3.1.3 Advantages and Disadvantages of Photopolymerization..44
3.2 3D Printing..47
3.2.1 Stereolithography (SLA)..49
3.2.2 Digital Light Processing (DLP)..50
3.3 References..51
Chapter 4: Materials and Methods..53
4.1 Materials..53
4.1.1 PEGDA Mn 250 and PEGDA Mn 575..53
4.1.2 Ionic Liquid Monomers (ILMs)..54
4.1.3 Photoinitiator: BAPO..55
4.1.4 Pigments: Methyl Red..56
4.2 Preparation of the Formulations..57
4.2.1 Formulation Characterization: Photo Rheometry..58
4.3 DLP-3D Printing..59
4.4 Characterization Methods..60
4.4.1 IR Spectroscopy..60
4.4.2 Extraction in Chloroform..61
4.4.3 Differential Scanning Calorimetry (DSC)..61
4.4.4 Dynamic Mechanical Thermal Analysis (DMTA)..63
4.4.5 Optical Microscope and SEM (Scanning Electron Microscope)..64
4.5 VOCs' Absorption Tests..65
4.5.1 Experimental Set-Up..66
4.6 Desorption Tests..67
4.7 References..68

Chapter 5: Results *70*

5.1 Efficiency of the Photopolymerization **70**

5.1.1 Photo-Rheometry 71

5.1.2 Production of solid objects via 3D Printing 75

5.1.3 IR Spectroscopy 78

5.1.4 Extraction in Chloroform 84

5.1.5 Observation of 3D Printed objects: SEM and Optical Microscope 85

5.2 Analysis of Thermo-Mechanical Properties **93**

5.2.1 DSC (Differential Scanning Calorimetry) 93

5.2.2 DMTA 97

5.2.3 Considerations on DSC-DMTA Results 102

5.3 Absorption Capacity **103**

5.3.1 Acetone 103

5.3.2 Isopropyl Alcohol 105

5.3.3 Ortho-dichlorobenzene 106

5.3.4 Acetonitrile 107

5.3.5 Chloroform 108

5.4 Desorption Capacity **109**

5.4.1 Acetone 109

5.4.2 Isopropyl Alcohol 110

5.4.3 Ortho-dichlorobenzene 110

5.4.4 FTIR Spectroscopy to monitor Absorption and Desorption of Chloroform 111

5.5 Discussion of the Results **116**

5.5.1 Realization of PILs-based solid objects via DLP-3D Printing 116

5.5.2 Absorption and Desorption Capacities 116

5.5 References **121**

Chapter 6: Conclusions *123*

Bibliography *125*

Sitography *134*

Riassunto in Italiano

I. Obiettivi

Lo scopo di questo lavoro è la valutazione della capacità di assorbimento di composti organici volatili (acetone, 2-propanolo, orto-diclorobenzene, acetonitrile e cloroformio) da parte di materiali polimerici, caratterizzati dalla presenza di *Poly(Ionic Liquid)s* (PILs) in diverse concentrazioni.

Inoltre, è stata studiata la possibilità di produrre tali materiali tramite il processo di stampa 3D (DLP), in modo tale da costituire strutture più o meno complesse.

II. Liquidi Ionici e *Poly(Ionic Liquid)s*

I liquidi ionici sono dei sali organici non volatili, che si presentano come liquidi a temperatura ambiente, in quanto sono caratterizzati da una temperatura di fusione inferiore ai 100°C.

Tali composti ionici possono essere molto variabili, sia dal punto di vista chimico, che per quanto riguarda le relative proprietà fisiche: così come riportato in Fig. I, differenti cationi e anioni possono formare liquidi ionici con caratteristiche differenti e modulabili in relazione alla tipologia di ioni costitutivi.

I liquidi ionici possono essere classificati secondo diversi criteri: uno dei più significativi è quello basato sulla loro struttura chimica. Infatti, si possono distinguere liquidi ionici protici, aprotici e zwitterionici. In particolare, i primi sono quelli di maggiore interesse, in quanto prevedono una struttura ionica che consente loro di formare facilmente legami a idrogeno con altre specie che si comportano da acidi o da basi.

In generale, i liquidi ionici possono essere definiti monofunzionali, se caratterizzati da una sola carica ionica, mentre sono bifunzionali o multifunzionali se presentano due o più cariche ioniche nella struttura.

Essi sono caratterizzati da una buona stabilità termica, non solo volatili non sono infiammabili. Le loro polarità e solubilità spiccate consentono di utilizzare tali liquidi come solventi, nei quali far avvenire reazioni chimiche o processi di estrazione di altre specie affini, in fase liquida o gassosa (come nel caso della CO_2 o di composti organici). La loro struttura ionica garantisce una certa conducibilità elettrica, grazie alla quale, spesso tali sostanze possono essere impiegate in applicazioni elettrochimiche (realizzazione di sensori, attuatori, celle a combustibile, …).

I liquidi ionici polimerizzabili (o *Poly(Ionic Liquid)s*), sono caratterizzati da uno ione che dispone di gruppi funzionali in grado di essere coinvolti in processi di polimerizzazione radicalica. Tali gruppi possono essere provvisti di doppi legami, per esempio, come i sostituenti vinilici.

La polimerizzazione degli ioni genera una struttura polimerica interconnessa, caratterizzata da zone con carica positiva, che interagiscono con gli ioni dalla carica opposta, mobili nel materiale (Fig. II).

Anche i PILs possono essere classificati in base alla loro struttura ionica: per esempio, possono essere policationi (se la polimerizzazione coinvolge i cationi), polianioni (se gli anioni sono sottoposti a polimerizzazione) o copolimeri.

Essendo caratterizzati da proprietà simili a quelle dei liquidi ionici, anche nel caso dei PILs, la ricerca in questi ultimi anni si è concentrata maggiormente nello studio di tali materiali, utilizzati come conduttori ionici per la realizzazione di dispositivi elettrochimici; oppure nella caratterizzazione di membrane polimeriche in grado di garantire l'assorbimento selettivo di gas, in particolare di anidride carbonica.

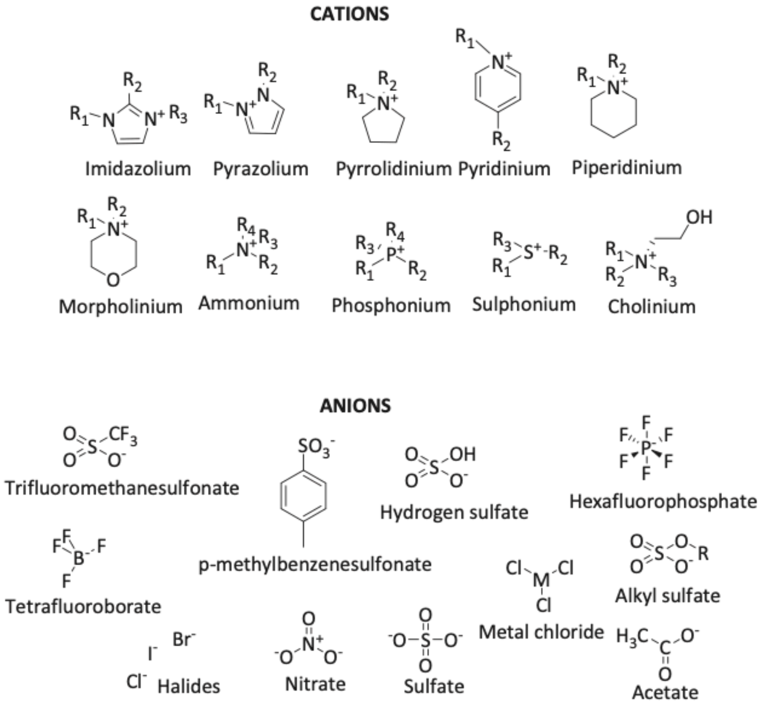

Figura I. Cationi e anioni che comunemente costituiscono Liquidi Ionici

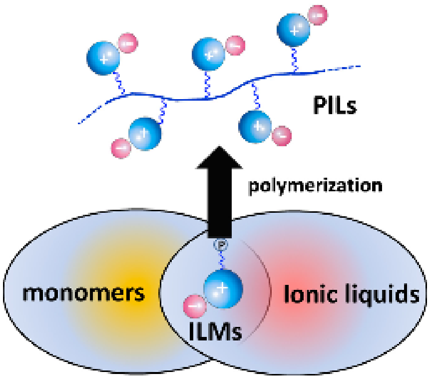

Figura II. Polimerizzazione di liquidi ionici: struttura di PILs

III. Fotopolimerizzazione radicalica

La fotopolimerizzazione consiste in una reazione di polimerizzazione, innescata dall'assorbimento di luce (UV-Visibile) da parte della formulazione polimerica di partenza.

La fotopolimerizzazione radicalica, nello specifico, si basa su meccanismi di poliaddizione che vengono reiterati grazie alla radicalizzazione di monomeri, che, addizionandosi alle catene già formatesi, ne consentono la crescita.

Le formulazioni che sono predisposte alla fotopolimerizzazione sono sempre costituite dai seguenti componenti:

- Un **fotoinizatore**, ovvero una molecola sensibile all'assorbimento di luce UV-Visibile, in seguito al quale sviluppa scissione, formando dei radicali in grado di dare inizio al processo di polimerizzazione (fotoiniziatore di tipo I);

- **monomeri**, con più gruppi funzionali insaturi in grado di prendere parte al processo di polimerizzazione (come vinili, acrilati,…);

- Un **solvente**, utile per controllare la viscosità della formulazione;

- **Additivi**, per conferire specifiche proprietà al materiale polimerico (pigmenti, stabilizzanti, plasticizzanti, …).

a)

$$In \ \to^{kd} In\cdot$$
$$In\cdot + M \ \to^{ki} M\cdot$$
$$k_d < k_i$$

b)

$$M_n\cdot + M \ \to^{kp} \ M_{n+1}\cdot$$
$$M_{n+1}\cdot \ + M \ \to^{kp} \ M_{n+2}\cdot$$
$$\dots$$

c)

$$M_n\cdot + M_m \ \cdot \to^{kt} \ M_{n+m}$$

$$M_n\cdot + In\cdot \to^{kt} \ M_n$$

Figura III. Meccanismo di fotopolimerizzazione radicalica

La fotopolimerizzazione radicalica avviene in tre fasi fondamentali: durante la prima fase, il fotoiniziatore viene attivato dall'assorbimento di luce, si scinde in due radicali che reagiscono con i monomeri, radicalizzandoli a loro volta (Fig. III.a). La seconda fase, invece, è quella di propagazione: la crescita delle catene polimeriche per poliaddizione avviene effettivamente, attraverso un processo reiterativo, in cui nuovi monomeri radicali si formano e si addizionano alle catene già formate (Fig. III.b). Tale processo si conclude con la fase di terminazione, in cui, attraverso meccanismi differenti, i radicali vengono spenti, concludendo definitivamente la crescita delle catene polimeriche (Fig. III.c).

Nel caso in cui i monomeri siano multifunzionali, tale processo consente la formazione di un reticolo polimerico estremamente interconnesso, denominata *cross-linking*.

IV. Stampa 3D: Digital Light Processing

In generale, le tecniche di stampa 3D rientrano nell'ambito dell'Additive Manufacturing, che prevede la realizzazione di un oggetto tramite la deposizione di strati successivi, dallo spessore micrometrico, a partire da un modello CAD del prodotto desiderato. Tali metodi produttivi possono essere applicabili su diverse categorie di materiali, tra cui i materiali polimerici.

Tra i vari processi di 3D Printing, il metodo chiamato *Digital Light Processing* (Fig. IV*)* prevede la polimerizzazione di ogni strato costituente l'oggetto finito, attraverso la proiezione di luce, con una specifica lunghezza d'onda, sul fondo trasparente di una vaschetta contenente la formulazione polimerica. L'irraggiamento avviene su tutta l'area di interesse, che costituirà l'estensione del layer in fase di formazione. Il materiale polimerizzato aderisce sulla superficie di una piattaforma, posizionata in modo tale da essere a diretto contatto con la formulazione stessa. Dopo la polimerizzazione di ogni layer, la piattaforma si alza per poi ricollocarsi in prossimità della formulazione, tenendo in considerazione lo spessore dei layer già formati.

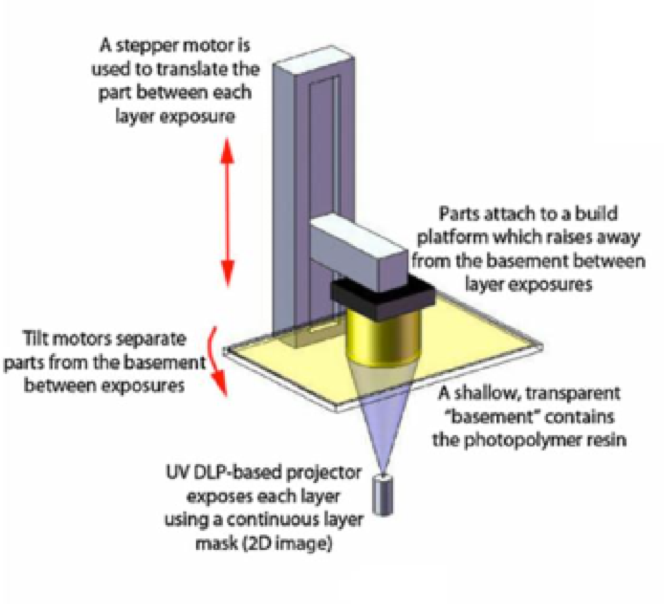

Figura IV. Digital Light Processing

V. Materiali e Metodi

Per perseguire l'obiettivo di questo lavoro, sono state prodotte sei differenti formulazioni, contenenti un quantitativo variabile di liquidi ionici monofunzionali o bifunzionali. In particolare, i liquidi ionici utilizzati sono i seguenti:

- Liquido Ionico Monofunzionale: *3-Ethyl-1-vinylimidazolium bis(trifluoromethanesulfonyl) imide* (Fig.V.a)*;*
- Liquido Ionico Bifunzionale: *1,4-Butandyl-3,3'-[bis-(1-vinyl)-imidazolium]di-bis(trifluoromethanesulphonyl)imide* (Fig.V.b)

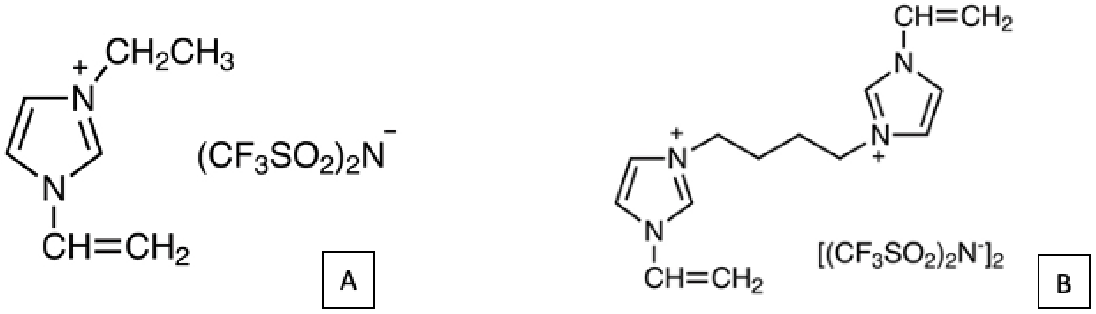

Figura V. Liquidi Ionici considerati

In alcune formulazioni è presente anche il PEGDA, con pesi molecolari differenti (Mn 250, Mn 575). In tutte le formulazioni è stato additivato il fotoiniziatore BAPO, in concentrazione 2% in peso, e lo 0,1% in peso di colorante Methyl Red.

Le sei formulazioni si caratterizzano come segue:

1. PEGDA Mn 250
2. PEGDA Mn 575
3. 50% (wt.) PEGDA Mn 250 + 50% (wt.) Liquido Ionico Monofunzionale
4. 50% (wt.) PEGDA Mn 575 + 50% (wt.) Liquido Ionico Monofunzionale
5. 90% (wt.) Liquido Ionico Monofunzionale + 10% (wt.) Liquido Ionico Bifunzionale
6. 90% (wt.) Liquido Ionico Monofunzionale + 10% (wt.) PEGDA Mn 575

Dopo aver eseguito le prove di foto-reologia su ogni formulazione, per verificarne l'efficienza della fotopolimerizzazione, diversi oggetti (caratterizzati da forme più o meno complesse) sono stati realizzati, tramite stampa 3D. La stampante utilizzata è ASIGA Pico2, che lavora con luce visibile (λ= 405 nm).

Tutti i materiali sono stati successivamente caratterizzati, per verificare l'efficienza della loro fotopolimerizzazione e per valutare le rispettive proprietà termomeccaniche.

I metodi di caratterizzazione considerati sono:

- *Spettroscopia IR (FTIR)*: per valutare la percentuale di conversione dei polimeri in seguito alla polimerizzazione, considerando l'area sottesa ai picchi relativi a gruppi funzionali coinvolti nella reazione;

- *Estrazione in Cloroformio*: per valutare la quantità di monomeri residui dalla polimerizzazione, estratti dal materiale polimerico imbevuto in tale solvente per 24 ore;

- *DSC (Calorimetria a Scansione Differenziale):* per valutare la temperatura di transizione vetrosa dei materiali polimerici;

- *DMTA (Analisi Dinamo-Meccanica in Temperatura):* per valutare la temperatura di transizione vetrosa dei materiali e la loro risposta meccanica a sollecitazioni sinusoidali in differenti condizioni di temperatura (monitorando G' e G'');

- *SEM e Microscopio Elettronico:* per osservare in modo dettagliato i solidi polimerici, ottenuti tramite stampa 3D, valutando l'affidabilità di tale processo.

Infine, l'assorbimento di composti organici volatili (quali acetone, 2-propanolo, orto-diclorobenzene, acetonitrile, cloroformio) da parte di tali materiali è stato considerato.

Le prove di assorbimento sono state condotte all'interno di contenitori in vetro, chiusi ermeticamente, entro i quali i campioni dei diversi materiali sono stati collocati, in modo tale che non fossero a diretto contatto con il solvente liquido presente. L'evaporazione e il conseguente assorbimento di tali composti sono stati incentivati da una temperatura costante di 40°C. I test di assorbimento sono stati eseguiti con una durata di 24 ore.

Anche i test di desorbimento sono stati efettuati nelle medesime condizioni di temperatura e con le stesse tempistiche.

VI. Risultati

VI.I Foto-Reologia

Le prove di foto-reologia sono state condotte monitorando l'andamento del modulo conservativo G' e di quello dissipativo G'' in funzione del tempo. Il reometro piatto-piatto è stato utilizzato in modalità oscillatoria, con una frequenza costante di 1 Hz, ricavata dalla zona di viscoelasticità lineare osservata preliminarmente. Dopo 60 secondi dall'inizio della prova, una luce (visibile) di intensità pari a 0,5 mW/cm^{-2} è stata irradiata sulla formulazione di interesse, causando l'inizio della polimerizzazione.

In Fig. VI, a titolo esemplificativo, si riportano le curve relative alla variazione del modulo conservativo per quattro materiali significativi: in ogni caso, si osserva che la polimerizzazione va a buon fine, in quanto G' cresce per arrivare ad un plateau. Il materiale caratterizzato unicamente dalla presenza di PILs polimerizza con una velocità minore ed è caratterizzato da un valore finale di G' inferiore. La presenza di PEGDA nelle formulazioni migliora notevolmente le condizioni in cui avviene la polimerizzazione, a prescindere dalla concentrazione di liquidi ionici.

Tali test hanno confermato l'idoneità dei materiali di interesse per essere utilizzati nel processo di stampa 3D.

VI.II Stampa 3D

Il processo di stampa 3D ha permesso la produzione di oggetti caratterizzati da forme più o meno complesse: sono stati ottenuti campioni rettangolari, pellets porosi, oggetti cavi cilindrici (Fig. VII). Le dimensioni di tali oggetti sono riportate in Tab.I.

I parametri di stampa ottimizzati per l'ottenimento di tali oggetti sono riportati in Tab. II: essi sono risultati variabili a seconda del materiale considerato e della complessità della forma da ottenere.

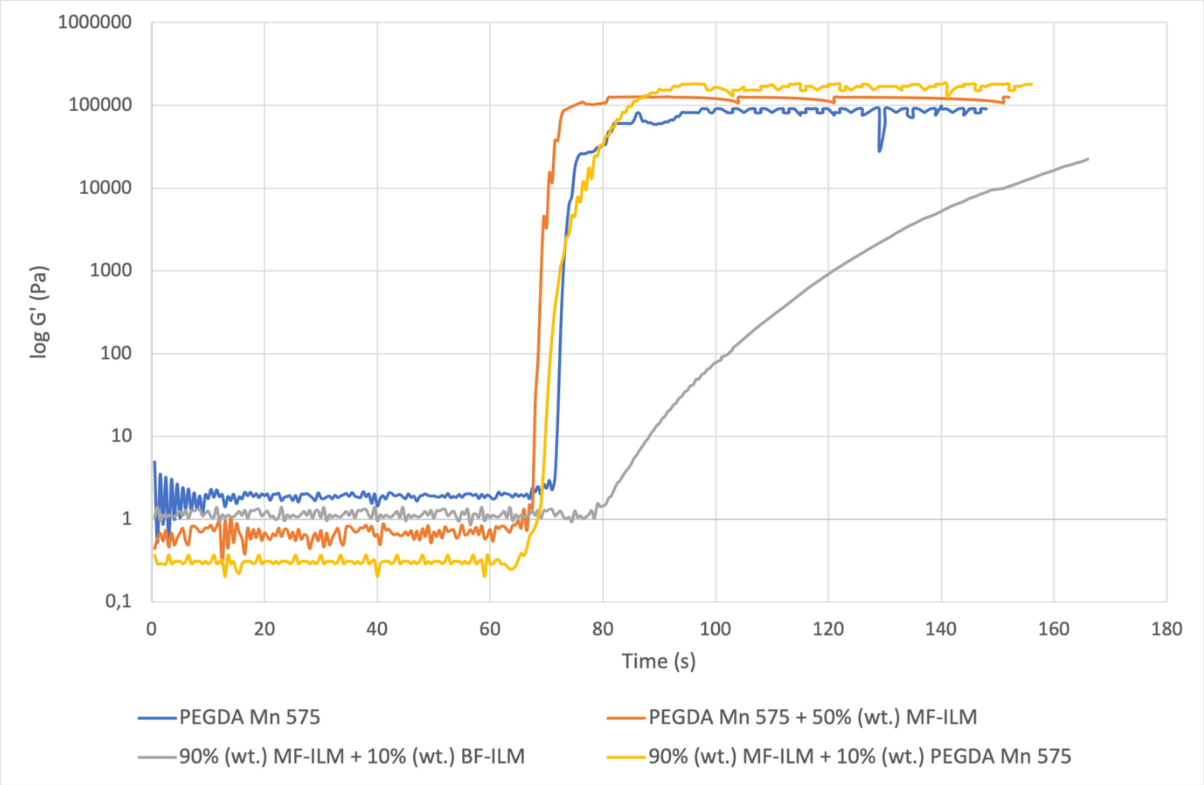

Figura VI. Foto-Reologia

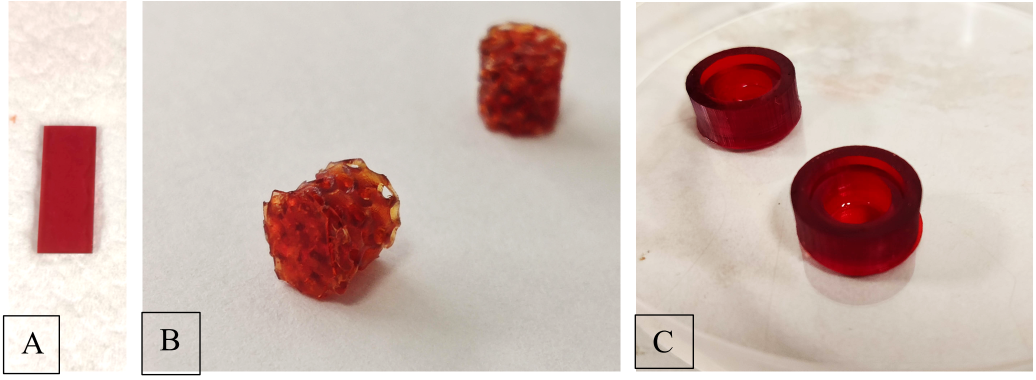

Figura VII. a) Campioni rettangolari; b) Pellets porosi c) Cilindri cavi

Campioni Rettangolari	7 x 25 x 0,7 mm
Pellets	Ø5x5 mm; Ø2,5x2,5 mm
Cilindri	Ø13x10 mm

Tabella I. Dimensioni oggetti

Campioni rettangolari	Formulazioni con PEGDA (1,2,3,4)	**Intensità (mW/cm^2)**	32
		Tempo di Esposizione	0.8 s
	Formulazioni con PILs (5,6)	**Intensità (mW/cm^2)**	40
		Tempo di Esposizione (BURN IN, 100 µm)	2 s
		Tempo di Esposizione	1.5 s
Pellets Porosi	Formulazioni con PEGDA (1,2,3,4)	**Intensità (mW/cm^2)**	32
		Tempo di Esposizione	0.8 s
	Formulazioni con PILs (5,6)	**Intensità (mW/cm^2)**	40
		Tempo di Esposizione (BURN IN, 100 µm)	3 s
		Tempo di esposizione	1.5 s
Cilindri cavi	Layer in PILs	**Intensità (mW/cm^2)**	40
		Tempo di Esposizione (BURN IN, 500 µm)	3 s
		Tempo di esposizione	1.5 s
	Pareti in PEGDA	**Intensità (mW/cm^2)**	32
		Tempo di Esposizione	0.8 s

Tabella II. Parametri di stampa ottimizzati

VI.III Spettroscopia IR

I grafici derivanti dalla spettroscopia IR sono stati analizzati considerando i picchi significativi per ogni sistema: per ogni materiale lo spettro relativo alla formulazione è stato confrontato con quello riferito al solido polimerico, in particolare comparando l'intensità dei picchi associati a gruppi funzionali significativi per la polimerizzazione. Essi sono:

- 1800-1700 cm^{-1} : stretching del carbonile nel PEGDA;
- 1675-1665 cm^{-1} : stretching dei doppi legami degli acrilati del PEGDA;
- 995 cm^{-1}: bending del legame singolo che lega il Gruppo vinile all'imidazolo dei liquidi ionici

In Tab.III sono riportate le percentuali di conversione relative alla polimerizzazione di ogni formulazione studiata. Anche questi risultati confermano l'efficienza del processo di polimerizzazione per i materiali considerati.

I dati ottenuti, relativi alla quantità di monomeri estratti in cloroformio, sono coerenti con questi risultati, in quanto la percentuale di monomeri residui per tutti i materiali non supera il 15%.

Materiale	**% Conversione**
PEGDA Mn 250	88,3 %
PEGDA Mn 250 + 50% (wt.) MF-LI	90 %
90% (wt.) MF-LI + 10% (wt.) BF-LI	76 %
90% (wt.) MF-LI + 10% (wt.) PEGDA Mn 575	70 %

Tabella III. Percentuali di conversione nella polimerizzazione, derivanti da spettri FTIR

VI.IV Osservazione al SEM e Microscopio Ottico

Le immagini ottenute tramite il Microscopio Ottico e il SEM consentono di confrontare visivamente le strutture ottenute con PEGDA e quelle realizzate con PILs.

È evidente che i campioni in PEGDA (Fig.VIII) presentino una definizione maggiore degli strati che li costituiscono, mentre gli stessi campioni ottenuti con PILs (Fig.IX) sono caratterizzati da una minore risoluzione e una maggiore interconnessione tra i layer succcessivi.

In generale, le dimensioni dei modelli CAD sono in linea con quelle riscontrate negli oggetti ottenuti tramite stampa 3D, perciò si può dire che in tutti i casi il processo abbia avuto successo.

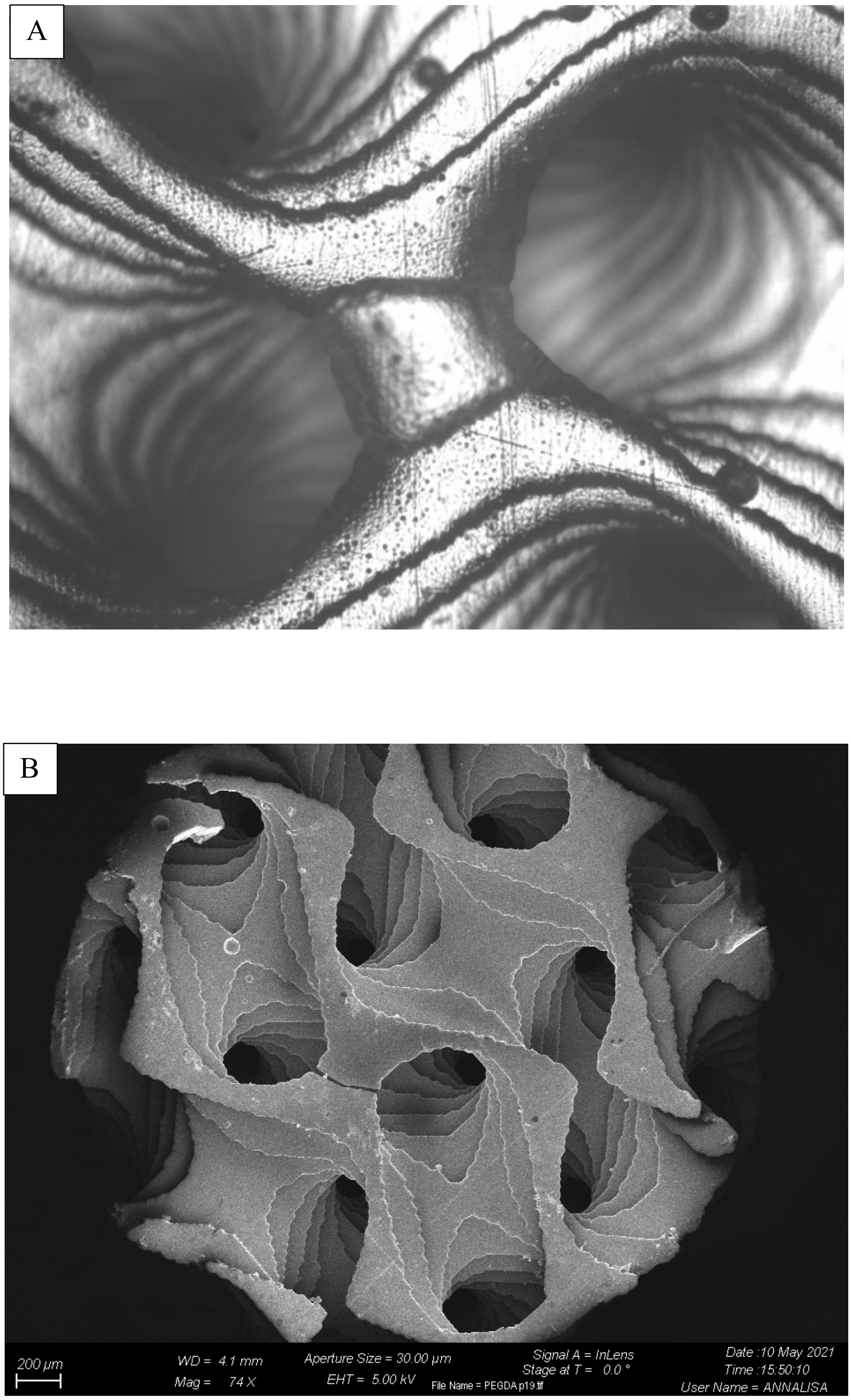

Figura VIII. PEGDA Mn 250: a) Microscopio Ottico; b) SEM

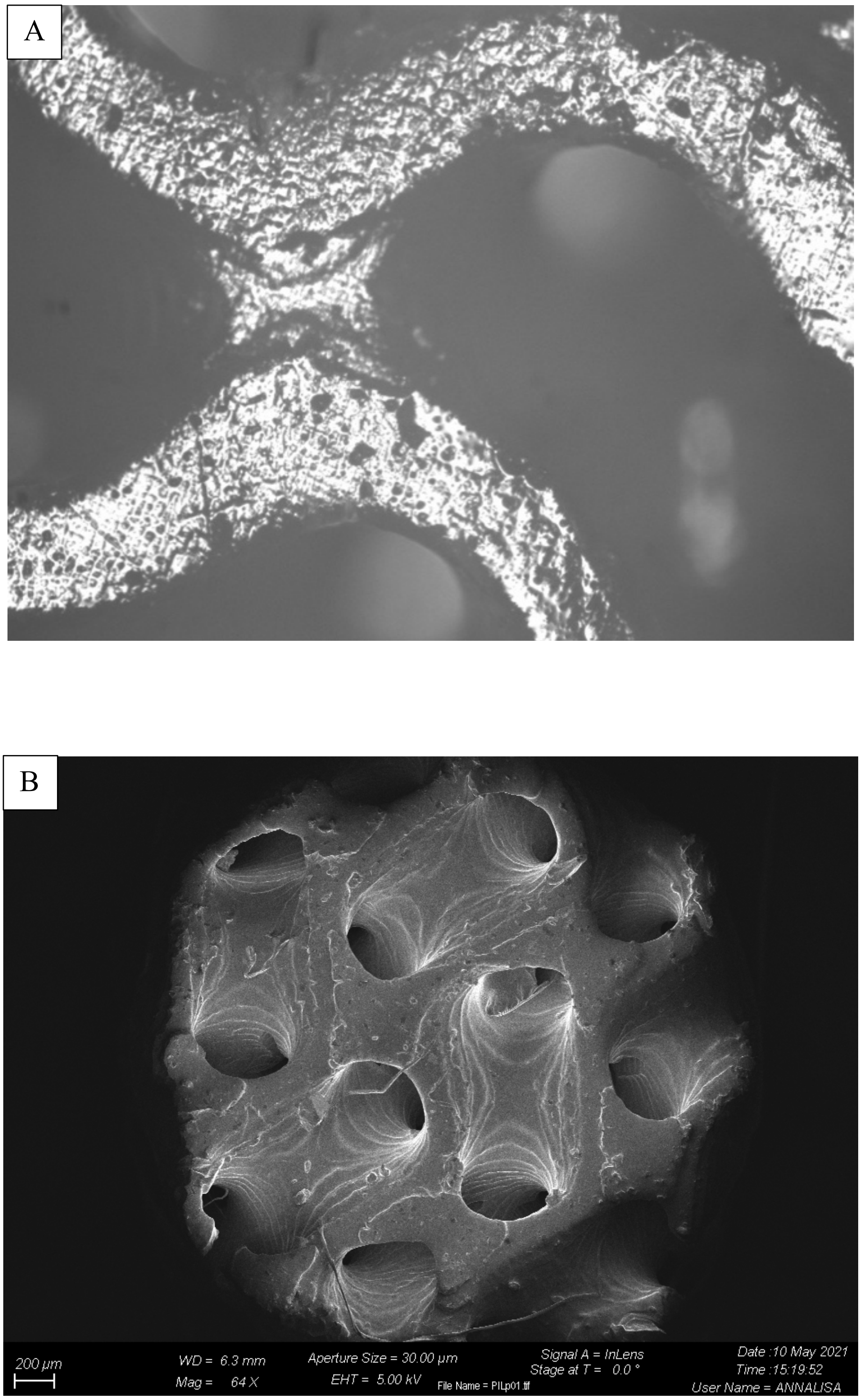

Figura IX. PILs: a) Microscopio Ottico; b) SEM

VI.V DSC e DMTA

Le prove di DSC e DMTA sono state utilizzate per valutare, comparando i risultati ottenuti da entrambe, la temperatura di transizione vetrosa dei sei materiali polimerici in analisi.

Le temperature di transizione vetrosa rilevate da entrambi i metodi di analisi sono riportate in Tab. IV. In generale si è osservata coerenza tra i valori di T_g ricavati dalla DSC e quelli individuati tramite DMTA. Nel caso dei materiali con il più alto contenuto di PILs, la DSC non è stata sufficiente per valutare la T_g : tale valore è stato individuato con maggiore precisione mediante i risultati della DMTA.

Materiale	**T_g**
PEGDA Mn 250	60 °C
PEGDA Mn 575	-20 °C
PEGDA Mn 250 + 50% (wt.) MF-LI	40 °C
PEGDA Mn 575 + 50% (wt.) MF-LI	-10 °C
90% (wt.) MF-LI + 10% (wt.) BF-LI	40 °C
90% (wt.) MF-LI + 10% (wt.) PEGDA Mn 575	30 °C

Tabella VI. IV. Temperatura di transizione vetrosa (da DSC e DMTA)

Osservando i dati ottenuti, è possibile dire che la temperatura di transizione vetrosa sia influenzata dalla concentrazione di PILs nel materiale: infatti, si osserva che la T_g cresce o diminuisce tanto maggiore è la quantità di PILs presenti. La T_g del materiale costituito unicamente da PILs si aggira attorno ai 40 °C.

La Tg dei materiali può essere influenzata dalle interazioni intramolecolari, accentuate dalla presenza di PILs, oppure può variare a seconda della densità del reticolo macromolecolare, anch’essa modulabile in funzione della quantità di PILs presenti nel materiale polimerico.

VI.VI Prove di Assorbimento e di Desorbimento di VOCs

Le capacità di assorbimento e di desorbimento dei materiali polimerici sono state valutate attraverso la differenza di peso dei campioni: esso è stato rilevato prima e dopo l'assorbimento di vapori organici.

Tale valore è stato rapportato all'entità del peso iniziale dei campioni, come riportato in eq. I ed eq.II.

$$Capacit\grave{a}\ di\ assorbimento\ \% = \frac{Peso\ finale - \ Peso\ iniziale}{Peso\ iniziale} x\ 100$$

Equazione I. Capacità di Assorbimento

$$Capacit\grave{a}\ di\ desorbimento\ \% = \frac{Peso\ iniziale - \ Peso\ finale}{Peso\ iniziale} x\ 100$$

Equazione II. Capacità di desorbimento

a) *Acetone*

I materiali caratterizzati da una maggiore concentrazione di PILs sono quelli che presentano la massima capacità di assorbire acetone (55 % circa) (vedi Fig. X). Si osserva, in generale, che la quantità di acetone assorbito aumenta con l'incremento della concentrazione di questo solvente.

I materiali contenenti PEGDA Mn 575 presentano, inoltre un comportamento intermedio in termini di assorbimento, migliore rispetto a quelli di PEGDA Mn 250.

Per quanto riguarda la capacità di desorbimento di acetone (Fig. XI), essa è buona per tutti i materiali considerati. I PILs, tendono ad avere una capacità di rigenerazione leggermente più bassa.

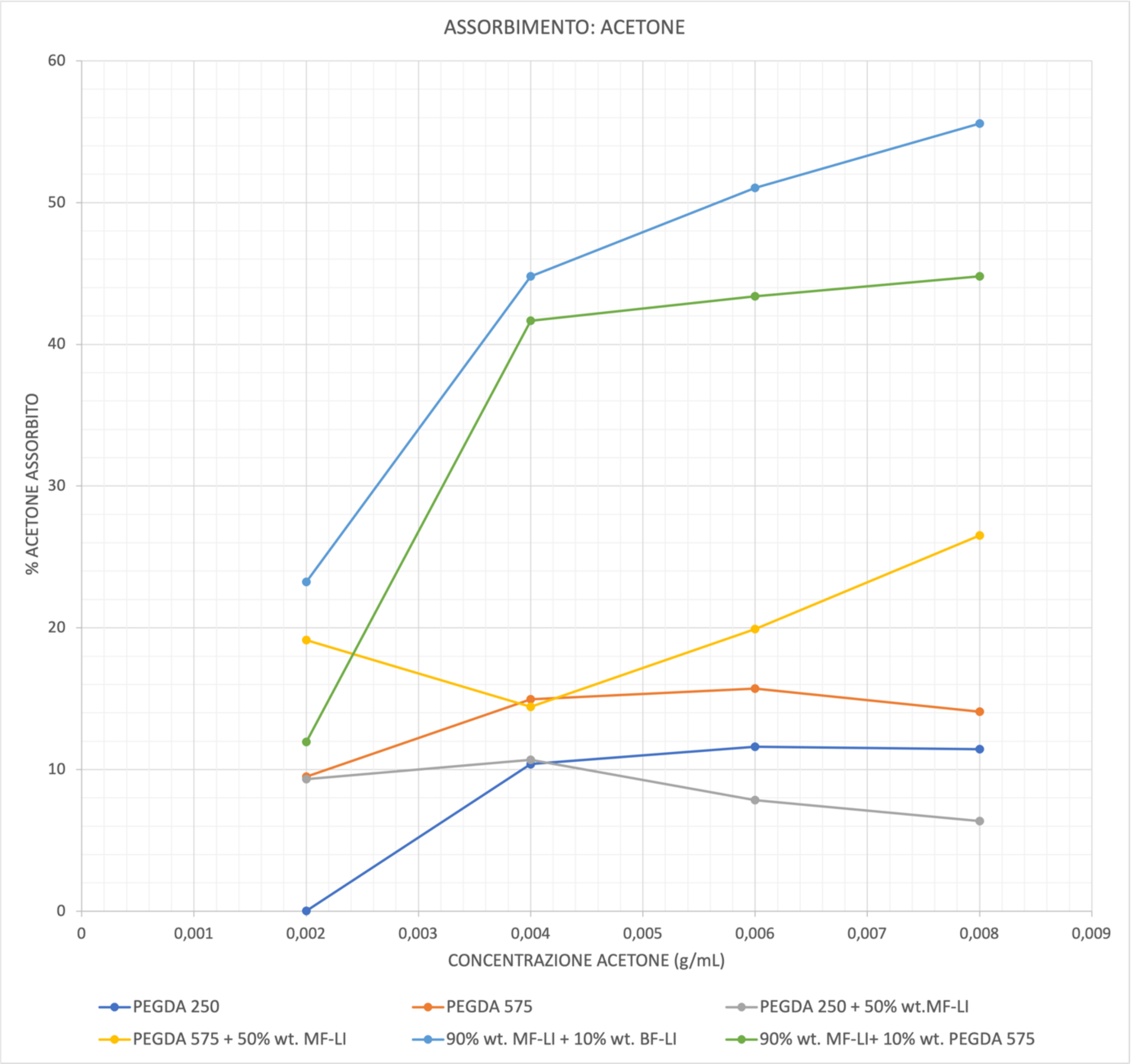

Figura X. Assorbimento di Acetone

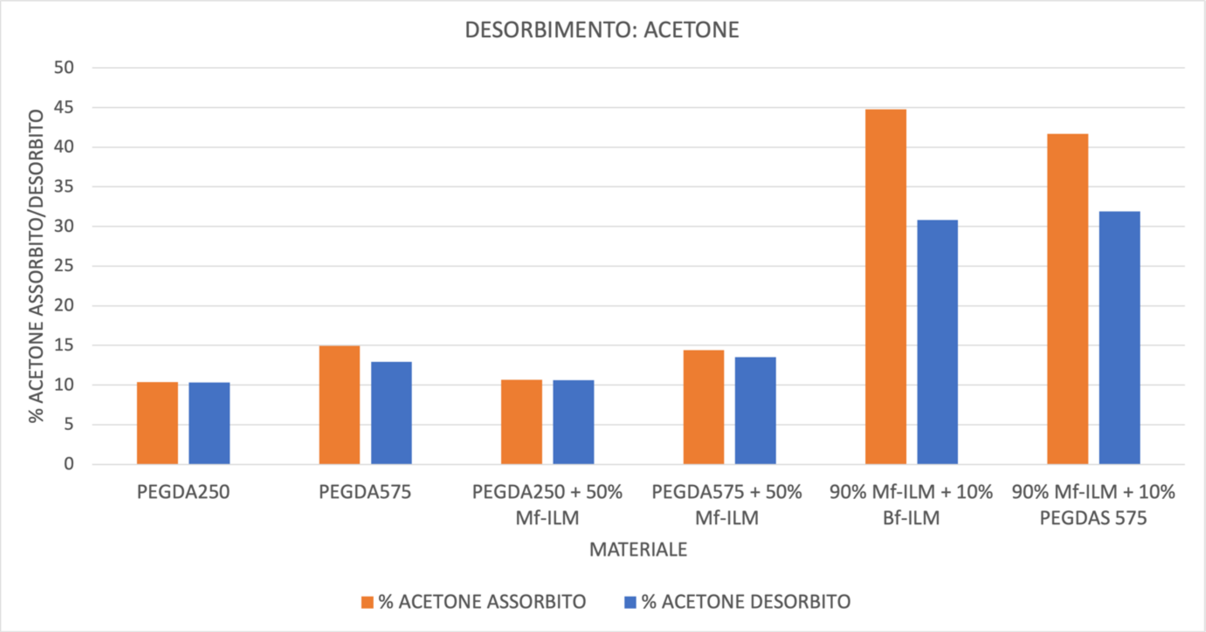

Figura XI. Desorbimento di Acetone

b) 2-propanolo

Le capacità di assorbimento di 2-propanolo da parte dei materiali studiati (Fig. XII) è molto minore rispetto a quella rilevata per l'acetone. Infatti, la massima capacità di assorbimento di tale solvente si ferma al 8% ed è associata a materiali contenenti PEGDA Mn 575.

La presenza di PILs sembra che non provochi un miglioramento netto della capacità di assorbimento dei materiali polimerici.

In questo caso, inoltre, l'aumento della concentrazione di 2-propanolo non influenza la quantità di vapore organico assorbito dai materiali.

Per quanto riguarda il desorbimento di 2-propanolo, esso avviene in modo efficiente per tutti i campioni (Fig. XIII).

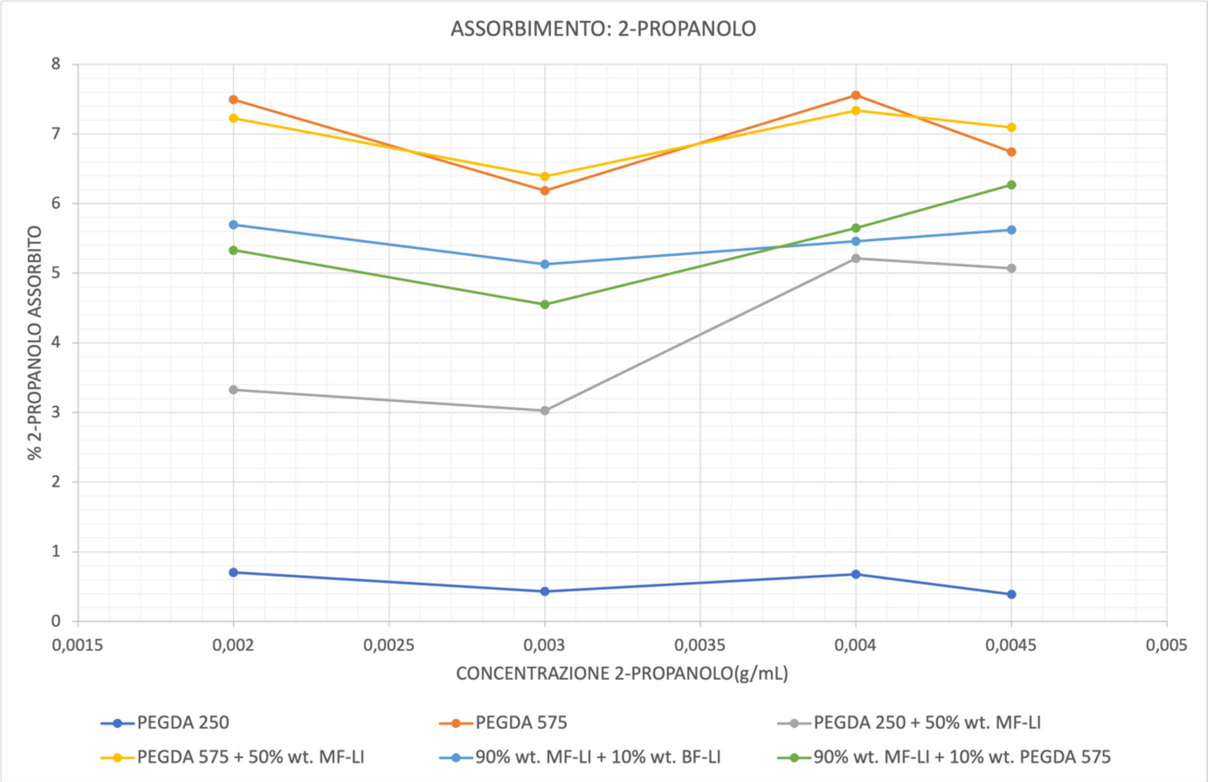

Figura XII. Assorbimento di 2-Propanolo

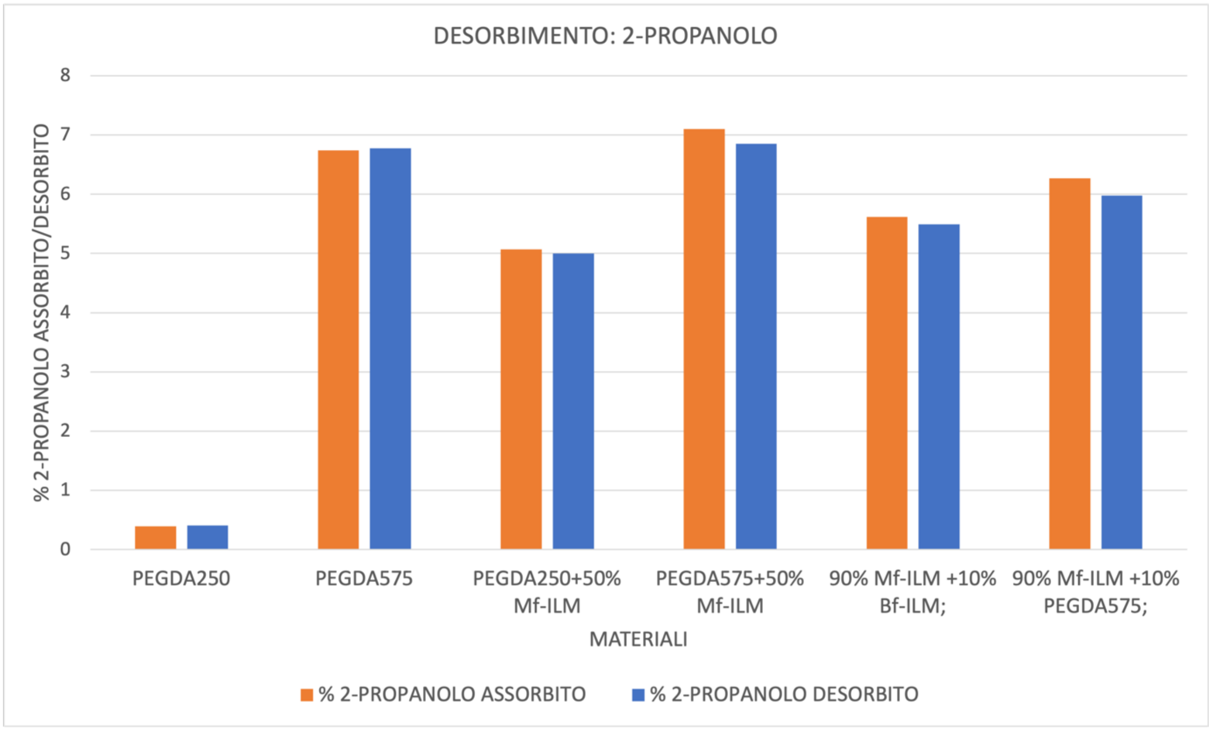

Figura XIII. Desorbimento di 2-propanolo

c) Orto-diclorobenzene

L'orto-diclorobenzene viene assorbito in modo più efficace da materiali caratterizzati da una matrice di PEGDA Mn 575, con capacità di assorbimento massima di 30 % circa (Fig. XIV).

I PILs, invece, presentano una capacità di assorbimento intermedia (10 %). Anche in questo caso i materiali con PEGDA Mn 250 presentano le capacità di assorbimento minori.

Il desorbimento di orto-diclorobenzene (Fig. XV) avviene in modo efficace per tutti i campioni, anche se quelli che presentano PEGDA Mn 575 tendono a desorbire il solvente con maggiore difficoltà.

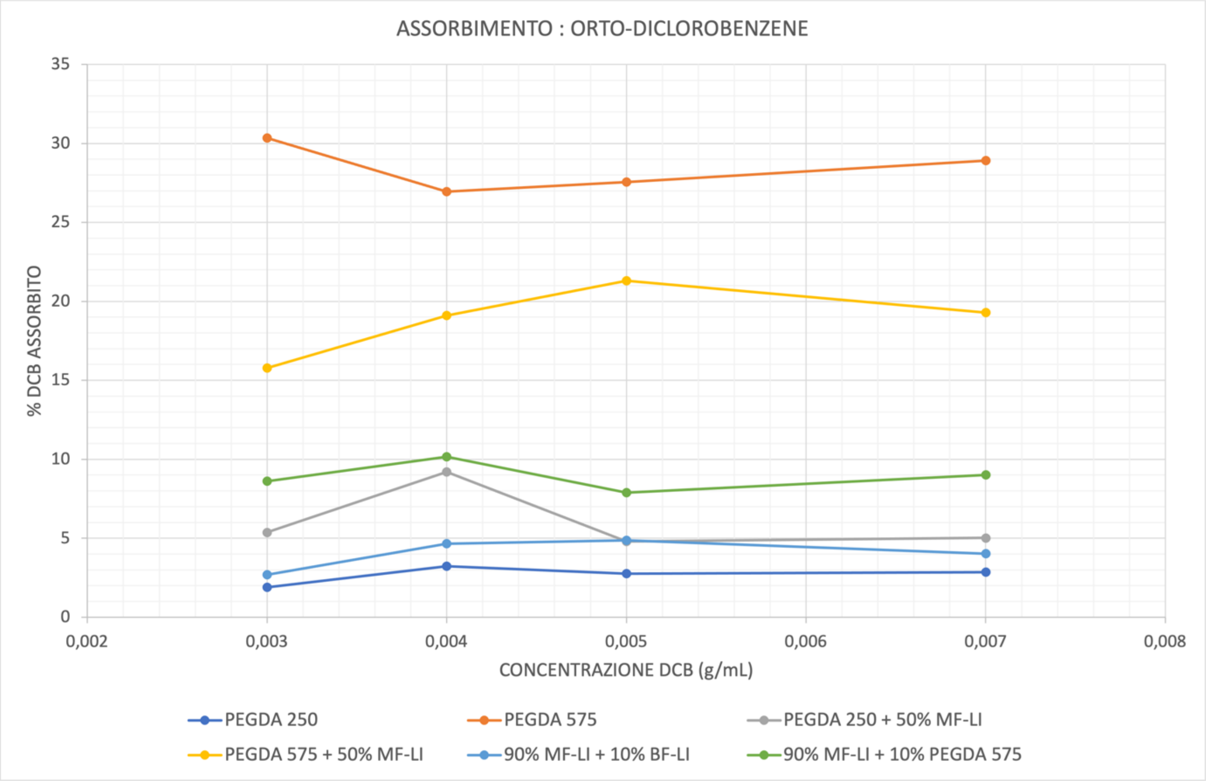

Figura XIV. Assorbimento di Orto-diclorobenzene

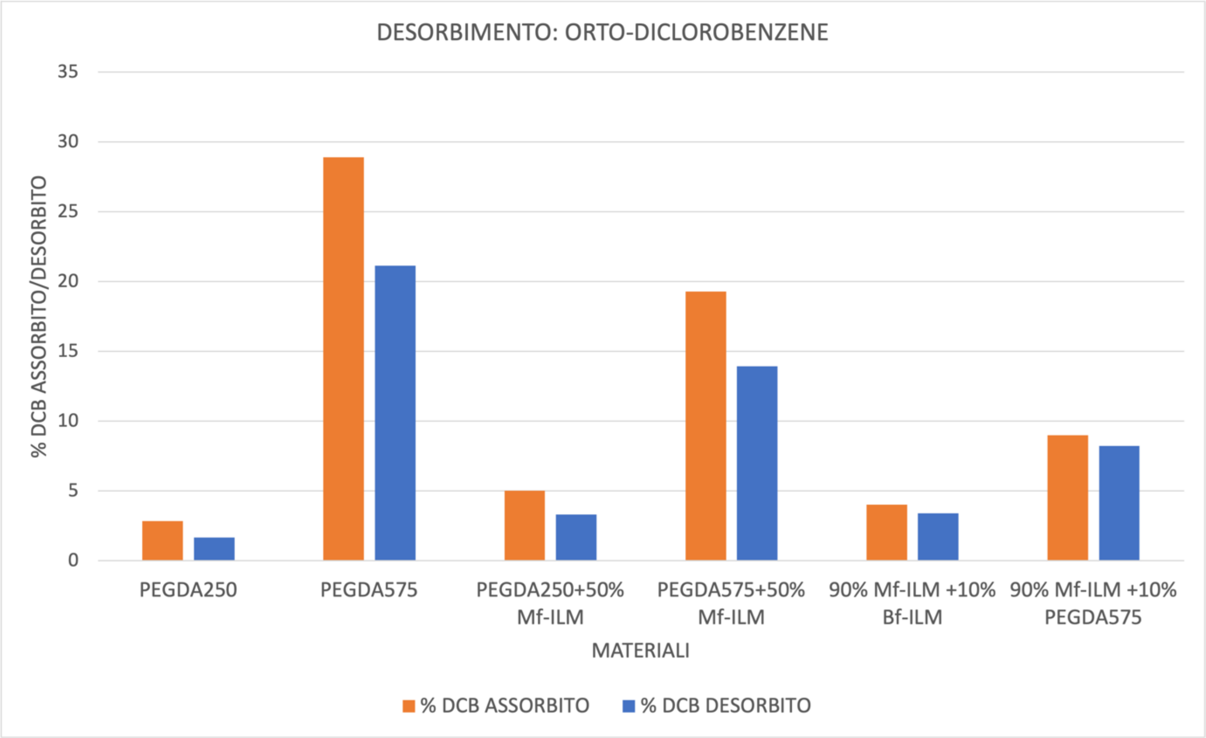

Figura XV. Desorbimento di Orto-diclorobenzene

d) Acetonitrile

Le prove di assorbimento di acetonitrile sono state eseguite per valutare la dipendenza di tale fenomeno dalla costante dielettrica dei solventi organici (associata alla loro polarità): infatti, l'acetonitrile è caratterizzato da una costante dielettrica maggiore rispetto a tutti gli altri VOCs utilizzati.

In effetti, così come nel caso dell'acetone (con costante dielettrica elevata), la capacità di assorbimento di acetonitrile è maggiore per materiali contenenti PILs in alte concentrazioni (55%, vedi Fig. XVI).

e) Cloroformio

Le prove di assorbimento di cloroformio sono state condotte per valutare l'interazione di PILs con un solvente organico molto volatile e dalla costante dielettrica molto più bassa rispetto ai VOCs precedentemente considerati.

La massima capacità di assorbimento (Fig. XVII) è stata riscontrata per PEGDA Mn 575 (75%).

Anche i PILs hanno garantito l'assorbimento di una considerevole quantità di vapore organico (40%).

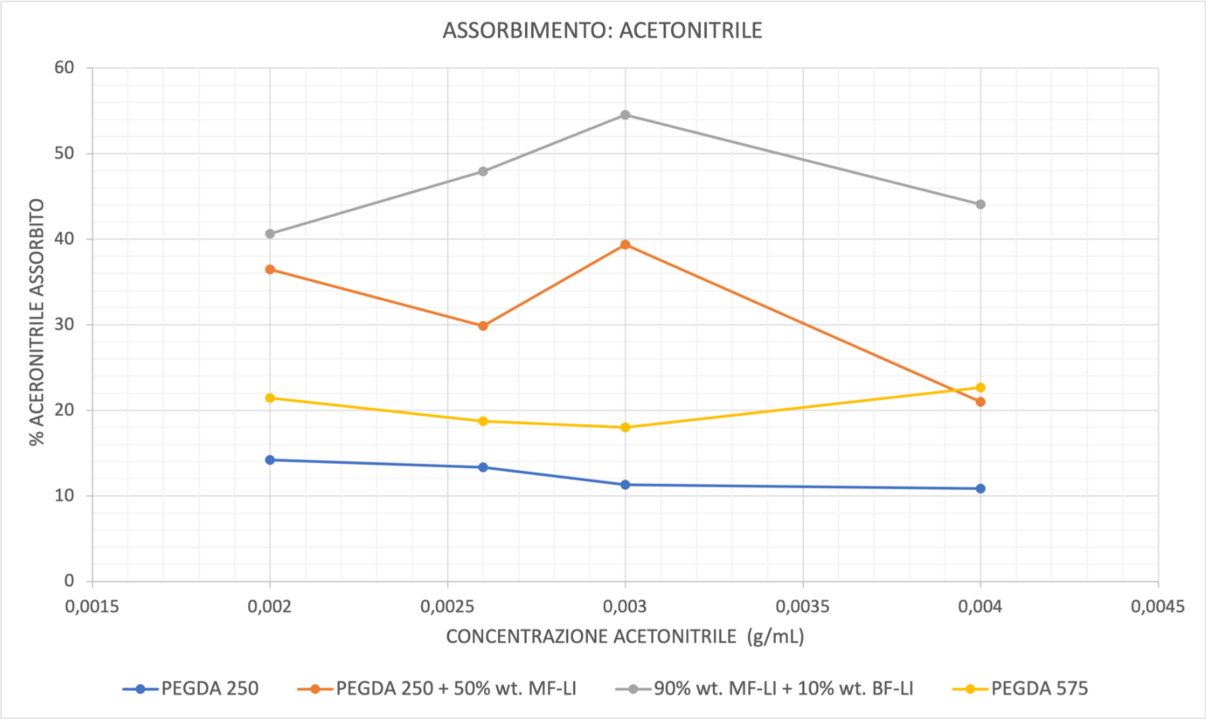

Figura XVI. Assorbimento di Acetonitrile

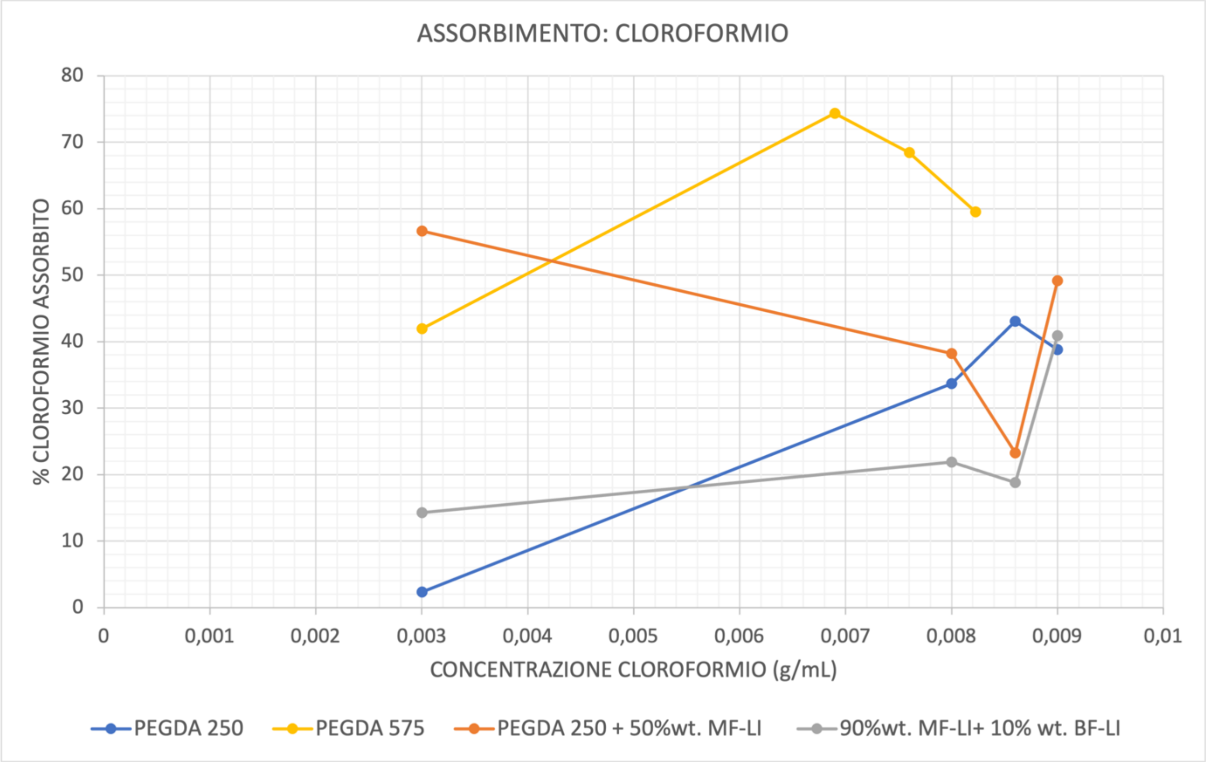

Figura XVII. Assorbimento di Cloroformio

VII. Conclusioni

Con il presente lavoro è stato dimostrato che è possibile realizzare oggetti, anche di forma complessa, con materiali polimerici a base di *Poly(Ionic Liquid)s*, tramite un processo di stampa 3D (DLP). Tale risultato è stato confermato dalle prove di foto-reologia, di spettroscopia IR e attraverso l'osservazione diretta dei campioni ottenuti tramite SEM e Microscopio Ottico.

Le proprietà termo-meccaniche di tutti i materiali considerati, caratterizzati da diverse concentrazioni di PILs e dalla presenza di PEGDA Mn 250 e PEGDA Mn 575, sono state valutate tramite le prove di DSC e DMTA. Si è osservato che la temperatura di transizione vetrosa è influenzata dalla presenza di PILs nei materiali: essa varia tanto più la loro concentrazione è elevata.

La capacità di assorbire composti organici volatili (come acetone, 2-propanolo, orto-diclorobenzene, acetonitrile, cloroformio) relativa ai materiali caratterizzati da PILs è stata studiata tramite prove di assorbimento alla temperatura di 40°C, dalla durata di 24 ore.

Si è osservato che l'acetone e l'acetonitrile, entrambi caratterizzati da costanti dielettriche alte, siano stati assorbiti in modo particolarmente efficace da parte dei PILs. Al contrario, 2-propanolo, orto-diclorobenzene e cloroformio vengono assorbiti preferenzialmente da materiali costituiti da PEGDA Mn 575.

Tali risultati possono derivare da più fattori che possono influenzare il modo in cui il solvente organico interagisce con i materiali polimerici. Oltre alla costante dielettrica, che è un indicatore della polarità dei solventi, è importante considerare anche la capacità che tali molecole hanno di interagire attraverso legami a idrogeno; o la loro affinità con i cationi e gli anioni costituenti i PILs.

Per esempio, il cloroformio, che ha una costante dielettrica molto bassa, è stato assorbito sufficientemente bene dai PILs, grazie alla sua capacità di costituire legami a idrogeno. Nonostante ciò, la sua affinità con la struttura chimica del PEGDA è probabilmente maggiore rispetto a quella che ha con i cationi e anioni costituenti i PILs.

Il 2-propanolo, invece, nonostante sia caratterizzato da una costante dielettrica elevata, non viene assorbito efficacemente dai PILs: questo può essere spiegato considerando che la solubilizzazione di tale solvente nei *Poly(Ionic Liquid)s* può essere inibita dalla presenza di catene alchiliche corte presentate dai policationi.

Per quanto riguarda l'orto-diclorobenzene, la capcità di assorbimento di tale solvente è stata maggiore per i materiali a base di PEGDA Mn 575. Nonostante ciò, anche i PILs hanno dimostrato una buona capacità di assorbire tale solvente, non solo grazie alla sua polarità, ma anche tramite interazioni $\pi - \pi$, legami a idrogeno e forze di Van der Waals che esso è in grado di instaurare con gli ioni.

Anche le proprietà termo-meccaniche dei polimeri, come la temperatura di transizione vetrosa, sono fondamentali per dare un senso ai risultati ottenuti. A temperature superiori alla T_g dei polimeri, infatti, il volume libero presente tra le macromolecole è maggiore. Tale condizione, garantirà la propensione del materiale all'assorbimento di molecole organiche. Questo può spiegare, almeno parzialmente, il fatto che molti VOCs siano stati assorbiti preferenzialmente da PEGDA Mn 575, che presenta una T_g estremamente bassa (- 20°C).

Per quanto riguarda il desorbimento di VOCs, tutti i materiali hanno dato buone prestazioni in relazione a tutti i solventi organici considerati: la forza delle interazioni secondarie che consentono l'assorbimento non è consistente, al punto che, se sottoposti a una temperatura di 40°C, i materiali polimerici sono in grado di desorbire tutti i composti organici efficientemente.

Aim of the Work

Volatile Organic Compounds (VOCs) are carbon-containing compounds, volatile at room temperature, commonly found in the atmosphere. They derive mostly from industrial processes, oil refining and petrol storage, agriculture and engines' exhausted products, but they are also quite common in indoor environments and activities. Considering that Volatile Organic Compounds affect the human health and enhance many threatening environmental issues, it is clear that their removal from the atmosphere is necessary.

Various existing methods to achieve this have been considered: the aim of this work is to verify if the absorption of VOCs may be provided by polymeric filters, with a porous structure, realized by DLP- 3D printing.

In particular, the considered polymeric material must be characterized by a certain amount of Poly (Ionic Liquid)s, which have been studied a lot recently for their versatility and their ability to capture volatile pollution agents, such as CO_2.

In this case, the goal is to know how the presence of PILs influence the absorption capacity of the polymeric matrix, and, in general, to investigate their efficiency as VOCs' absorbents.

This analysis has been made for different organic solvents as absorbates (acetone, isopropyl alcohol, 1,2-dichlorobenzene, acetonitrile and chloroform) in order to study how their different physical and chemical properties affect the efficiency of the absorption process.

Furthermore, the possibility to obtain even complex structures through DLP-3D Printing of PILs has been evaluated. The efficiency of this process and the properties of the obtained solid materials have been investigated.

Chapter 1: Introduction

1.1 Volatile Organic Compounds (VOCs)

Volatile Organic Compounds are defined by the European Union's Council Directive 199/13/EC of March 11th, 1999 as "*any organic compound having at 293,15 K a vapour pressure of 0,01 kPa or more, or having a corresponding volatility under the particular conditions of use*." [1].

Furthermore, the World Health Organization defines them as any organic compound whose boiling point is in the range of 50-250°C (ISO 1600) [2].

VOCs could be also considered as carbon-containing compounds, volatile at room temperature and easily found in the atmosphere, different from carbon dioxide, carbon monoxide, carbonic acid, metallic carbides or carbonates and ammonium carbonate. [3, 4].

VOCs which are present in the ground level atmosphere are mostly originated by industrial processes, oil refining and petrol storage, agriculture and engines' exhausted products, but they are also quite common in indoor environments and activities.

A little amount of VOCs is also produced by plants, whose metabolism is actually influenced by the higher CO_2 concentration and the global warming effects. Because of those abiotic and biotic stresses, as a defence strategy, they produce a more consistent amount of VOCs, consequently dispersed in the atmosphere [5].

This term indicates a wide variety of solvents, that differ from one another because of their chemical, physical, molecular properties. This is the reason why it is quite difficult to consider a unique way to classify those organic compounds: for example, the World Health Organisation categorise VOCs as indoor pollutants according to their volatility, as summarised in Tab.1 [4].

NAME	BOILING POINT (°C)	EXAMPLES
VERY VOLATILE ORGANIC COMPOUNDS (VVOC)	<0 to 50-100	Propane, butane, methyl chloride
VOLATILE ORGANIC COMPOUNDS (VOC)	50-100 to 240-260°C	Formaldehyde, toluene, acetone, ethanol, 2-propanol, hexanal, 1,2-dichlorobenzene
SEMIVOLATILE ORGANIC COMPOUNDS (SVOC)	240-260°C to 380-400°C	Pesticides (DDT, chlordane, plasticizers as phthalates, fire retardants as PCBs and PBB)

Table 1.5. Volatile Organic Compounds classification [4]

As those organic solvents are very different from each other, also the potential impact on the outdoor and indoor environments in which they are found is variable: in fact, it depends on their volatility, their degradation mechanisms and the time required to complete them. There are some compounds which are extremely stable, such as chlorofluorocarbons (CFCs, used as refrigerants), characterized by a lifetime that could last decades; and others with a very short lifetime, such as formaldehyde, which degrades quickly.

In general, the main problems concerning the presence of VOCs in the outdoor or indoor atmosphere are:

- Toxicity of the organic solvents, that is predominant in the indoor environment in which VOCs could be more concentrated. The inhalation of those vapors may, in fact, cause acute or chronic diseases to people.

- Secondary effects caused by the presence of VOCs in the atmosphere, even if in smaller concentrations: they are basically due to the reactivity of the volatile organic compounds that in certain conditions determines the formation of other pollutant agents and particulates, called also photochemical smog. This could have a strong impact on the greenhouse effect and the global warming issues deriving from that [6].

1.1.1 Direct Exposure to VOCs

The high volatility of VOCs at room temperature makes them more susceptible to fast volatilization and their consequent gathering in indoor environments. Their concentration in those cases is way higher than in outdoor atmosphere: indoor concentrations of VOCs are commonly 2-5 times greater than outdoor ones [7]. This led people to be prone to inhalation and direct exposure of those organic vapors, whose sources are basically furniture materials, printing machines, household products (such as those used for cleaning, cooking, home-working), perfumes and fragrances, cosmetics, glues, smoking and working environments [7,8].

The constant exposure to VOCs may be problematic because of the toxicity of some solvents and their irritant nature: even though often the indoor air quality is considered an underrated feature to be monitored, the amount of time spent by people in closed environment makes it actually way more decisive than expected for human health.

In fact, it has been demonstrated that the prolongated exposure to VOCs may cause acute or chronic respiratory, cardiovascular and neurological diseases and inflammatory reactions, considering also the fact that many organic compounds are carcinogenic [7,9].

In particular, Total Volatile Organic Compound (TVOC) is an indicator discussed by Mølhave, L. (2009) [10] used to identify the concentration of similar VOCs in the air and their combined effects that may lead to perceived irritation and discomfort.

It has been proven that 2 mg/m^3 is the VOCs' concentration limit above which discomfort, physical stress and irritation are perceived, while at 25 mg/m^3 a subacute stress reaction may often occur. The correlation between VOCs concentration and its effect on human health in indoor circumstances is illustrated in Tab.2.

Normally, about 50-300 different VOCs are found in an air sample on non-industrial indoor environment, in which toluene is one of the most common to be found.

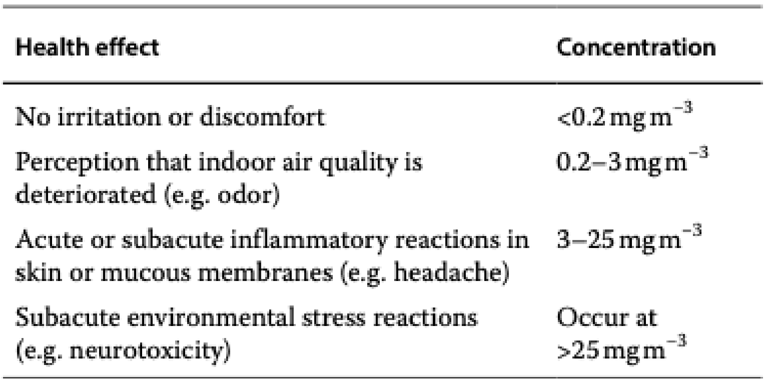

Health effect	Concentration
No irritation or discomfort	<0.2 mg m^{-3}
Perception that indoor air quality is deteriorated (e.g. odor)	0.2–3 mg m^{-3}
Acute or subacute inflammatory reactions in skin or mucous membranes (e.g. headache)	3–25 mg m^{-3}
Subacute environmental stress reactions (e.g. neurotoxicity)	Occur at >25 mg m^{-3}

Table 1.6. Health effects of different VOCs concentrations [7,10]

1.1.2 Secondary Effects of VOCs: Impact on the Atmosphere

The presence of VOCs in the atmosphere may lead to two different problems, connected to the ozone concentration:

- The increase of the concentration of ozone in the troposphere (which is the part of the atmosphere closer to the Earth surface, extending for 10-15 km above it), thus enhancing the amount of pollutants and the devastating effects of global warming;
- The depletion of ozone in the stratosphere, where this gas is useful to keep some UV radiations potentially dangerous for living beings from arriving to the Earth surface.

The two phenomena are determined by different mechanisms and different types of VOCs: CFCs for example, are mainly responsible for the depletion of ozone, because of their long lifetime which permits them to gather in the stratosphere; while other organic compounds more prone to photochemical degradation mechanisms are the ones causing the first process that has been described.

Whereas the effects of the first phenomenon are attributable to localized urban areas, the ones given by the latter are considered in a global perspective [6].

1.1.2.1 Effects on the Troposphere: Increase of Ozone Concentration

The reactivity of VOCs with other elements available in the ground level atmosphere, such as nitrogen oxides, causes the progressive increase of the amount of ozone in the troposphere.

In fact, the following reaction occurs, which basically represent a degradation mechanism of those organic compounds, activated by the sunlight.

$$\text{VOC} + \text{NO}_x + \text{Sunlight} = \text{O}_3 + \text{NO}_x + \text{other products}$$

The "other products" obtained are particulates, carbon monoxide, formaldehyde or organonitrates, defined also as secondary products.

The ozone formation is primarily controlled by VOCs and NO_x concentrations: it has been demonstrated that the lowering of VOCs concentration is more effective than the one made for NOx, in order to diminish the amount of ozone produced via this photochemical process.

Furthermore, different types of VOCs have different chemical characteristics and reactivity, from which the formation of ozone depends [2].

Ozone is a greenhouse gas: in the ground level atmosphere it is able to absorb the infrared radiations arriving from the Earth surface, after it is warmed up by the absorption of the sunlight. Ozone (as CO_2 and methane) is also capable of re-emitting the energy provided by the infrared thermal radiations absorbed, in all directions, towards the Earth surface too. This increases the temperature perceived on Earth, which is not only given by the direct exposure to sunlight but it is also enhanced by the thermal radiations re-emitted by greenhouse gasses (Fig.1.1).

If the concentration of those gasses progressively increases in the troposphere, the consequences of this cycle that gradually warms up our planet's surface will be intensified more and more. Global warming and climate changes derive also from this mechanism, whose control is becoming decisive [6, 11].

Moreover, the exposure to ozone and secondary pollutants may become a human health issue: while ozone causes respiratory and cardiovascular diseases, formaldehyde is carcinogenic and fine particulates may lead to irritation, inflammation and chronic illnesses [10].

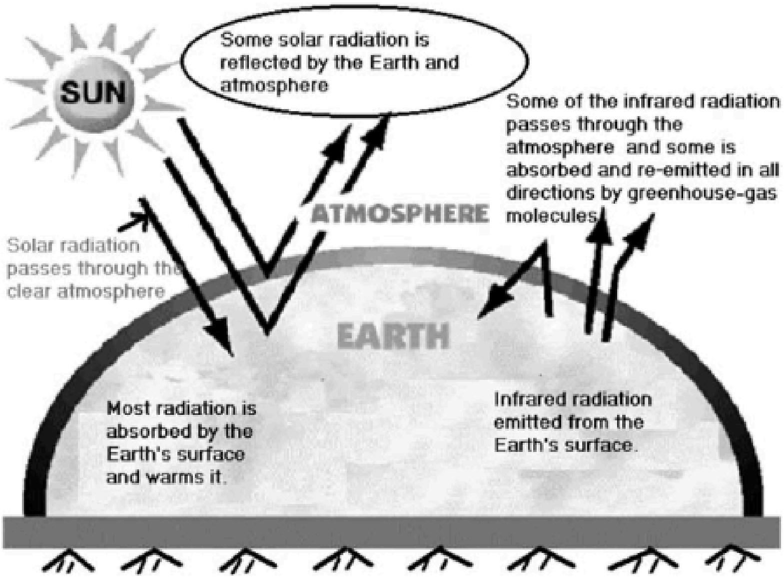

Figure 1.1. Greenhouse effect [11]

1.1.2.2 Effects on the Stratosphere: Ozone Depletion

Ozone is also present in the stratosphere, where it absorbs more than the 90% of UV radiations characterized by a wavelength between 200 to 315 nm, which could be potentially damaging for beings living on the Earth surface.

The ozone concentration of the stratosphere is not uniform, but it should be maintained constant by the photolysis of oxygen through UV light irradiation, and the consequent combination of the oxygen atoms to O_2 molecule to form O_3:

$$O_2 + h\nu = O + O$$

$$O + O_2 = O_3$$

Ozone may be destroyed by the reaction with other compounds, such as nitrogen oxides and compounds that bring chlorine or bromine to this part of the atmosphere, which act as catalysts for the whole reaction. This one may be repeated several times, so the amount of ozone depleted grows exponentially.

Those compounds may be CFCs, for example, that are characterized by a slow degradative mechanism occurring in the troposphere, so that they are led to gather on the stratosphere, enhancing the demolition of ozone:

$$Cl + O_3 = ClO + O_2$$

$$ClO + O = Cl + O_2$$

$$\text{Net reaction: } O_3 + O = O_2$$

The diminishing quantity of ozone in certain areas of the stratosphere leads UVB radiations which are potentially dangerous for human beings, plants and animals to permeate the stratosphere and reach the Earth surface [6].

1.2 VOCs Removal: Existing Methods

Considering all the consequences given by the presence of a significant amount of VOCs in the atmosphere, it is important to reduce their concentration as much as possible.

This goal could be achieved through the modification of the industrial processes and the relative equipment needed, which is a complicated solution, with many limits [12].

Other alternatives may be represented by the destruction or the recovery of VOCs, that should be separated efficiently from the other gasses constituting atmospheric air. Those two types of methods are deepened in the following paragraphs.

1.2.1 Destruction of VOCs

There are different methods that provide the degradation of VOCs, through:

- Oxidation (thermal, catalytical)
- Bio-filtration

1.2.1.1 Oxidation Methods

Oxidation reactions represent a very efficient method to degrade the majority of VOCs produced by many different processes, so that they won't be released in the atmosphere.

Those techniques are able to transform the volatile organic compounds into less harmful gasses such as carbon dioxide and water vapor. If chlorine- or sulfur-based compounds are degraded, it is possible to obtain HCl or SO_2 as products as well as nitrogen compounds in the case of nitrogen-based VOCs [13].

The reactions occurring in order to decompose VOCs require oxygen and a certain amount of heat, which is useful to reach the activation energy.

1.2.1.2 Thermal oxidation

This method requires the use of heating sources in order to increase the temperature of the VOCs entering a reaction chamber (that is maintained around 650-1000°C). The heat, in this case, is the only way to activate the oxidation of those organic compounds, which may take from 1 to 2 seconds to complete [14]. The operating temperature to be provided depends on the kind of organic compound that has to be thermally degraded, on its concentration in the entering stream and on the desired efficiency required for the whole process.

There are different types of thermal oxidation, according to the different designed system and process:

- Direct fired thermal oxidation

  This process provides the oxidation of the VOCs stream into a combustion chamber, through burners specifically designed to make the vapors reach the desired temperature. No heat recovery is generally provided by this method [14].

- Recuperative thermal oxidation

  This method is suitable for streams with low VOCs concentration, it provides not only the thermal decomposition of those compounds, but also the recovery of the thermal energy generated by VOCs' oxidation. This one may be used to pre-heat the entering VOCs stream or, alternatively, it could be applied on external systems by which heat is required.

  Thermal recovery is generally guaranteed by the use of shell-and-tube or plate-type heat exchangers. This could be convenient in order to diminish the amount of external energy required to heat up the VOCs stream, and consequently to lower the quantity of auxiliary fuel needed to increase the temperature in the chamber, through its combustion. Typically, the amount of recovered energy may vary between 60% and 80% [12,13,14].

- Regenerative thermal oxidation

  Similarly to recuperative thermal oxidation, the regenerative method guarantees the recovery of the heat associated with oxidized VOCs stream: in this case, the hot gas passes through more than one ceramic beds, capable of extracting the heat from them, lowering their temperature so that they can be released to the atmosphere. The hot ceramic beds, then, could be useful in order to pre-heat the feed VOCs stream, so that the process of their decomposition may continue cyclically. Moreover, the ceramic bed cools down thanks to this process, so that it may be available again in order to lower the temperature of oxidized gasses.

  Those systems may be characterized by at least two ceramic beds and valves that regulate the gas flux's directions according to the thermal conditions of the considered heat exchangers. This may lead to the recovery of 95% of the heat involved in the process, so that no additional fuel is required to maintain it [12,13,14].

- Catalytic oxidation

  This oxidation method, differently from the previous ones, involves the use of catalysts supported by honeycomb or monolithic structures. Those materials enhance the reactivity of VOCs even at lower temperature (400-500°C), so that the amount of thermal energy required to activate the oxidation mechanism diminishes. The reaction takes place at the catalysts' surface [12,14].

1.2.1.3 Bio-filtration

Low concentrations of VOCs are removed from the atmosphere thanks to bio-filtration, which is based on the permeation of those volatile compounds through porous filters where a population of micro-organisms resides. Those microbes are able to digest many organic compounds transforming them in carbon dioxide, water and biomass.

The characteristics of the microbes' environment (like pH, moisture content, temperature and pressure) must be carefully controlled.

The complexity of the organic compound determines the efficiency of its bio-degradation process: the degree of adsorption of the vapor by the filters depends on its water solubility, molecular weight and Henry's constant; the biodegradability of VOCs is connected to their chemical properties and structures: for example, simpler alcohols, ketones and aromatics show better biodegradability than certain anthropogenic compounds or more complex ones such as phenols, chlorinated or aromatic hydrocarbons. This means that though bio-filtration is an effective, inexpensive and less impacting degradation method for VOCs, its efficiency is not maximized, especially for those compounds that present a greater complexity [12,15].

1.2.2 Recovery of VOCs

The methods that provide the recovery of VOCs, determining the possibility to reuse those organic compounds again during the same process they derive from, or a different one, are:

- Condensation processes
- Absorption processes
- Adsorption processes

1.2.2.1 Condensation

In order to separate VOCs by the gas stream contaminated by them, the technique of condensation may be considered. It is based on the transformation of the vapor into liquid.

This could be achieved by the oversaturation of the gas stream, the reduction of temperature at constant pressure, or the increase of pressure at constant temperature. The efficiency of the condensation process depends on the physical properties of the organic compound, its concentration and the environmental conditions. This method is not suitable for streams with high concentrations of VOCs, though it is cheap and efficient [12,16].

1.2.2.2 Absorption

Absorption processes provide the removal of VOCs from a gas mixture through the direct contact between the contaminated stream and a liquid, in which VOCs are easily soluble.

The absorbent liquids (such as water, mineral oils, non-volatile petroleum oils [17]) must be compatible with the organic compound to be recovered and they have to be as cheap as possible. In particular, the efficiency of an absorption process depends on the solubility of the organic compound in the liquid solvent, on the concentration of VOCs to be removed from the air, the temperature, the liquid/gas ratio and the surface contact area.

The two most common absorption methods are based on the use of packed bed towers and mist scrubbers with a spray nozzle system that atomizes the liquid in order to create droplets that enhance the surface contact area with the surrounding gas [12,16].

1.2.2.3 Adsorption

Adsorption is defined as the process through which molecules, atoms, ions (adsorbate) adhere to the surface of a specific material, called adsorbent. This could be achieved thanks to physical or chemical interactions between the adsorbate and the surface. It differs from *absorption*, because the phenomenon is not related to the bulk of the considered material but it is connected to mechanisms acting only on the surface of it.

It is a reversable process: desorption may be provided by an increase of the temperature of the adsorbent or by a reduction of the pressure surrounding it.

VOCs adsorption is mainly due to physical mechanisms, consisting, for example, of Van der Waals forces or dipole-dipole attraction, depending on the polarity of the molecules involved [12].

It is a suitable process for the removal of low concentrated VOCs from the atmosphere, provided by adsorbents with a highly porous structure and maximized specific surface. The most common ones are:

- *Activated Carbons* [12,16,18], which generally operates at temperatures lower than 40°C and a relative humidity lower than 50% in order to avoid the inhibition of the adsorptive capacity. This one also increases with the polarity of the molecules, that makes the interaction with the surface even stronger; their degree of cyclization and their molecular weight. When the activated carbons are saturated by the adsorbate, they are regenerated through an increase of temperature, that favors the desorption of VOCs. The released VOCs are then condensed by cooling and eventually separated by gravity decanting or distillation; whereas the activated carbon may be reused.
  Activated carbons are flammable, they may promote the polymerization or the oxidation of some solvents and they may be hard to be regenerated from high boiling solvents and they require high operating and maintenance costs.

- *Zeolites* [12,19], that are less common than the materials presented previously, but they are able to be efficient even at higher temperature and variable relative humidity.
  The majority of zeolites used with this purpose are hydrophobic high-silica ones, with a minimum Si/Al ratio of 75, which determines the hydrophobicity, the reactivity, thermal stability and the crystalline structure's characteristics of zeolites. Their efficiency is high, but they are expensive.

1.2.3 Recent Developments

Recently other effective methods to remove VOCs from the atmosphere have been investigated, in order to improve the consolidated techniques or to propose other innovative solutions.

For example, ionic liquids (ILs) were studied as liquid absorbents of these organic compounds: thanks to their designable structure, made by organic cations and anions, they provide interactions with VOCs that are strong enough to determine their extraction from liquids or the solubilization of these vapors. In many cases imidazolium-based ionic liquids are used for this purpose, as they presented sufficient compatibility with the chemical structure of the organic solvents: for example [2-Mim][NTf_2] was combined with activated carbons and demonstrated excellent selectivity and solubility in ammonia adsorption [20]. In general, ionic liquids may impregnate polymeric membranes (as in the case of SILMs, described in paragraph 2.5.2.2) or they may be also immobilized in hollow or porous polymeric fibers so that mechanical support and high interfacial surface are guaranteed [21]. The membranes impregnated with ILs also take advantage of pervaporation mechanism: this is based on the permeation of a liquid VOC into the porous membrane and its consequent evaporation, and it is used especially in the separation of two liquids phases.

Other porous adsorbents were also investigated: for instance, novel mesoporous materials such as hypercrosslinked mesoporous polymeric membranes, which are different from activated carbons and zeolites because of their tunable pore structure that enhances the adsorption ability of these systems [22]. Other mesoporous structures that have been discussed are Metal Organic Frameworks (MOFs), which are crystalline, organic or inorganic materials with specific structures, characterized by maximized porosity and surface area: they are based on the presence of unsaturated metals, that interact with VOCs [23].

Also carbon nanotubes and graphene-based materials have been considered [24]: for example, CNTs functionalized with sulfonic acid demonstrated good adsorption capacity for benzene, thanks to the interactions involving π– electrons and the hydrophobicity of their surface. Despite their good performances, they are used rarely because of their high cost.

Graphene oxide and reduced graphene oxide also present good adsorption capacities for VOCs: in particular, the reduced graphene oxide provided the best behavior in the adsorption of non-polar organic compounds (such as benzene and toluene), as its structure is more hydrophobic. In general, they demonstrated higher adsorption capacities than the ones of activated carbons, because of their increased specific area and the stronger interactions involving graphene [25].

For the catalytic oxidation of VOCs, innovative catalysts have been studied, such as porous Ru-$5Co/TiO_2$ or $CuMn_2O_4$.

Nevertheless, the photocatalytic oxidation of these organic compounds was investigated more deeply, as it permits to degrade them at lower temperature, compared to the ones reached in thermal oxidation, thus requiring low energy consumption. The catalysts start their activation process thanks to the low increase of temperature, and then complete it with the absorption of UV light. The photothermocatalysis may be provided by a photocatalyst that absorbs UV radiations (a semiconductor such as titania) together with a thermocatalyst that takes advantage of the heat, which is generally a transition metal. This process may be also guaranteed by a single system providing both the effects, acting simultaneously.

The catalysts are usually based on mesoporous titania, obtained by sol-gel methods, which may be functionalized with Pt nanoparticles or Zr dopants that enhance its performance in the catalysis. Also mesoporous structures based on CeO_2 have been studied and specifically functionalized.

Considering that this one is a thermocatalyst and that titania provides the photocatalysis, the combination of the two of them has been provided: the properties of the resulting material have been investigated for the removal of benzene. Other examples may be represented by Au/TiO_2 catalysts to degrade ethanol and MnO_x-CeO_2 materials to oxidate formaldehyde [24, 26].

1.3 References

[1] European Union Council Directive 1999/13/EC on the limitation of emissions of volatile organic compounds due to the use of organic solvents in certain activities and installations, 11th March 1999; Official Journal of the European Communities.

[2] Berenjian A., Chan N., Malmiri H.J.; 2012; Volatile Organic Compounds Removal Methods: A Review; American Journal of Biochemistry and Biotechnology; 8(4); 220-229.

[3] Derwent R.D.; 1995; Sources, Distributions and Fates of VOCs in the Atmosphere; in “Volatile Organic Compounds in the Atmosphere”; Hester R.E., Harrison R.M. Eds; Royal Society of Chemistry.

[4] https://www.epa.gov/indoor-air-quality-iaq/technical-overview-volatile-organic-compounds

[5] Copolovici L., Popitanu A.C., Copolovici D.M.; 2021; Volatile Organic Compound emission and residual substances from plants in light of the globally increasing CO_2 levels; Aleya L., Uddin S., Bungau S. G. Eds; Environmental Health: Interdisciplinary medical research in the field of public and environmental health; 19: 100216.

[6] Roy W. R.; 2019; Environmental Impact of Solvents in “Handbook of Solvents, 3rd Edition. Volume2. Use, Health and Environment”; Wypych G. Ed.; Chapter 16; ChemTech Publishing; Toronto.

[7] Miller S.L.; 2018; Indoor Air Pollution in “Handbook of Environmental Engineering”; Kuts M. Ed; Wiley; chapter 17.

[8] Wickliffe J.K., Stock T.H., Howard J.L., Frahm E., Simon-Friedt B.R., Montgomery K., Wilson M.J., Lichtveld M.Y., Harville E.; 2020; Increased long-term health risks attributable to select volatile organic compounds in residential indoor air in southeast Louisiana; Nature; 10:21649.

[9] Lin Y., Egeghy P., Rappaport S.; 2008; Relationships between levels of volatile organic compounds in air and blood from the general population; Journal of Exposure Science and Environmental Epidemiology; 18, 421-429.

[10] Mølhave L.; 2009; Volatile Organic Compounds and Sick Building Syndrome in “Environmental Toxicants: Human Exposures and their Health Effects, 3rd Edition”; Chapter 8; Lippmann M. Ed.; Van Nostrand Reinhold; New York.

[11] Tiwari G.N., Mishra R.K.; 2012; General Introduction in “Advanced Renewable Energy Sources”; chapter 1; RSC Publishing; Cambridge.

[12] Khan F.I., Ghoshal A.K.; 2000; Removal of Volatile Organic Compounds from polluted air; Journal of Loss Prevention in the Process Industries; 13, 527-545.

[13] Kohl A.L., Nielsen R.B.; 1997; Thermal and Catalytic Conversion of Gas Impurities in “Gas Purification. 5th Edition”; Chapter 13; Gulf Publishing Company; Houston.

[14] Hutten I.M.; 2016; Federal Law and Regulatory Activity That May Relate to Nonwoven Filter Media in “Handbook of Nonwoven Filter Media”; Chapter 10; Butterworth-Heinemann (Elsevier).

[15] Kumar T.P., Kumar R.M.A.; Chandrajit B.; 2011; Biofiltration of Volatile Organic Compounds (VOCs)-An Overview; Research Journal of Chemical Sciences; 1(8); 83-92.

[16] Goldberg E., Min M.K.; 1997; Environmental Concerns in “Fermentation and Biochemical Engineering Handbook-Principles, Process Design, Equipment, 2nd Edition”; Chapter 15; Vogel H.C., Todaro C.L. Eds.; Noyes Publications; Westwood, USA.

[17] Ozturk B., Yilmaz D.; 2006; Absorptive Removal of Volatile Organic Compounds from Flue Gas Streams; Process Safety and Environmental Protection; 84(B5), 391-398.

[18] Control of Odors and Emissions from Wastewater Treatment Plants Task Force of the Water Environment Federation; 2004; Chemical and Physical treatment of Odors in “Control of Odors and Emissions from Wastewater Treatment Plants”; Chapter 13; Water Environment Federation; Alexandria, USA.

[19] Dunne S.R.; 2010; Industrial has Phase Adsorptive Separations in “Zeolites in Industrial Separation and Catalysis”; Chapter 9; Kulprathipanja S. Ed.; Wiley-VHC; Des Plaines, USA.

[20] Yu M. *et al.;* 2021; Ionic liquid-based adsorbents in indoor pollutants removal; Green and Sustainable Chemistry; 27, 100405.

[21] Salar-Garcia M.J. *et al.*; 2016; Ionic liquid technology to recover volatile organic compounds (VOCs); Journal of Hazardous Materials; 321, 484-499.

[22] Wang S. *et al.*; 2014; Enhanced adsorption and desorption of VOCs vapor on novel micro-mesoporous polymeric adsorbents; Journal of Colloid and Interface Science; 428, 185-190.

[23] Li X. *et al.*; 2020; Adsorption materials for volatile organic compounds (VOCs) and the key factors for VOCs adsorption process: A review; Separation and Purification Technology; 235, 116213.

[24] Teimoori S. *et al.* ; 2020; A Review, Methods for removal and adsorption of volatile organic compounds from environmental matrixes; Analytical Methods in Envirionmental Chemistry Journal; 3 (2), 34-58.

[25] Zhu L. *et al.*; 2020; A critical review on VOCs adsorption by different porous materials: Species, mechanisms and modification methods; Journal of Hazardous Materials; 389, 122102.

[26] Wei L. *et al.* ; 2021; Recent advances in VOCs and CO removal via photothermal synergistic catalysis; Chinese Journal of Catalysis; 42, 1078-1095.

Chapter 2: Ionic Liquids

2.1 Definition and Nomenclature

Ionic liquids (ILs) are nonvolatile organic salts composed only by poorly coordinated ions: they are liquids at room temperature because of their melting point which is usually below 100°C [1]. They are therefore called also Room Temperature Ionic Liquids (RTILs).

They are often characterized by an asymmetric structure: organic cations are generally bigger while anions are smaller and they may be both organic and inorganic. This asymmetry limits the crystallization of these salts, providing their typical low melting point defined previously. In fact, differently from ILs, inorganic salts melt at temperatures above 800°C, having higher viscosity [2].

As represented in Fig. 2.1, there are a lot of different cations and anions that may potentially constitute ionic liquids, in fact several potentially existing ILs may be identified on the order of 10^{18} [3].

The possibility of combining different ions gives these salts the feature of having unique variable properties, which depend on the type of ions considered: ILs may present different polarity, hydrophobicity, thermal and chemical stability, ionic conductivity (which is always high), density, viscosity, reactivity according to the chosen combination of them. This is the reason why ILs are also called “designer solvents”.

These properties depend also on the kind of interactions occurring between cations and anions: they are mainly due to coulomb forces, but also hydrogen bonds, Van der Waals forces, dipole-dipole and π- π interactions are present. They are obviously correlated to the considered type of ions forming the liquid salt.

This is the main reason why in the recent decades ionic liquids have been studied a lot: about 90000 articles have been published on this topic in 20 years (2000-2020), according to a research made on SCOPUS [4] writing “ionic liquids” as the key word. The interest in those compounds is constantly increasing, considering that about the 80% of papers mentioned before were written from 2010 to 2020.

Though the possible combinations of ions are very numerous, the ILs studied in literature most commonly are based on imidazolium, pyrazolium, pyrrolidinium, ammonium, sulphonium as cations; while the anions considered more often are trifluoromethanesulphonate, hexafluorophosphate, halides, nitrates, sulfates, etc.

Considering the great variety of ions involved in the formation of ILs, a specific nomenclature has been defined, based on abbreviations of each ion’s full name. In Tab. 2.1 [5] some examples are reported.

According to this nomenclature, for example, 3-Ethyl-1-vinylimidazolium bis(trifluoromethansolfonyl)imide could be indicated as [EVIM][NTf_2] and 1-butyl-3-methyl-imidazolium tetrafluoroborate is [BMIM][BF_4].

CATIONS		ANIONS	
Full name	**Nomenclature**	**Full name**	**Nomenclature**
Methylimidazolium	[MIM]	Bromide, Chloride	Br^-, Cl^-
Ethylimidazolium	[EIM]	Hexafluorophosphate	$[PF_6]$
Vinylimidazolium	[VIM]	Tetrafluoroborate	$[BF_4]$
Pyridinium	[Py]	Trifluoromethanesulfonate	$[CF_3SO_3]$
Pyrrolidinium	[Pyrr]	Trifluoromethansulfonylimide	$[N(SO_2CF_3)_2]$, $[NTf_2]$
Phosphonium	[P]	Alkylsulfate	$[RSO_4]$
Sulfonium	[S]	Toluenesulfonate	$[CH_3C_6H_4SO_3]$
Ammonium	[N]	Alkylcarboxylate	$[RCO_2]$
Thiazolium	[Thia]	Hydrogen Sulfate	$[HSO_4]$

Table 2.7. Nomenclature of common Ionic Liquids [5]

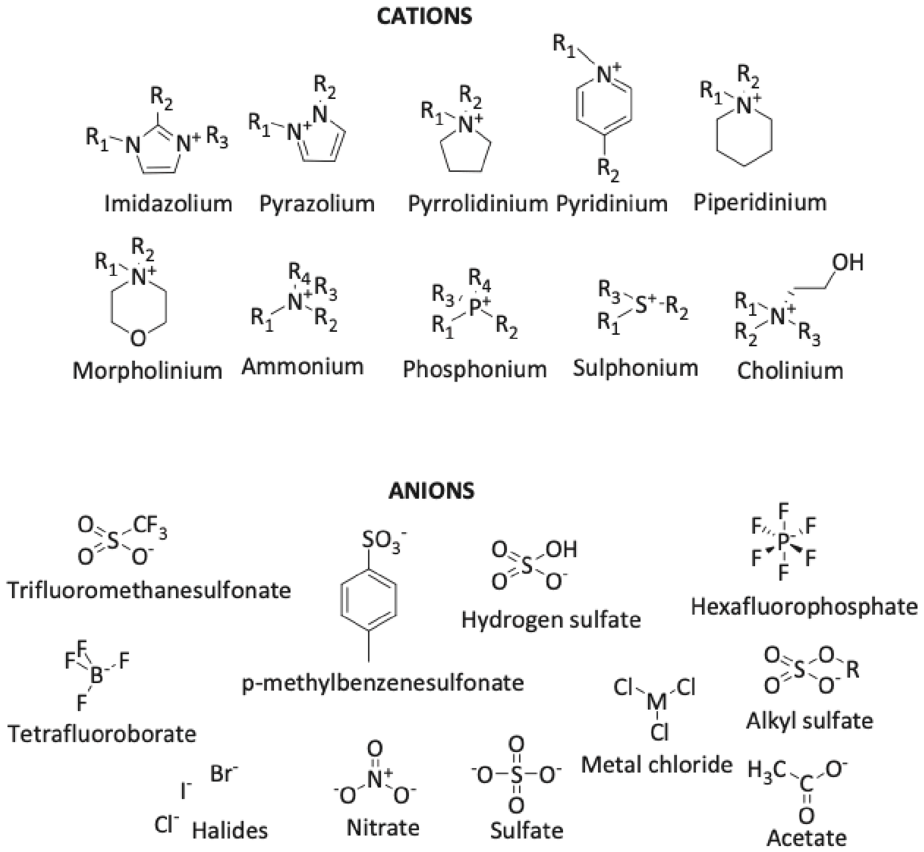

Figure 2.2. Common Cations and Anions that constitute Ionic Liquids [6]

2.2 Classification of ILs

The variety of ILs makes it hard to evaluate a single general way to classify them.

One way to do that is considering their history: the first salt (ethylammonium nitrate) which was identified as liquid at room temperature was studied in 1914 by Walden [7]. After that first study, this particular type of salts was investigated a lot, leading to the definition of different generations of ILs, according to their chemical characteristics, their physical properties, their applications and the period of time in which they were analyzed the most (Fig. 2.2) [8]:

- *1st generation*: RTILs based on 1-alkyl-3-methylimidazolium and tetrachloroaluminate. They were first studied by Wilkes *et al.* in 1982 [9].
- *2nd generation*: RTILs based on the ones previously discovered, whose anion was substituted with others, such as tetrafluoroborate, making these salts more stable when in contact with air and water. This was made in 1992 [10] and has been successful in different applications as an organic reaction media.
- *3rd generation*: these ILs are also called "Task specific ILs", as they are characterized by a functional group that is covalently bonded to their cation or anion in order to give them tunable desired properties. They were introduced by Davis [11] in 2000.

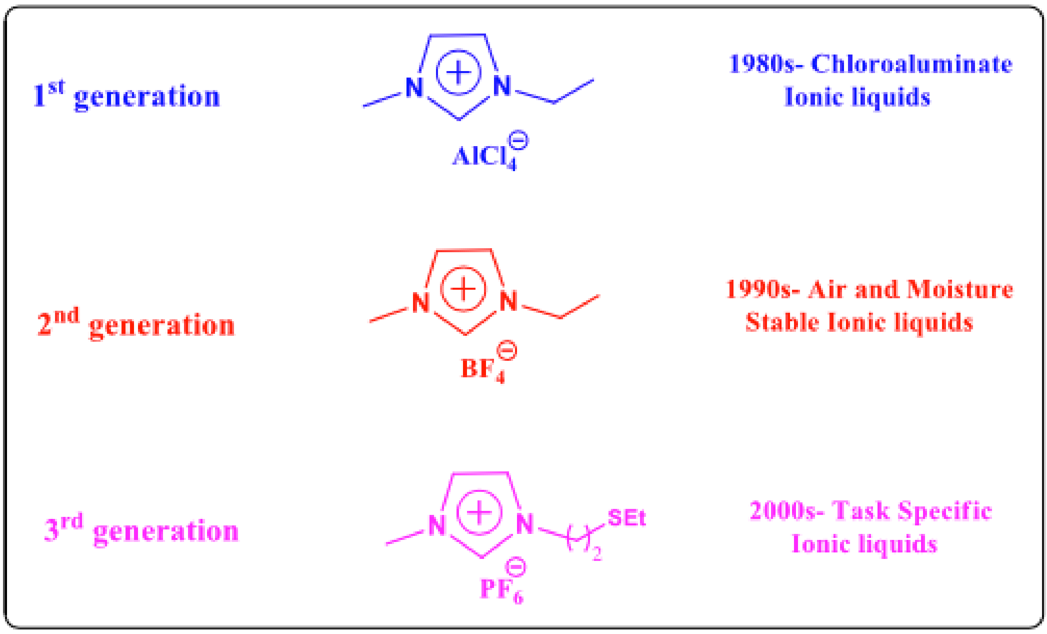

Figure 3.2. Generations of ILs [8]

Another criterion through which ILs may be classified in a more general way is their chemistry. In fact, some of them (Fig. 2.3) could be defined as [1]:

- *Protic ILs*: they derive from a reaction between a Brønsted acid (AH) and a Brønsted base (B), involving a proton exchange. This provides the formation of the salt $[BH^+][A^-]$, as reported in the following equation:

  $$[AH] + [B] = [BH^+][A^-]$$

  The chemical structure of protic ILs, which is based on the presence of a proton-donor site and a proton-acceptor one, allows the formation of hydrogen bonds between these ions, creating a network. Generally, the generation of the salt is enhanced by the strength of the acid or the base involved in the reaction.

- *Aprotic ILs*: they are generated by a synthetic reaction, because in this case a substituent group (such as an alkyl one) replaces the labile proton, typical of protic ILs. The reaction occurring in order to form an aprotic ionic liquid, then, is generally more complex than the one considered for protic ILs.

- *Zwitterionic ILs*: they may be similar to aprotic ILs, except for the fact that the positive and negative charges are both localized on the same chemical spices.

There are also several other ILs' categories, very specific and different from each other, due to the tunability of the properties associated to these chemical spices, such as biological ILs, switchable polarity solvents, chiral ILs, polymeric ionic liquids (PILs), etc.

As briefly described in Fig. 2.3, every type of ionic liquid is more suitable for different specific applications: for example, aprotic ILs are commonly used as supercapacitors and lithium batteries; protic ILs may be found in fuel cells while zwitterionic ILs are valid for ionic-liquid-based membranes.

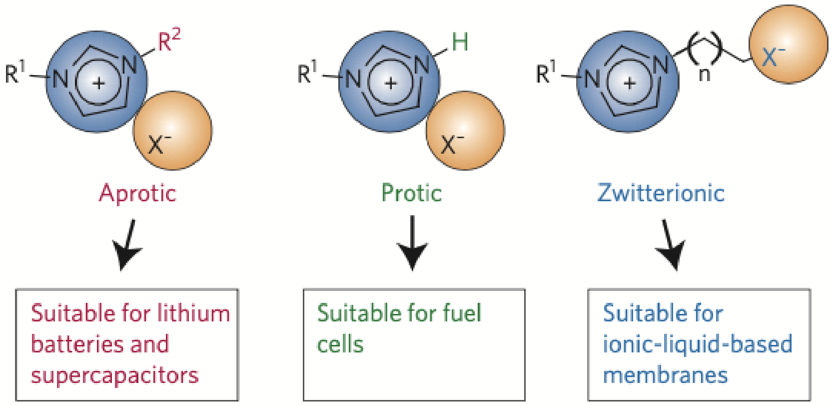

Figure 2.4. Classification of ILs according to their chemical nature [12]

2.3 General properties of ILs

The huge number of possible existing ionic liquids leads to the fact that they are difficult to be characterized in a very general way. In fact, they may present properties very different from one another, depending on the type of ions involved in the formation of that specific organic salt.

Another important issue deriving from this is the lack of information and studies concerning many ILs, which have been less popular and thus analyzed less frequently than others.

The following paragraphs describe very general properties that could be associated with the majority of ionic liquids, or at least, with the most studied ones [1, 13].

2.3.1 Thermal properties

In order to define ionic liquids, their melting point represent an essential parameter to be considered: in fact, their melting point is lower than 100°C, making them liquids at room temperature. This property may depend on the chemical structure of the ions, their symmetry and the function groups that characterize it: for example, if the cation presents long alkyl groups, low symmetry and good distribution of charge, it will be more likely to produce a decrease in the melting point of its ionic liquid. Moreover, a lower size of the anion implies an increase of it.

The nature of the anion influences also the decomposition temperature of those organic compound, which could be up to about 400°C: for example, the higher their hydrophobicity, the lower the decomposition temperature of ILs.

2.3.2 Density

The density range of the majority of ILs is 1.05-1.35 g cm^{-3}, at ambient pressure and temperature. Even this property is connected to the nature of cations and anions considered: in Fig. 2.4 a graph relative to the ionic liquid 1,3-dialkylimidazoliumtetrachloroaluminate. It is evident that the longer the alkyl groups of the cation (in the horizontal axis: 1)R=Me, R'=Me; 2) R= Me, R'=Et; 3) R= Me, R'= Pr; 4) R= Me, R'= Bu; 5) R= Bu, R'= Bu), the lower the overall density of the salt; while if the anion is substituted with another one similar to it, such as bromoaluminate, the density increases. Those two effects given by different cations and anions may present simultaneously, determining the effective density of the ionic compound, just as the relationship between abscissa and ordinate explained in the graph.

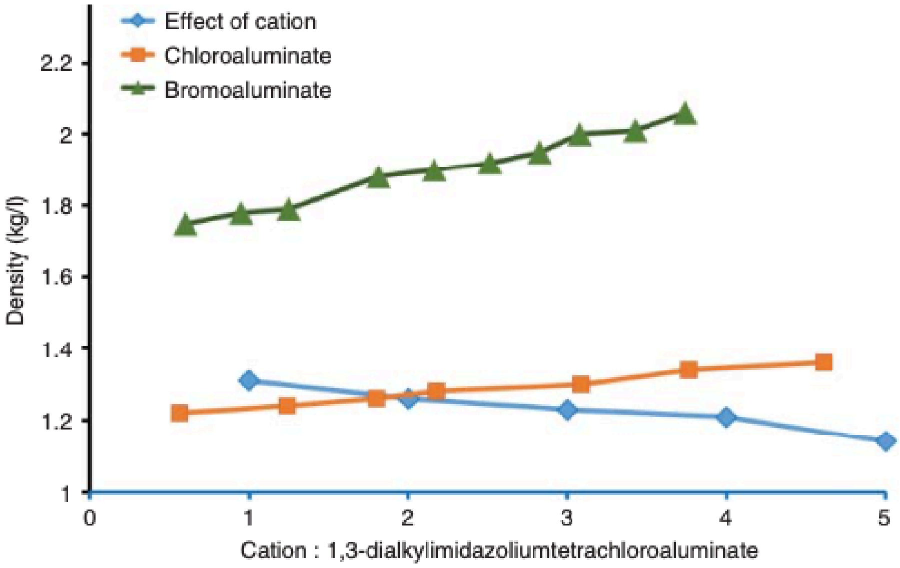

Figure 2.5. Effect of cations and anions on density of ILs. In abscissa, the effect of different cation's alkyl functional groups: 1) R=Me, R'=Me; 2) R= Me, R'=Et; 3) R= Me, R'= Pr; 4) R= Me, R'= Bu; 5) R= Bu, R'= Bu [1]

2.3.3 Volatility and Nonflammability

The vapor pressure of ionic liquids is basically considered negligible at room temperature: this means that their volatility is very low. Nevertheless, they could be distilled if low pressures and high temperatures (200-300°C) are provided, because of their large vaporization enthalpies (around 120-200 kJ mol^{-1}) due to their ionic nature.

Those characteristics, together with their nonflammable nature, make them suitable as solvents which can be considered "green" and less threatening than the organic ones commonly used for different purposes.

2.3.4 Viscosity

The viscosity of many ILs could be defined in the range of 66-1110 cP at room temperature. Those values are 1-3 orders of magnitude higher than the viscosities associated to conventional organic solvents.

Though the amount of data regarding viscosity is scarce in literature, it is possible to state that also this property depends strongly on the chemical structure of the ionic liquid considered (as the example in Fig. 2.5), and most of all, it derives from the strength of the physical interaction between the ions: hydrogen bonds, coulombian forces and Van der Waals interactions have different impact on the viscosity of the organic compounds, considering their different intensities.

Viscosity is also important to determine the mass transport capability of these liquid salts, so that properties like the diffusion coefficient and the ionic electrical conductivity may be influenced by it.

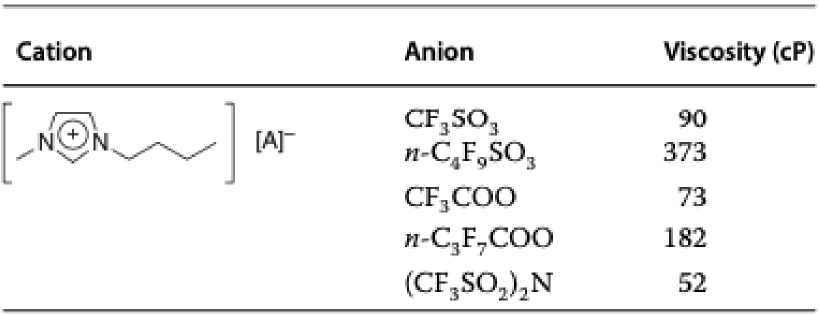

Cation	Anion	Viscosity (cP)
$[A]^-$	CF_3SO_3	90
	$n\text{-}C_4F_9SO_3$	373
	CF_3COO	73
	$n\text{-}C_3F_7COO$	182
	$(CF_3SO_2)_2N$	52

Source: Wasserscheid and Keim (2000). Reproduced with permission of John Wiley & Sons.

Figure 2.6. Influence of different anions in the viscosity of imidazolium-based IL. [1]

2.3.5 Polarity

Considering the chemistry of ionic liquids, they are definable as highly polar. The variety of ionic liquids and their peculiar nature make it hard to define a unique way to measure their polarity: many studies have been published, in which the definition of a polarity scale for ILs is analyzed and the physical and chemical aspects that influence this characteristic are investigated.

Though there is not a unique parameter of polarity, it is possible to state that it is given by their chemical structure and the physical interactions they are involved in. In fact, Van der Waals forces, H-bonds and coulombian interaction let those ionic solvents interact quite easily with some solutes. As an example to create a comparison, it has been proven that the ionic liquid based on 1,3-dialkyl imidazolium have a polarity similar to that of short-chain alcohols; while pyridinium-based ILs present a polarity comparable to that of some solvents characterized by the capability of creating less intense hydrogen bonds [14].

The dielectric constant ε, which is one of the most common parameters to define the polarity of molecular solvent, is not suitable in order to define the polarity of ionic liquids because it gives some incongruences in the comparison between the characteristics of different ILs. Thus, other different scales have been considered, and Guan W. *et al.* (2017) [15], for example, proposed a new one based on their vaporization enthalpies, which is compatible with the information given by the dielectric constant for common molecular solvents.

2.3.6 Solubility

The capability of ionic liquids to dissolve other substances depends on their chemical structure and on the interaction occurring between cations and ions. In general, ILs are good solvents because of their polarity and the tunability of their properties, making them even more versatile from this perspective.

The solubilization process may be defined by three steps: a cavity with a proper size has to be created in the solvent, in order to let the solute reside there, compatibly with the solvent surrounding it. Then, the presence of the solute polarizes the solvent, reorienting the entire ionic structure.

This process is completed only if it is convenient from an energetic point of view: the formation of the cavity in the solvent implies the removal of some solvent ions, which cost the system hundreds of kcal/mol, considering that each ion has about 5-8 other counterions surrounding it, attracted one to another through strong coulombian interactions, hydrogen bonds or dispersion forces. This means that only the spices that accommodates into those ionic solvents without causing a considerable perturbation in their structure will be easily solvated by ILs [14].

This explains why the physical interaction acting between cations and anions in an ionic liquid are so important to define their efficiency as solvents.

2.3.7 Electrical Conductivity

As cations and anions constitutes ionic liquids, their electrical conductivity is given by their ion mobility. Their conductivity could be defined in the range of 0.1-20 mS/cm. This value may be influenced by other characteristics of IL, such as its viscosity, its chemical properties and the environmental conditions.

In fact, it has been demonstrated that ILs' electrical conductivity is enhanced if the temperature is higher, because it improves the ions' mobility. On the contrary, it is not favored by ions containing long-chain functional groups, which cause an increase of the viscosity of the system, diminishing the mobility of the charges.

2.4 Applications

Considering the tunable characteristics of ILs, they have been applied in many realms, different from each other. The main ones are [16, 17]:

- *Solvents and Catalysis*

  Because of the tunability of their properties, their low volatility, and their high decomposition temperature, ILs are defined as "green" or "designable" solvents, as they are safer and act specifically with reactants to promote their reactions.

  They may be applied for the synthesis of both organic and inorganic species, replacing the volatile organic solvents, commonly used for this purpose. I

  ons could be specifically functionalized accordingly to the type of contribution they must give to the reactive system, those compounds are called "Task-specific ILs (TSILs)".

  They may be involved not only in organic reactions like hydrogenations, isomerizations, dimerizations, alkylations, (etc.), but also in the formation of nanoparticles, porous materials (such as zeolites), metal organic frameworks, transition metals and metal clusters: through the variation of the properties of ionic liquids, it is possible to define different product's characteristics.

- *Solvent Extraction*

  Thanks to the modulable solubility and polarity of ILs, they are used in order to separate compounds with different chemical and physical compatibility, creating two different immiscible liquids.

  This mechanism is often exploited for the removal of toxic pollutants from water, in order to purify it and, for example, for fuel desulfurization.

- *Electrochemical applications*

  As ionic liquids are entirely based on ions, they have greater concentration of charge carriers than any other diluted salt.

  Nonetheless, their electrical conductivity is limited by their viscosity which may hinder the ion diffusion and influenced by temperature and the types of cations and anions [18]. This is the reason why ionic liquids may be applied in the electrochemical field: they are used as electrolytes for supercapacitors, batteries, fuel cells and dye-sensitized solar cells.

ILs are suitable for those applications because of their large electrochemical window and resistance to high temperatures, and they are more conductive and safer than electrolytic solutions based on water or organic solvents, which are commonly used in those contests.

Another field in which ionic liquids may be used as electrolytes is the electrodeposition of metals: they give the advantage of operating at lower temperature and with higher conductivity than the commonly used molten salts.

- *Gas adsorption/separation*

One of the most studied application of ILs are gas adsorption systems. There are different possible solutions involving ionic liquids, which are likely to capture industrial waste gasses such as CO_2, SO_2, H_2S, VOCs, separating them from natural atmosphere.

The mechanism through which this is possible could be defined as physical absorption (based on the physical interaction between ionic liquids and gas molecules, such as hydrogen bonds, Van der Waals interactions or electrostatic forces) or chemical absorption (ILs are often functionalized in order to improve even more their absorption ability, so chemical interactions occur mainly between the functional groups of the ions and the gas molecules involved in the process).

RTILs or TSILs may be used for this purpose, even though they present some limitations, such as the requirement of long time for their regeneration, their instability due to their liquid status, their need for supports and their cost.

Supported Ionic Liquid Membranes (SILMs) have been proposed in order to give RTILs a stable structure: they are made by a porous membrane, polymeric (PVDF, PTFE, PES) or silica-based, in which ionic liquids are impregnated and immobilized. However, they may become unstable at high temperature, because of a possible extraction of ILs from the pores.

Composite membranes based on polymers and ionic liquids have also been studied, which are made mainly by PVDF, PVDF-HFP, PVP. They are different materials compared to SILMs, because in this case a unique composite object is created, characterized by ILs dispersed in a polymeric matrix, not interacting with that. Ionic liquids provide the sorption capability of those composites, which present better stability and higher gas permeability than SLIMs: nevertheless, if the amount of ILs integrated in the material increases significantly, a phase separation may occur, generating isolated microcapsules of ILs.

Another type of membranes based on ionic liquids, created in order to enhance the gas sorption and at the same time providing better mechanical stability for the system, is given by ionic liquids with polymerizable functional groups. They are called “Polymerized Ionic Liquids” or “Poly(ionic liquids)”(PILs) and they are able to create a polymeric backbone creating a macromolecular structure with the same characteristics of classic ionic liquids.

Those membranes have been studies especially for their ability to absorb CO_2, with improved performances compared to the ones related to RTILs [19,20].

2.5 Polymerized Ionic Liquids or Poly(Ionic Liquid)s (PILs)

Polymerized Ionic Liquids (also called Poly(Ionic Liquid)s or PILs) are defined as materials deriving from the polymerization of ionic liquids, that provides the formation of a macromolecular architecture in which the polymeric backbone, characterized by cationic or (rarely) anionic moieties, interacts with specific counterions (Fig. 2.6).

In recent years, the interest on PILs has been growing considerably, as the graph in Fig. 2.7 clearly explains. This is due to the unique properties of those materials, that combines the tunable characteristics of ionic liquids with the ones typical of polymers.

As ionic liquids, even PILs may be constituted combining different types of polymerized cations or anions, thus determining their specific properties and, consequently, their applications.

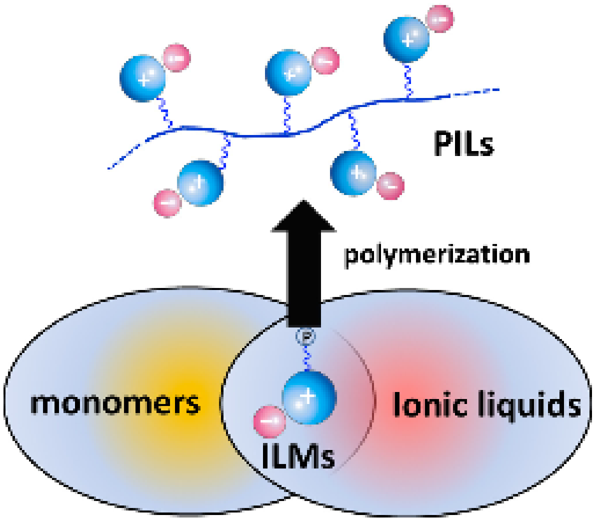

Figure 2.7. Poly Ionic Liquids [21]

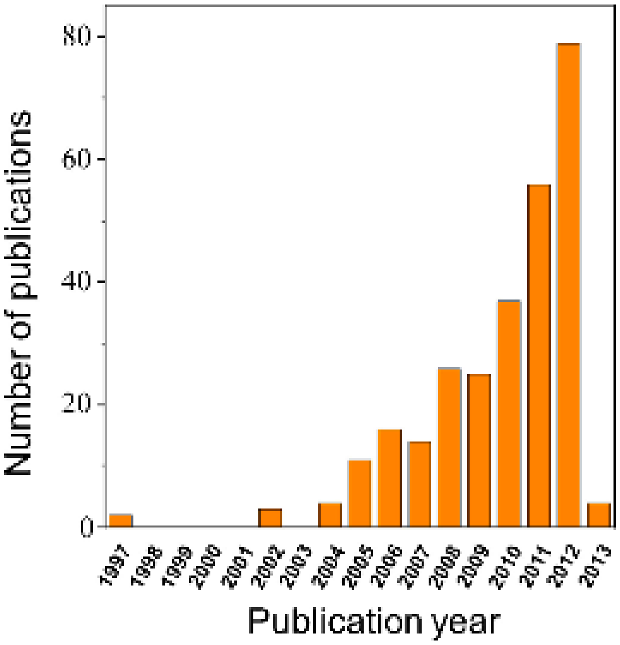

Figure 2.8. Number of pubblications from Web of Science searching for the topics "poly(ionic liquid)", "polymerized ionic liquid", "polymerizable ionic liquid", "ionic liquid monomer", "ionic liquid polymer" [21]

2.5.1 Classification and synthesis

In general, PILs could be classified not only according to the kind of ions they derive from, but also in terms of their chemical structure. The nature and the collocation of the ionic charges on the polymeric structure is crucial in order to distinguish different PILs, with variable characteristics and realized through various polymerization processes.

PILs' categories based on those criteria are (Fig. 2.8) [22, 23]:

- *Polycationic PILs*: the main polymeric backbone is characterized by positive-charged moieities, while anions are mobile and interact with them. The main types of cation included in the polymeric structure are imidazolium, pyridinium and pyrrolidonium; that are able to react between each other thanks to functional groups integrated on them, such as vinyl, styrenic, (meth)acrylic and (meth)acrylamide. The counterions are usually tetrafluoroborate, hexafluorophosphate, nitrate, bis(trifluoromethane)sulfonimide, etc.

- *Polyanionic PILs*: they are rarer than polycationic PILs. They are characterized by negative-charged moieties in their polymeric backbone, given, for example, by sulphonate, carboxylate, phosphoric, amide ions. The counterions may be alkyl-imidazolium or tetraalkylammonium.

- *Zwitterionic PILs*: those materials are based on polymers with both cationic and anionic charges located on the polymer backbone. They usually derive from the polymerization of molten salts instead of classical monomers.

- *Copolymeric PILs*: they may be random or block copolymers, obtained by the polymerization of different ionic or even neutral monomers. They may be realized in order to reduce the number of charged areas on the polymeric backbone (Fig. 2.8a), so that the properties related to the concentration of charges in the structure could be tunable; to obtain opposite charges located in the same polymer chain (Fig. 2.8b) or even to built the polymeric structure through different cationic monomers (Fig. 2.8c), which are able to interact with variable counterions.

- *Polymer blends*: they are obtained by the interaction of polyanionic chains with polycationic ones, without having mobile counterions surrounding them.

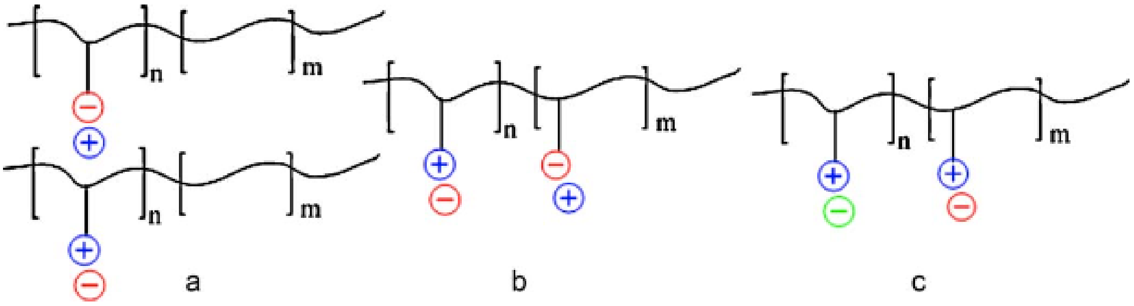

Figure 2.9. PILs copolymers [22]

The majority of PILs are obtained through direct free radical polymerization of ionic monomers, though other more specific reactions have been also considered, such as step growth polymerization, polycondensation, Atom Transfer Polymerization (ATRP) and Reversible Addition-Fragmentation Transfer Polymerization (RAFT).

Though direct free radical polymerization is the more common way to form PILs, it is sensitive to the presence of impurities in the reactants, which are difficult to be purified. The main monomers involved in this type of reactions are (meth)acryloyl-, N-vinylimidazolium- or styrene-based ones.

The ionic monomers may be characterized by a single reactive site or more than one functional group: this defines them as, respectively, mono-functional, bi-functional, multi-functional ionic monomers. The multiple number of reactive groups could be exploited by cross-linking processes obtained by radical polymerization, which provide the creation of an interconnected polymeric network. In those cases, the process could be carried out by UV-VIS photocuring or thermal curing, thanks to the addition of an initiator, activated by heat or light absorption [22, 23, 24].

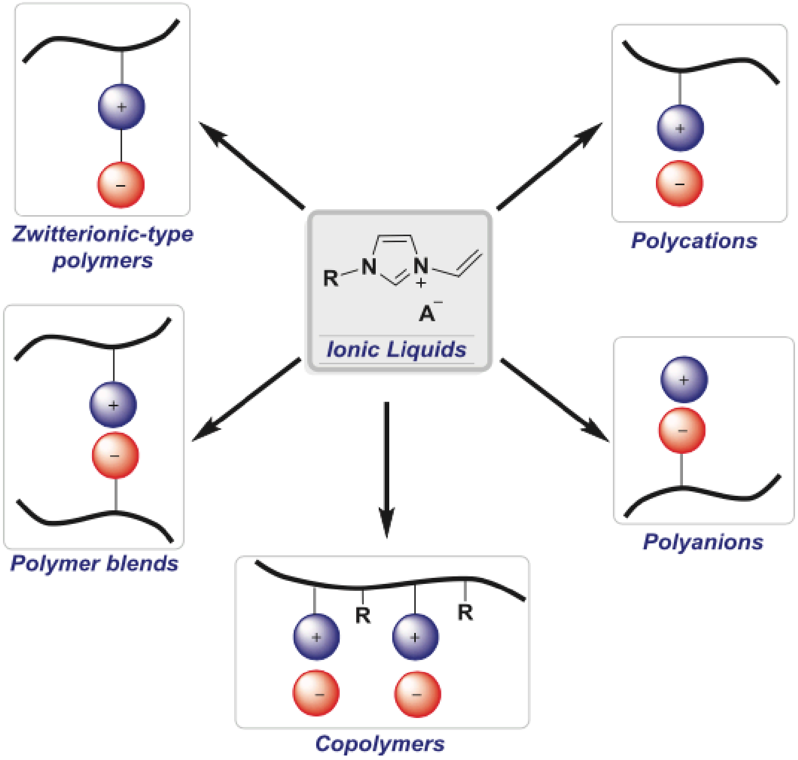

Figure 2.10. Different structures of PILs [23]

2.5.2 Properties and Applications of PILs

The characterization of Poly(Ionic Liquid)s has not been investigated deeply by scientists, because of their greater interest in the applications in which PILs may be used. Therefore, the information regarding the specific properties of those materials are way more general than the ones explained previously for RTILs. In many cases, in fact, the peculiarities of PILs may be derived from the studies of the specific applications in which they are involved.

In general, the properties of ILs described previously (may be associated with the ones concerning PILs, though they may present variations in terms of their effectiveness or their tunability, considering the physical differences between the two ionic liquids' categories.

In fact, it is possible to describe PILs, differently from Ionic Liquids, as amorphous solid materials with very low glass transition temperatures, included in wide ranges around -60°C. Their T_g depends most of all on the type of the anion interacting with the polymeric backbone [21, 22] and defines their tendency of having a plastic behavior at room temperature. This means that they are characterized by mechanical properties similar to the ones of generic polymers: this is the reason why they can be formed with well-known polymers production methods (extrusion, spin coating, film production, electrospinning), in order to create variable and stable shapes [21].

The application fields in which PILs have been analyzed are numerous and very different from each other: this is due to the versatility of those materials, given by their specific and tunable properties.

For instance, PILs have been studied for those main application areas [21, 22, 23, 24]:

- Ionic conductors in electrochemical devices
- Gas separation ad adsorption membranes
- Catalysts or catalyst supports
- Carbon precursors
- Dispersants

Considering the aim of this work, only the two former realms will be deepened, explaining the material's properties that are connected to each different use of PILs. Moreover, those two fields of PILs' application are also the most studied in literature, thus the most significative.

2.5.2.1 PILs as Ionic Conductors

As ionic liquids, PILs are ionic conductors, thanks to the presence of mobile ions in their structure. Nevertheless, the main difference between the two of them is related to the effectiveness of this property: in fact, the ion-conductivity of PILs is lower than the one of ILs monomers, due to the lower ion diffusivity caused by the covalent bonding of polymerized ions, which reduces the overall quantity of mobile charges.

The conductivity of PILs is strongly influenced by the polymeric structure and the type of ionic monomers from which they derive from: the choice of cations, anions, the characteristics of polymerizable functional groups that are present on the monomers are important to define the structural parameters affecting that specific PIL's electric behavior.

The ionic conductivity, more specifically, may depend on the glass transition temperature of PILs, as ion mobility is enhanced by the flexibility of polymeric chains. Also the size of ions is important in order to define their transport efficiency (the smaller the ions, the easier their movement into the polymeric structure); temperature also enhances ion mobility.

Imidazolium-based cations are generally the ones that present higher ionic conductivities while bis(trifluoromethyl sulfonyl)imide is the most conductive anion.

The advantage of using PILs for electrochemical applications is related to their easy processability, allowing the production of thin films, membranes, fibers, coatings or even complete circuits, with desired size and shape. Furthermore, they are safer as they are nonflammable.

The devices containing PILs that has been studied are very different from each other: lithium batteries [25], fuel cells [26], dye sensitized solar cells [27], actuator [28], sensors [29], etc. The interest for this application field is still developing and growing more and more [21-23].

2.5.2.2 PILs for Gas Separation and Sorption

The field for which PILs have been studied the most in literature is related to the gas sorption and separation. In particular, there has been a lot of interest in their efficiency in capturing CO_2.

It has been proved that PILs provide higher CO_2 absorption capacities compared to the ones of RTILs, and the gas thermal desorption is faster and completely achievable.

While for RTILs the anion is more decisive for determining CO_2 sorption ability, PILs' behavior in this application is influenced mostly by the nature of the cationic monomers and by the backbone structure deriving from their polymerization. Specifically, ammonium-based PILs present the best CO_2 sorption ability, while imidazolium-based ones are the worst cations for this purpose. As for anions, the ones giving better absorption capacity to PILs are BF_4 and PF_6.

Even though PILs' membranes are characterized by lower CO_2 permeability than the one of SLIMs (polymeric membranes impregnated with RTILs), they completely avoid the ILs' "blow-out" problem, connected to the presence of those liquid salts in the membrane pores, which may be extracted from them at transmembrane pressure differences of 1-2 atm and at higher temperature conditions.

Another interesting property of those PILs-based membranes is their permeation selectivity: they have been studied in order to verify their ability to separate CO_2 from typical waste gas mixtures like CH_4, N_2, H_2. The gas selectivity derives from its permeability, diffusivity and solubility in the considered material: those are properties that depend on the chemical nature of PILs, in particular of their cationic polymeric structure. The relationship between the chemical structure of PILs and their gas selectivity and permeability are not completely understood, and it is still a topic that many research groups are studying.

In order to enhance the absorption capacity of PILs, also porous membranes have been prepared, exploiting the higher specific surface area of them to capture a greater quantity of gas, thanks to the maximized number of moieties where physical interaction with gasses may occur.

The adsorption ability of PILs has been studied mostly for CO_2, while other gaseous substances such as Volatile Organic Compounds have been scarcely analyzed. In fact, the ability to absorb VOCs has been investigated mostly for RTILs, supported by porous membranes [21-24; 30-33].

2.5.2.3 3D Printing of PILs

3D Printing techniques are based on the photopolymerization of polymeric formulations. The realization of solid materials based on Poly (Ionic Liquid)s thanks to this method is possible, considering ionic liquid monomers with unsaturated functional groups.

In order to do so, the control of the rheological properties and the homogeneity of the formulations containing ILs must be carefully done. The ionic liquid monomers that are commonly used with this purpose are the ones with vinyl and (meth)acrylate functional groups, whose reactivity in photopolymerization is excellent. These one characterizes the cation structure (so that polycationic structure will result after the polymerization), while the anions may be variable. Furthermore, the use of multifunctional ionic liquid monomers permits the formation of a highly cross-linked and interconnected macromolecular structure.

Sometimes these ions could be copolymerized in presence of another type of monomers, such as PEGDA or DVB, to give higher mechanical stability and durability to the polymeric material. One of the possible applications deriving from the photopolymerization of ILs is the production of membranes, which present ionic conductivity and polarity, making them useful respectively for the realization of electrochemical devices or for the separation and absorption of gasses [34].

Schultz *et al.*, in 2014 published their results regarding the 3D Printing of phosphonium ILs thanks to Mask Projection Microstereolitography: they were the first to demonstrate that the formation of the PILs network is possible and successful via Additive Manufacturing techniques. In this case, diacrylate comonomers were added in the initial formulation, as comonomers. The ionic conductivity, the glass transition temperature and the thermal stability were investigated: they proved that these solid materials may be suitable as electroactive membranes for different purposes [35].

Indeed, this process has been considered a lot recently, for the realization of PILs-based materials applied in different realms:

- *Electronic devices, Soft Robotics, Energy Storage*: 3D Printed PILs have been studied a lot to produce electromechanical sensors and actuators, exploiting their ionic conductivity and their mechanical stability. For instance, piezoresistive tactile sensors were realized with 3D Printed 1-ethyl-3-methyl-imidazolium tetrafluoroborate [23, 36]; and soft somatosensitive actuators based on the 3D Printing of an ionogel containing ionic liquids (1-ethyl-3-methylimidazolium ethyl sulfate) and silica particles were realized [37].
  Recently PILs were used also as stabilizers in inks based on graphene, whose deposition through Additive Manufacturing methods permits to create 3D Printed graphene aerogels, useful in different applications as batteries and supercapacitors [38].
  The effect of imidazolium-based PILs was positive on the electrical conductivity of these materials, as their presence inhibited the graphene agglomeration.

- *Biomedical applications*: ionic liquids' tunable properties make them suitable for drug delivery applications as they are biocompatible, non-cytotoxic and they are able to solubilize efficiently many substances and biopolymers like cellulose [39]. They are also used as solvents in bioprinting (material jetting) to obtain biomedical products, such as antibacterial PILs' membranes or scaffolds for cellular growth.
  As an example, Zhang M. *et al.* realized biological scaffold based on 3D Printed ink based on PILs, gelatin and sodium alginate: it has been demonstrated that different PILs may influence the physicochemical properties of the scaffolds, and thus varting the cells' growth efficiency [40].

- *Gas Absorption:* as reported in 2.5.2.2, PILs are suitable for the selective absorption of pollutant gasses, such as CO_2, 3D Printed PILs have been studied considering their absorption capacities: for instance, Gillono M. *et al.* demonstrated that complex-shaped objects made with different PILs are obtainable by DLP-3D Printing: the PILs based on imidazolium and tetrafluoroborate with bis(trifluoromethylsulfonyl)imide did not inhibit the photopolymerization process. These materials turned out to be efficient in the absorption of CO_2, that may be enhanced by the design of their structures [41].

2.6 References

[1] Tiwana M.; 2020; Future Technology for Metal Extraction from Waste: II. Ionic Liquids in “Sustainable Metal Extraction from Waste Streams”; Chauhan G., Kaur P.J., Pant K.K., Nigam K.D.P. Eds.; Chapter 7; Wiley-VCH; Weinheim (Germany).

[2] Marcinkowski L. *et al.*; 2019; Nanoconfined Ionic Liquids, Properties and Analytical Applications in “Handbook of Smart Materials is Analytical Chemistry, Volume I”; de la Guardia M. Ed.; Chapter 2; Wiley.

[3] Morton S.A., Morton L.A.; 2010; Ionic Liquids for the Utilization of Lignocellulosics in “Thermochemical Conversion of Biomass to Liquid Fuels and Chemicals”; Crocker M. Es.; Chapter 12; RSC Publishing; Cambridge.

[4] https://www-scopus-com.ezproxy.biblio.polito.it/search/form.uri?display=basic#basic

[5] Kohli R.; 2013; Removal of Surface Contaminants Using Ionic Liquids in “Developments in Surface Contamination and Cleaning, Volume 6”; Kohli R., Mittal K.L. Eds.; Chapter 1; Elsevier; USA.

[6] Noorhisham N. A., Amri D., Mohamed A. H., Yahaya N., Ahmad N. M., Mohamad S., Kamaruzaman S., Osman H.; 2021; Characterisation techniques for analysis of imidazolium-based ionic liquids and application in polymer preparation: A review; Journal of Molecular Liquids, 326, 115340.

[7] Walden P.; Molecular weights and electrical conductivity of several fused salts; Bull. Acad. Imp. Sci. St Petersbg 8 (1914) 405-422.

[8] Vekariya R.L.; 2017; A review of ionic liquids: Applications towards catalytic organic transformations; Journal of Molecular Liquids; 227, 44-60.

[9] Wilkes J.S. *et al.;* 1982; Dialkylimidazolium chloroaluminate melts: a new class of room-temperature ionic liquids for electrochemistry, spectroscopy and synthesis; Inorg. Chem. 21(3) 1263-1264.

[10] Wilkes J.S. *et al.* ; 1992; Air and water stable 1-ethyl-3-methylimidazolium based ionic liquids; Journal of Chemical Society; 965-967.

[11] Davis H., James Jr.; 2004; Task-Specific Ionic Liquids; Chemistry Letters, 33 (9); 1072-1077.

[12] Armand M. *et al.*; 2009; Ionic-liquid materials for the electrochemical challenges of the future; Nature Materials; DOI: 10.1038/NMAT2448

[13] Aparicio S. *et al.;* 2010; Thermophysical Properties of Pure Ionic Liquids: Review of Present Situation; Ind. Eng. Chem. Res.; 49, 9580-9595.

[14] Chiappe C. *et al.;* 2009; Ionic Liquids: Solvation ability and polarity; Pure Appl. Chem.; 81(4), 767-776.

[15] Guan W. *et al.*, 2017; Determination and Prediction for the Polarity of Ionic Liquids; Journal of Chemical and Engineering Data; 62, 2610-2616.

[16] Ozokwelu D., Zhang S., Cheng W., Litombe N.; 2017; Properties of Ionic Liquids in "Novel Catalytic and Separation Processes Based on Ionic Liquids"; Chapter 3; Elsevier.

[17] Prado R., Weber C.C.; 2016; Applications of Ionic Liquids in "Application, Purification and Recovery of Ionic Liquids"; Kuzmina O., Hallett J.P. Eds.; Chapter 1; Elsevier.

[18] Nancarrow P. *et al.;* 2021; Comprehensive analysis and correlation of ionic liquid conductivity data for energy applications; Energy; 220, 119761.

[19] Rashid T.U.; 2021; Ionic liquids: Innovative fluids for sustainable gas separation from industrial waste stream; Journal of Molecular Liquids; 321, 114916.

[20] Do-Thanh C.L. *et al.*; 2020; Ionic Liquid-Based Membranes in "Materials for Carbon Capture"; Jiang D., Mahurin S.M., Dai S. Eds.; Wiley.

[21] Yuan J. *et al.;* 2013; Poly(ionic liquid)s: An update; Progress in Polymer Science; 38, 1009-1036.

[22] Mecerreyes D.; 2011; Polymeric ionic liquids: Broadening the properties and applications of polyelectrolytes; Progress in Polymer Science; 36, 1629-1648.

[23] Nulwala H. *et al.*; 2018; Ionic liquids and poly(ionic liquid)s for 3D printing – A focused mini-review; European Polymer Journal; 108, 390-398.

[24] Yuan J., Antonietti M.; 2011; Poly(ionic liquid)s: Polymers expanding classical property profiles; Polymer; 52, 1469-1482.

[25] Mecerreyes D. *et al.*; 2020; Innovative Polymers for Next-Generation Batteries; Macromolecular Chemistry and Physics; 221, 1900490.

[26] Liu F. *et al*.; 2021; Multifunctional poly(ionic liquid)s cross-linked polybenzimidazole membrane with excellent long-term stability for high temperature-proton exchange membranes fuel cells; Journal of Power Sources; 494, 229732.

[27] Thomas M., Rajiv S.; 2020; Porous membrane of polyindole and polymeric ionic liquid incorporated PMMA for efficient quasi-solid state dye sensitized solcar cell; Journal of Photochemistry and Photobiology A: Chemistry; 394, 112464.

[28] Tudor A. *et al.*; 2017; Poly(ionic liquid) thermo-responsive hydrogel microfluidic actuators; Sensors and Actuators B: Chemical; 247, 749-755.

[29] Jing M. *et al.*; 2019; Construction of multifunctional electrochemical sensor based on electroactivity-adjustable poly(ionic liquids)/reduced graphene oxide; 197, 277-283.

[30] Zhou X. *et al.;* 2019; Poly(ionic liquid)s: Platform for CO_2 capture and catalysis; Current Opinion in Green and Sustainable Chemistry; 16: 39-46.

[31] Tomè L.C. *et al.*; 2015; Polymeric ionic liquid-based membranes: Influence of polycation variation on gas transport and CO_2 selectivity properties; Journal of Membrane Science; 486, 40-48.

[32] Indra S. *et al.;* 2021; Interaction of volatile organic compounds acetone and toluene with room temperature ionic liquid at bulk and the liquid-vacuum interface; Journal of Molecular Liquids; 331, 115608.

[33] Yan X., et al.; 2021; Toluene removal from gas streams by an ionic liquid membrane: experiment and modeling; Chemical Eng. Journal; 404, 127109.

[34] Guterman R., Smith C. A.; 2019; Photopolymerization of Ionic Liquids – A Mutually Beneficial Approach for Materials Fabrication; Isr. J. Chem.; 59, 803-812.

[35] Schultz A. R. *et al*.; 2014; 3D Printing Phosphonium Ionic Liquid Networks with Mask Projection Microstereolitography; ACS Macro Letters; 3, 1205-1209.

[36] Lee J. *et al.*; 2017; Effect of degree of crosslinking and polymerization of 3D printable polymer/ionic liquid composites on performance of stretchable piezoresistive sensors; Smart Mater. Struct.; 26, 35043.

[37] Truby R.L. *et al.* ; 2018; Soft Somatosensitive Actuators via Embedded 3D Printing; Advanced Materials; 30, 1706383.

[38] Tran T.S.; 2020; Poly(ionic liquid)-Stabilized Graphene Nanoinks for Scalable 3D Printing of Graphene Aerogels; ACS Applied Nano Materials; 3, 11608-11619.

[39] Markstedt K. *et al*.; 2014; 3D Bioprinting of Cellulose Structures from an Ionic Liquid; 3D Printing and Additive Manufacturing, 1(3).

[40] Zhang M. *et al.*; 2021; 3D Printing for Biological Scaffolds using Poly(Ionic Liquid)/Gelatin/Sodium Alginate Ink; Macromolecular Materials and Engineering; 2100084.

[41] Gillono M. *et al.*; 2019; Study on the Printability through Digital Light Processing Technique of Ionic Liquids for CO_2 Capture; Polymers; 11, 1932.

Chapter 3: Photopolymerization and 3D Printing

3.1 Photopolymerization

Photopolymerization (also called radiation curing, or photocuring) is a process that provides the formation of a solid polymeric material through the polymerization of a liquid formulation, activated by light adsorption (Fig.3.1). In this way, thanks to many consecutive reactions occurring after the adsorption of photons with specific energy, a network of interconnected polymers may be created, and even cross-linked structures may be obtained. [1]

The typical formulation that can be photopolymerized presents [2]:

- *A Photoinitiator*: a chemical species which is sensitive to UV-VIS irradiation. In fact, it absorbs light with a specific energy, in order to initiate the polymerization by activating the reactions between monomers;

- *A diluent*: which regulates the rheology and the viscosity of the formulation, and in some e cases it is capable of participating to the reaction;

- *A monomer*: generally speaking, it is characterized by more than one functional group that takes part in the polymerization. The chemical properties of these functional groups are decisive to define the proper polymerization mechanism occurring and the physical properties of the polymeric material deriving from this process.

- *Additives*: they are useful to control the properties of the final polymeric material. They may be pigments, stabilizers, wetting agents, etc.

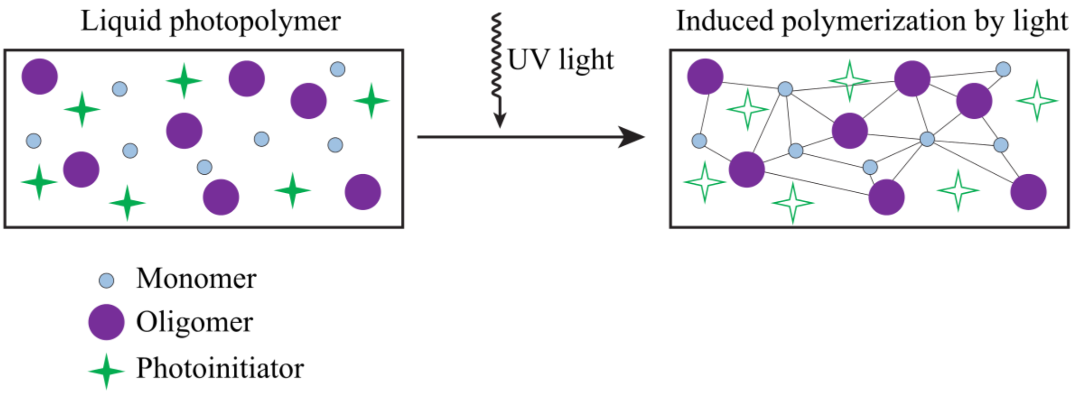

Figure 3.11. Photopolymerization [3]

3.1.1 Reaction Mechanisms

Photopolymerization starts from the decomposition of the photoinitiator, which is achieved through the absorption of UV-VIS light by this molecule.

According to the type of chemical spices obtained by the activation of the photoinitiator, it is possible to define two different polymerization processes [4]:

- *Free Radical Photopolymerization*: in which the activation process consists of the decomposition of the photoinitiator in two radicals, that will be added to the double bonds (typical of reactive groups such as vinyls, acrylates, etc.) present on the monomers, in order to generate different reactive radicals. This chain process is based on polyaddition mechanism, and involves the continuous creation of radical spices, which may be combined between each other.

- *Ionic Photopolymerization:* which is activated by the transformation of the photoinitiator in a strong Lewis acid or a Brønsted one. It is a process that requires the use of photoinitiators that are different from the ones chosen for the radical polymerization. Generally speaking, this mechanism is mostly defined as cationic photopolymerization, and it is less common than the one explained previously.

Considering that Free Radical Photopolymerization is more common than the other one and it is, in particular, the polymerization process that may explain the reaction occurring between ionic liquid monomers to obtain PILs, it will be discussed more deeply in the following paragraphs.

3.1.1.1 Free Radical Photopolymerization

This polymerization mechanism is applicable especially for those monomers characterized by groups with unsaturated bonds: in this category the acrylates (and methacrylates) are the most common ones (Fig. 3.2). In fact, the presence of a vinyl group in the molecule makes it suitable for its rapid radicalization, and consequently for the polymerization process.

When the considered monomers are multifunctional, the reactive spots in the molecules are not singular, and the polymerized structure will be a thermoset polymer that means a stable and cross-linked network [5]. When monofunctional monomers are reacted, only a linear chain can be obtained with the formation of the thermoplastic polymer.

The most common radical photocurable monomers are acrylates, unsaturated polyester resins, thiol-ene systems [2].

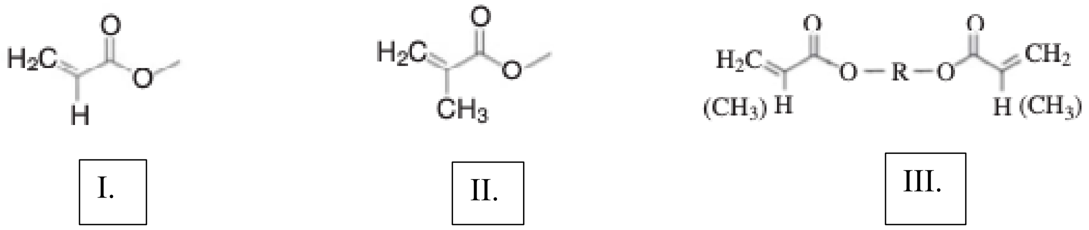

Figure 3.12. I) Acrylate functionality II) Methacrylate functionality III) Multifunctional (meth)acrylate; R= polyester, polyether, polyurethane, bisphenol A,…[5]

Free Radical Polymerization is a polyaddition that requires the following steps in order to be completed [5]:

- *Initiation*: the photoinitiator absorbs the light, characterized by a specific energy, thus generating primary radicals. This process is defined kinetically by the constant k_d.
  Lastly, these radicals are added to monomers, forming new radical spices which can actively take part to the polymerization. The rate determining step of this phase is the radical formation (with the rate constant k_d), which is the slowest process.

$$In \ \rightarrow^{kd} In \cdot$$
$$In\cdot \ +M \ \rightarrow^{ki} M\cdot$$

$$k_d < k_i$$

- *Propagation:* it is the decisive step to build up the entire polymeric structure. It is based on the addition of the radical monomer to the other monomers, so that a gradual growth of the polymeric chain is achieved. This main reaction may be hindered by side reactions, such as *chain transfer*: the radical does not react with other monomers, but with another small molecule. This may cause the premature termination of the polymerization and the formation of another simple radical.
  The rate of propagation can be defined as dependent on the concentration of monomers and of the radical spices, which are connected to this parameter through the constant k_p.

$$M_n\cdot + M \ \rightarrow^{kp} \ M_{n+1}\cdot$$
$$M_{n+1}\cdot \ + M \ \rightarrow^{kp} \ M_{n+2}\cdot$$
$$\ldots$$

Chain transfer: $M_n\cdot \ + RH \ \rightarrow^{ktr} \ M_nH + R\cdot$

- *Termination:* in this step the growth of the polymeric chain is definitively stopped by different possible reactions. For instance, it is possible to have *bimolecular termination (1)*, which provides the reaction between two macroradicals so that a final polymer is achieved from the combination of the two of them. If the reaction occurs between two primary radicals, such as the ones deriving from the decomposed photoinitiator, the final dead polymer appears differently (2). The radicals may also be trapped in the polymeric structure without having the capability of reacting anymore. This is called *monomolecular termination* (3) and it can be resolved by increasing the temperature of the system, enhancing the mobility of the radicals and improving their reactivity.

$$1)\ M_n \cdot + M_m \ \cdot \rightarrow^{kt} \ M_{n+m}$$

$$2)\ M_n \cdot + In \cdot \rightarrow^{kt} \ M_n$$

$$3)\ M_n \cdot \rightarrow^{kt} \ (M_n)_{trapped}$$

This process may also cause the formation of a cross-linked structure if multifunctional monomers are used. The reaction occurs for every functional group in the macromolecules, so that not only the growth of the polymeric chains could be achieved, but also the formation of an interconnected network is possible thanks to the presence of pendant double bonds reacting between each other and, lastly, the formation of loops caused by the reaction between these pendant double bonds and the radical spot on the same polymeric chain (Fig.3.3).

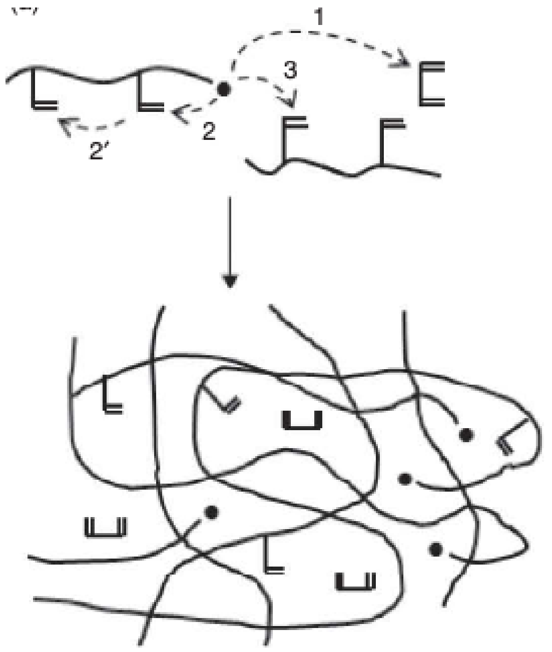

Figure 3.13. Cross-linking process: 1) chain growth; 2,2') loop formation 3) cross-linking: reaction between pendant double bonds [5]

3.1.2 Radical Photoinitiators

Photoinitiators are useful to provide the activation of the polymerization process: they are able to absorb light with specific wavelength, so that radical reactive spices are formed.

Every radical photoinitiator, in fact, must have the following properties [6]:

- High absorptivity in the region of activation (UV-VIS);
- High quantum yield, which is the ratio between the amount of radicals formed through the decomposition of the photoinitiator induced by light absorption and the number of photons absorbed by it in order to achieve this purpose [7];
- Non-toxic, non-yellowing;
- Cheap, chemically stable,and easily processed.

Radical photoinitiators may be divided in two different categories, according to the kind of reaction occurring to decompose these molecules, generating the reactive spices. These categories are:

- α –cleavage (Type I) photoinitiators
- H-abstraction (Type II) photoinitiators

3.1.2.1 *α-cleavage (Type I) photoinitiators*

Type I photoinitiators are able to provide the formation of two free radicals in the α position, by undergoing a direct photofragmentation after the absorption of light with a specific wavelength.

The majority of these photoinitiators are aromatic carbonyl compounds, different from each other thanks to variable functional groups; for instance, they may be benzil ketals, acetophenones, aminoalkyl phenones, phosphine oxides, etc.

The radicals formed by α –cleavage are mainly benzoyl and benzyl radicals, which are able to initiate polymerization.

An example of this process is reported in Fig. 3.5, where the photolytic cleavage of benzoin is reported.

These photoinitiators generally activate the free radical polymerization of vinyl groups and acrylate double bonds [8].

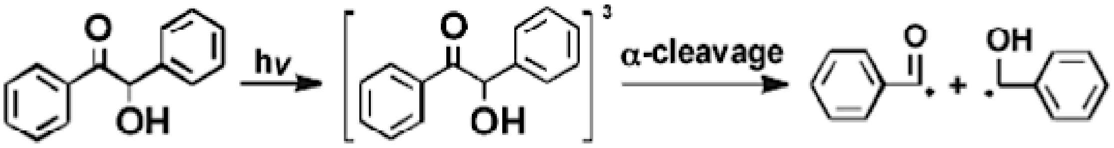

Figure 3.14. a-cleavage of benzoin photoinitiator [8]

3.1.2.2 *H-abstraction (Type II) photoinitiators*

Type II photoinitiators' functionality is based on the extraction of a hydrogen atom from molecules constituting the resin or the solvent surrounding them. This hydrogen atom provides the decomposition of the double bond, for example, in a carbonyl group that has acquired this atom from the hydrogen donor.

This process causes the formation of two radicals: the one deriving from the H donor (that lost its hydrogen atom), and the one given by the modification of the bonds in the carbonyl group of the photoinitiator. This mechanism is obviously activated by the absorption of UV-VIS light, depending on the specific kind of molecule than has been considered.

The most common Type II photoinitiators are the ones based on benzophenone (Fig. 3.6): they are characterized by low cost, high efficiency, high quantum yield, but they may cause yellowing and migration of these products from the polymerized material [9].

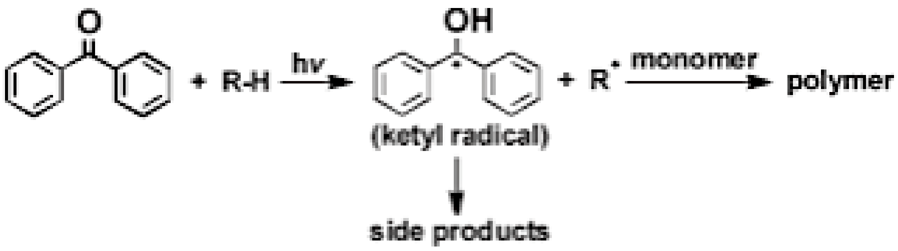

Figure 3.15. Type II photoinitiators'mechanism: benzophenone and H-donor [8]

3.1.3 Advantages and Disadvantages of Photopolymerization

The main advantage of choosing a photopolymerizable system is connected to the rapidity of this type of polymerization and the low temperatures required in order to activate it. In fact, the majority of these processes could be achieved at room temperature, without influencing the mechanical stability of the materials during their own formation, and with high productivities.

There are also ecological advantages such as the lower organic solvent consumption (and VOCs' emission) and the possibility of recycling the products. Furthermore, the process requires low space and capital investments, though the development of a curing equipment is compulsory.

The polymeric materials obtained by photopolymerization are durable, tough, and resistant to abrasion, stain and chemical substances. The variety of polymeric materials obtainable with this process makes it very versatile and easily reproducible.

The possible drawbacks may be connected to the necessity of carefully controlling the composition of the initial formulations, in order to achieve the perfect viscosity (which may hinder the mobility of the molecules, thus lowering the polymerization rate and efficiency), and to obtain the perfect combination of photoinitiator, monomers and additives, according to the dimensions and the thickness of the final product. Moreover, the presence of fillers or pigments may influence the behavior of the formulation during the polymerization [1,2].

Two common phenomena may occur, hindering the efficiency of photopolymerization: the so called "Oxygen Inhibition" and shrinkage, which are explained in the following paragraphs.

3.1.3.1 Oxygen Inhibition

Oxygen Inhibition affects free radical polymerization in most cases, especially when the process is extended on an industrial scale.

This issue is connected to two processes occurring with the presence of atmospheric oxygen during the photopolymerization: the first one is called *quenching*, the latter is *scavenging*.

As represented in Fig. 3.7, quenching reaction makes the photoinitiator unexcited, because the oxygen molecule steals its reactive state. The O_2 radical is way less reactive than the photoinitiator's one, so the polymerization's efficiency is threatened.

Scavenging reactions, on the other hand, provides the formation of peroxides' radicals through the interaction between O_2 and the propagating radicals, thus slowing down and hindering the entire chain process [10].

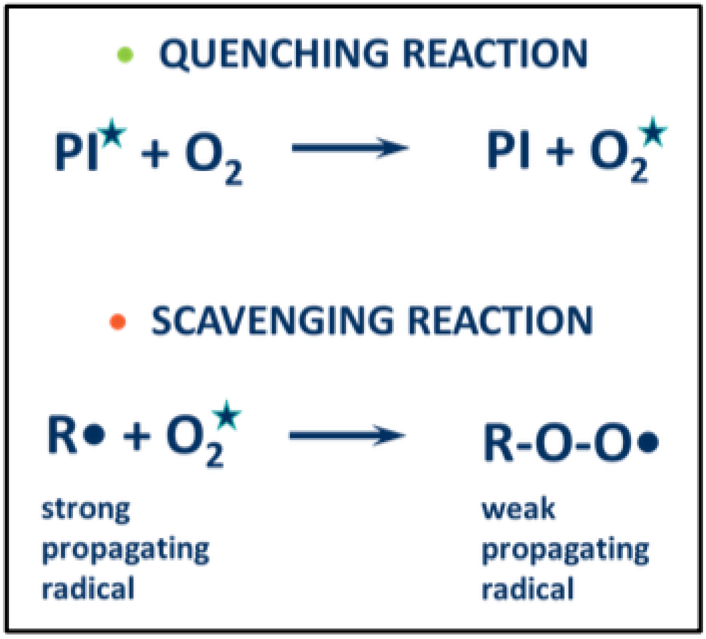

Figure 3.16. Oxygen inhibition precesses [10]

In order to minimize this problem, the main solutions that have been adopted are the following ones:

- The use of inert atmospheres (N_2, for instance), so that the presence of atmospheric oxygen is avoided during the photopolymerization. This is an effective solution, but it is expensive, especially for industrial processes. Other less expensive solutions may be the use of waxes to isolate the polymers from the outer atmosphere, even though they may prejudice the final quality of the product;

- The increase of photoinitiator's concentration, so that the impact of the oxygen inhibition on the entire system is compensated by the greater quantity of initiating radicals: in this way, the polymerization rate does not become too low. This could provide the increase of the amount of undesired residual products from polymerization;

- The increase in the intensity of UV-VIS light impacting on the material to activate the polymerization;

- The use of chemicals such as thiols, amines, ethers which are reactive with oxygen and they are able to eliminate it from the atmosphere (as reported in Fig. 3.8 for amines) surrounding the polymerizing formulation. They may cause problems like strong odor, yellowing and moisture sensitivity of the final product.

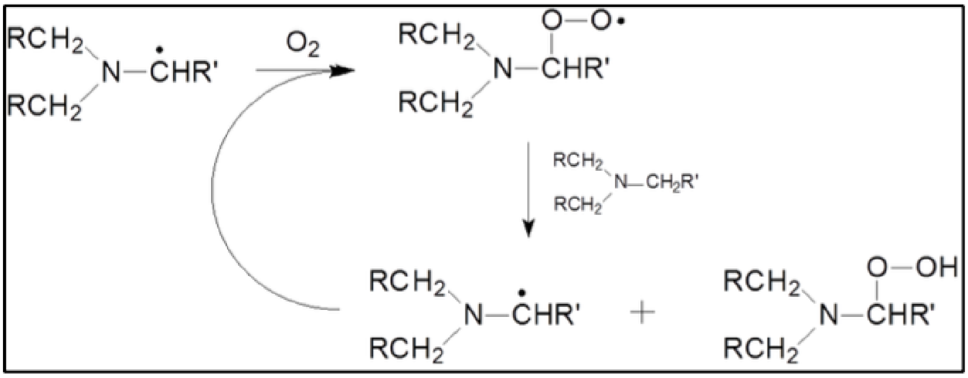

Figure 3.17. Reaction of Amines with O_2 [10]

3.1.3.2 Shrinkage

Considering that the polymerization involves the decomposition of double bonds (in acrylates or methacrylates groups, for example), which are substituted with single bonds between the atoms, also the distance between these atoms changes after the process is completed. In fact, the covalent bonds resulting from the polymerization define a shorter distance between the atoms involved in the reaction: this causes the reduction of the total volume of the final product, which is defined as *shrinkage*.

Different shrinkages may occur, depending on the type of monomers that take part to the polymerization and on the degree of conversion of this process: for instance, methacrylates are characterized by lower shrinkage than acrylates, because of their lower reactivity and degree of conversion [5].

3.2 3D Printing

The term "*3D Printing*" refers to different manufacturing processes that provide the realization of an object through the formation of consecutive layers, thus it is also called "*layer-based technology*".

The process is automated, and it is part of the general realm of Additive Manufacturing techniques: it is applied in many application fields, such as automotive, biomedical, aerospace industries; where the production of small lots of complex or customizable components is required. In fact, even though the geometrical precision provided by these techniques is excellent, their productivity rates are slow, making them expensive.

Additive Manufacturing techniques are named *direct processes*, as they provide the formation of an object without requiring any physical prototype or mold, but by building it up layer by layer starting from a CAD file, thanks to which the product is designed. The opposite of this definition is the one concerning *indirect processes*, that don't involve the deposition of consecutive layers to realize the entire object, but they are basically copy works, where prototypes (usually obtained by AM's processes) are used to generate a mold that guarantees the production of the final products [11].

Every direct process starts with the definition of the part to be produced in a CAD file, given by specific software or imaging processes (such as computerized tomography).

The digital model is then elaborated by the software so that it is divided into layers (Fig. 3.9), with specific thickness (in the order of 25-100 μm) and characterized by a geometry which correspond to different cross-sections of the object. In general, these layers extend in the x-y plane, and they are positioned one on another along the z-axis.

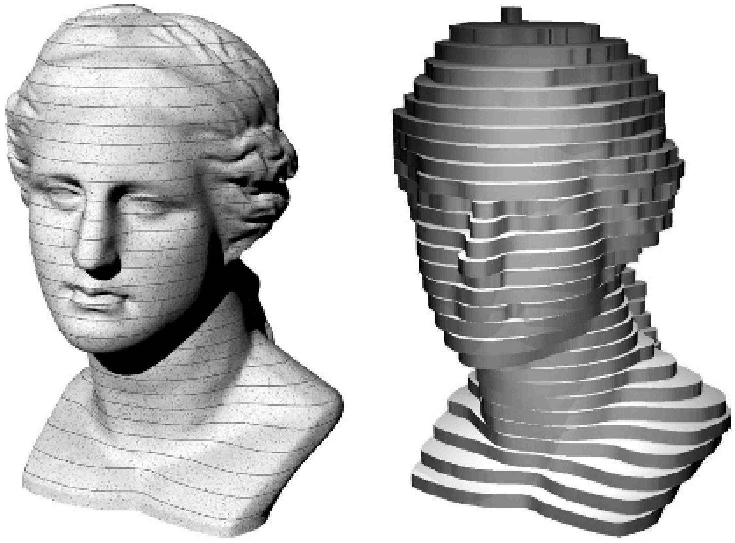

Figure 3.18. Slicing of CAD model: layers are characterized with equal thickness but different geometry [12,13]

After this initial step, the AM Process starts effectively, and single layers are gradually generated one after another and then, they are connected between each other to form a continuous object.

AM may be used to obtain pieces of different kind of materials, such as metals, ceramics and polymers. In this work, only the latter category will be considered [12].

There are different types of techniques that provide the formation of a polymeric final product through a layer-by-layer process: some of them are based on photopolymerization and these are the only ones that will be considered in this work. In particular, the main ones are:

- Stereolithography (SLA)

- Digital Light Processing (DLP)

3.2.1 Stereolithography (SLA)

Stereolithography was invented by the founder of 3D Systems, Charles Hull, in 1986.

This technique exploits the photopolymerization of a liquid formulation, activated by the irradiation of a laser beam on it.

In fact, the SLA system is typically made of a build volume, defined by a reservoir into which the liquid formulation resides, a building platform that is placed into this tank. Its position on the z-axis is controlled by a stepper motor that permits its translation during the process.

The polymerization is initiated by a laser beam (with a wavelength in the UV range) that is positioned on the top of the build volume: it is able to move in x-y directions so that the punctual absorption of its light by the liquid makes it possible to polymerize it, thus generating the shape of the solid layers constituting the desired object. A laser scanner determines the orientation and the movement of the laser beam, according to the desired shape of the layer to be polymerized.

When a layer is completely formed on the building platform, it translates downwards into the formulation so that another layer may be deposited on the previous one, repeating the same process (Fig. 3.10).

SLA provides precision and accuracy in the realization of the final object: these are the main advantages of choosing this process: in fact, the tolerances on a part deriving from SLA are less than 0.05 mm. The surfaces of the object are smooth, that is why these components may be used as prototypes, molds or preforms for other manufacturing processes [12, 14].

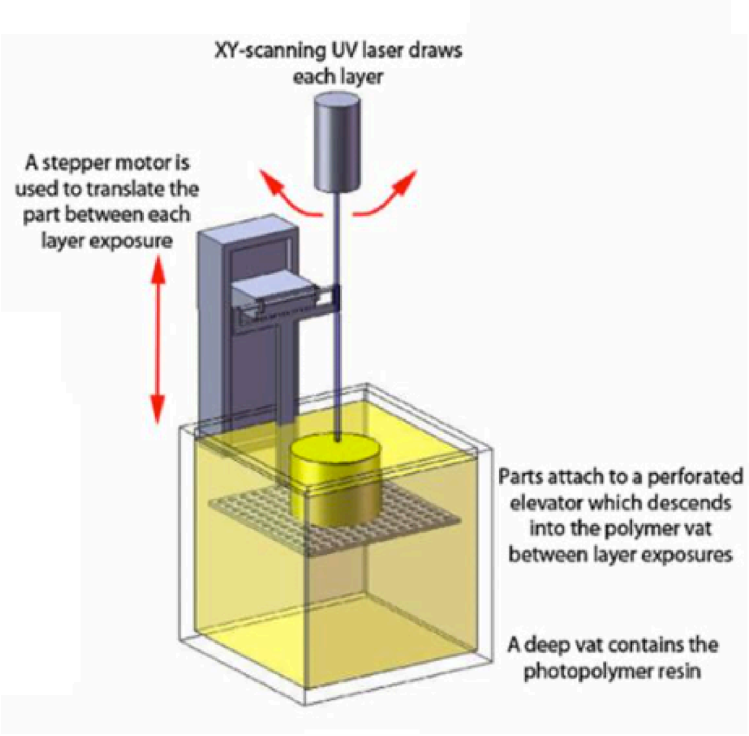

Figure 3.19. Stereolithography [15]

3.2.2 Digital Light Processing (DLP)

Digital Light Processing differs from SLA because it does not provide the polymerization through a laser beam, but with a projected light: the light is projected on the formulation according to the whole cross-section of the object.

Even for DLP the light is characterized by wavelength in the UV-VIS range, and the formulation is contained in a tank, right above the projector. This reservoir is characterized by a glass or transparent plastic bottom, so the projected light could be irradiated on the formulation, providing its solidification. The formation of the layer occurs on a mobile platform, positioned upside-down, so its surface may be in direct contact with the liquid formulation. The growth of the desired object is possible because of the capability of the platform to move upward when the formation of a layer is completed, and then moving towards the formulation, so that the previous process may start over (Fig. 3.11).

DLP guarantees very good resolutions (under 30 μm) and production times that depend on the dimension of the object to be manufactured. It is faster than SLA because the photopolymerization is not activated punctually but simultaneously for an entire layer [12,14].

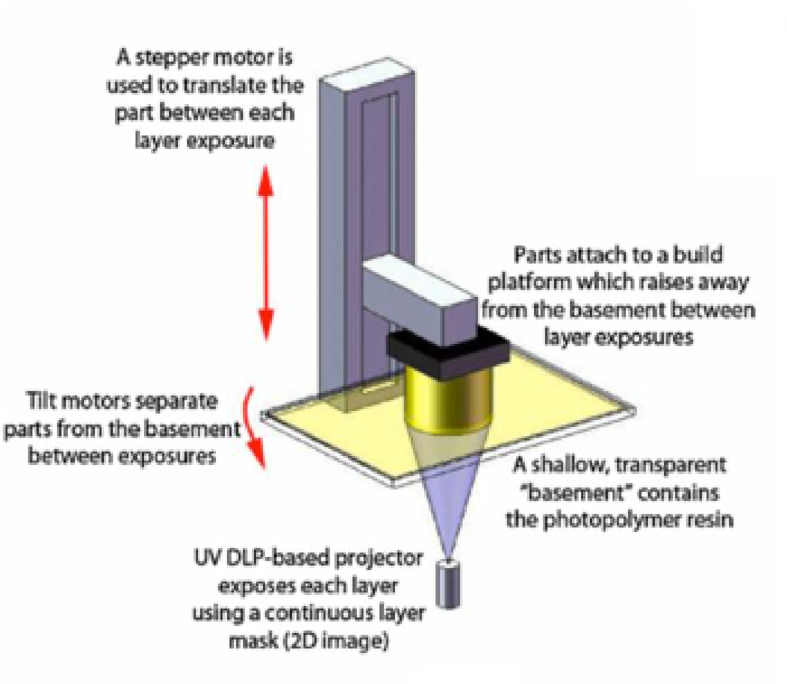

Figure 3.20. Digital Light Processing [15]

3.3 References

[1] Pappas S.P.; 2013; Radiation Curing: A Personal Perspective in “Radiation Curing: Science and Technology”; Chapter 1; Springer Science & Business Media.

[2] Slides: “Scienza dei materiali polimerici” lessons by M. Sangermano; 2018.

[3] https://en.wikipedia.org/wiki/Photopolymer

[4] Deflorian F., Fedel M.; 2014; UV-curable organic polymer coatings for corrosion protection of steel in “Handbook of Smart Coatings for Materials Protection”; Chapter 20; Makhlouf A.S.H. Ed.; Woodhead Publishing, Elsevier.

[5] Andrzejewska E.; 2016; Free Radical Photopolimerization of Multifunctional Monomers in “Three-Dimensional Microfabrication Using Two-Photon Polymerization, Fundamentals, Technology and Applications; Baldacchini T. Ed.; Elsevier.

[6] Allen N.S.; 1996; Photoinitiators for UV and visible curing of coatings: mechanisms and properties; Journal of Photochemistry and Photobiology A: Chemistry; 100, 101-107.

[7] https://en.wikipedia.org/wiki/Quantum_yield

[8] Schwalm R.; 2001; Photoinitiators and Photopolymerization in “Encyclopedia of Materials, Vol. 1 A-B”; Jürgen Buschow K. H., Cahn R.W., *et al*. Eds.; pp. 6946-6948.

[9] Avci D., Nur Eren T.; 2018; Monomeric and Polymeric Photoinitiators in “Photopolymerization Initiating Systems”; Lalevée J., Fouassier J.P Eds.; Royal Society of Chemistry.

[10] Ann j.; 2014; Mitigation of Oxygen Inhibition in UV LED, UVA and Low Intensity UV Cure; Allnex USA Inc., Allnex Belgium SA.

[11] Gebhardt A., Kessler J., Thurn L.; 2019; Basics of 3D Printing Technology in “3D Printing, Understanding Additive Manufacturing, 2nd Edition”; Chapter 1; Hanser Publishers, Munich.

[12] Gebhardt A., Kessler J., Thurn L.; 2019; Additive Manufacturing Processes/3D Printing in "3D Printing, Understanding Additive Manufacturing, 2nd Edition"; Chapter 2; Hanser Publishers, Munich.

[13] GoetheLab, University of Applied Science, Aachen.

[14] Kocovic P.; 2017; 3D Printing Technologies in "3D Printing and its Impact on the Production of Fully Functional Components: Emerging Research and Opportunities"; IGI Global; USA.

[15] Slides: "Materiali Nanostrutturati" lessons by M. Sangermano, 2019.

Chapter 4: Materials and Methods

This chapter presents the materials involved in this study, the adopted preparation procedures and a brief description of the characterization techniques used.

In the end, the specific set up for the adsorption and desorption tests is defined.

4.1 Materials

In order to evaluate the influence of PILs on the behavior and the absorption capacity of a polymeric matrix, six different formulations have been prepared with variable amount of ionic liquid monomers into them.

In particular, *poly (ethylene glycol) diacrylate* (PEGDA) at different molecular weights (250 and 575) has been used as polymer matrix; samples containing the neat matrices and others involving also ionic liquid monomers in different concentrations have been prepared.

The chosen ionic liquid monomers are both based on the imidazolium cation, but one of them is a monofunctional molecule, while the other one is bifunctional. This choice is due to the interest in finding out how the functionality of ionic liquid monomers may influence the efficiency of their photopolymerization and the properties of the materials obtained by it.

All the formulations present a certain amount of photoinitiator, which is BAPO, *phenylbis (2,4,6-trimethylbenzoyl) phosphine oxide,* and a pigment, that is Methyl Red.

4.1.1 PEGDA Mn 250 and PEGDA Mn 575

In Fig. 4.1 the molecular structure of PEGDA is represented: it is characterized by two acrylic groups at the ends, so the free radical photopolymerization occurs thanks to this bifunctional structure.

PEGDA Mn 250 and PEGDA Mn 575 differ because of their molecular weight, given by the number of groups that are repeated on the polymeric chain, separating the two acrylic ends: this means that the polymerized structure will be more open, the higher the molecular weight of PEGDA.

Both of them have been purchased from Sigma-Aldrich: in general, these reactants may be used in tissue engineering, drug delivery, and applications involving gas separating membranes or flexible coatings [1,2].

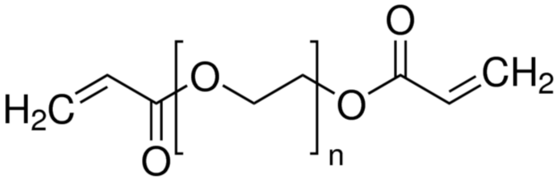

Figure 4.21. Molecular structure of PEGDA [1]

4.1.2 Ionic Liquid Monomers (ILMs)

Though the variety of ionic liquid monomers is extended, only two types of ILMs have been chosen in this work: both of them are characterized by the imidazolium cation and the trifluoromethanesulphonyl anion and they have been purchased from Solvionic. These are:

- Monofunctional ILMs: *3-Ethyl-1-vinylimidazolium bis(trifluoromethanesulfonyl) imide* (Fig. 4.2A)*;*
- Bifunctional ILMs: *1,4-Butandyl-3,3'-[bis-(1-vinyl)-imidazolium]di-bis(trifluoromethanesulphonyl)imide* (Fig. 4.2B)

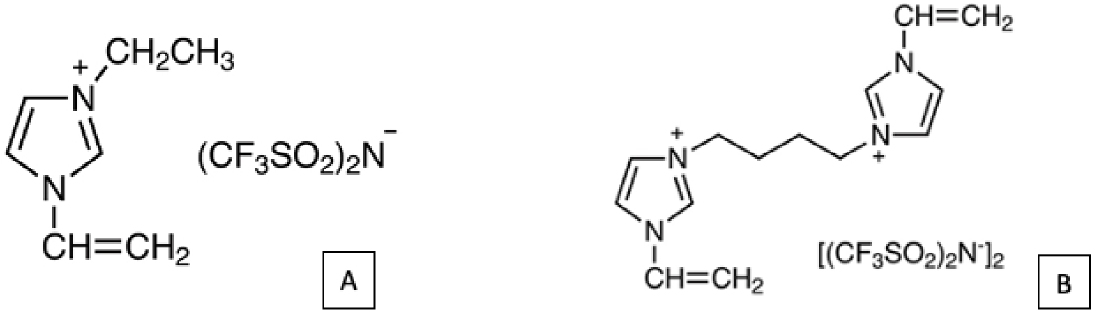

Figure 4.22. A) Monofunctional ILM; B) Bifunctional ILM [3,4]

Imidazolium based ionic liquids exhibit low melting point, high chemical stability and they are prone to ionization, thanks to the aromatic structure presented by it, in which nitrogen atoms play an important role. As represented in Fig. 4.3, in fact, two nitrogen atoms are involved in imidazole ring: the first one (1) is a hydrogen donor, while the other (3) is an acceptor. This structure makes it able to provide amphoteric behavior: the quaternization[1] of the ring provides a stable positive charge that allows it to be a proton donor or acceptor, according to the conditions that it undergoes.

---

[1] Quaternization (or Menshutkin reaction) is a reaction occurring between a tertiary amine and a compound characterized by alkyl, aryl groups (for instance, halides) in order to convert them into a quaternary ammonium salt [6].

Ionic liquids based on imidazolium cations are often used in different applications like sensors, absorption and catalysis. They are often chosen as monomers for the creation of Poly (Ionic Liquid)s [5].

As for the chosen ionic liquid monomers present vinyl groups (one in the monofunctional and two in the bifunctional) that allow their polymerization: their double bonds are involved in the free radical photopolymerization and provide the formation of a cross-linked structure.

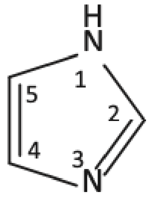

Figure 4.23. Imidaziole ring [6]

4.1.3 Photoinitiator: BAPO

The photoinitiator used in all the formulation is *phenylbis (2,4,6-trimethylbenzoyl) phosphine oxide*, also called BAPO (Fig. 4.4). It is a Type I photoinitiator, that activates the polymerization through the absorption of UV-Visible light (it absorbs in the range of 365-405 nm [7]).

It is a powder, it was bought from Sigma-Aldrich and it is commonly used to polymerize unsaturated monomers, in photocurable formulations [8].

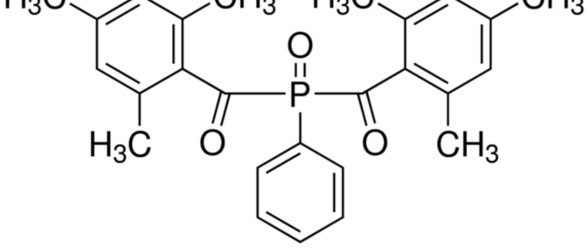

Figure 4.24. BAPO molecular structure [8]

4.1.4 Pigments: Methyl Red

Methyl Red (MR) *2-((4-dimethylaminophenylazo) benzoic acid, Acid Red 2, 4-Dimethylaminoazobenzene-2'-carboxylic acid*) whose molecular structure is represented in Fig. 4.5., was added to all the formulations as a dye.

It is a powder, that is added into the formulation in order to enhance the resolution of the photopolymerization when the solidification of the polymeric materials occurs during 3D Printing.

Methyl Red could be used also as a pH-indicator, as it changes its color when the acidity of a solution varies: it becomes red at lower pH and yellow at higher ones. As it is represented in the absorption spectrum in Fig. 4.6, both at higher and lower pH conditions, Methyl Red absorbance is maximized in the range of UV-Visible light (400-600 nm) [9].

This is positive for the purpose of photopolymerization, because the pigments' absorption range does not coincide completely with the one of the photoinitiator, so it does not interfere with its role.

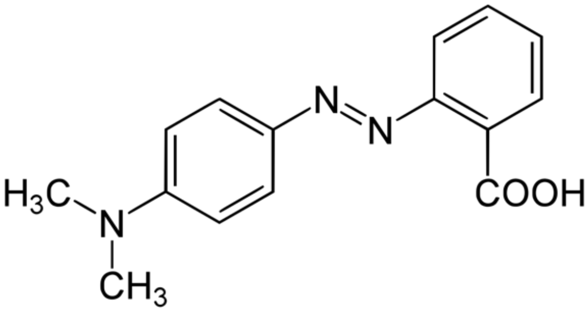

Figure 4.25. Methyl Red: molecular structure [10]

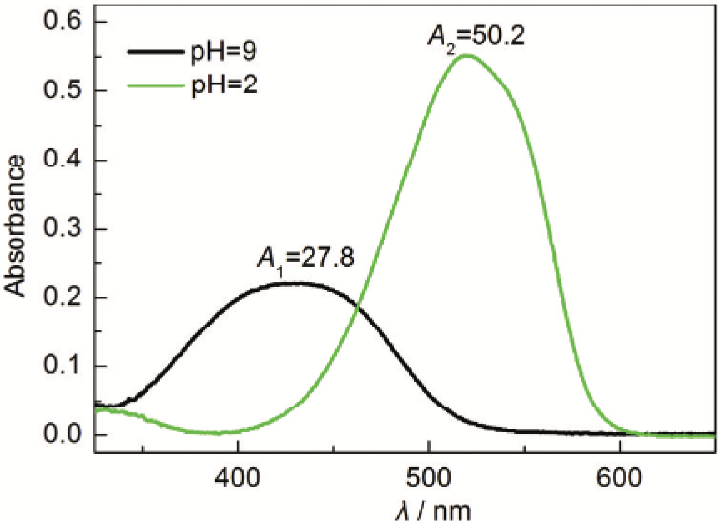

Figure 4.26. Absorption spectrum of Methyl Red, according to different pH conditions [9]

4.2 Preparation of the Formulations

Considering that the purpose of this work is to compare the behavior of different polymeric materials, characterized by variable concentrations of PILs, in terms of their VOCs' absorption capacity, six formulations have been prepared:

1. PEGDA Mn 250
2. PEGDA Mn 575
3. 50% (wt.) PEGDA Mn 250 + 50% (wt.) Monofunctional ILM
4. 50% (wt.) PEGDA Mn 575 + 50% (wt.) Monofunctional ILM
5. 90% (wt.) Monofunctional ILM + 10% (wt.) Bifunctional ILM
6. 90% (wt.) Monofunctional ILM + 10% (wt.) PEGDA Mn 575

In these different formulations the concentration of ionic liquid monomers increases, so that it is possible to consider their influence in the absorption capability of the material; furthermore, the polymeric matrices based on PEGDA, with different molecular weights, make it possible to evaluate the neat polymer efficiency in the VOCs' absorption, and then comparing it with the one presented by PILs.

It is also interesting to create these comparisons, in order to find out which mechanism is predominant in the absorption of different organic solvents, and so which property is specifically required for the material that is considered to be the most suitable for this purpose.

In all the formulations, the concentrations of BAPO and MR were maintained constant, as reported in Tab. 4.1.

Photoinitiator (BAPO)	2 % wt.
Methyl Red	0,1 % wt.

Table 4.8. Concentration of photoinitiator and pigment in the formulations

All the formulations have been sonicated for variable amount of time, to solubilize all the components homogeneously. In general, the amount of time required to achieve the complete solubilization of the different components is around 10 minutes.

On the other hand, the presence of components that are powdery (and thus prone to agglomeration), in some cases causes the need for longer sonication times: for instance, the formulation nr.5, characterized by the bifunctional ILM, required sonication times around 20-30 minutes.

As all the formulations are photosensitive, it is important to protect them from sunlight during their utilization, so that the photopolymerization does not initiate earlier than expected.

4.2.1 Formulation Characterization: Photo Rheometry

The photo rheometry permits the evaluation of the rheological properties of all the considered formulations, even during their photopolymerization, induced by light absorption.

This allows to consider the reactivity of the formulations, their polymerization kinetics and the basic mechanical parameters defining the obtained solid material.

In particular, in this work an Anton Paar MCR 302 parallel-plate rotational rheometer has been used, equipped with a lamp emitting light in the range of visible.

Each formulation has been positioned on a quartz plate, completely transparent to visible light, and the upper plate has been lowered considering a gap between the plates of 0,2 mm. The tests took place at room temperature.

The aim of the photo rheological tests is to identify the rheological behavior of formulations during their polymerization through parameters such as G', G'' in function of time. This is the reason why tests in oscillation mode were carried out, with constant frequency of 1 Hz and amplitude of 1%, deriving from the preliminary test in which the linear viscoelastic region was determined.

The lamp was switched on after 60 seconds from the start of each test: in these conditions, both the storage modulus G' and the loss one G'' are expected to grow: the first one, the storage modulus, represents the elastic behavior of the polymerized material, and becomes constant when the polymerization process is ended, while the latter, the storage modulus, represents the viscous component of the material behaviour. In a liquid formulation G'' usually results higher than G' while during the irradiation, and thus the polymerization of the formulation, the elastic component becomes predominant until the reaching of the plateau level. The cross-point in which G'=G'' is defined as the gel point. Furthermore, the slope of the linear part of the graph, defining the growth of G' in function of time is important to be considered in order to define the polymerization rate.

The light irradiating on the formulation was characterized by an intensity of 0,5 mW/cm^{-2}, and two measurements were taken for each second.

4.3 DLP-3D Printing

The realization of different objects was carried out by using a DLP-3D Printer (ASIGA Pico2), that worked with light in the rage of visible (λ=405 nm) (Fig. 4.7).

The process parameters were progressively optimized for each formulation, according to its characteristics and its reactivity, that were specifically investigated with the photo-rheological tests described previously.

After the 3D Printing process has completed, the objects were removed from the building platform and immersed in ethanol, so that the residual formulation has been extracted.

In conclusion, they have been subjected to post-curing, in a UV curing device, for about 5 minutes, in order to complete definitively the photopolymerization of monomers.

Figure 4.7. ASIGA Pico2 [11]

4.4 Characterization Methods

In this paragraph the analysis that have been made on the polymeric materials will be presented in detail. The aim of this part of the work is the characterization of every material, defining their physical, mechanical, and chemical properties. Some tests provided also information about the efficiency of the photopolymerization that permitted the formation of the solid objects.

The characterization methods that have been considered are:

- IR Spectroscopy
- Extraction in Chloroform
- DSC
- DMTA
- SEM and Optical Microscope

4.4.1 IR Spectroscopy

IR Spectroscopy is a non-destructive technique that is useful to identify the main functional groups presented by molecules or polymeric materials. Through this analysis it is possible to evidence which functional groups take part to the polymerization and which is its efficiency.

It is based on the phenomenon through which an infrared radiation with a specific energy is absorbed by a molecule that, in these conditions, is able to provide a vibrational transition.

The identification of different functional groups is based on the fact that each of them absorbs a different discrete energy to provide the vibrational transitions: the wavelength of the IR radiation that is required to do so, is monitored and it is associated to the functional group itself through tables that are available in literature.

Specifically, FT-IR Spectroscopy (Fourier Transformate IR Spectroscopy) has been considered, because of the higher resolution of its spectra and the wide wavelength range that it considers.

The outcome of this analysis is a spectrum that represents absorbance (the intensity of electromagnetic radiation absorbed by the functional group) in function of the wavelength of the infrared radiation absorbed by the studied material.

The spectra were obtained for each liquid formulation and for the corresponding polymerized material.

After having identified the significant peaks in the IR spectra, some considerations may be derived from them, for instance, the conversion efficiency of the system. It is calculated through equation 4.1, in which $P_{\text{formulation}}$ stands for the area of the peak associated to the functional groups participating in the polymerization presented by the spectrum relative to the formulation, while $P_{Polymerized}$ is the area of the peak associated with the same functional group, in the spectrum of the 3D printed material. Both the areas of the peaks are normalized considering the area of a peak that is associated to a functional group which is not involved in the polymerization.

$$\%conversion = \frac{P_{formulation} - P_{Polimerized}}{P_{formulation}}\ x\ 100$$

Equation 4.1.

4.4.2 Extraction in Chloroform

The extraction in chloroform was done to evaluate the amount of unreacted monomers after the polymerization, so that the results deriving from it may be compared to the IR Spectroscopy ones.

First, each specimen's initial weight was registered, then the sample has been packed into a metallic net and immersed in chloroform for 24 hours.

In the end, the final weight has been evaluated for each specimen, and the difference between this one and the initial weight has been calculated. This parameter is significative, especially in relation to the initial weight of the materials: it is possible to derive the percentage of monomers that didn't take part to the polymerization reaction, lowering the overall efficiency of it.

4.4.3 Differential Scanning Calorimetry (DSC)

DSC is a thermal analysis method that provides the identification of the melting temperature, the glass transition temperature or the crystallization temperature of a polymeric material.

It is based on the application of a temperature slope on two crucibles: one of them contains the material to be analyzed, while the other acts like a reference for the measurement.

While the system heats up progressively, an inert atmosphere is created into the chamber, which is usually filled with a flux of N_2, in order to avoid interferences of a reactive atmosphere with the specimens at high temperature.

The principle through which DSC works, is based on the fact that different materials require different heat fluxes in order to maintain the same temperature: in fact, endothermic or exothermic reactions may occur at certain temperature, so that the heat flux which is necessary to guarantee the thermal equilibrium between the analyzed material and the reference is variable.

The relationship between the heat flux required to provide thermal equilibrium and the temperature at which this condition must be maintained is represented on the graph deriving from this thermal analysis.

As it is represented in Fig. 4.8, different peaks or inflection points may be present in the DSC outcoming graph: they define the glass transition temperature (inflection point), the melting point (negative peak considering an exothermic heat flow), the crystallization point (positive peak for exothermic heat flow) and other features like cross-linking, oxidation, or degradation of the material.

In this work the DSC has been provided by subjecting the specimens at three consecutive temperature slopes, to eliminate residual tensions on the materials before testing it:

- Increasing temperature slope: from -20°C/-50°C to 120°C/60°C
- Decreasing temperature slope: from 120°C/60°C to -20°C/-50°C
- Increasing temperature slope (the one effectively considered as outcome): from -20°C/-50°C to 120°C/60°C

In all cases the temperature increases or decreases with a rate of 10°C per minute.

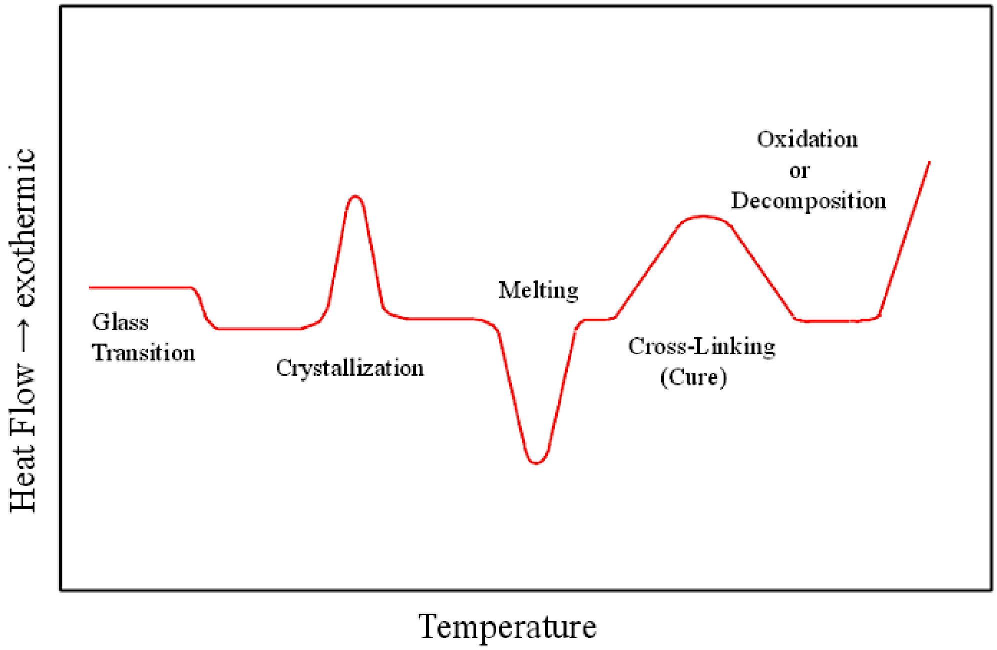

Figure 4.8. DSC graph: significative peaks and inflection points [12]

4.4.4 Dynamic Mechanical Thermal Analysis (DMTA)

DMTA is a thermo-mechanical analysis that is useful to study the viscoelastic behavior of a polymeric material: this is achieved by subjecting a specimen to sinusoidal strain ε, with constant frequency, while its temperature increases during the test.

The viscoelastic behavior of the material should be identified observing the shift of the stress σ (which is also sinusoidal) connected to the applied strain.

In fact, for perfectly elastic materials the mechanical behavior is descripted by Hook’s law:

$$\sigma = E\varepsilon$$

Equation 4.2

The viscous fluids, instead, are characterized by a mechanical behavior defined by Newton’s law:

$$\sigma = \eta \frac{\partial \varepsilon}{\partial t}$$

Equation 4.3.

Considering that strain is a sinusoidal function, eq. 4.2 and 4.3 become:

$$\varepsilon = \varepsilon_0 \, sin\,(\omega t)$$

Equation 4.4

$$\sigma = E\varepsilon = E\varepsilon_0 \, sin\,(\omega t) = \sigma_0 sin\,(\omega t)$$

Equation 4.5

$$\sigma = \eta \frac{\partial \varepsilon}{\partial t} = \eta\varepsilon_0 \, \omega \cos(\omega \, t) = \sigma_0 \sin(\omega \, t + \delta); \quad \delta = \frac{\pi}{2}$$

Equation 4.6

So, it is possible to say that for a phase lag δ equal to zero, the material presents a completely elastic behavior, while when it is equal to $\frac{\pi}{2}$, it is a viscous fluid: δ that is included in the range defined by these extremes represents a viscoelastic behavior of the material.

This is the reason why the mechanical behavior is generally defined by two moduli: G’ is called elastic or storage modulus, while G’’ is loss modulus (eq. 4.7, 4.8).

$$G' = \frac{\sigma_0}{\varepsilon_0}\cos\delta$$

Equation 4.7

$$G'' = \frac{\sigma_0}{\varepsilon_0}\sin\delta$$

Equation 4.8

$$\tan\delta = \frac{\sin\delta}{\cos\delta} = \frac{G''}{G'}$$

Equation 4.9

Equation 4.9 defines one of the parameters monitored in DMTA, which is tan δ: it indicates the shift that occurred between the sinusoidal stress and strain.

DMTA’s outcome is a graph representing how G’ and G’’ vary with the sinusoidal solicitation in function of the increasing temperature; and at the same time, it monitors how tan δ changes during this process: in particular, a peak of this parameter may be identified for a certain temperature, that turns out to be the glass transition point of the analyzed material. This has been compared to the data deriving from other thermal analysis, such as DSC, to evaluate their coherency.

All the analyses have been carried out at constant frequency (1 Hz) and with a temperature slope of 3°C per minute, starting from -40°C to 100°C. Liquid nitrogen has been fluxed into the specimens’ chamber, in order to considerably lower their temperature before the test started.

4.4.5 Optical Microscope and SEM (Scanning Electron Microscope)

In order to evaluate the quality of the 3D printed objects, especially the ones characterized by more complex shapes, they were observed in detail thanks to optical microscope and SEM.

In particular, the porous pellets made with PEGDA Mn 250, and the ones only based on PILs have been compared, to identify the precision and resolution of their structures.

The images obtained by optical microscope are characterized by a magnification of 5x: both the bigger pellets and the smaller ones were observed, even though this technique didn’t provide the evaluation of the conformation of layers constituting the objects. Another problem that occurred during the use of optical microscope was the lack of sufficient illumination to obtain clear and defined images.

The specific observation of the superficial characteristics of the material and of the layered structure on which the objects are based, was achieved by using Scanning Electron Microscope. The magnification was chosen in the range of 70x - 300x, according to the kind of observation that had to be provided.

4.5 VOCs' Absorption Tests

The aim of this work is basically the evaluation of the VOCs' absorption capacity of PILs-based polymeric materials: in order to achieve this, a very simple experimental set-up has been defined.

The absorption of organic solvents, different from each other was carried out. They have been chosen considering their dielectric constant, their boiling temperature and taking into account the ones that are more commonly used in different realms. In Tab. 4.4 are indicated the Volatile Organic Compounds that have been used, with their own main characteristics [13, 18].

	VOC	Density	Boiling T	Dielectric const. ε	Molecular structure
1	Acetone	0,79 g/cm^3	56,2 °C	21	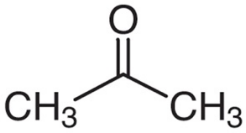 [14]
2	Isopropyl alcohol	0,79 g/cm^3	82,6°C	18	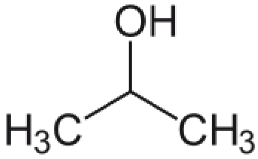 [15]
3	Ortho-Dichlorobenzene	1,31 g/cm^3	180 °C	10	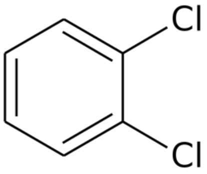 [16]
4	Acetonitrile	0,78 g/cm^3	82°C	37,5	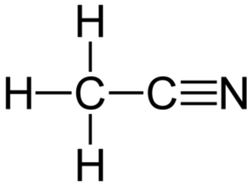 [17]
5	Chloroform	1,50 g/cm^3	61°C	4,81	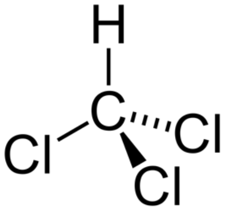 [18]

Table 4.9. Volatile Organic Compounds used in this work [13-18]

4.5.1 Experimental Set-Up

Every absorption test has been carried out using glass jars with hermetic closure, into which different amounts of organic solvents have been put.

The rectangular specimens of each type of material were positioned into the jar, separately from the liquid solvent surrounding them, thanks to little beakers used as containers.

Four different concentrations in volume of the liquid solvents were put into the jars (Tab. 4.5): they were the same for each solvent, that evaporated differently in the system, due to its own characteristics.

	Concentration of liquid VOC (in volume, mL/mL)
Test 1	0,002
Test 2	0,005
Test 3	0,02
Test 4	0,04

Table 4.10. Concentration in volume of liquid VOCs for tests made with each solvent

The jars were carefully closed and put in an oven at the constant temperature of 40°C for 24 hours (Fig. 4.9) the reported temperature was chosen as a compromise to facilitate the solvent evaporation at relatively low temperature. During the 24 hours, the organic solvents were expected to evaporate, so that the gaseous VOC would have been present into the jar and absorbed by the specimens.

Figure 4.9. Experimental Set-Up: Absorption Tests

The absorption capacity of the materials was determined by the difference in their weight after the absorption tests: their initial weight was recorded right before every test, and their final one was evaluated after the vapors' absorption.

Their absorption capacity was calculated as described by equation 4.10.

$$Absorption\ capacity\ \% = \frac{Final\ weight - \ Initial\ weight}{Initial\ weight} x\ 100$$

Equation 4.10

Then, the absorption capacities were considered in function of the VOC's concentration in the jar, expressed in grams of evaporated liquid solvent per milliliter of the jar's volume (g/mL).

This concentration is different from the one referred to the volume of the liquid solvent in the jar, because it considers only the grams of solvent evaporated (by evaluating how much residual solvent has been found after the absorption tests) in relation to the total volume of the jar.

4.6 Desorption Tests

In this work, the desorption ability of each material in relation to each volatile organic compound was also tested.

The conditions were similar to the ones defined for absorption: the specimens were put in the oven at 40°C for 24 hours.

The desorption ability is also based on the difference of weight of the specimens after the test (eq. 4.11): even in this case their initial weight was measured before the desorption and their final one was registered after this process.

The absorption capability of the materials was evaluated only once, so the possibility of using and regenerating the absorbent materials more than once has not been considered.

$$Desorption\ capacity\ \% = \frac{Initial\ weight - \ Final\ weight}{Initial\ weight} x\ 100$$

Equation 4.11

4.7 References

[1] https://www.sigmaaldrich.com/IT/en/product/aldrich/475629

[2] https://www.sigmaaldrich.com/IT/en/product/aldrich/437441?context=product

[3] https://www.tcichemicals.com/HK/en/p/E1280

[4] https://www.tcichemicals.com/GB/en/p/B5421

[5] Noorhisham N.A. *et al.*; 2021; Characterisation techniques for analysis of imidazolium-based ionic liquids and application in polymer preparation: A review; Journal of Molecular Liquids; 326, 115340.

[6] https://en.wikipedia.org/wiki/Menshutkin_reaction

[7] Dietlin C. *et al.*; 2020; New Phosphine Oxides as High Peformance Near-UV Type I Photoinitiators of Radical Polymerization; Molecules; 25, 1671.

[8] https://www.sigmaaldrich.com/IT/en/product/aldrich/511447

[9] Chang-wei Xu; 2021; Determination of Acidic Dissociation Constant of Methyl Red by Multi-Peaks Gaussian Fitting Method Based on UV-Visible Absorption Spectrum; Acta Physica Sinica-Chinese Edition; 28, 1030-1036.

[10] https://en.wikipedia.org/wiki/Methyl_red

[11] https://www.asiga.com/products/printers/pico2/

[12] Slides from “Polymer Science” lessons; M. Sangermano, 2018.

[13] https://en.wikipedia.org/wiki/Acetone

[14] https://www.carlroth.com/com/en/xylene-alternatives/acetone/p/cp40.5

[15] https://en.wikipedia.org/wiki/Isopropyl_alcohol

[16] https://en.wikipedia.org/wiki/1,2-Dichlorobenzene

[17] https://en.wikipedia.org/wiki/Acetonitrile

[18] https://en.wikipedia.org/wiki/Chloroform

Chapter 5: Results

In this chapter, the results deriving from the different tests described previously are presented.

Firstly, the efficiency of the considered systems in terms of their photopolymerization, occurring during 3D Printing is shown, together with the optimization of the 3D printing parameters to obtain the desired objects. Then, the physical properties of the materials are evaluated. In the end, the data referred to the VOCs' absorption (and desorption) capacity are presented.

5.1 Efficiency of the Photopolymerization

Different techniques have been considered in order to define the efficiency of the photopolymerization for the considered formulations.

Right before the 3D Printing of the desired objects, the photo-rheological tests were carried out on all the considered formulations, in order to verify their reactivity.

After that, the realization of objects with different shapes and complexities has been done by DLP-3D Printing, thanks to the optimization of the process' parameters.

Then, the efficiency of the photopolymerization that occurred during the realization of the solid objects via 3D Printing was evaluated, thanks to these analyses:

- IR Spectroscopy (FTIR)
- Extraction in Chloroform
- Observation of structures obtained with 3D Printing via SEM or Optical Microscope

5.1.1 Photo-Rheometry

The graphs obtained by rheological tests are useful to verify the efficiency of the photopolymerization of each formulation. This has been made by monitoring the values of the storage modulus G' and the loss modulus G'' in function of time, during the irradiation of the considered formulation. This permitted also to compare the reactivity of different formulations, and to evaluate the influence of ionic liquid monomers on it.

In general, all the considered formulations completed efficiently the photopolymerization process, that started quite immediately (a few seconds) after the irradiation with visible light, meaning that they are suitable for 3D Printing process.

As it is possible to see from Fig. 5.1- Fig. 5.6, at the end of the reaction the storage modulus is higher, constant and greater than the loss modulus: this means that the material behaves more like a rigid solid, rather than being a viscous liquid.

The graphs represent also the gel point of each formulation, that is individuated when G' is equal to G''.

Even the formulation based only on ionic liquid monomers polymerized efficiently, even though the polymerization rate is way lower than the one of the other formulations containing PEGDA and the final G' is smaller than the one considered for the other cases.

In Fig. 5.7, it is possible to compare the rheological behavior of different formulations: in particular, the influence of increasing content of monofunctional ionic liquid monomer has been evaluated.

The presence of ionic liquid monomers does not influence the polymerization rate of PEGDA, as the slope of the linear part of each curve is similar, nor it inhibits the initiation of the reaction: in fact, it occurs always about 10 seconds after the start of the irradiation, differences observed among the samples can be considered in order of the measurement error. Even the final storage modulus does not vary significantly with the increase of ILM's concentration.

In the case of PILs-based formulation (90% wt. Monofunctional ILM + 10% wt. Bifunctional ILM), the initiation of the polymerization is delayed: in fact, it occurs after 20 seconds from the start of the irradiation.

If the rheological behavior of this material is compared to the one of the formulation characterized by the same amount of monofunctional ionic liquid monomer, but containing 10% (wt.) of PEGDA 575, it is evident that the presence of PEGDA enhances the stability of the polymerization and increases its rate. This is due to the much lower reactivity of vinyl groups with respect to acrylates in a free radical polymerization reaction.

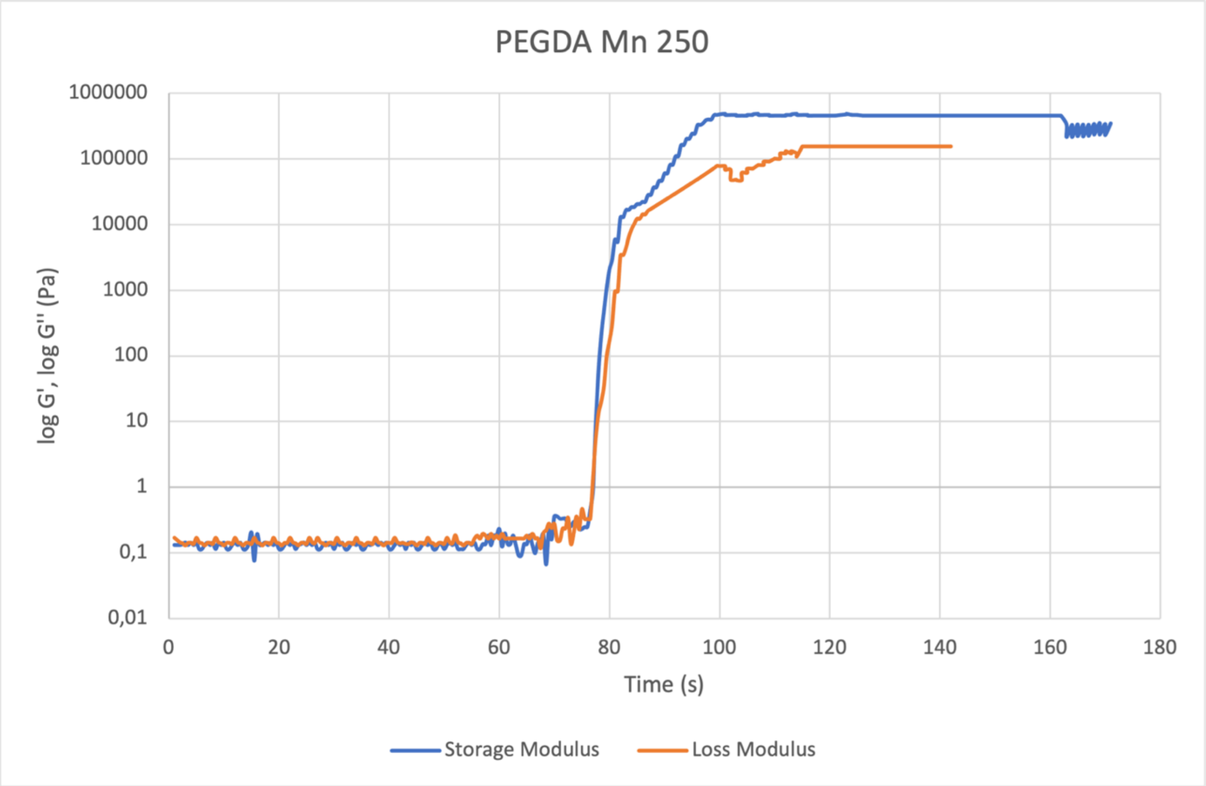

Figure 5.27. Photo-Rheometry of PEGDA Mn 250

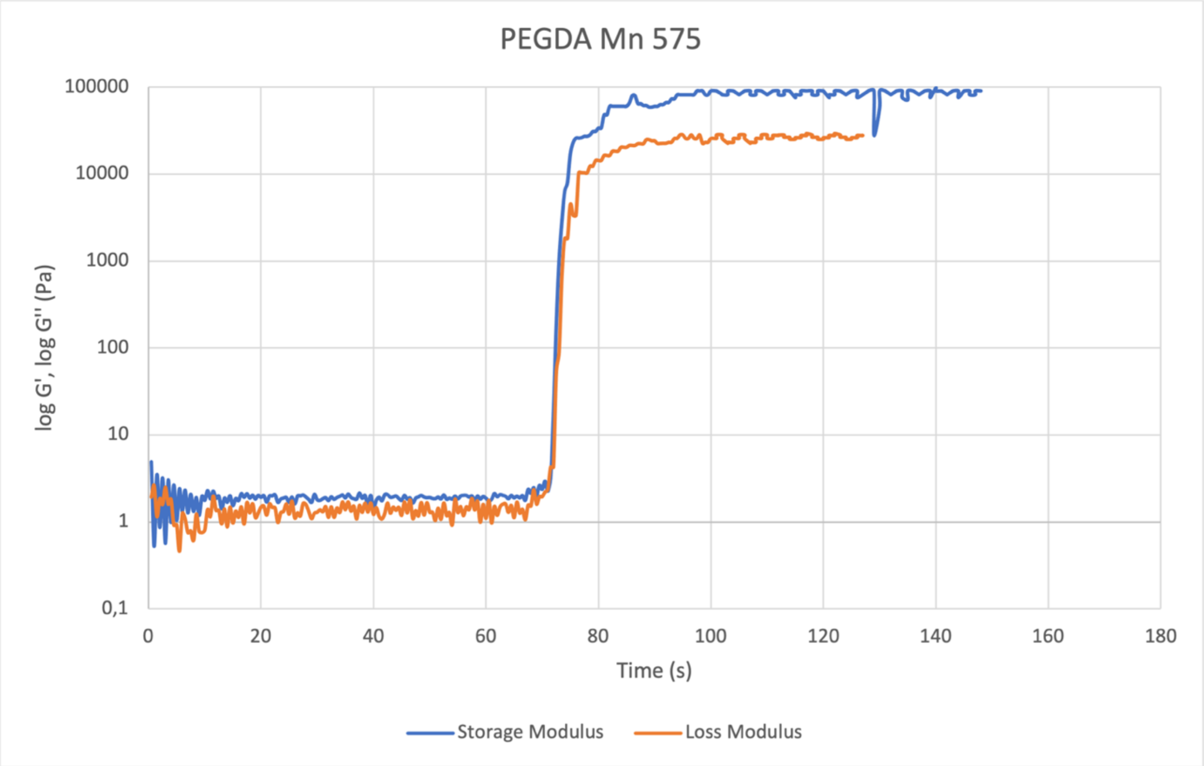

Figure 5.28. Photo-Rheometry of PEGDA Mn 575

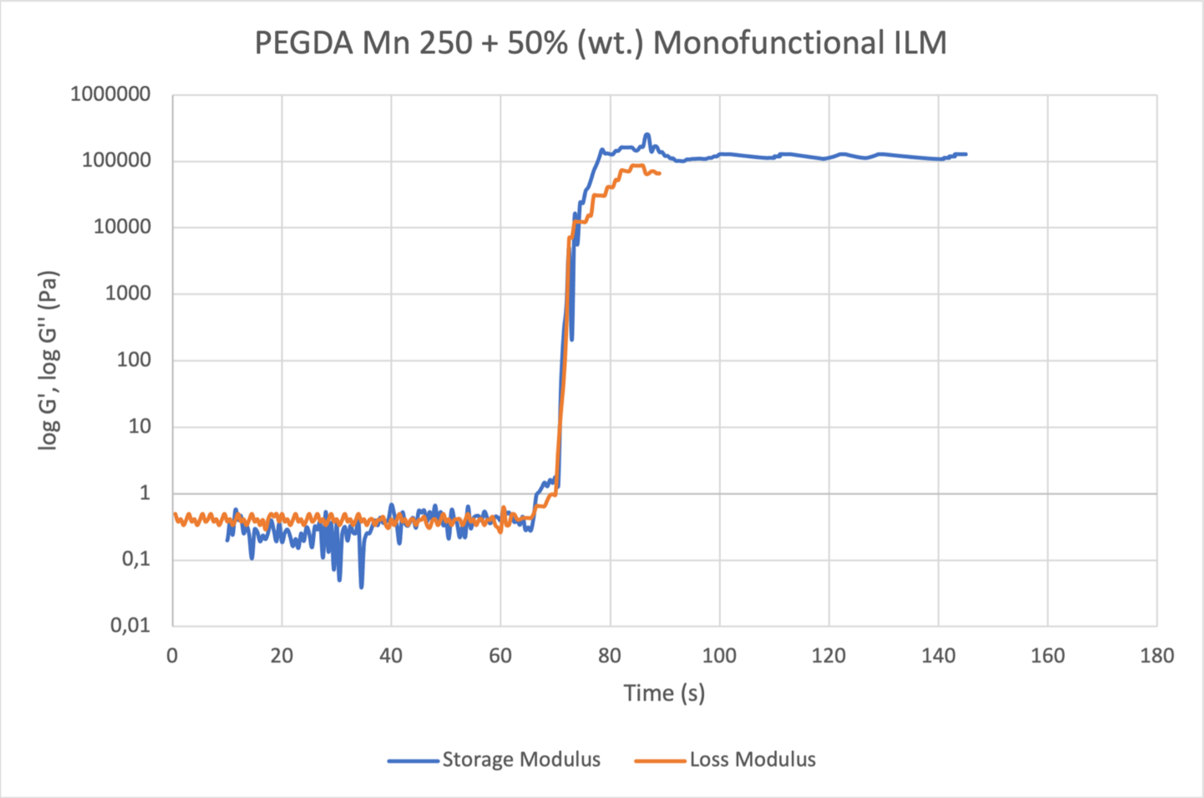

Figure 5.29.Photo-Rheometry of PEGDA Mn 250 + 50% (wt.) Monofunctional ILM

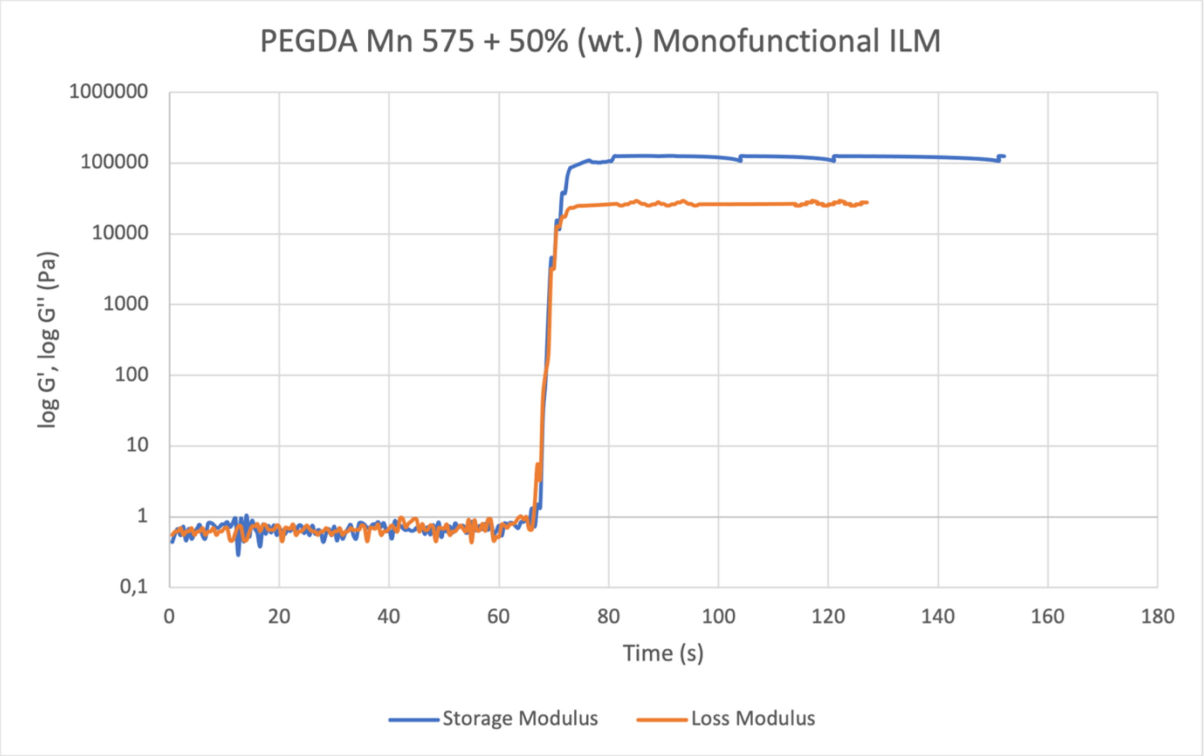

Figure 5.30. Photo-Rheometry of PEGDA Mn 575 + 50% (wt.) Monofunctional ILM

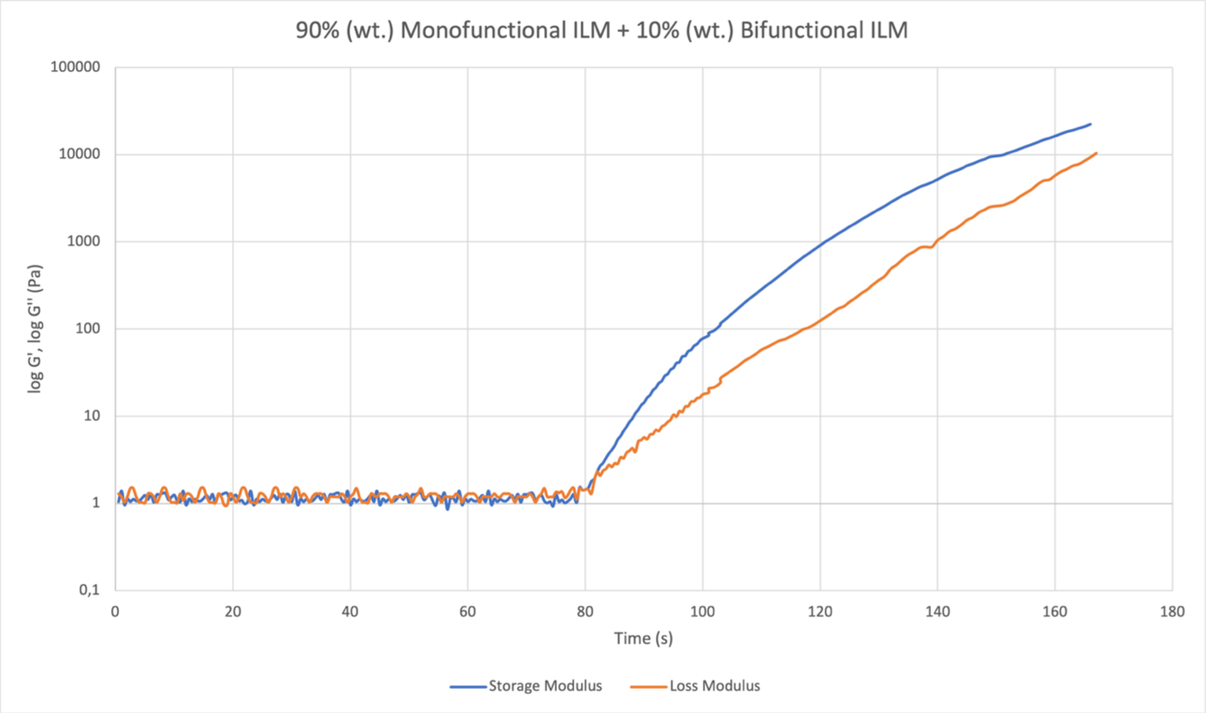

Figure 5.31.Photo-Rheometry of 90% (wt.) Monofunctional ILM + 10% (wt.) Bifunctional ILM

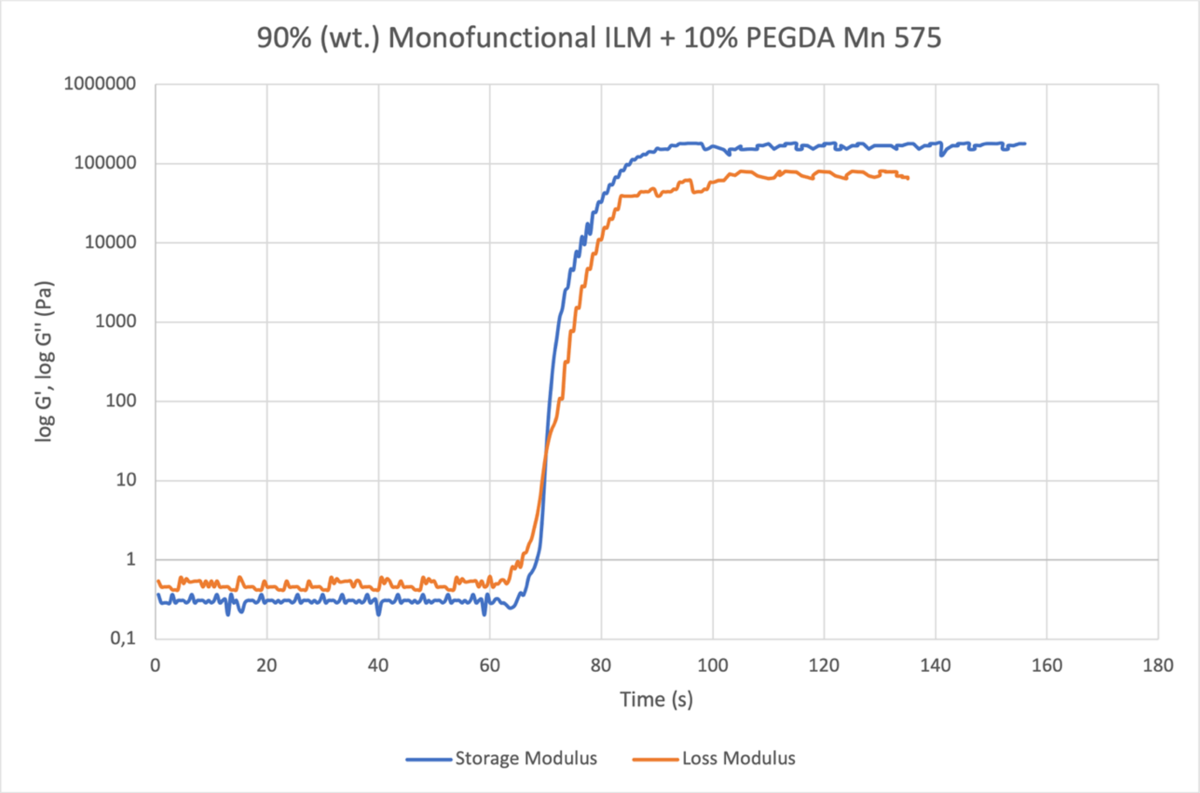

Figure 5.32. Photo-Rheometry of 90% (wt.) Monofunctional ILM + 10% (wt.) PEGDA Mn 575

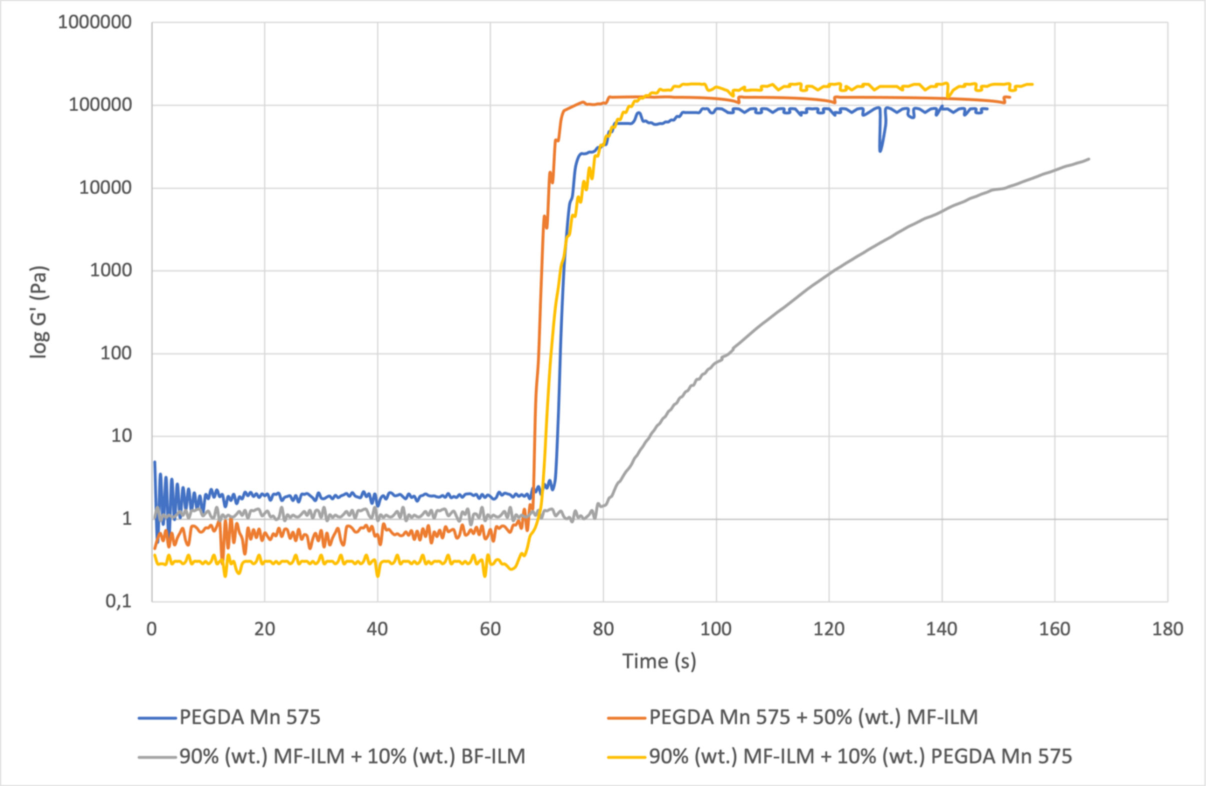

Figure 5.33. Comparison between significative G' trends for different materials

5.1.2 Production of solid objects via 3D Printing

After having confirmed the possibility to photopolymerize the formulations, plenty of objects were obtained thanks to DLP-3D Printing technique, involving all the formulations described in 4.2: the fact that simple shapes and also more complex ones were obtained, confirms once more that these formulations are suitable for this AM technique.

In particular, two different structures have been printed: rectangular specimens (Fig. 5.8), more complex porous pellets (Fig.5.9) and also cylindrical caps (Fig. 5.10): their dimensions have been reported in Tab. 5.1.

Rectangular objects	7 x 25 x 0,7 mm
Pellets	Ø5x5 mm; Ø2,5x2,5 mm
Cylindrical Caps	Ø13x10 mm

Table 5.1. Dimensions of object obtained by DLP

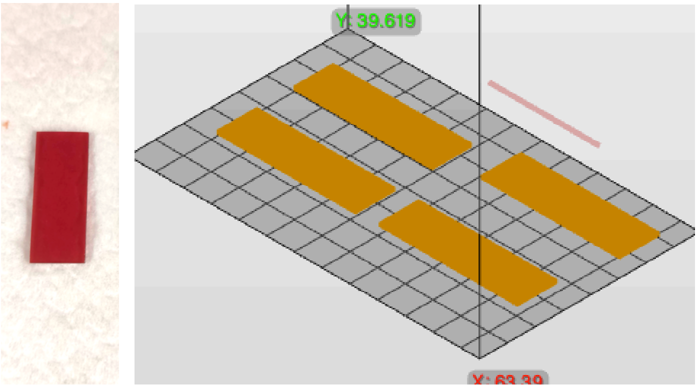

Figure 5.8. Rectangular specimens: final object and CAD prototype [1]

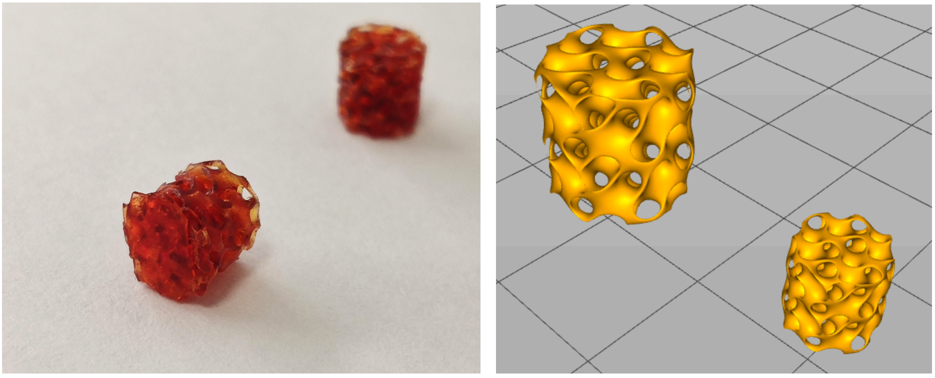

Figure 5.9. Porous pellets: final objects and CAD prototype [1]

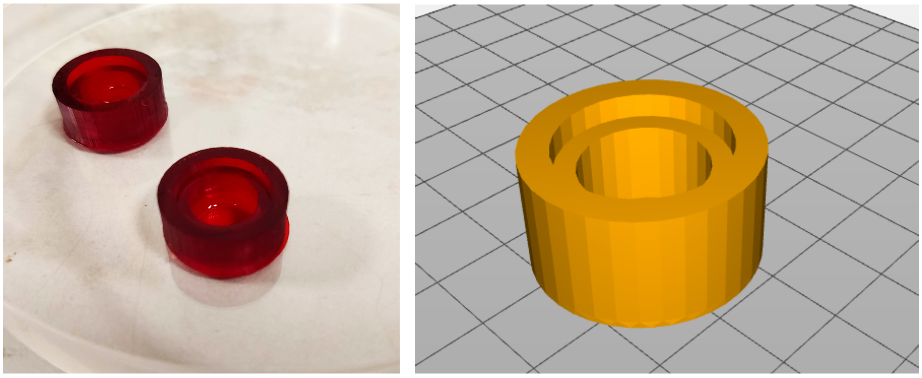

Figure 5.10. Cylindrical caps: final objects and CAD prototype [1]

Rectangular objects	PEGDA-based formulations (1,2,3,4)	**Intensity (mW/cm^2)**	32
		Exposure Time	0.8 s
	PILs based formulations (5,6)	**Intensity (mW/cm^2)**	40
		Exposure Time (BURN IN, 100 µm)	2 s
		Exposure Time (other layers)	1.5 s
Porous Pellets	PEGDA-based formulations (1,2,3,4)	**Intensity (mW/cm^2)**	32
		Exposure Time	0.8 s
	PILs-based formulations (5,6)	**Intensity (mW/cm^2)**	40
		Exposure Time (BURN IN, 100 µm)	3 s
		Exposure Time (other layers)	1.5 s
Cylindrical Caps	PILs' layers	**Intensity (mW/cm^2)**	40
		Exposure Time (BURN IN, 500 µm)	3 s
		Exposure Time (other layers)	1.5 s
	PEGDA walls	**Intensity (mW/cm^2)**	32
		Exposure Time	0.8 s

Table 5.2. Parameters for DLP 3D Printing of different objects with ASIGA Pico2.

The parameters through which the realization of the different object has been possible, are different between each other: for PEGDA-based formulations they were determined more easily, and they were quite similar for every object that has been realized; while the formulations with a higher amount of ILMs, were printed in a more difficult way, determining new parameters for every shape (Tab. 5.2). In particular, in order to improve the adhesion between the PILs and the building platform, during the realization of the pellets with formulations characterized by higher content of ILMs, an initial layer made of PEGDA was deposited.

As for cylindrical caps, the base has been realized with the formulation nr. 5 (completely based on PILs), while the walls were built up with PEGDA Mn 250. The aim of producing this shape was the identification of a possible set up for measuring the permeability of PILs-based membranes (the bottom of these caps).

Every object has been built up with layers photocured one on another, characterized by a thickness of 50 µm. Every printing process was carried out with a separation velocity of the building platform of 3 mm/s.

5.1.3 IR Spectroscopy

FTIR Spectroscopy was used to observe the disappearance of the characteristic peaks of double bonds from vinyls and acrylate groups after the polymerization reaction. In this way, the efficiency of the photopolymerization may be quantified, as explained in 4.4.1 (equation 4.1).

The significative peaks were identified thanks to tables that have been found in literature [2].

The most important ones are:

- 1800-1700 cm^{-1} : stretching of carbonyl in PEGDA;

- 1675-1665 cm^{-1} (weak): stretching of carbon double bonds in the acrylic groups of PEGDA;

- 995 cm^{-1}: bending of single bond that connects the vinyl groups to the imidazolium cation of ionic liquid monomers [3].

5.1.3.1 PEGDA Mn 250

In Fig. 5.8 the FTIR spectrum of PEGDA Mn 250 is represented. The conversion's efficiency has been determined considering the area of the peak at 1675-1665 cm^{-1}, that diminishes after the completed polymerization. The peaks have been normalized by the area of the one referred to carbonyl groups, which are not involved in the polymerization, and so their relative peak does not vary after the reaction has completed. The percentage of functional groups that took part to the polymerization has been identified around 88,3 %.

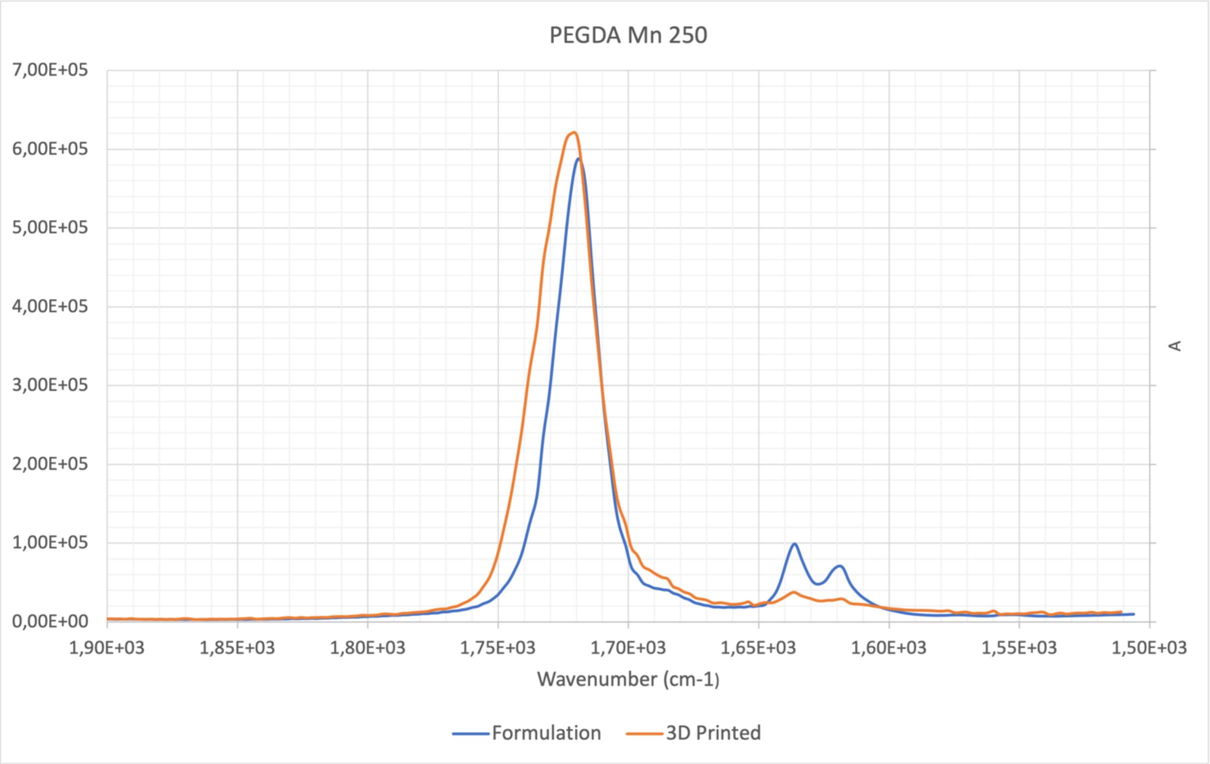

Figure 5.34. FTIR spectrum: PEGDA Mn 250

5.1.3.2 PEGDA Mn 250 + 50% (wt.) of Monofunctional ILM

In Fig. 5.9 and 5.10 the spectrum relative to PEGDA Mn 250 + 50% (wt.) of Monofunctional ILM is reported: in this case the polymerization' efficiency has been calculated taking into account the areas of the peak at 995 cm^{-1}, associated with the reactive groups (vinyls) of the ionic liquid monomer's cations; and the ones of the double bonds in the acrylic groups of PEGDA. The considered normalizing peak is the one referred to the carbonyl group of PEGDA. The percentage of functional groups converted during the polymerization has been defined around 91,3%, considering the efficiency of PEGDA's functional groups; while it is around 89% if the functional groups of ionic liquid monomers are considered.

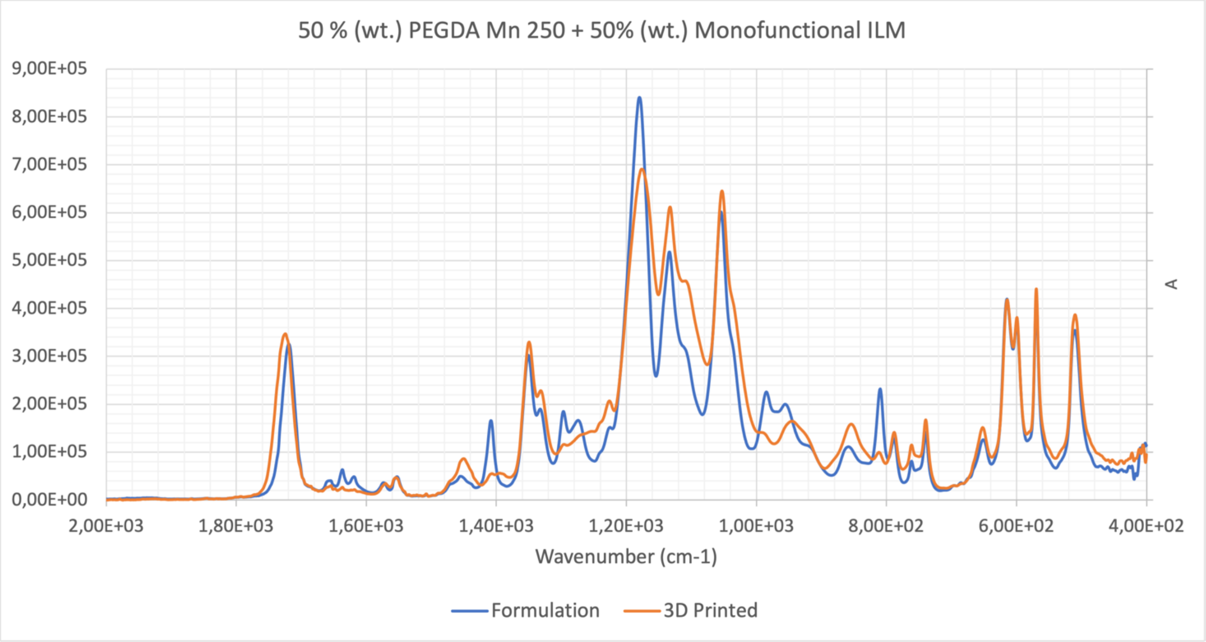

Figure 5.35. FTIR spectrum: PEGDA Mn 250 + 50% (wt.) Monofunctional ILM

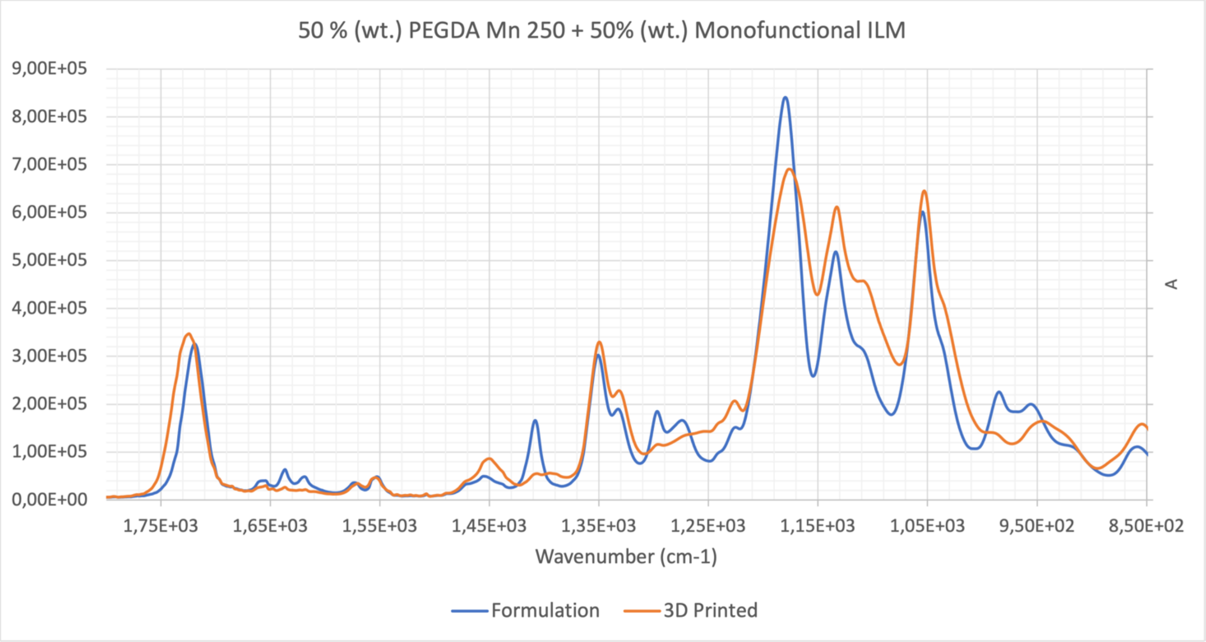

Figure 5.36. Zoom on significative peaks: FTIR spectrum of PEGDA Mn 250 + 50% (wt.) Monofunctional ILM

5.1.3.3 90% (wt.) of Monofunctional ILM + 10% (wt.) of Bifucntional ILM

The FTIR spectrum of the material only based on PILs is represented in Fig. 5.11 and 5.12: the area of the peak at 995 cm^{-1} has been considered in order to define the conversion's efficiency of this system. The normalizing peak that has been defined is the one at 1090-1000 cm^{-1}, as it does not vary after the polymerization. The percentage of functional groups that took part to the polymerization has been identified around 76%.

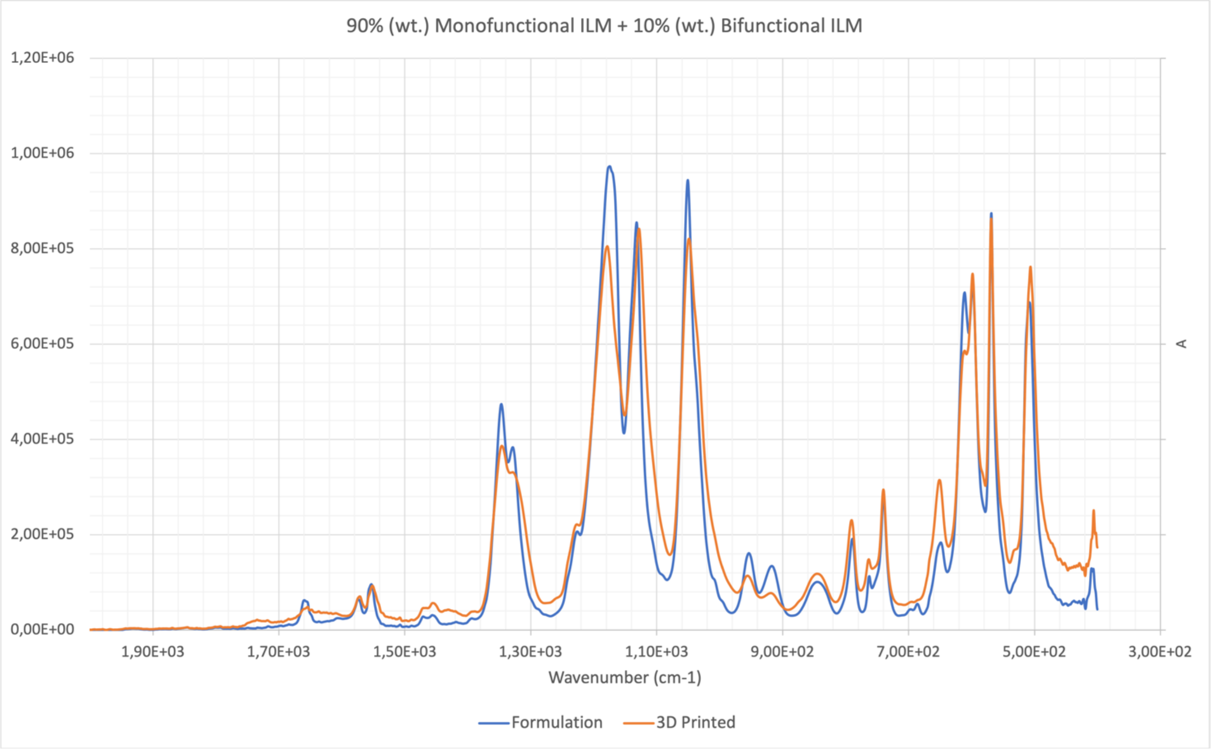

Figure 5.37. FTIR spectrum: 90% (wt.) Monofunctional ILM + 10% (wt.) Bifunctional ILM

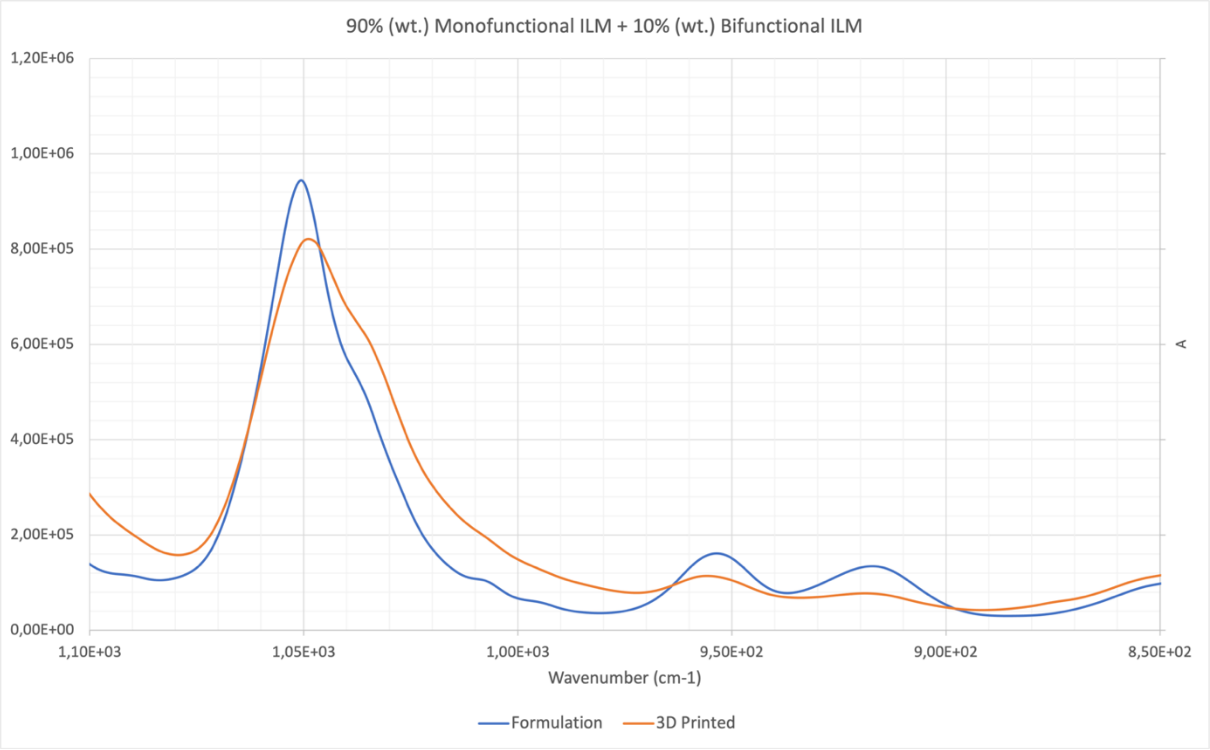

Figure 5.38. Zoom on significant peaks: FTIR spectrum of 90% (wt.) Monofunctional ILM + 10% (wt.) Bifunctional ILM

5.1.3.4 90% (wt.) of Monofunctional ILM + 10% (wt.) of PEGDA Mn 575

The FTIR spectrum of the material based on 90% (wt.) of Monofunctional ILM + 10% (wt.) of PEGDA Mn 575 is presented in Fig. 5.13 and 5.14. As in the previous case, in which PEGDA and ionic liquid monomers are both present in the formulation, the significant peaks of both these elements have been considered in order to define the conversion' efficiency. It was calculated to be 78,2% if the area of the peak relative to PEGDA's acrylic group is considered; while it is 52,3% if the ILM's functional groups are taken into account. This result is coherent with the information determined by the rheological tests: the presence of PEGDA has a strong and positive influence on the polymerization efficiency of the considered systems.

Nevertheless, the efficiencies that has been calculated demonstrate that all the formulations are able to provide a high degree of polymerization.

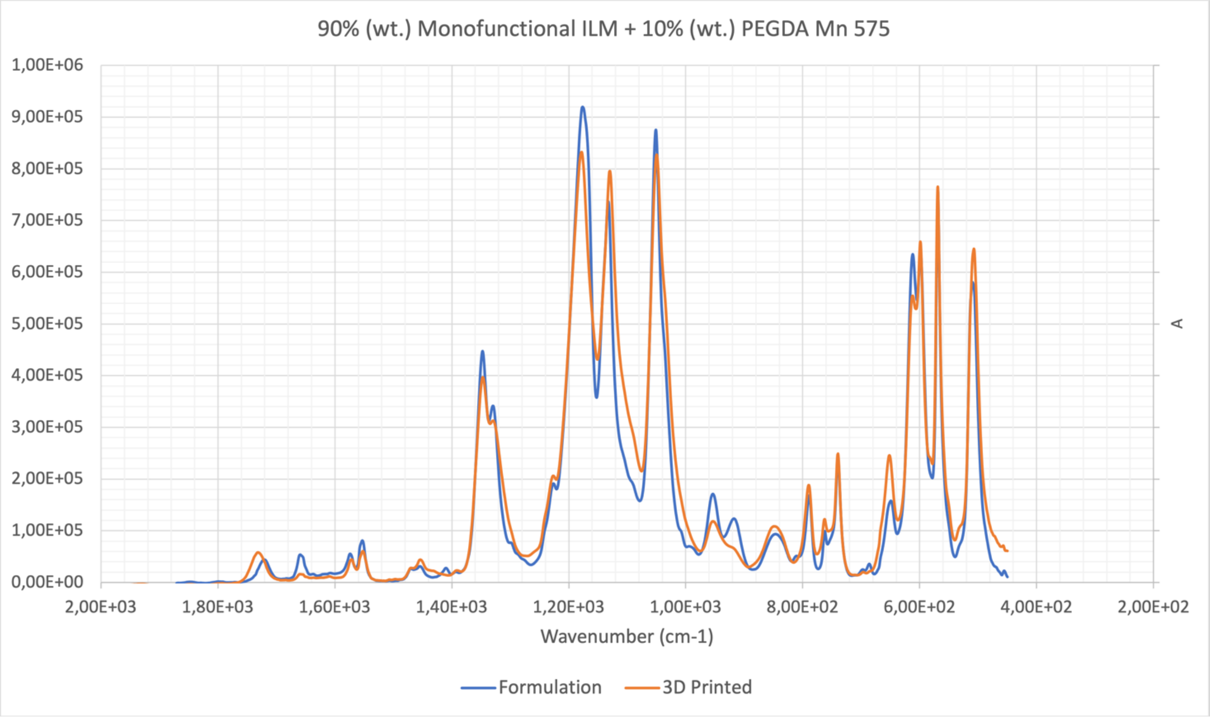

Figure 5.39. FTIR spectrum: 90% (wt.) Monofunctional ILM + 10% (wt.) PEGDA Mn 575

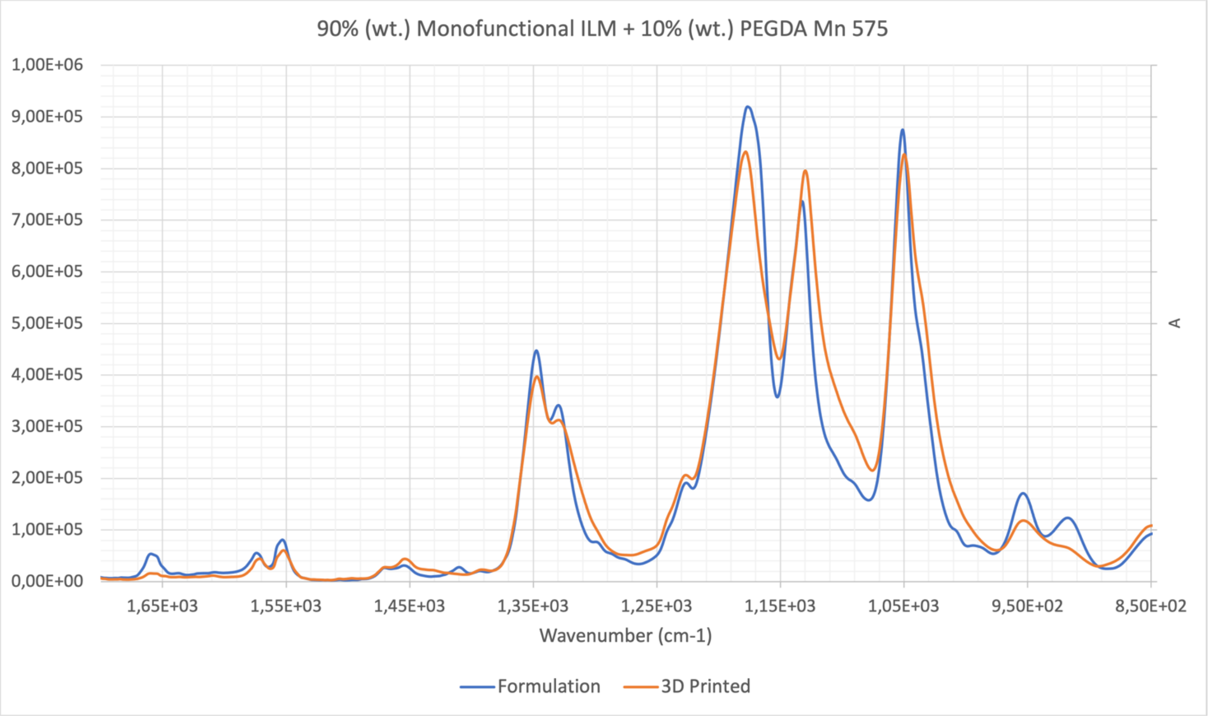

Figure 5.40. Zoom on significant peaks: FTIR spectrum of 90% (wt.) Monofunctional ILM + 10% (wt.) PEGDA 575

5.1.4 Extraction in Chloroform

The extraction in chloroform is another useful method to identify the amount of monomers that didn't take part to the polymerization.

In the graph in Fig. 5.15 the results deriving from this test are reported: in particular, the percentage of monomers extracted from the material has been calculated, considering the difference in the weight of the specimen right before and after the immersion in chloroform in relation to their initial weight.

This test also confirmed that the photopolymerization of all the considered formulations is possible and efficient: in fact, the percentage of extracted monomers does not exceed 15%.

It is lower for PEGDA, while the presence of ionic liquid monomers increases it slightly. Nevertheless, the material completely based on PILs presented only 5% of unreacted monomers, which were residue from the photopolymerization.

These data are coherent with the conversion's percentages that were calculated thanks to FTIR spectra, so they may be considered reasonable.

The higher extraction obtained for the samples based on PEGDA and Ionic Liquids can be ascribed to the different reactivity of the unsaturated groups: the higher reactivity of acrylates in a radical polymerization will lead to the fast formation of the acrylic network in which only a part of the monofunctional vinyl groups will be bounded.

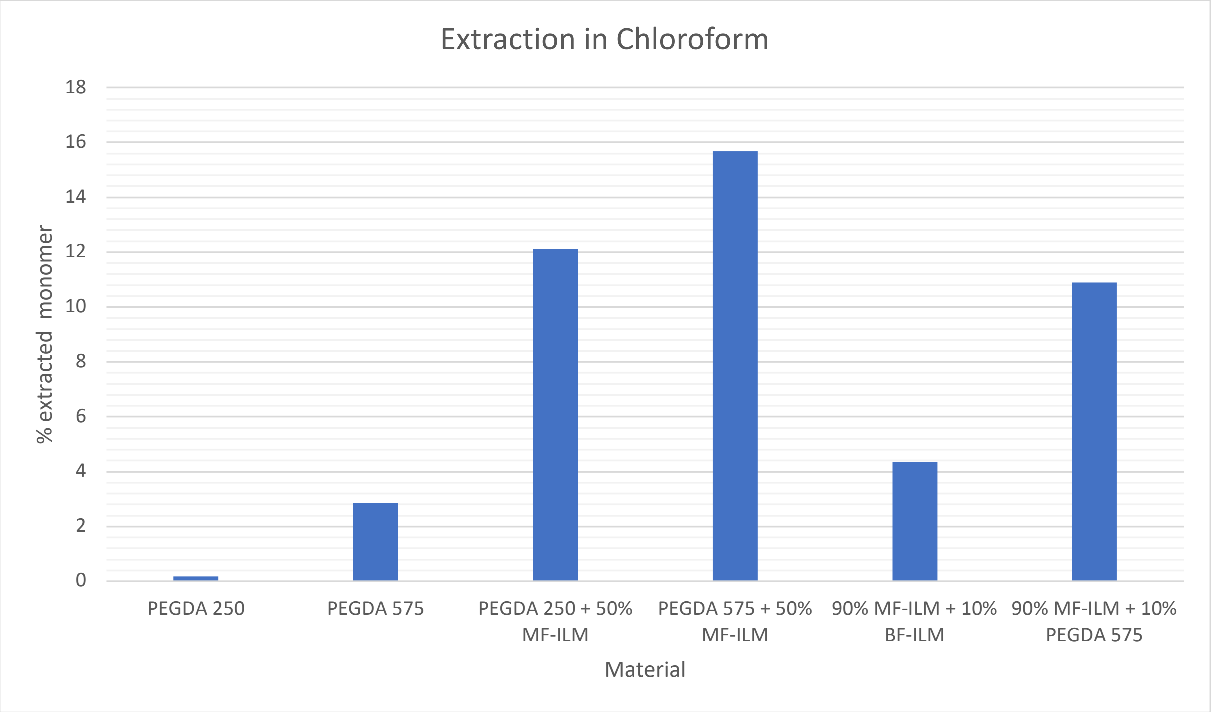

Figure 5.41. Extraction in Chloroform: results

5.1.5 Observation of 3D Printed objects: SEM and Optical Microscope

The evaluation of the efficiency of the 3D Printing technique, applied for the realization of complex structure, such as the porous cylinders that were introduced previously, was carried out thanks to the observation of these objects by optical microscope and SEM.

It was interesting to compare, in particular, the precision through which the complex shapes were obtained and the definition of their layered structure.

In Fig. 5.16 it is possible to observe the images provided by the optical microscope, with a magnification of 5x: the porous interconnected structure is evident, especially for the objects made by PEGDA Mn 250, that turned out to be more defined.

In Fig. 5.17 and 5.18 the comparison between the CAD model and the 3D printed object are represented. The distance between two significative points in the object has been compared: the one measured in the CAD model was very similar with the actual dimension of the object observed via optical microscopy. This could be said both for the PEGDA and the PILs-based specimens (Fig. 5.18) and confirmed that the precision of 3D printing technique in the realization of these objects, is effective.

The images obtained for PILs-based porous cylinders are darker because of the PEGDA layer that was deposited initially, in order to let PILs remain attached more easily to the building platform of the 3D printer: this caused the light to illuminate less intensely the observed object.

In order to achieve higher magnifications and better images' resolution, SEM has been used to observe in detail these complex shapes.

As it is evident comparing Fig. 5.19 with Fig. 5.20, PEGDA-based porous cylinders are characterized by higher layer definition than the one made of PILs. This is due to the higher reactivity of PEGDA in photopolymerization, that is confirmed also by the calculations made on IR spectra's significative peaks and by the results of photorheological tests. Nevertheless, PILs' objects are characterized by good resolution, high definition of complex shapes and they present layers that are less defined but with a smoother connection between each other.

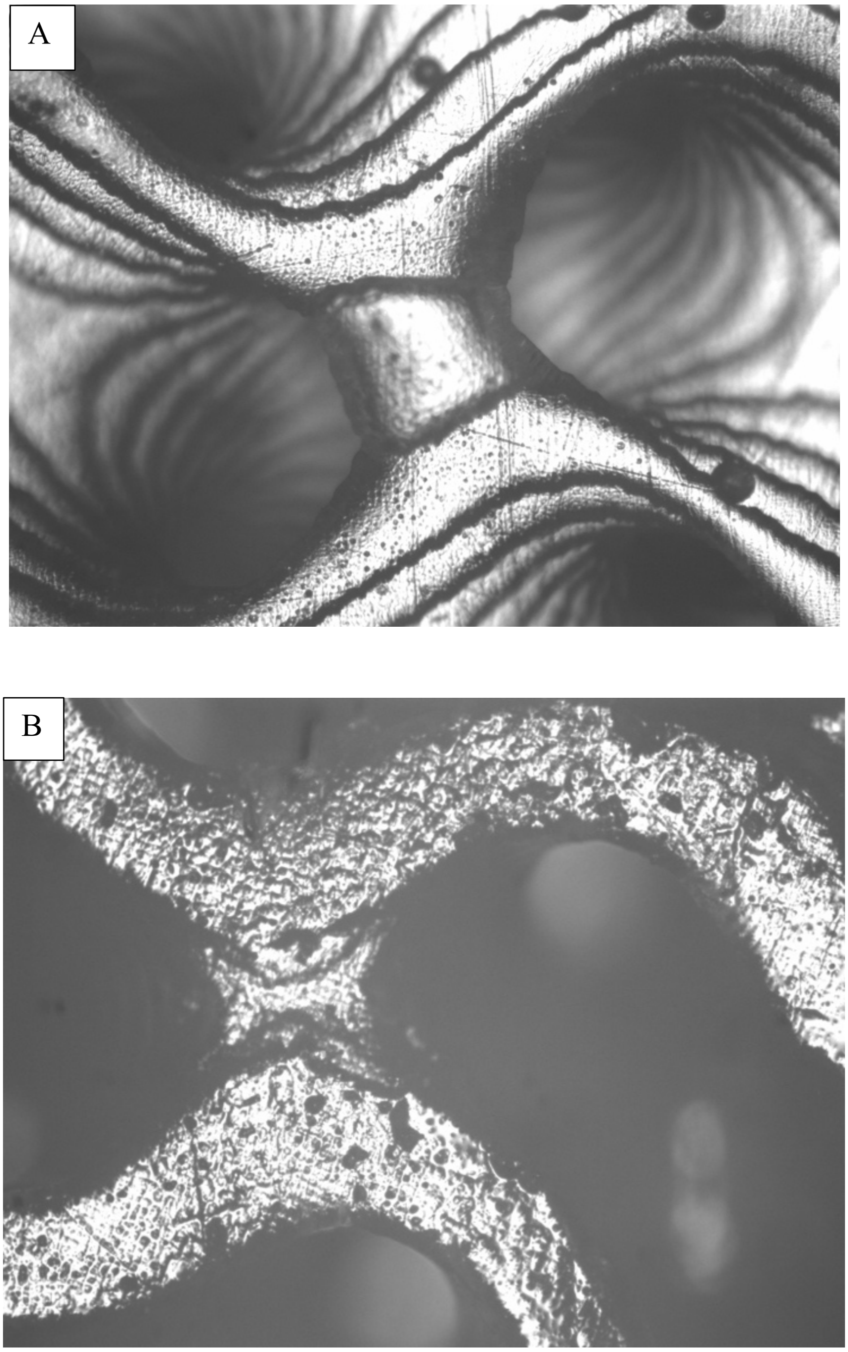

Figure 5.42. Optical Microscope: a) Porous structure in PEGDA 250 b) Porous structure made by PILs

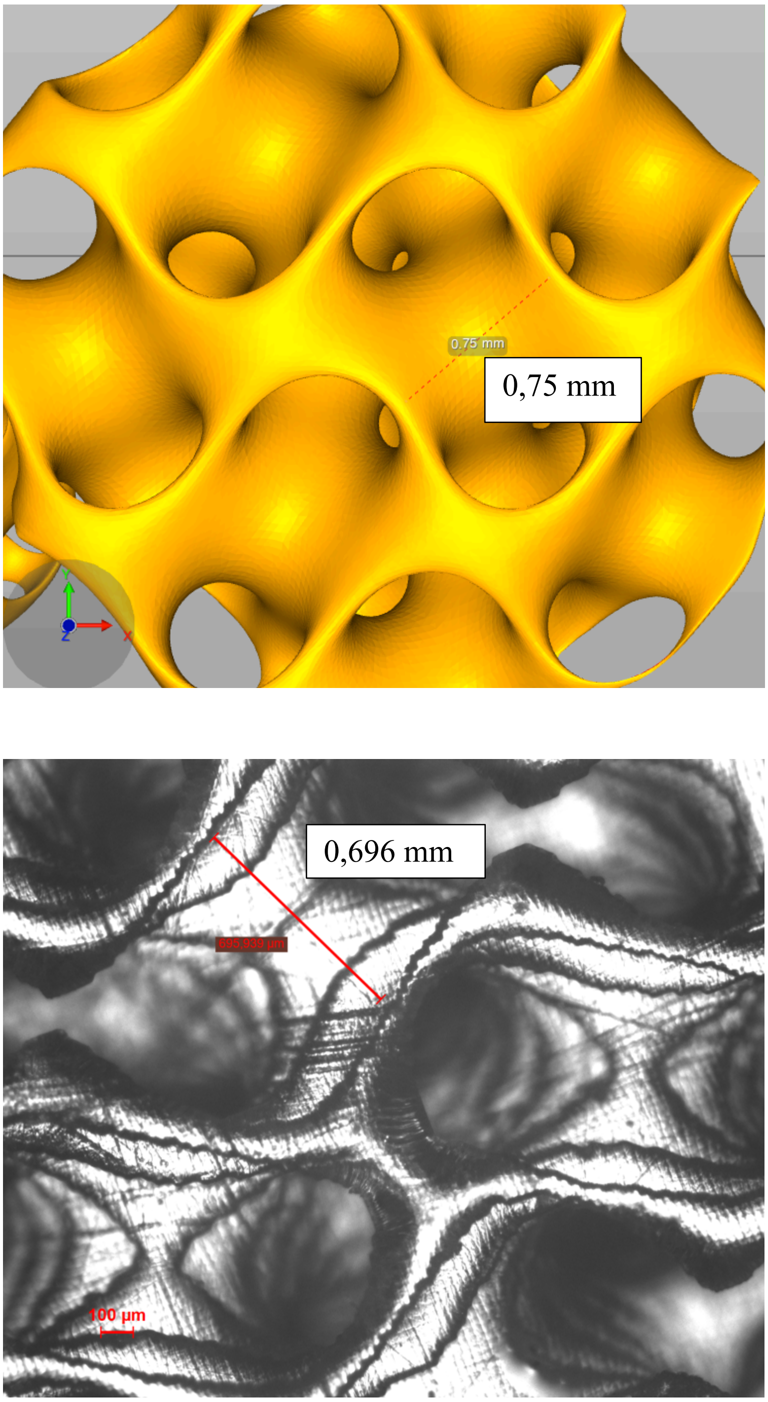

Figure 5.43. Comparison between CAD model and 3D Printed object (PEGDA Mn 250): dimensions [1]

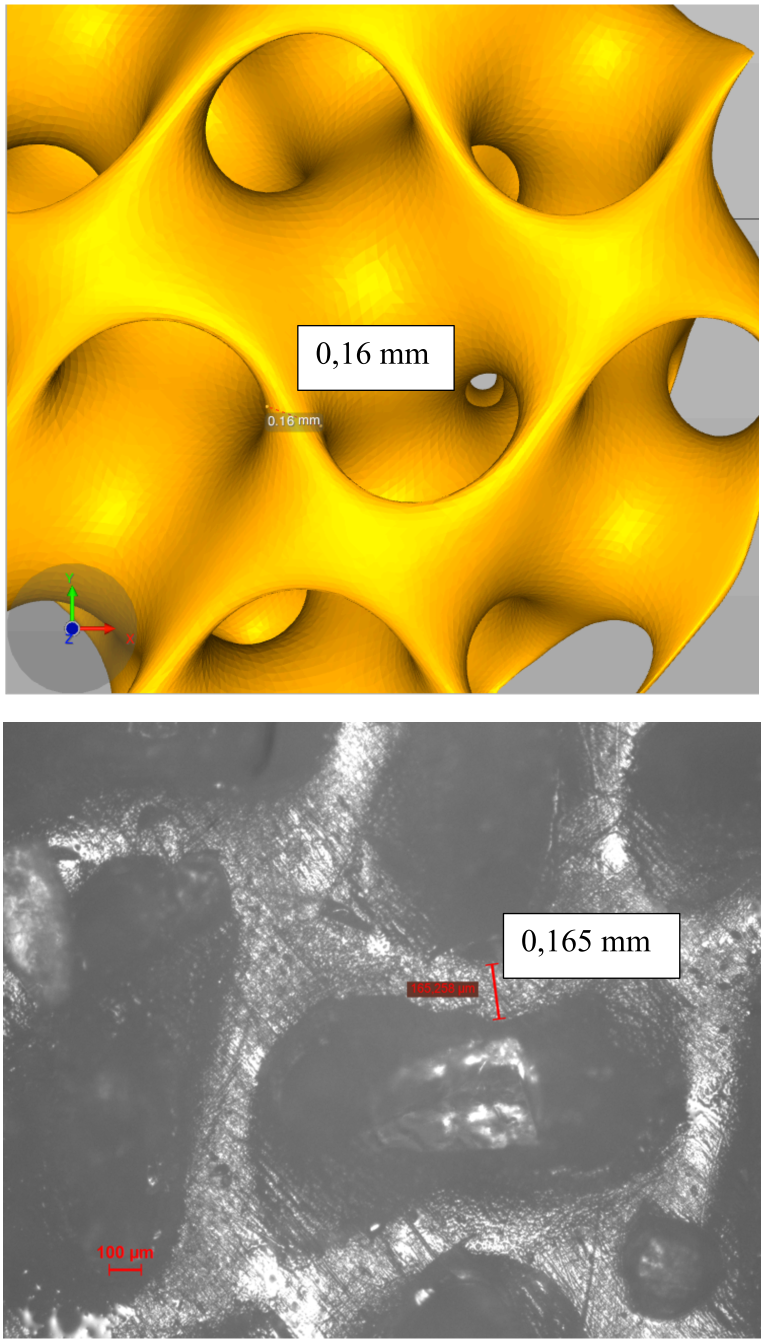

Figure 5.44. Comparison between CAD model and 3D Printed object (PILs): dimensions [1]

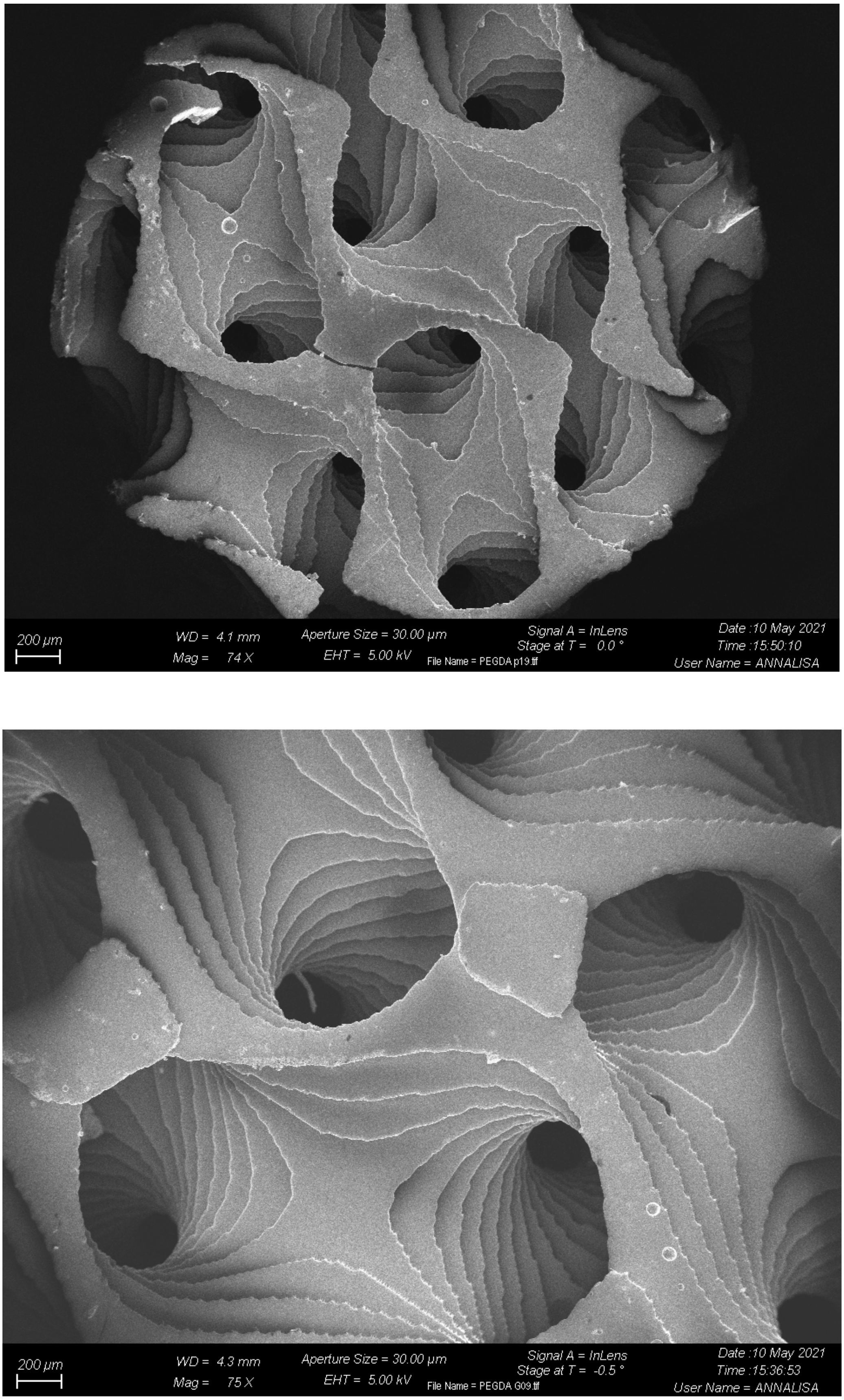

Figure 5.45. SEM images: porous cylinder (PEGDA Mn 250)

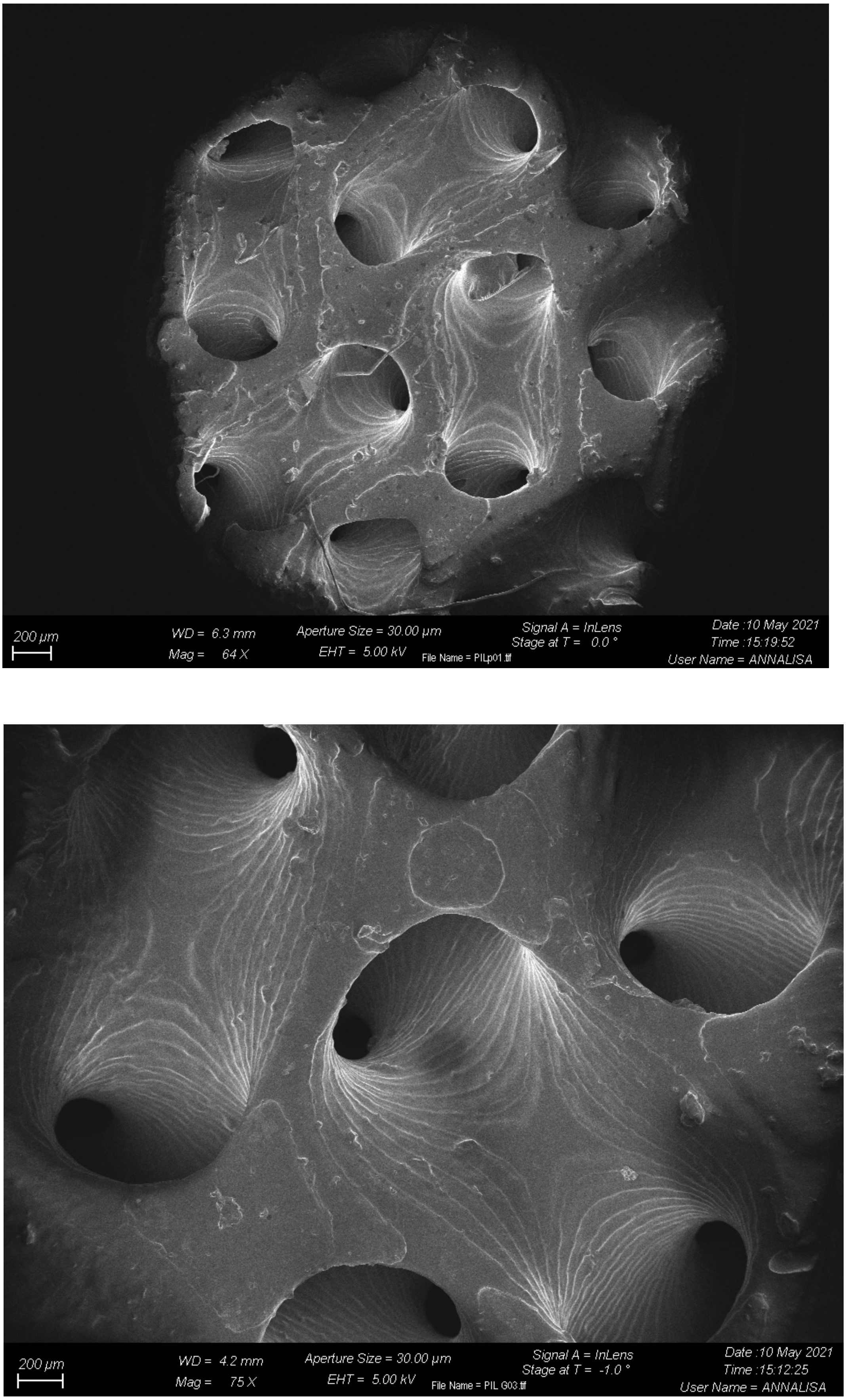

Figure 5.46. SEM images: porous cylinders (PILs)

These results were confirmed also by the images obtained by the 3D scanning provided by 3shape® software and hardware.

In Fig. 5.21 and 5.22 the images deriving from the scanning of the PEGDA-based objects and the ones made by PILs are reported. The different colors represent how much the scanned 3D image is similar to the original CAD model: the green or yellow parts are the ones with less displacement between the two of them. Considering that many green and yellow areas may be seen in these figures, it is possible to say that the reproduction of the CAD model with DLP-3D printing of PEGDA and PILs has been successful.

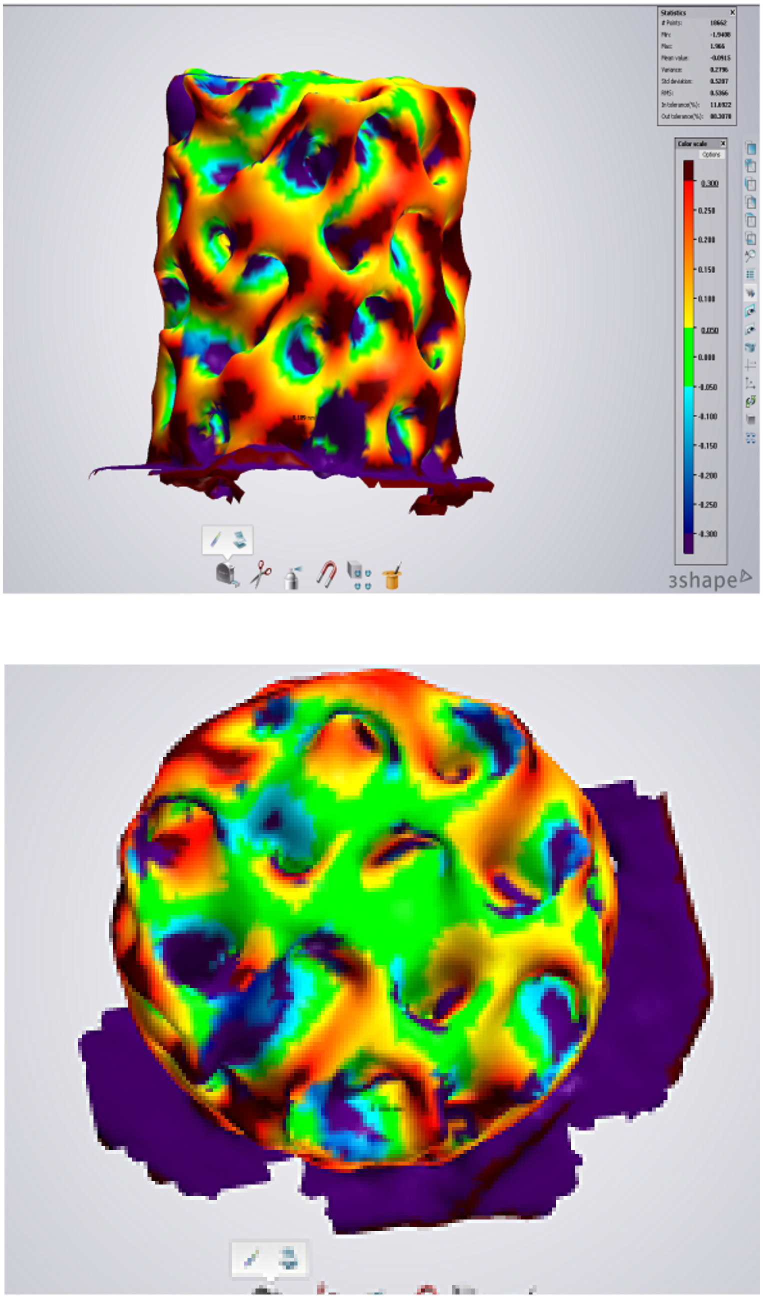

Statistics
Points: 10662
Min: -1.9408
Max: 1.966
Mean value: -0.0915
Variance: 0.2796
Std deviation: 0.5287
RMS: 0.5366
In tolerance(%): 11.6922
Out tolerance(%): 88.3078

Figure 5.47. 3D scanning of objects based on PEGDA Mn 250 [4]

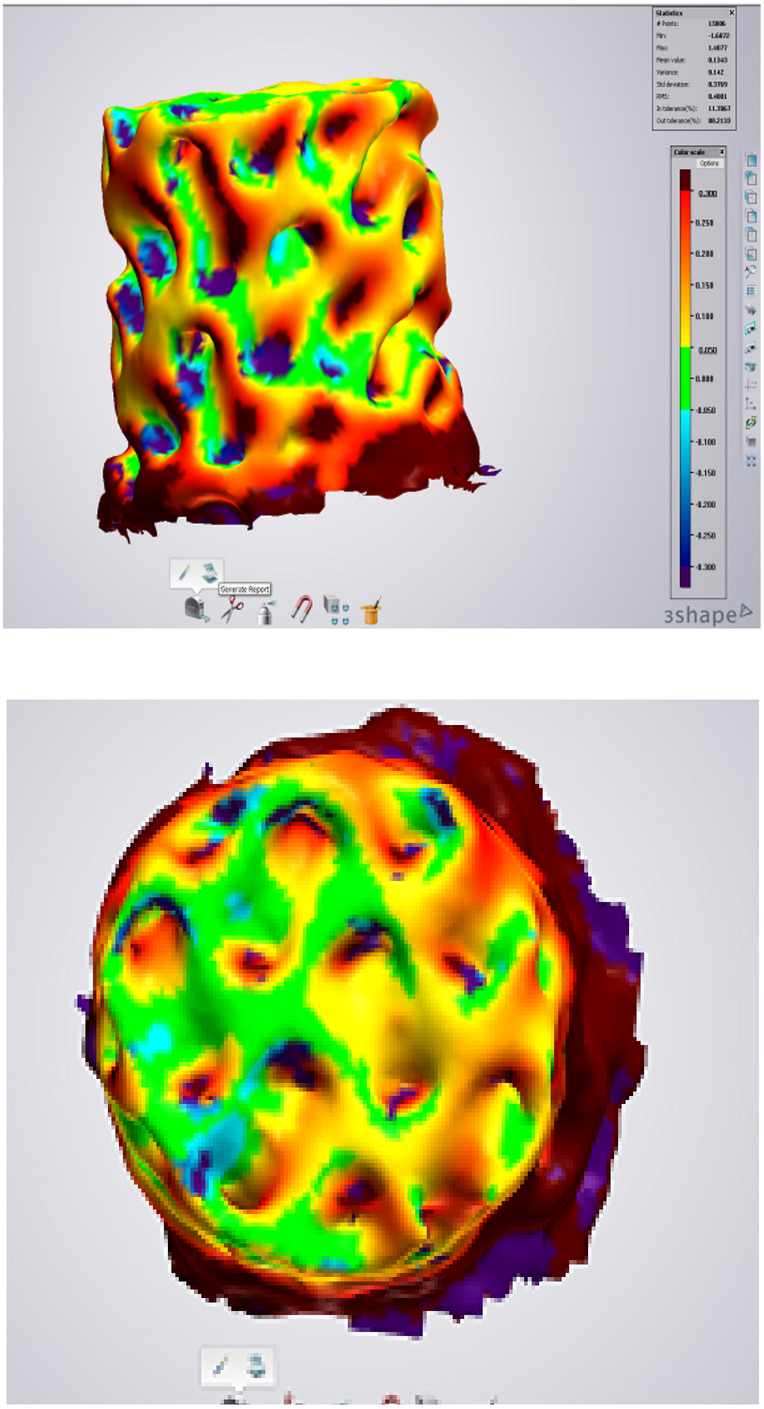

Statistics
Points: 15806
Min: -1.6872
Max: 1.4077
Mean value: 0.1343
Variance: 0.142
Std deviation: 0.3769
RMS: 0.4001
In tolerance(%): 11.7867
Out tolerance(%): 88.2133

Figure 5.48. 3D scanning of objects based on PILs [4]

5.2 Analysis of Thermo-Mechanical Properties

The study of the main physical properties of the studied materials has been carried out considering two techniques, which are DSC and DMTA.

In particular, the glass transition temperature of the materials has been investigated, considering that they are all amorphous, and so they are not characterized by other characteristic temperatures.

Though the two analyses are based on different principles and their results derive from different mechanisms, the data obtained from the two of them were compared in order to evaluate their reliability.

5.2.1 DSC (Differential Scanning Calorimetry)

As explained in 4.1.3, each material was subjected to three consecutive temperature slopes during a test. The results presented in this paragraph consider only the relationship between the heat flow and the temperature regarding the last temperature slope that was applied (increasing temperature, from -20°C/-50°C to 120°C/60°C), as in those conditions the material lost all the residual tension that would have influenced its behavior.

The definition of the T_g was provided by the software that was used to carry out DSC analysis, as well as by the observation of how the curvature changes.

5.2.1.1 PEGDA Mn 250

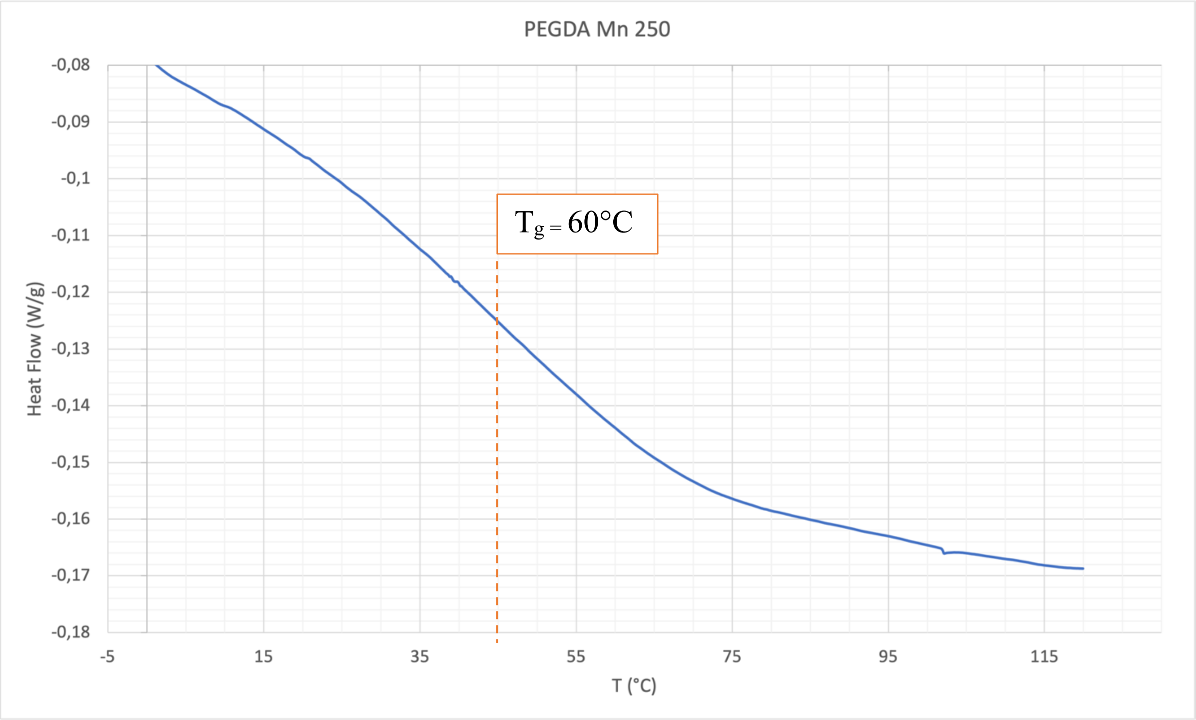

Figure 5.49. DSC: PEGDA Mn 250

In Fig. 5.23 the graph relative to the DSC test of PEGDA Mn 250 is represented: the glass transition temperature of this material has been identified around 60°C.

5.2.1.2 PEGDA Mn 575

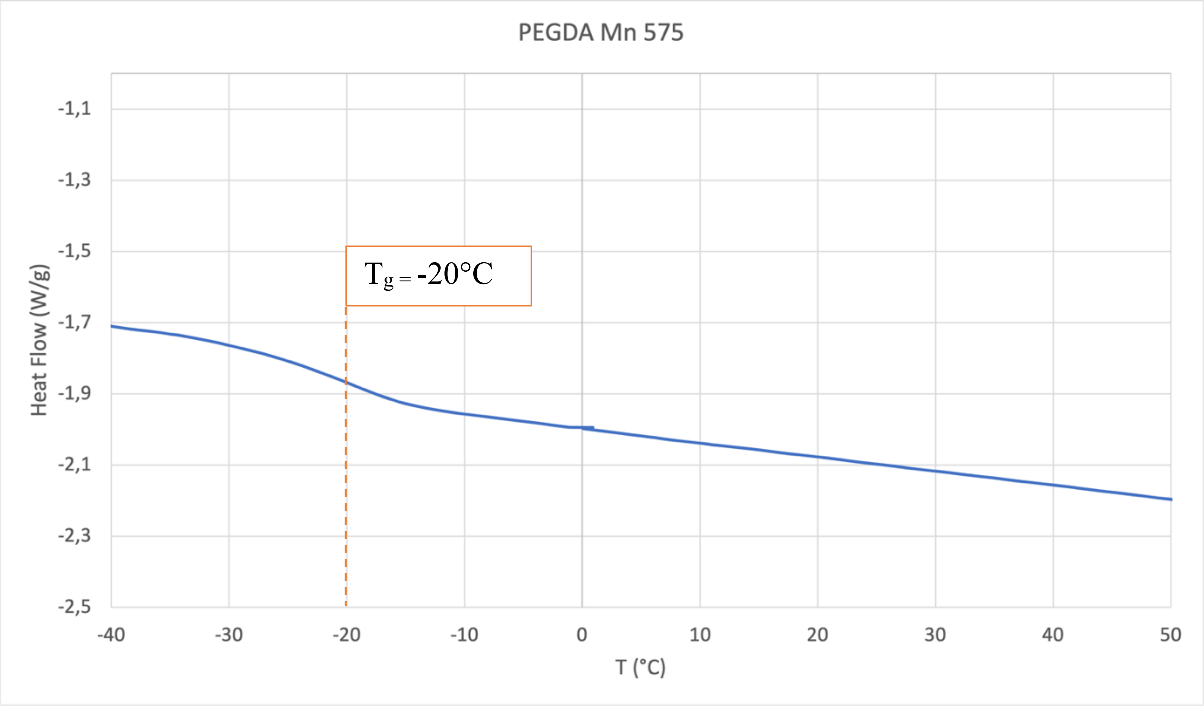

Figure 5.50. DSC: PEGDA Mn 575

As reported in the graph in Fig. 5.24, the glass transition temperature of PEGDA Mn 575 has been identified around -20°C. It is lower than the one of PEGDA Mn 250, as the molecular weight of the first one is higher: this cause the fact that the functional groups involved in the polymerization are less numerous, and therefore the cross-linked structure is more open and less dense, having higher amount of free volume between the polymeric chains. In fact, PEGDA Mn 575 is less rigid and more flexible than PEGDA Mn 250 at room temperature.

5.2.1.3 PEGDA Mn 250 + 50% (wt.) of Monofunctional ILM

The glass transition temperature deriving from DSC analysis is around 40°C (Fig. 5.25).

It is lower than the T_g of the material based only on PEGDA Mn 250, meaning that probably the presence of Poly (Ionic Liquid)s with certain concentration influence the physical properties of the polymeric material: specifically, they lower its glass transition temperature, thus making it less rigid at room temperature.

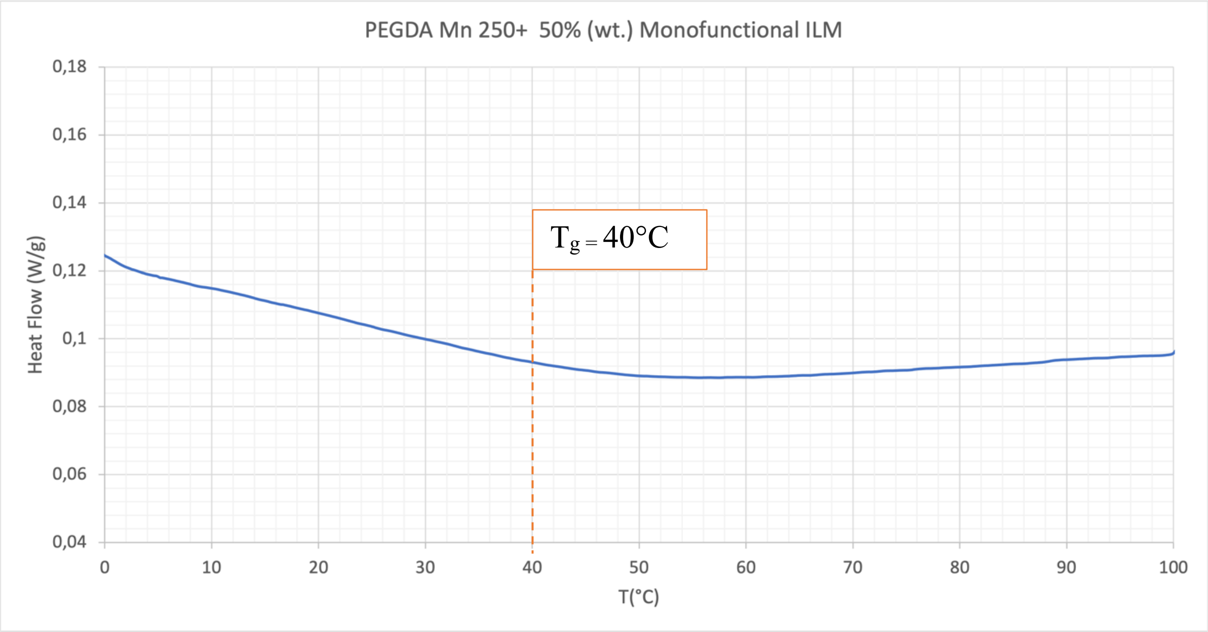

Figure 5.51. DSC: PEGDA Mn 250 + 50% (wt.) of Monofunctional ILM

5.2.1.4 PEGDA Mn 575 + 50% (wt.) of Monofunctional ILM

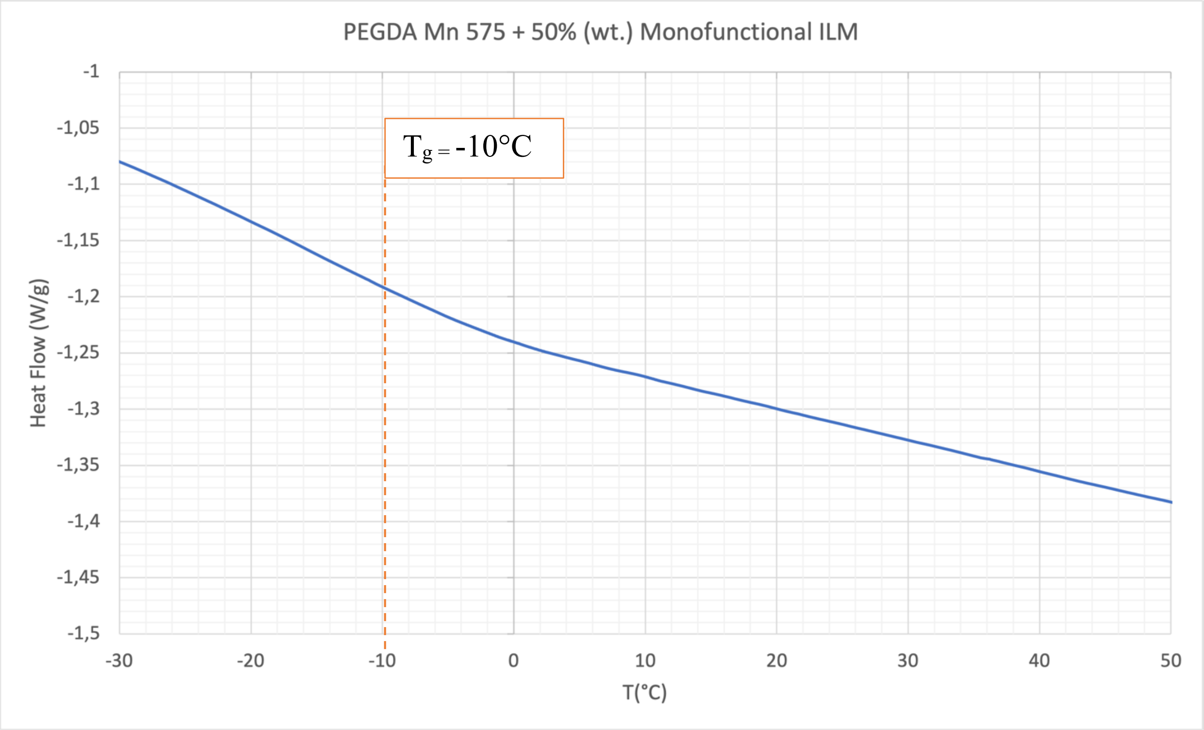

Figure 5.52. PEGDA Mn 250 + 50% (wt.) of Monofunctional ILM

In Fig. 5.26 the graph relative to the DSC of PEGDA Mn 575 + 50% (wt.) of Monofunctional ILM is reported: the glass transition temperature of this material has been defined around -10°C.

It is greater than the one of PEGDA Mn 575: even in this case, probably, the presence of PILs influences the thermomechanical properties of the material, that becomes slightly more rigid than the pure PEGDA Mn 575 at room temperature.

5.2.1.5 90% (wt.) of Monofunctional ILM + 10% (wt.) of Bifunctional ILM

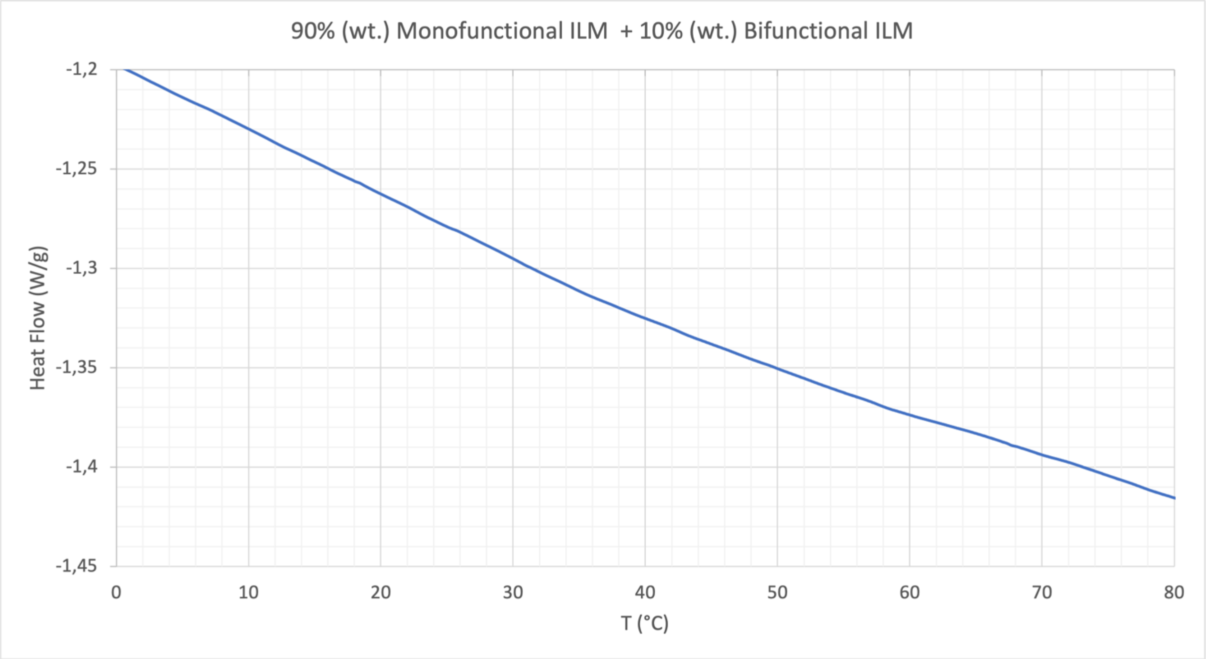

Figure 5.53. DSC: 90% (wt.) of Monofunctional ILM + 10% (wt.) of Bifunctional ILM

The material based only on PILs does not shows a clear change in the curvature of the graph resulting from its DCS analysis (Fig. 5.27). This is the reason why this test has been carried out more than once for this material, in order to obtain more significant curves. The glass transition temperature may be derived also from the DMTA analysis, that could be helpful to achieve more precise results.

5.2.1.6 90% (wt.) of Monofunctional ILM + 10% (wt.) of PEGDA Mn 575

Even for the material based on 90% (wt.) of Monofunctional ILM + 10% (wt.) of PEGDA Mn 575 (Fig.5.28) the identification of the glass transition temperature through DSC analysis turned out to be quite difficult. It may be evaluated in the range between 20-40 °C. The more precise value of T_g may be defined thanks to the results given by DMTA.

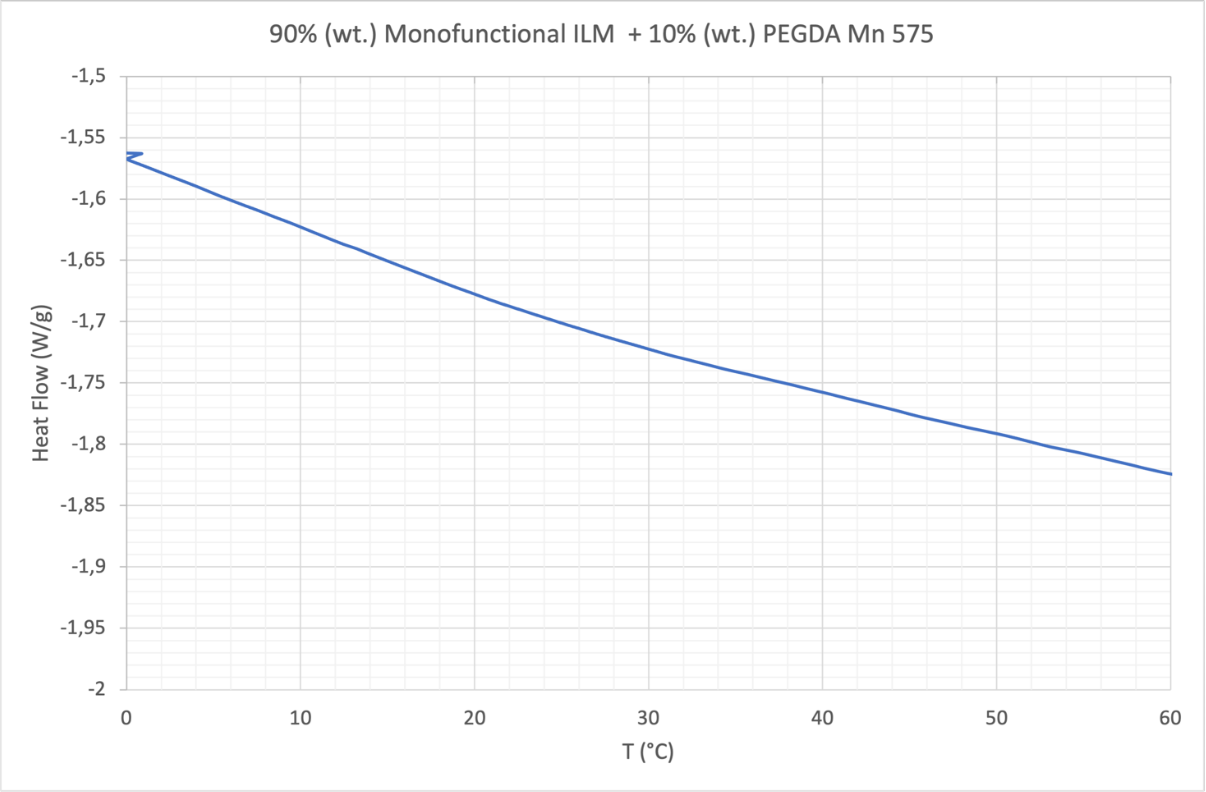

Figure 5.54. DSC: 90% (wt.) of Monofunctional ILM + 10% (wt.) of PEGDA Mn 575

5.2.2 DMTA

The interest in the results deriving from this thermo-mechanical analysis is connected to the possibility of monitoring how the storage modulus and the loss modulus of the materials vary at different temperatures, while the specimens are subjected to sinusoidal deformation.

In particular, the most important parameter to observe is tan δ, that usually presents a peak at the glass transition temperature's range. According to the presence of this peak of tan δ, the storage modulus G' should become drastically lower, as the material that in the first place had a rigid-elastic behavior, gradually presents a more viscous response.

The graphs deriving from the DMTA analysis of all the considered materials are presented, and the respective value of T_g have been discussed.

5.2.2.1 PEGDA Mn 250

In Fig. 5.29 the graph relative to the DMTA analysis of PEGDA Mn 250 is represented: the tan δ peak is evident at the temperature range around 60°C. This is coherent with the results given by the DSC analysis on the same material.

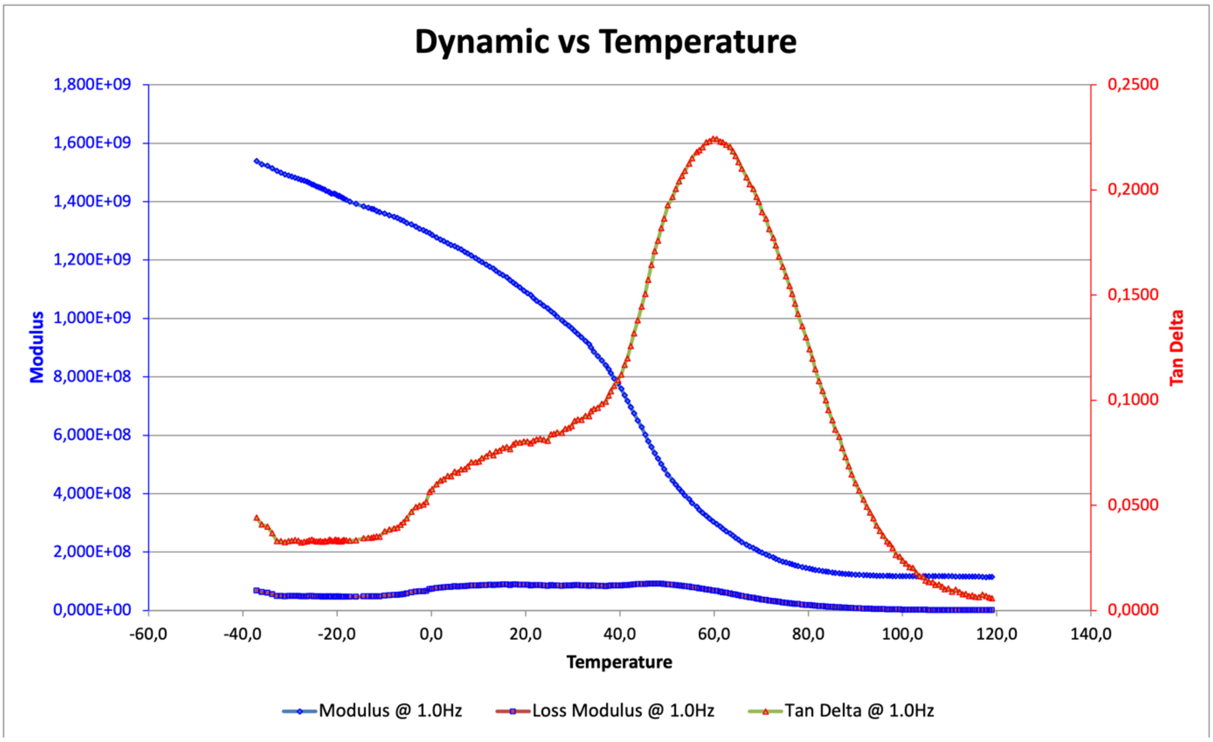

Figure 5.55. DMTA: PEGDA Mn 250

5.2.2.2 PEGDA Mn 575

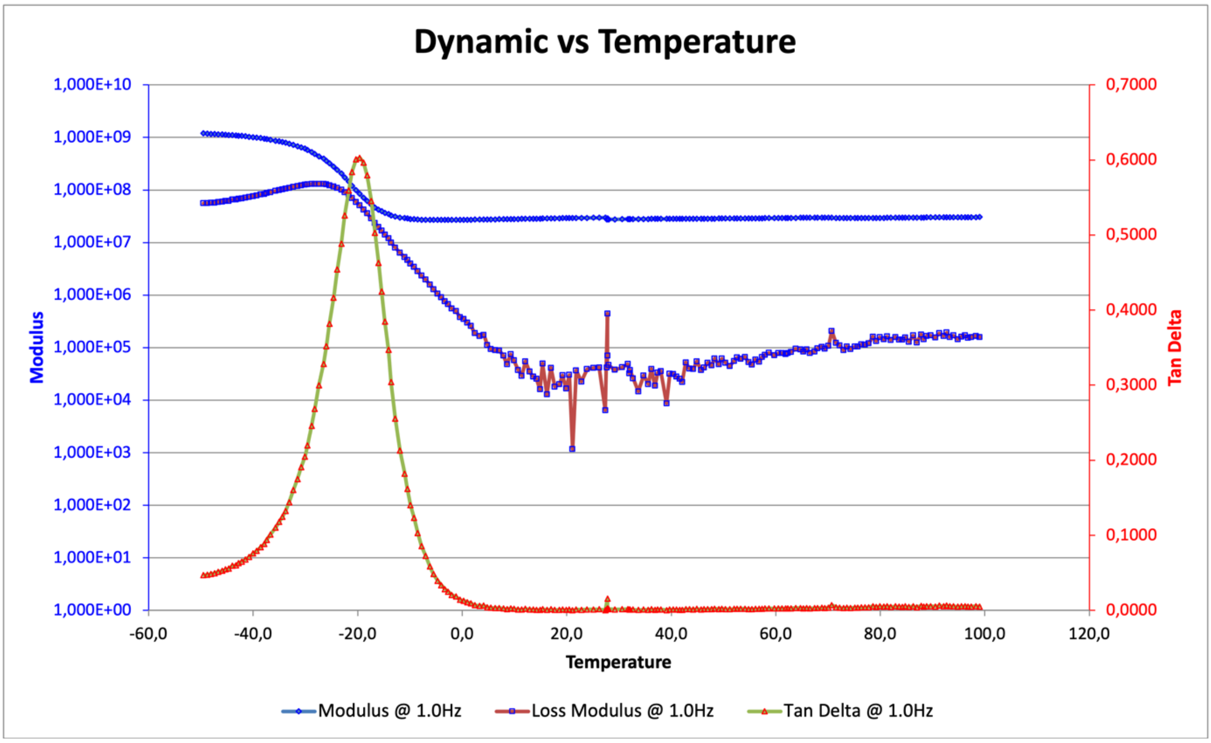

Figure 5.56. DMTA: PEGDA Mn 575

The graph in Fig. 5.30 demonstrates that a peak of tan δ is achievable around -20°C, in agreement with the decrease of G'. This glass transition temperature is very similar to the one identified by DSC analysis for PEGDA Mn 575.

5.2.2.3 PEGDA Mn 250 + 50% (wt.) Monofunctional ILM

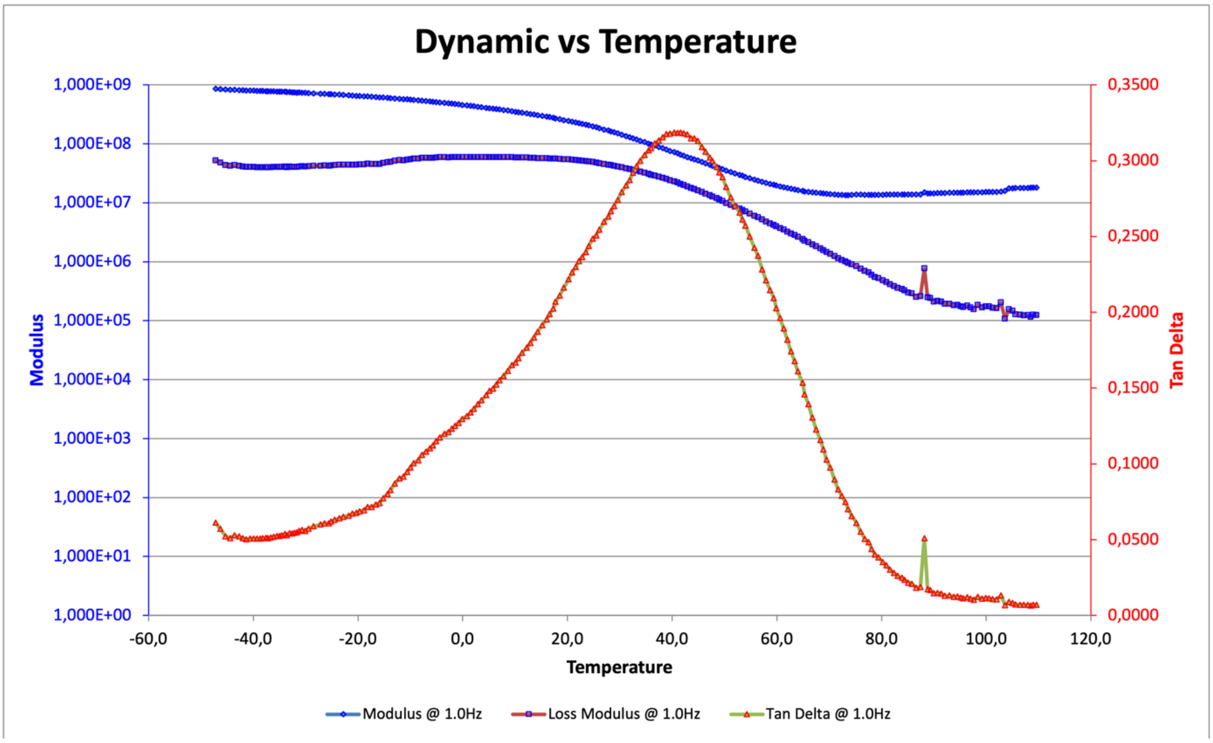

Figure 5.57. DMTA: PEGDA Mn 250 + 50% (wt.) Monofunctional ILM

In Fig. 5.31 the results of DMTA analysis made on PEGDA Mn 250 + 50% (wt.) Monofunctional ILM are reported: the tan δ peak is evident in a temperature range around 40°C, coherently with what derived from the DSC analysis concerning the glass transition temperature of this material.

5.2.2.4 PEGDA Mn 575 + 50% (wt.) Monofunctional ILM

The graph outcoming from the DMTA analysis of PEGDA Mn 575 + 50% (wt.) Monofunctional ILM is represented in Fig. 5.32: the glass transition temperature is observable around -10°C, considering the tan δ peak and the simultaneous decrease of the storage modulus G'. This T_g value confirms the reliability of the DSC's results.

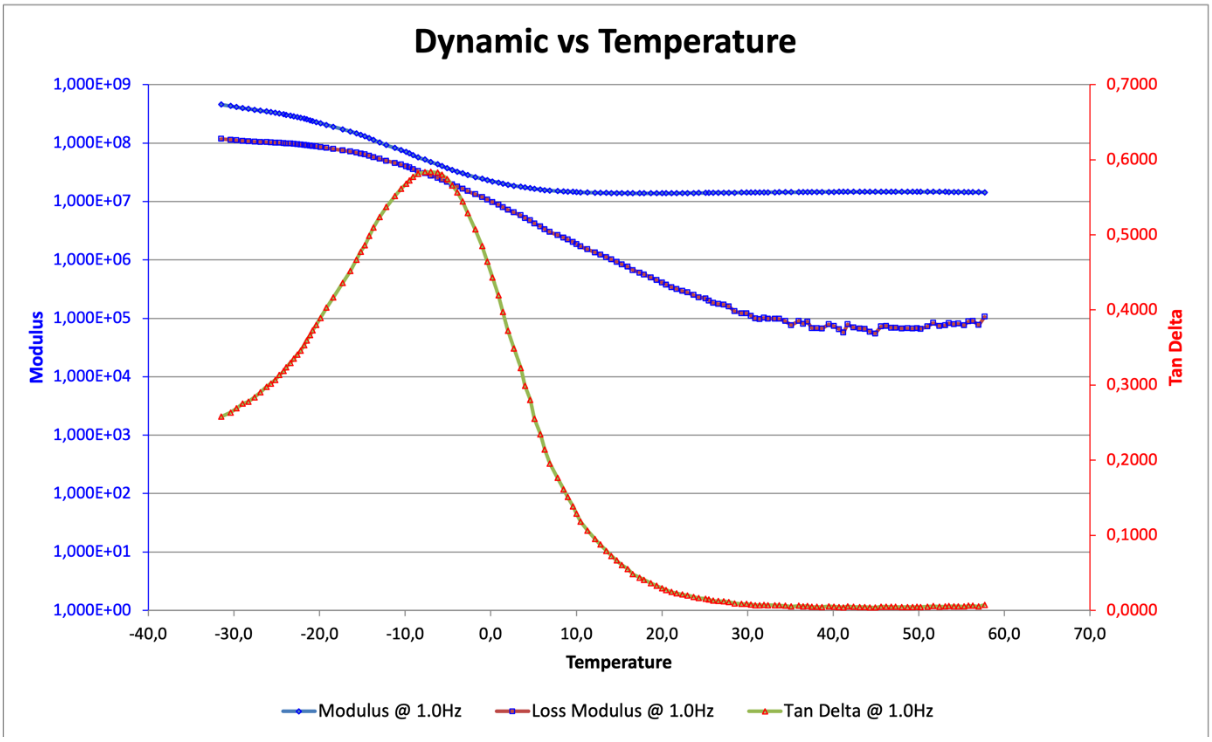

Figure 5.58. DMTA: PEGDA Mn 575 + 50% (wt.) Monofunctional ILM

5.2.2.5 90% (wt.) of Monofunctional ILM + 10% (wt.) of Bifunctional ILM

The results deriving from the DMTA analysis of the material based only on PILs (90% (wt.) of Monofunctional ILM + 10% (wt.) of Bifunctional ILM) are different from the ones provided for the other materials (Fig. 5.33): in particular, the peak of tan δ is not that evident, even though the storage modulus G’ decreases as expected.

Even though many DMTA tests have been provided for this material, in order to improve its outcoming graph, the same results have been obtained.

Nevertheless, it is possible to identify the glass transition temperature of this material with the temperature range within which the storage modulus decreases more rapidly, that is around 40°C.

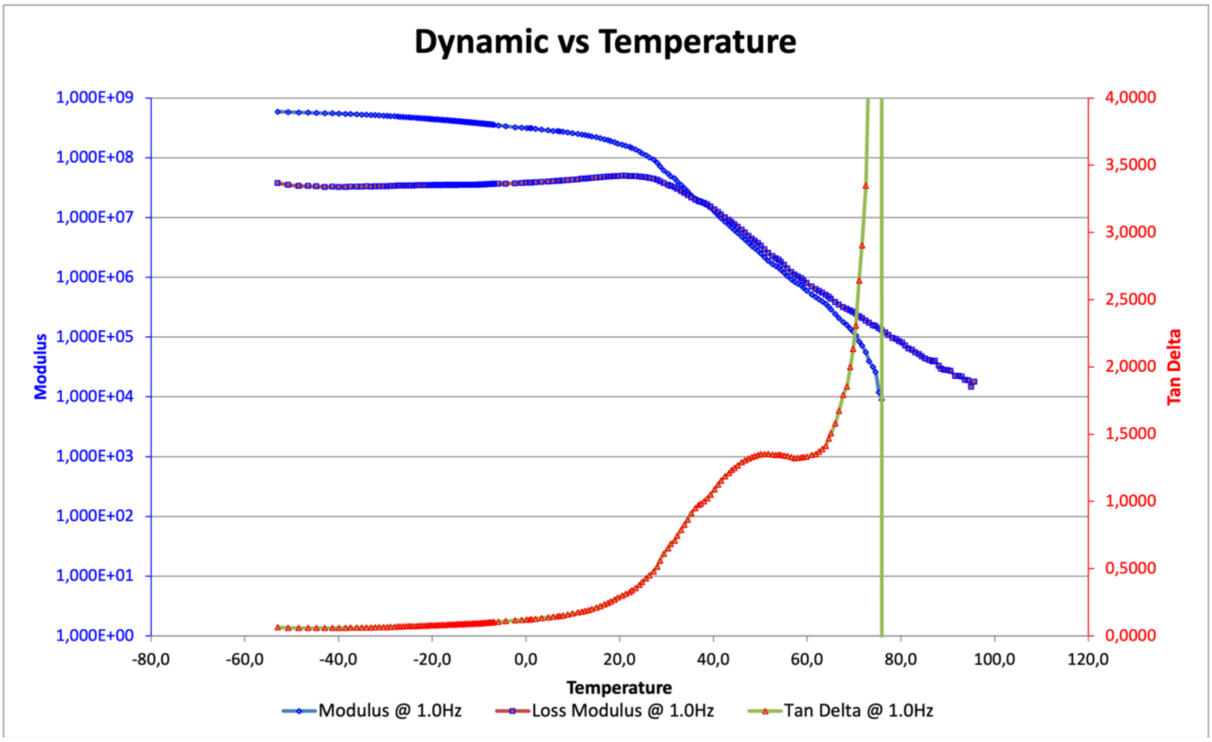

Figure 5.59. DMTA: 90% (wt.) of Monofunctional ILM + 10% (wt.) of Bifunctional ILM

5.2.2.6 90% (wt.) of Monofunctional ILM + 10% (wt.) of PEGDA Mn 575

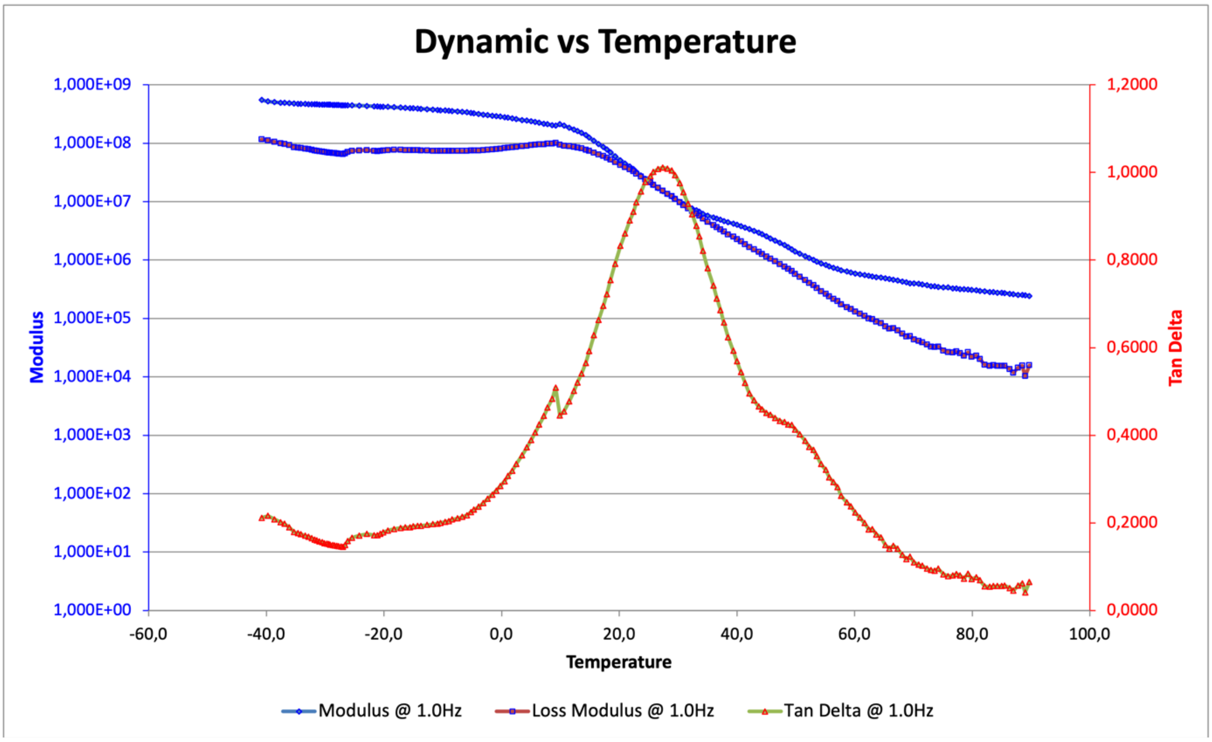

Figure 5.60. 90% (wt.) of Monofunctional ILM + 10% (wt.) of PEGDA Mn 575

The graph in Fig. 5.34 shows that the material based on 90% (wt.) of Monofunctional ILM + 10% (wt.) of PEGDA Mn 575 presents a glass transition temperature in a range around 30°C.

This could be defined observing the tan δ peak and the decrease of G' and it is coherent with the considerations made for the other materials characterized by the presence of PEGDA and PILs, for instance, the one discussed in 5.2.2.4. This one, is characterized by a lower concentration of PILs, and a lower T_g, meaning that there may be a correlation between the concentration of PILs into the polymeric material and the variation of its glass transition temperature.

In the case of materials based on PEGDA Mn 575, considering its low T_g (-20°C), the presence of PILs increases this parameter, with the increase of the concentration of Poly (Ionic Liquid)s themselves (that have a T_g higher than the one of PEGDA Mn 575, as reported in 5.2.2.5). This may be due to the high molecular interactions given by the ionic species of the ILs.

5.2.3 Considerations on DSC-DMTA Results

Material	**T_g**	**G' (RT) [Pa]**	**G'(T_g + 50°C) [Pa]**
PEGDA 250	60 °C	$1{,}025 \times 10^9$	$1{,}176 \times 10^8$
PEGDA 575	-20 °C	$2{,}96 \times 10^7$	$2{,}78 \times 10^7$
50% (wt.) PEGDA 250+ 50% (wt.) MF-ILM	40 °C	$1{,}917 \times 10^8$	$1{,}449 \times 10^7$
50% (wt.) PEGDA 575+ 50% (wt.) MF-ILM	-10 °C	$1{,}402 \times 10^7$	$1{,}457 \times 10^7$
90% (wt.) MF-ILM + 10% (wt.) BF-ILM	40 °C	$1{,}096 \times 10^8$	$8{,}923 \times 10^3$
90% (wt.) MF-ILM + 10% (wt.) BF-ILM	30 °C	$2{,}153 \times 10^7$	$3{,}018 \times 10^5$

Table 5.3 Main results from DSC and DMTA

Analyzing the data obtained from DSC and DMTA (Tab. 5.3), it is possible to make some considerations:

- When a rubbery (at room temperature) matrix is used (PEGDA 575) the addition of a monofunctional polymerizable ionic liquid seems to induce two opposing effects, indeed the addition of a monofunctional monomer leads to the formation of a more loosely network with lower crosslinking density (represented by the lower G' in the rubbery state), nevertheless the ionic nature of the monofunctional IL induces strong molecular interactions that leads to an increase of the T_g.

- On the contrary, when a glassy matrix at room temperature is considered (PEGDA 250) the decrease of the crosslinking density plays a major role leading to the decrease of the T_g when the ILM is added to the matrix.

- The material completely based on PILs is characterized by a broad T_g range that starts at about 20°C and presents its maximum above 40°C indicating that the material at room temperature is close to its T_g. Furthermore, above the tan δ peak, the material presents a complete loss of the mechanical properties: the low crosslinking density due to the low amount of bifunctional monomer, less reactive than PEGDA, leads to a very soft material above the T_g region.

5.3 Absorption Capacity

The absorption capacity of the six considered materials was investigated as reported in 4.2. The tests were carried out for all the solvents described in that paragraph, and the absorption capacity has been expressed in function of the concentration of the gaseous volatile organic compound interacting with the materials.

In the first place, the absorption of acetone, isopropyl alcohol and ortho-dichlorobenzene was evaluated. Then, after having considered the results given by these tests, the absorption of acetonitrile and chloroform was investigated, in order to compare their behavior with the one of the solvents previously tested, in relation to their physical and chemical characteristics (such as their dielectric constant and their boiling temperature).

5.3.1 Acetone

As reported in the graph in Fig. 5.35, for the majority of the considered materials, their capacity in the absorption of acetone becomes higher with the increase of its concentration, until a plateau is reached. In general, the maximum absorption capacity is around 55%, while the lowest is less than 0,5%.

It is evident that the material based only on PILs (90% (wt.) of Monofunctional ILM + 10% (wt.) of Bifunctional ILM) is the one that presents the greatest absorption capacity for acetone, followed by the material characterized by 90% (wt.) of Monofunctional ILM + 10% (wt.) of PEGDA Mn 575.

This means that the presence of Poly (Ionic Liquid)s into the polymeric materials increases considerably their absorption capacity: for instance, the behavior of the material based on PEGDA Mn 575 + 50% (wt.) Monofunctional ILM is better than the one of PEGDA Mn 575. Furthermore, it is also clear that the higher the concentration of PILs in the polymeric material, the higher their capacity to absorb acetone.

The behavior of the materials based on PEGDA Mn 250 is the worst, in terms of their absorption capacities, as the dense molecular structure of this polymer does not facilitate the absorption and the diffusion of this solvent into it. In fact, the more open molecular structure of PEGDA Mn 575, let this material have higher absorption capacity than PEGDA Mn 250.

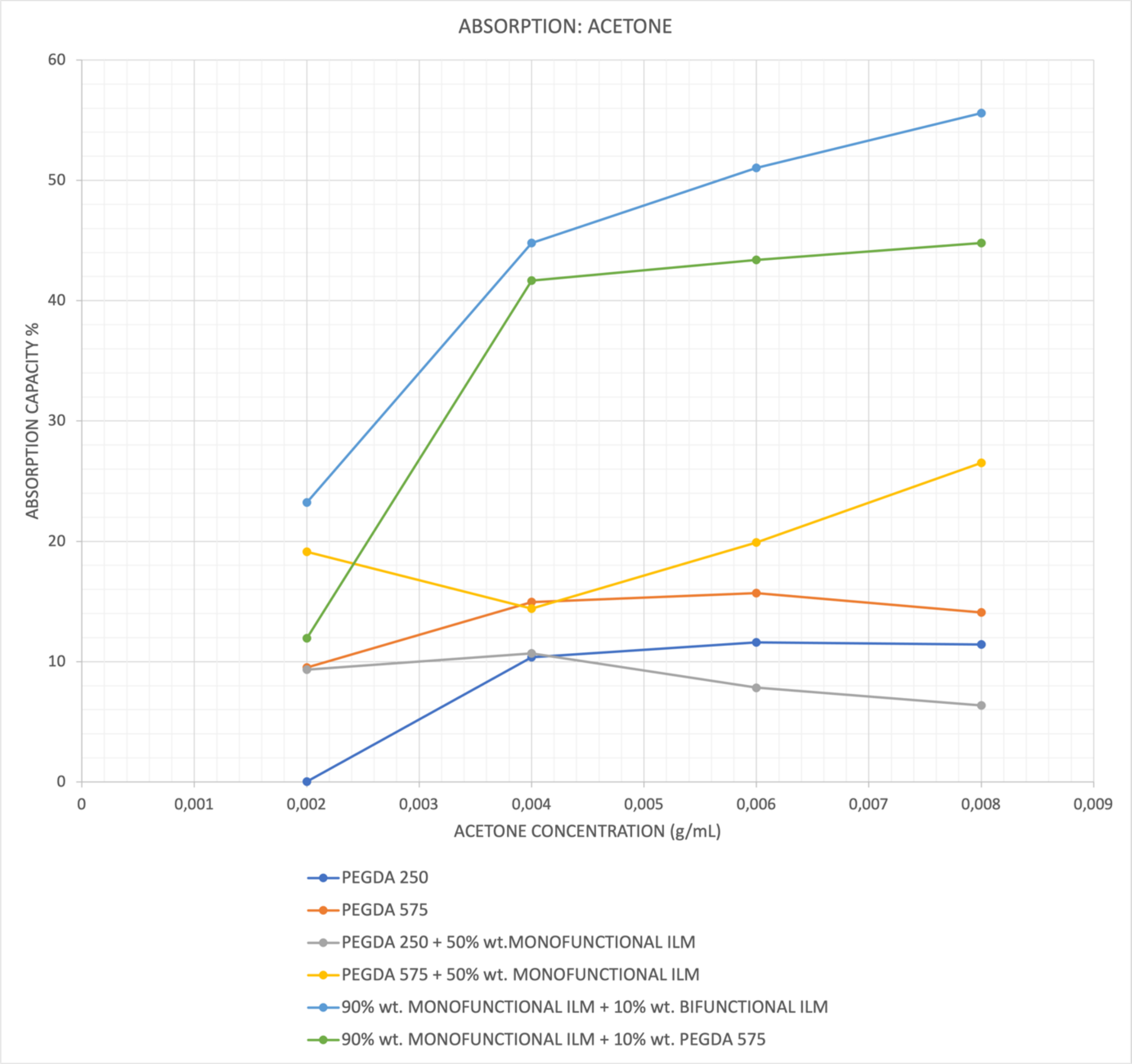

Figure 5.61. Absorption of Acetone

5.3.2 Isopropyl Alcohol

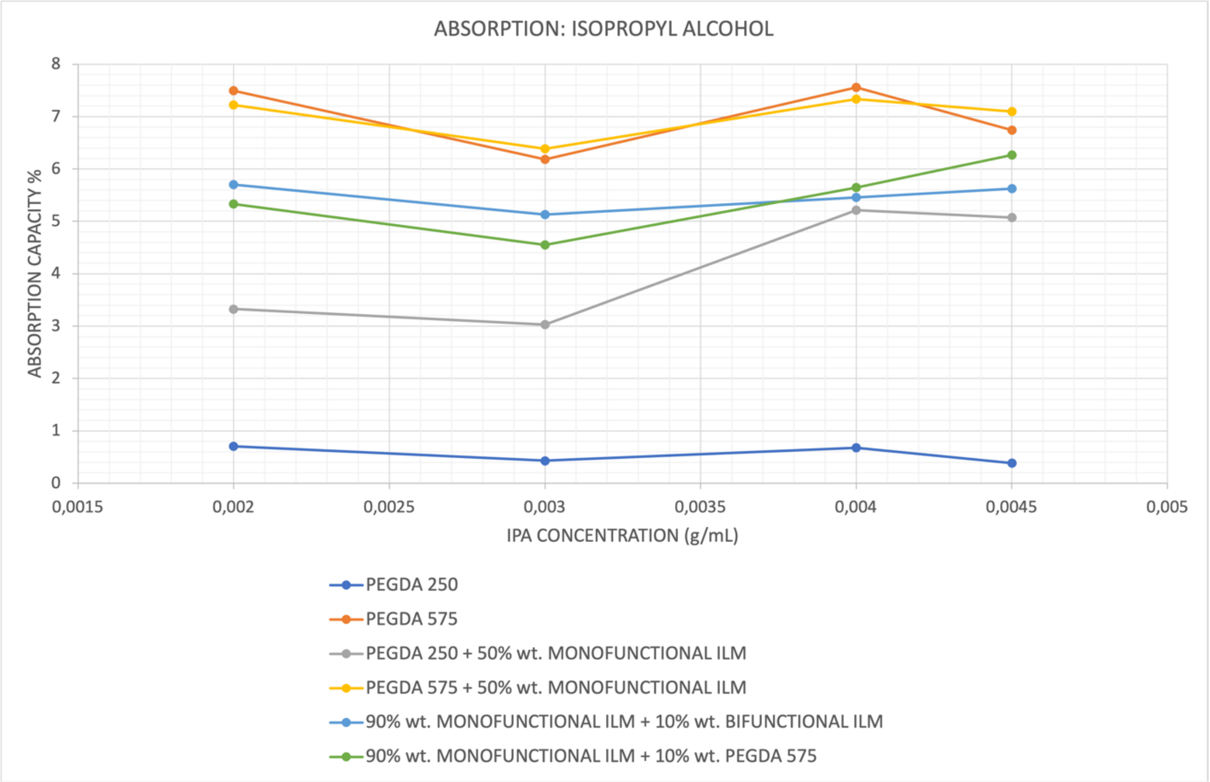

Figure 5.62. Absorption of Isopropyl Alcohol (IPA)

Differently from the results obtained for the absorption of acetone, the materials' absorption capacities relative to isopropyl alcohol (Fig. 5.36) do not vary considerably with the increase of the solvent's concentration. The maximum absorption capacity is around 8%, which is way lower than the one observed in the case of acetone.

Furthermore, in this case the materials with the highest capacity to absorb isopropyl alcohol are the ones based on PEGDA Mn 575. In fact, the presence of PILs into the polymeric structure seems not to influence considerably the ability of the materials to absorb isopropyl alcohol, not even when they are present in higher concentrations.

Also in this case, the materials based on PEGDA Mn 250 are the ones that provide the worst absorption capacities, due to their denser molecular structure.

5.3.3 Ortho-dichlorobenzene

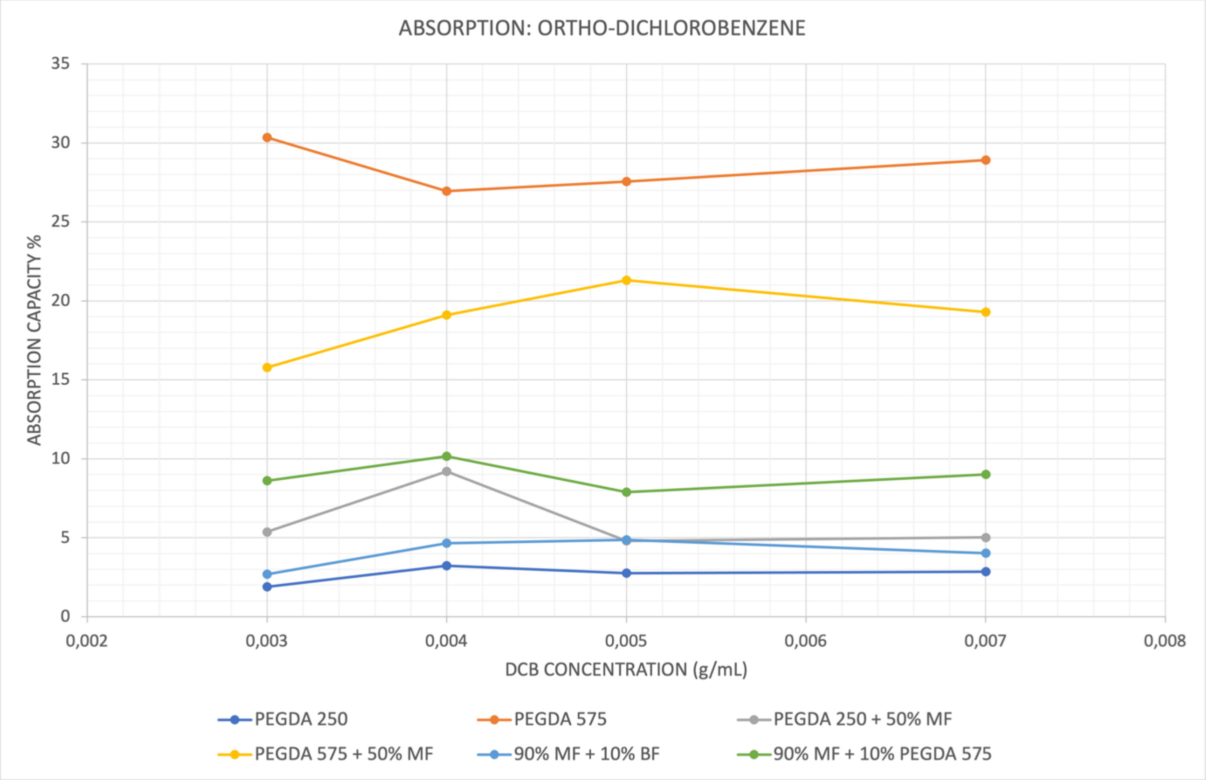

Figure 5.63. Absorption of Ortho-dichlorobenzene (ODB)

The graph in Fig. 5.37 shows the trends of the materials' capacities in the absorption of ortho-dichlorobenzene. Even in this case, the absorption capacities of these materials do not vary a lot with the concentration of the volatile solvent. The maximum absorption capacity is around 30% and it is presented by PEGDA Mn 575, followed by the materials based on PEGDA Mn 575 + 50%(wt.) of Monofunctional ILM.

The material based only on PILs (represented by the green curve), presents an intermediate absorption capacity, and so does the one characterized by 90% (wt.) of Monofunctional ILM + 10% (wt.) of PEGDA Mn 575. This means that probably the presence of higher concentration of PILs does not improve greatly the ability of the polymeric materials to capture ortho-dichlorobenzene.

On the contrary, the molecular structure of the polymers plays and important role in the definition of this property: while the open structure of PEGDA Mn 575 is the one characterized by the greater absorption ability, the denser one of PEGDA Mn 250 provides the worst behavior.

5.3.4 Acetonitrile

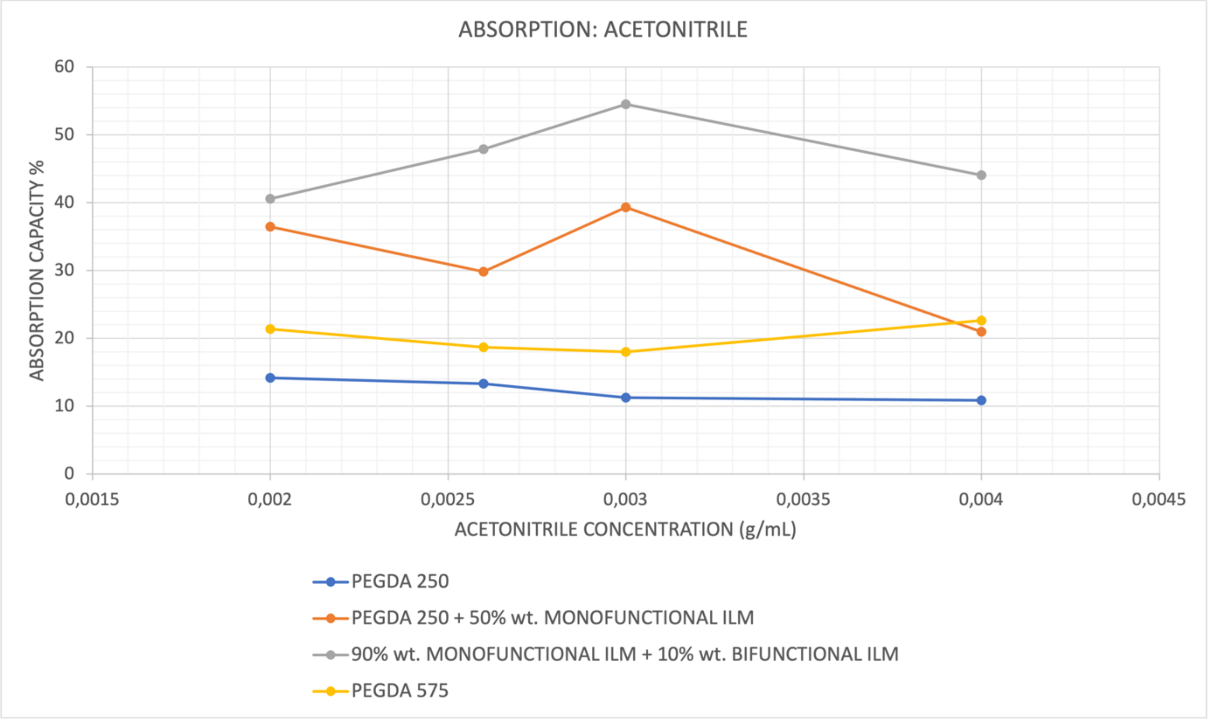

Figure 5.64. Absorption of Acetonitrile

It was chosen acetonitrile as the fourth volatile organic compound to be used, in order to test the absorption capacities of the materials, because of its physical and chemical characteristics.

In fact, it has a dielectric constant (that defines its polarity) which is higher than the ones of the solvents considered previously, while its boiling temperature (that may influence the amount of gaseous solvent interacting with the specimens) is similar to the one of isopropyl alcohol.

The behavior of the materials in the absorption of acetonitrile (Fig. 5.38) may be significant to identify which parameter characterizing the solvents is decisive to justify the effectiveness of its interaction with the different materials.

As expected, the material that presented the highest capacity to absorb acetonitrile was the one based only on PILs, with a maximum absorption capacity around 55% (as in the case of acetone), followed by the other material that is characterized by the presence of PILs, in lower concentration (PEGDA Mn 250 + 50% (wt.) Monofunctional ILM).

PEGDA Mn 250 and PEGDA Mn 575 presented the worst behavior in terms of their absorption capacity.

This test that involved acetonitrile, as the one involving acetone, are significative to explain the relationship between the dielectric constant (polarity) of the volatile organic compound to be absorbed and the Poly (Ionic Liquid)s' capacity to capture it efficiently. In fact, the two solvents previously mentioned, are characterized by the highest dielectric constants (compared to the ones of the other volatile organic compounds that have been considered) and they are absorbed more efficiently by the polymeric material based completely on PILs.

5.3.5 Chloroform

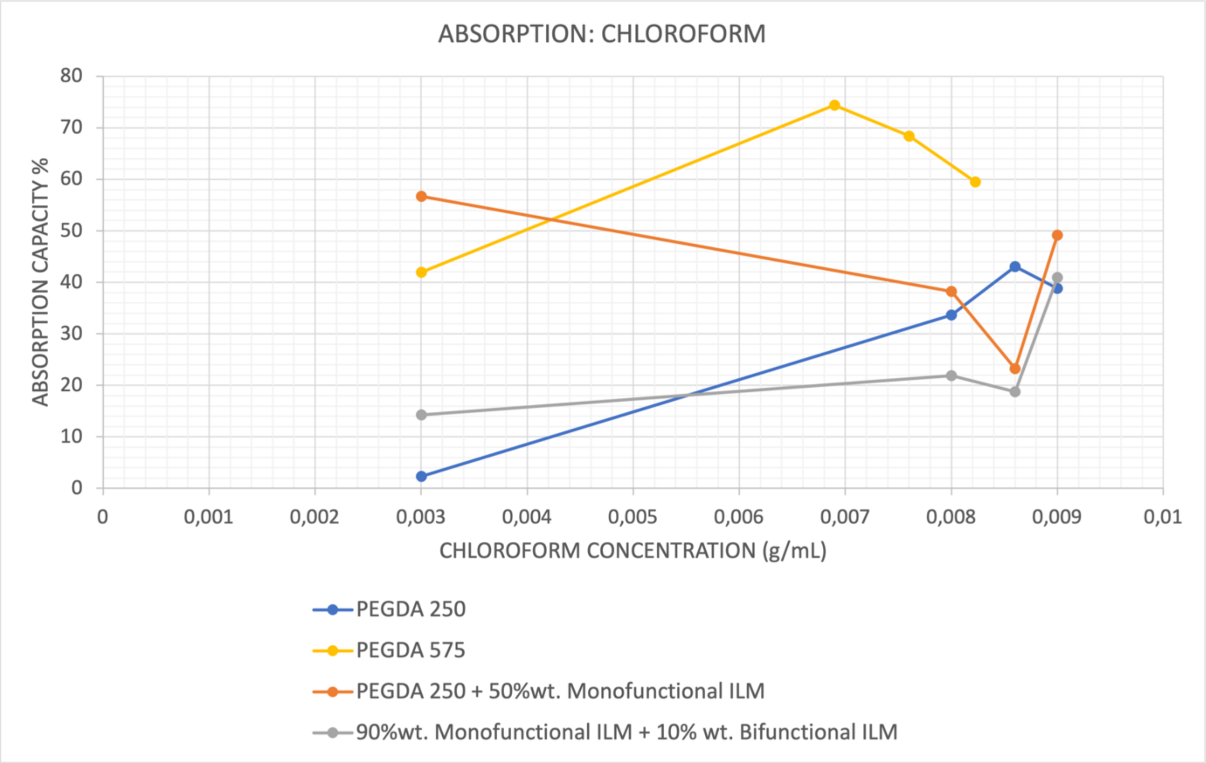

Figure 5.65. Absorption of Chloroform

The last absorption tests were carried out with chloroform (Fig. 5.39), that was chosen because of its dielectric constant and its boiling temperature, which are lower than the ones of the other volatile organic compounds that have been considered.

These tests were made to evaluate the influence of the low boiling temperature of the organic solvent in the absorption phenomena. In fact, these conditions provide easier evaporation of the VOC and so a higher concentration of gas interacting with the materials, by which the amount of organic vapor absorbed by the material may be influenced.

The material that presents the greatest ability to absorb chloroform is PEGDA Mn 575, whose maximum absorption is around 75%.

The materials based completely on PILs does not excel in the absorption of this solvent: this may indicate that, in order to maximize the absorption of chloroform, the presence of PILs is not decisive, and that, on the contrary, it is preferable to have a polymeric material with a molecular structure which is not too dense.

This is coherent with the hypothesis for which a higher dielectric constant of the solvent favors its interaction with the PILs-based materials that are supposed to absorb it.

5.4 Desorption Capacity

The desorption capacity of the six considered materials has been studied just for three significant volatile organic compounds, characterized with different properties. These are acetone, isopropyl alcohol, and ortho-dichlorobenzene.

The aim of these tests is to evaluate how solvents with different boiling temperature and polarity are desorbed from the variable polymeric materials, and if these parameters are actually important to define their ability to be regenerated.

All the regeneration tests were carried out as reported in 4.3.

5.4.1 Acetone

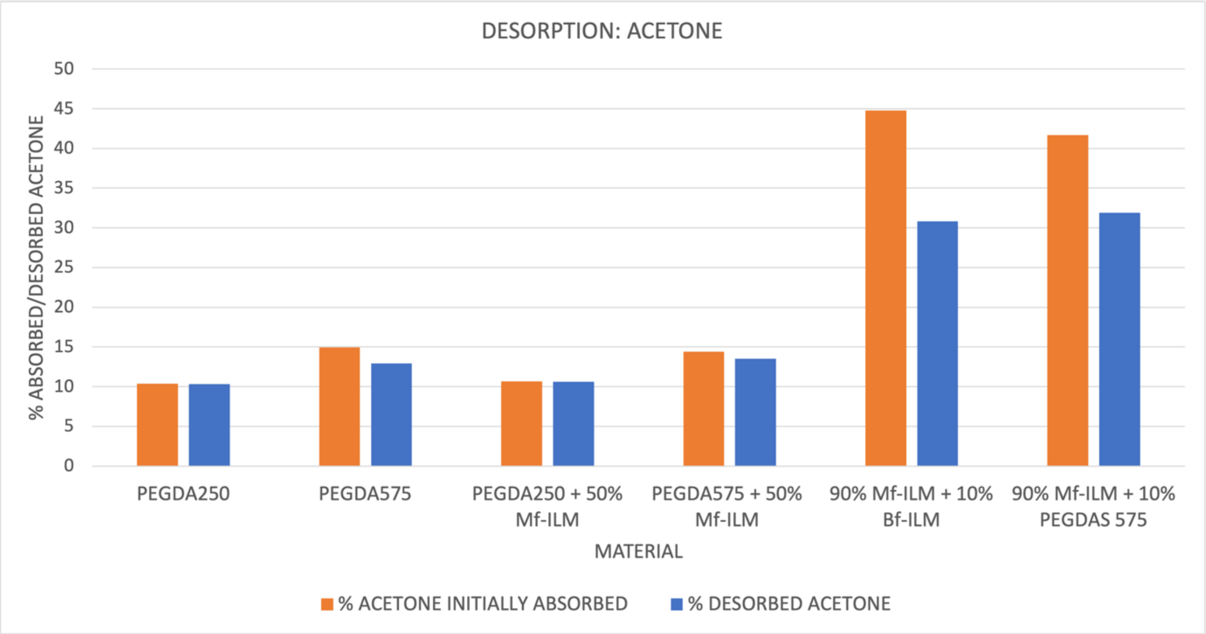

Figure 5.66. Desorption of Acetone

The histogram in Fig. 5.40 reports the comparison between the amount of acetone absorbed by the materials and the relative percentage of solvent desorbed from them.

In general, the two considered quantities are similar, if not equal, so it is possible to state that the regeneration of these materials from acetone is efficient.

The materials based completely on PILs show a slightly worse behavior than the others, as the difference in the quantities of absorbed and desorbed solvent is higher than the one presented by the other polymeric materials. This may be due to the interaction occurring between this polar solvent (with a dielectric constant of 21) and the Poly (Ionic Liquid)s.

5.4.2 Isopropyl Alcohol

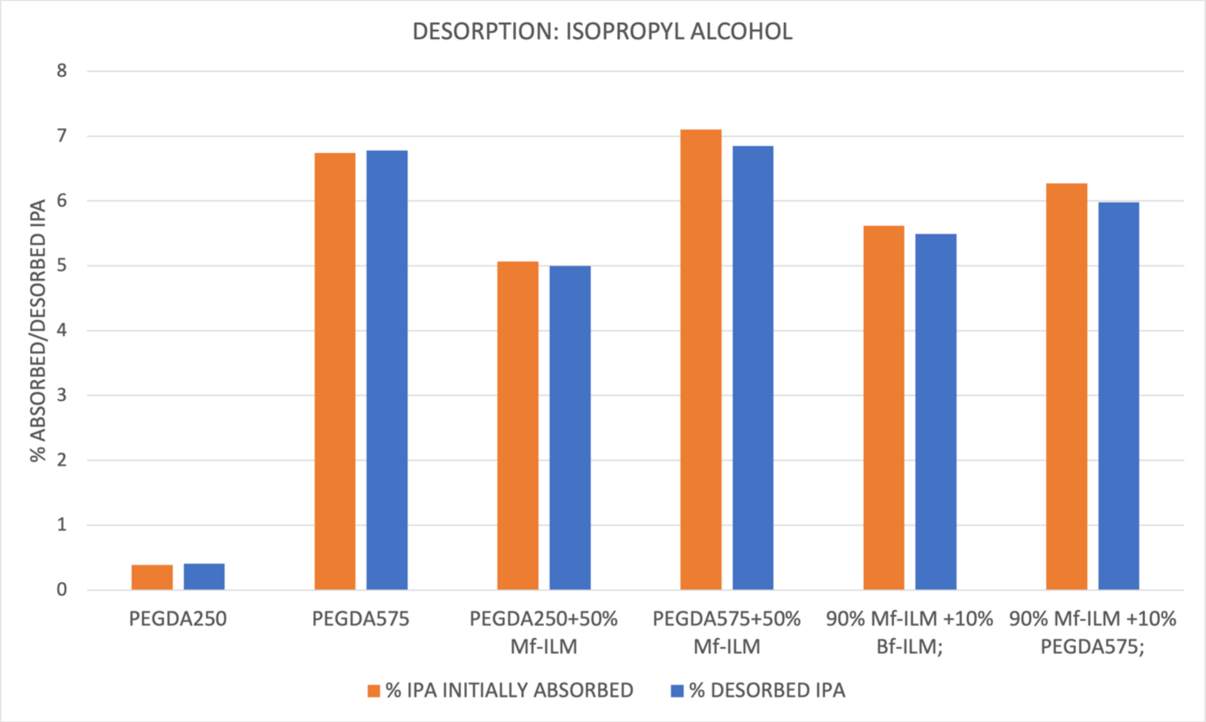

Figure 5.67. Desorption of Isopropyl Alcohol

In Fig. 5.41 the results relative to the desorption of isopropyl alcohol from the considered materials are reported: in general, it is evident that all the absorbed isopropyl alcohol is completely desorbed from each polymeric material.

This means that the regeneration of these materials not only is possible, but it may be also useful to make them re-usable for a second absorption of solvent.

5.4.3 Ortho-dichlorobenzene

The results of the desorption tests made with materials that had previously absorbed ortho-dichlorobenzene are presented in Fig. 5.42.

All the materials show good desorption capacity, considering that the amount of desorbed solvent is close to the one of VOC that was absorbed prior to this test.

The materials that provided the highest absorption capacity for ortho-dichlorobenzene, that are the ones based on PEGDA Mn 575, showed a slightly lower desorption ability.

This could be caused by the physical interactions occurring between the solvent and the polymers, like hydrogen bonds or electrostatic forces.

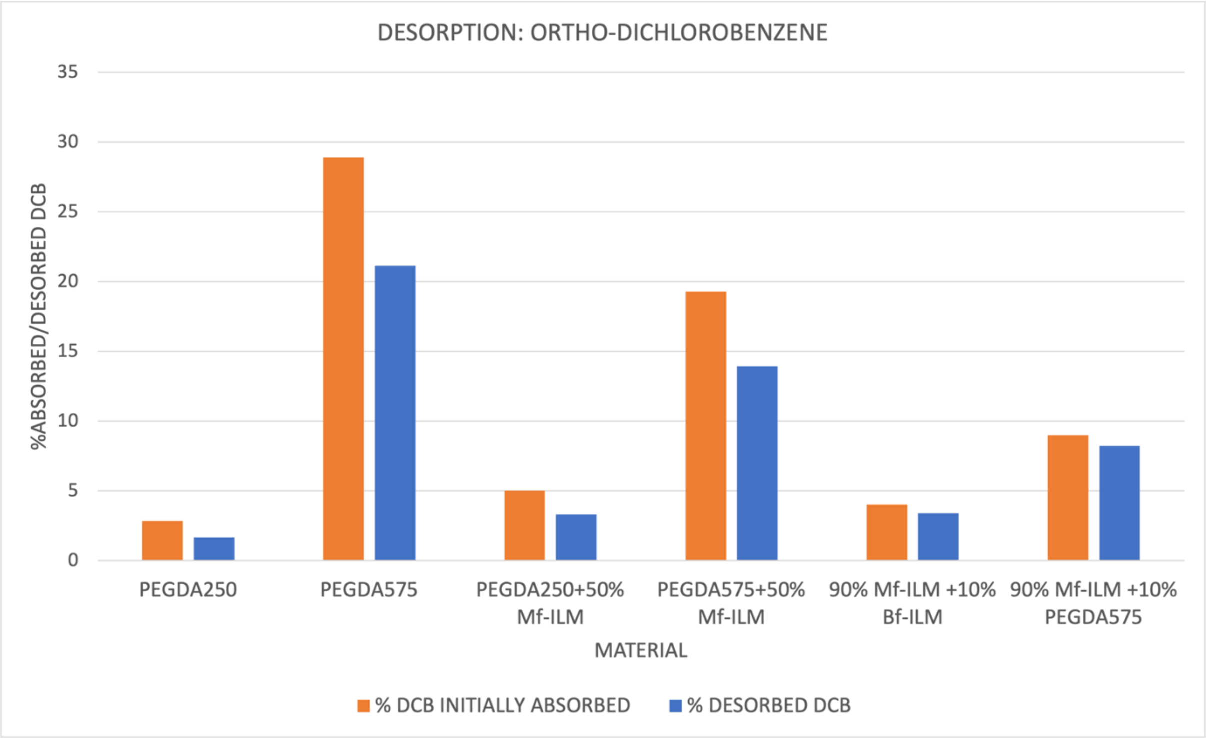

Figure 5.68. Desorption of Ortho-dichlorobenzene

5.4.4 FTIR Spectroscopy to monitor Absorption and Desorption of Chloroform

The desorption of chloroform was carried out in order to observe, thanks to FTIR spectroscopy, the presence and the absence of this volatile compound in the materials.

Wang *et al.* [5] reported on their paper different FTIR spectra made for Room Temperature Ionic Liquids to evaluate their regeneration ability after the absorption of toluene.

In this case, the behavior of Poly (Ionic Liquid)s has been taken into account, and the considered volatile organic compound is chloroform, though a similar technique has been adopted in order to evaluate the efficiency of the desorption.

In fact, this aim was pursued by analyzing the difference between the spectra collected in different conditions:

- A spectrum relative to the material that had not absorbed chloroform yet;

- A spectrum relative to the material after the absorption of chloroform;

- A spectrum relative to the material after the desorption of chloroform.

These spectra were also compared to the one of pure gaseous chloroform [6], reported in Fig. 5.43. The spectra were collected for three significative materials, interacting with chloroform: PEGDA Mn 250, PEGDA Mn 250 + 50% (wt.) of Monofunctional ionic liquid monomers, 90% (wt.) of Monofunctional ILM + 10% (wt.) of Bifunctional ILM.

In all the spectra represented in Fig. 5.44-5.49 it is possible to notice that the ones relative to the materials before the absorption of chloroform and the ones relative to the materials that had absorbed it, differs only for a peak around 700 cm^{-1} (indicated by the yellow circle), which is also visible in pure chloroform spectrum. This proves that the gaseous chloroform is actually present in the materials, despite its high volatility.

The spectra relative to the materials after chloroform's desorption are similar to the ones that characterized them before the absorption of this VOC. This is meaningful in the evaluation of the regeneration ability of the considered materials, and confirms the positive results given by the desorption tests of other solvents, presented previously.

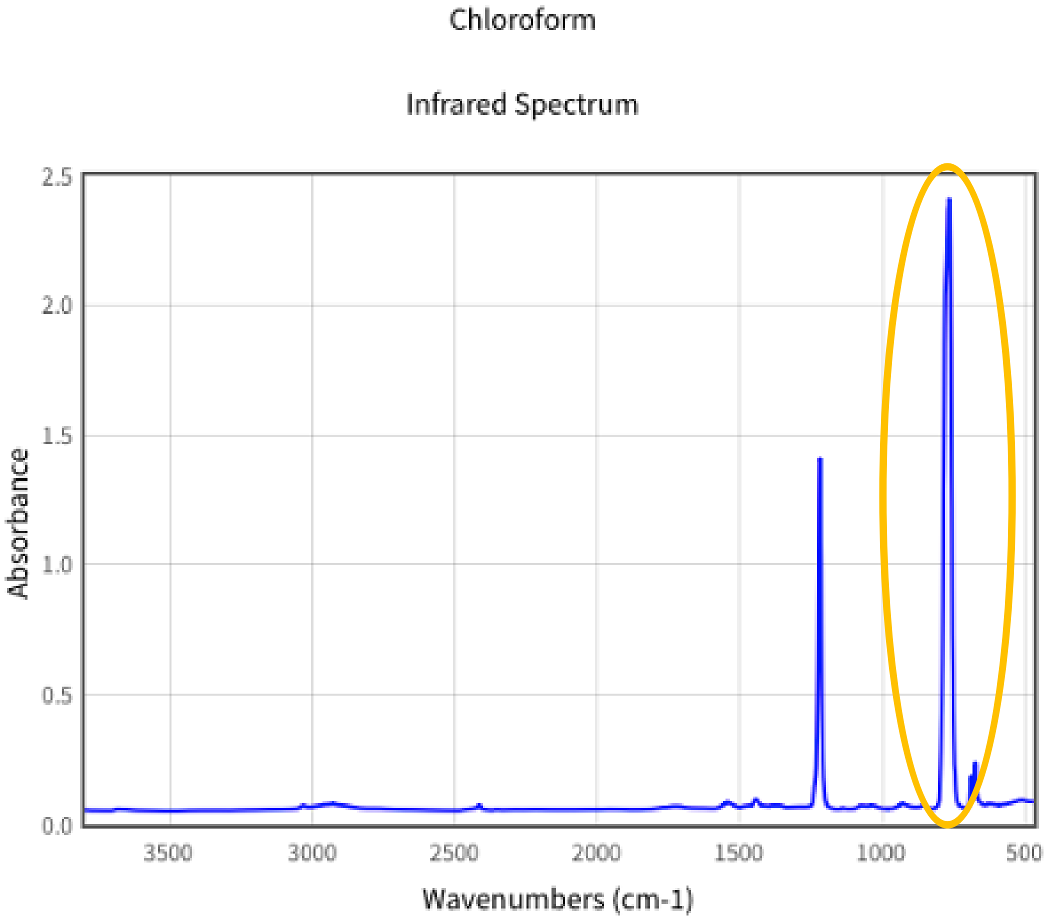

Figure 5.69. FTIR spectrum of gaseous chloroform [6]

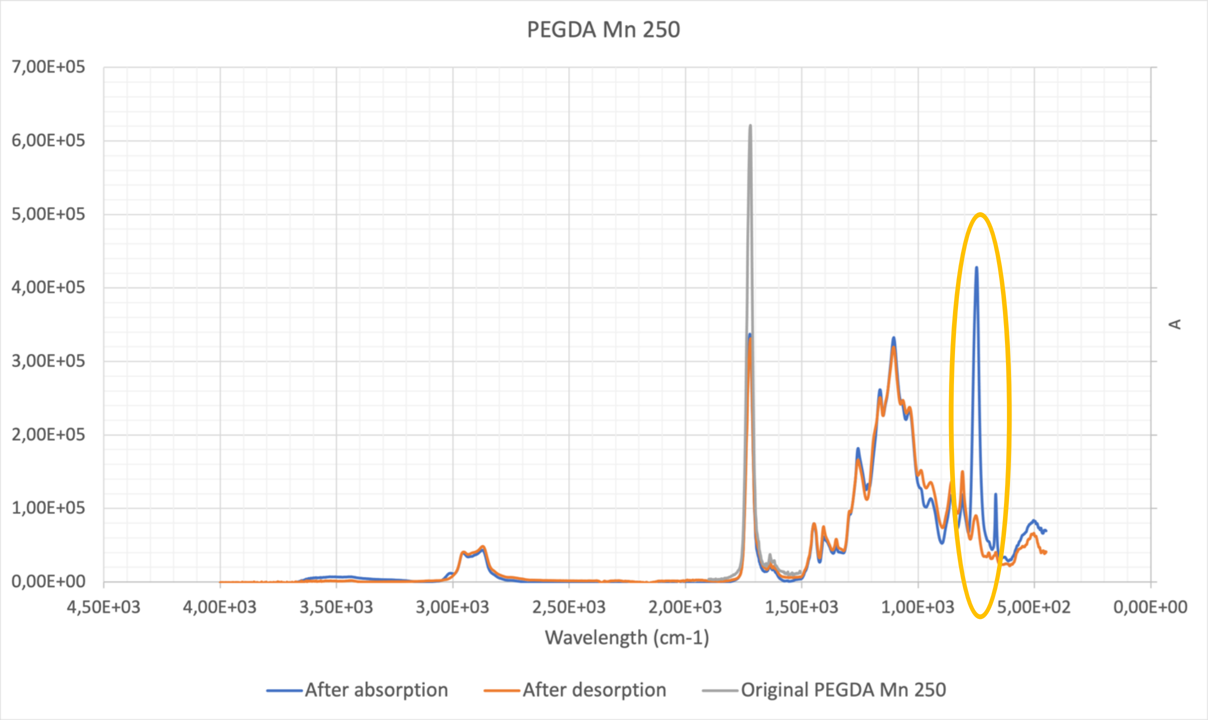

Figure 5.70. FTIR spectra: absorption/desorption of chloroform by PEGDA Mn 250

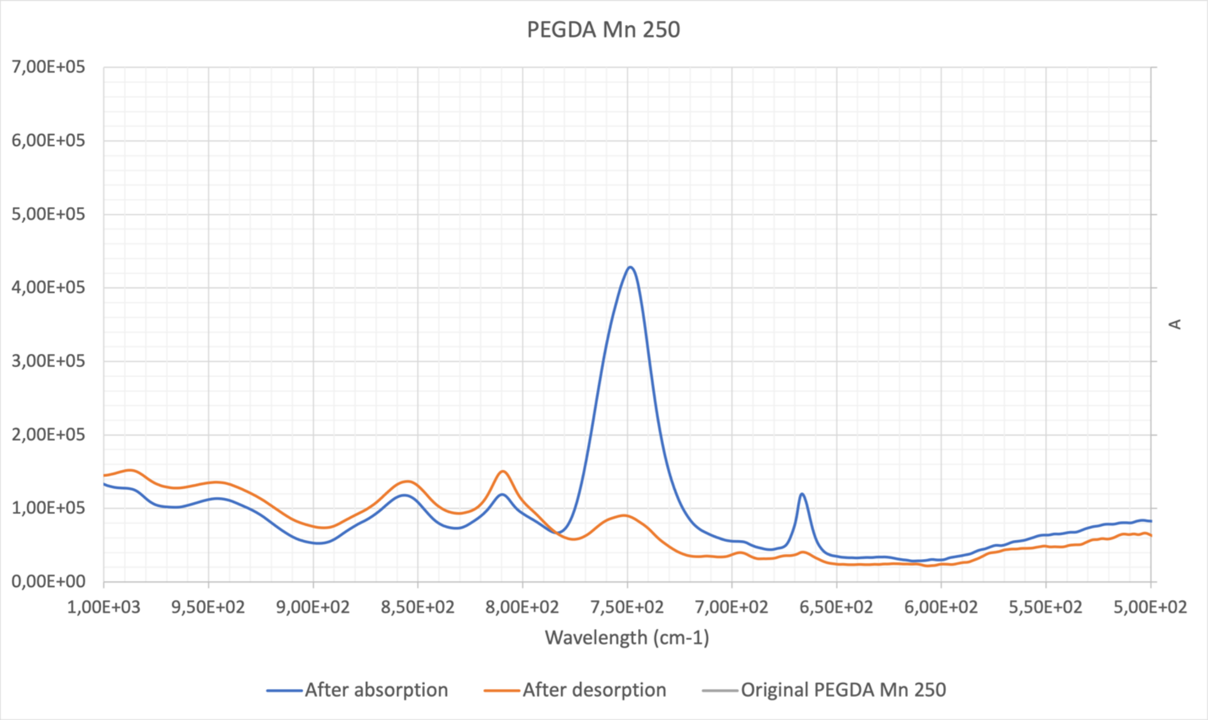

Figure 5.71. Zoom of FTIR spectra: absorption/desorption of chloroform by PEGDA Mn 250

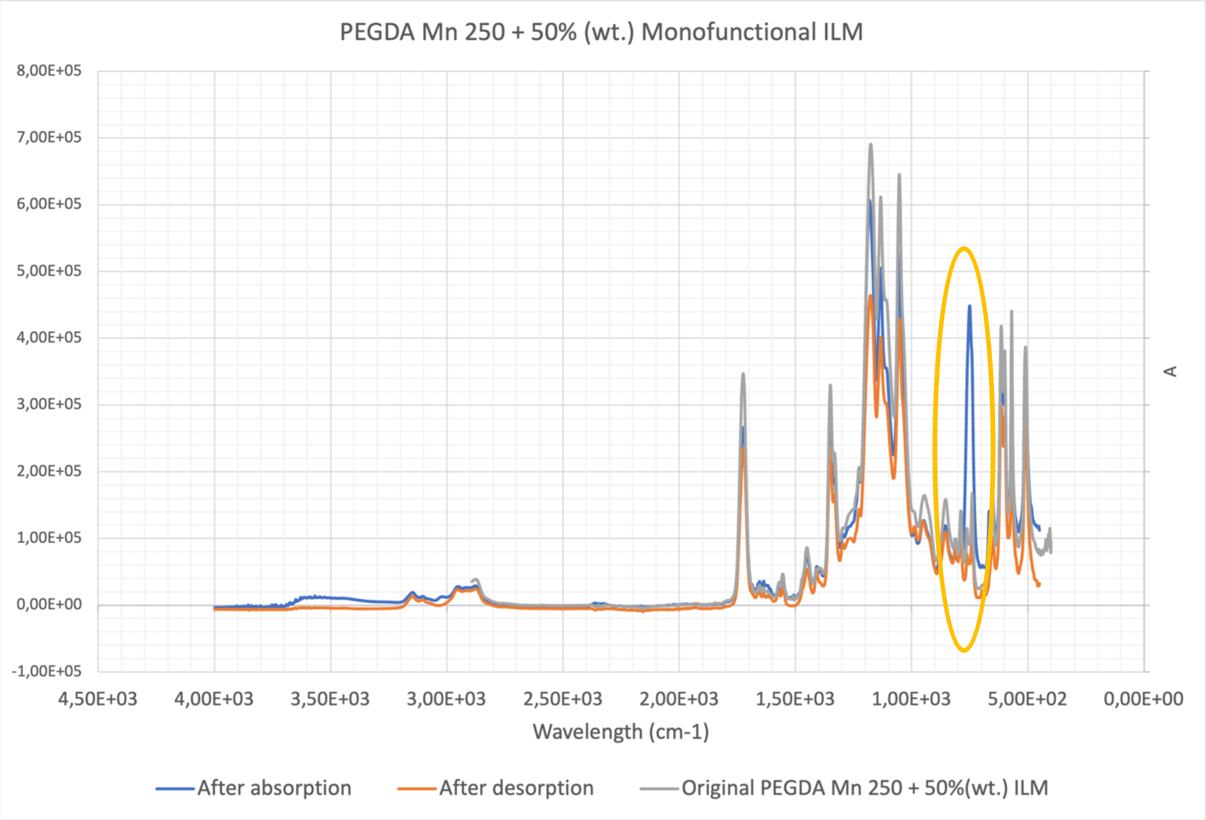

Figure 5.72. FTIR spectra: absorption/desorption of chloroform by PEGDA Mn 250 + 50% (wt.) of Monofunctional ILM

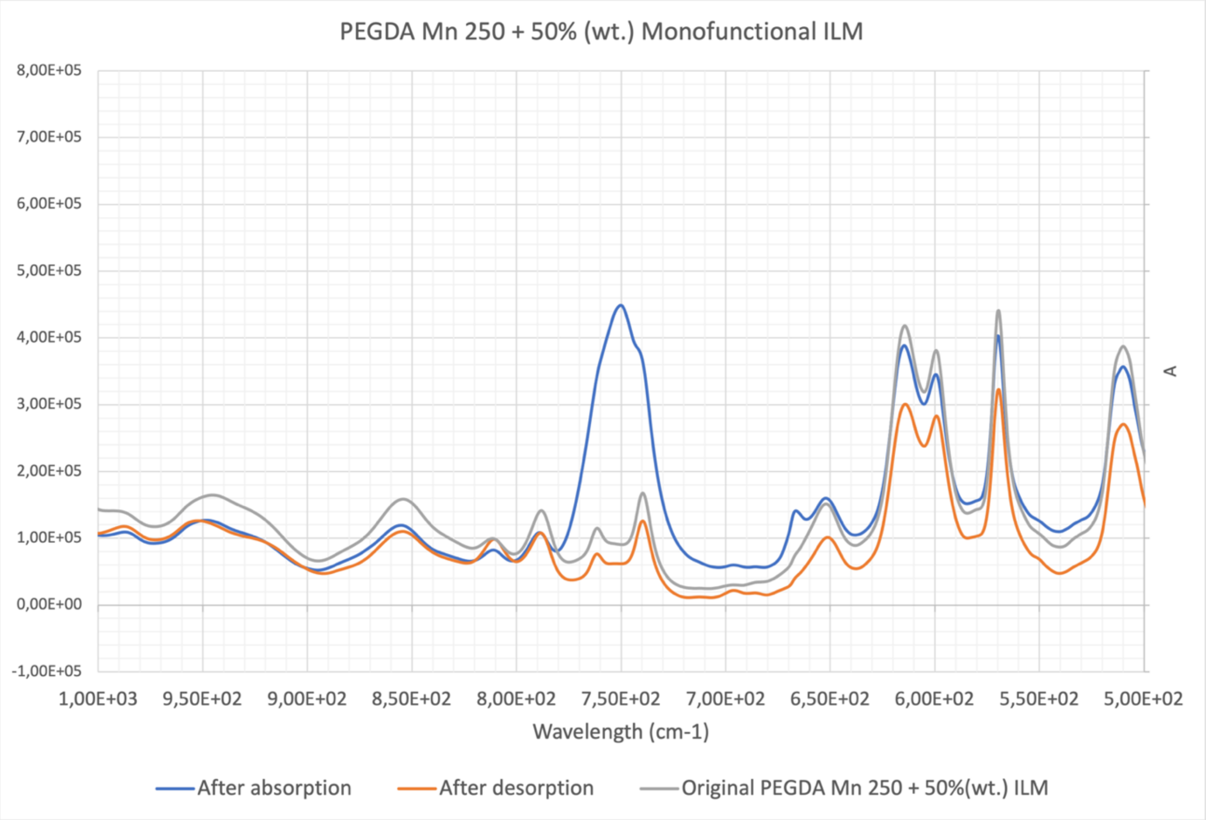

Figure 5.73. Zoom of FTIR spectra: absorption/desorption of chloroform by PEGDA Mn 250 + 50% (wt.) of Monofunctional ILM

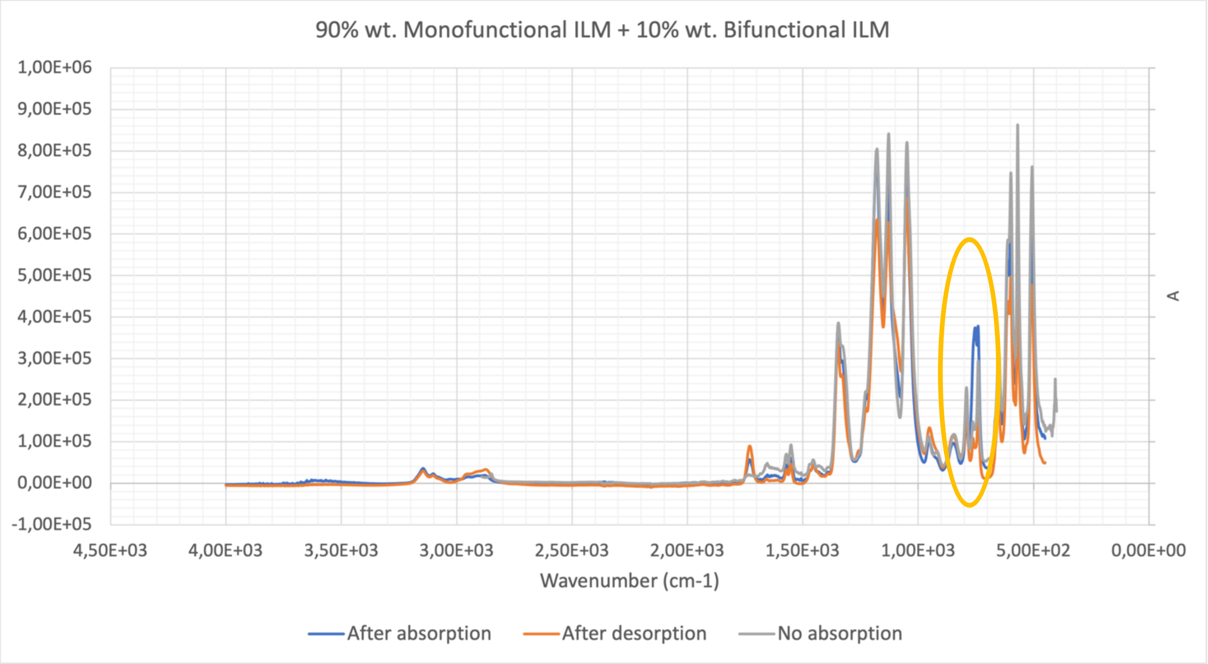

Figure 5.74. FTIR spectra: absorption/desorption of chloroform by 90% (wt.) of Monofunctional ILM + 10% (wt.) of Bifunctional ILM

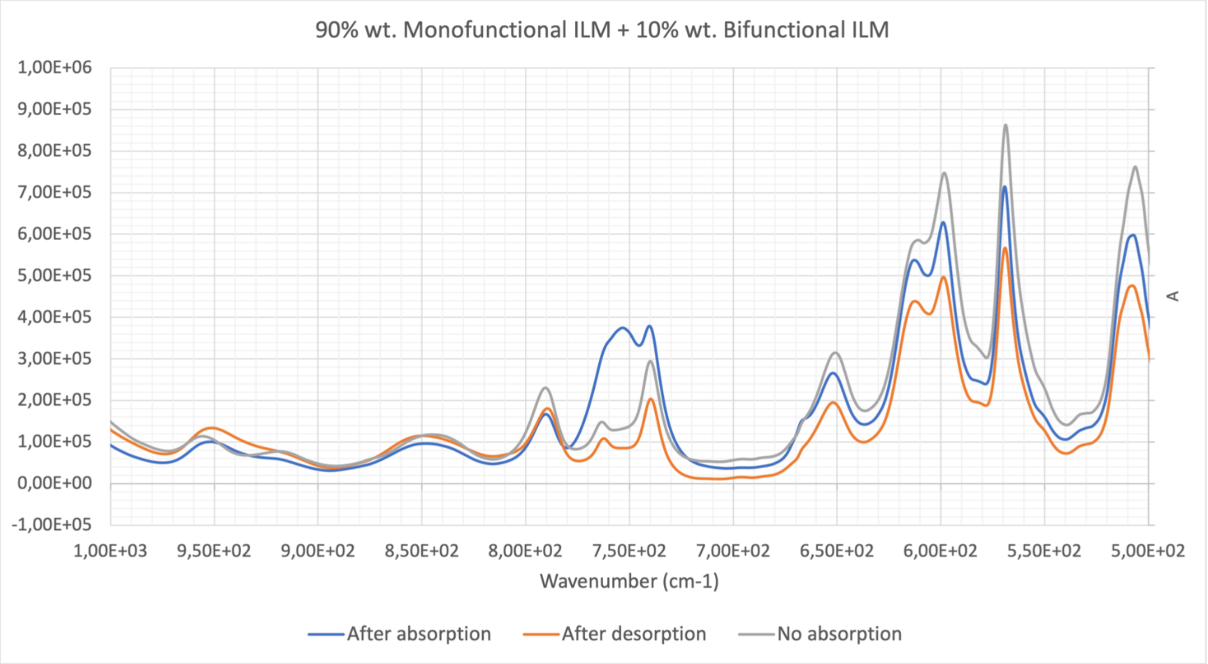

Figure 5.75. Zoom of FTIR spectra: absorption/desorption of chloroform by 90% (wt.) of Monofunctional ILM + 10% (wt.) of Bifunctional ILM

5.5 Discussion of the Results

5.5.1 Realization of PILs-based solid objects via DLP-3D Printing

The results given by the FTIR Spectroscopy confirm that the polymerization of all the considered materials, including the ones completely based on PILs, occurs efficiently. The comparison of the conversion's percentages relative to the considered materials demonstrates that the presence of PEGDA into the formulation improves the polymerization efficiency of PILs.

These considerations are confirmed also by the photo-rheological tests and by the images of the 3D Printed specimens, which were observed by optical microscope and SEM. This means that the DLP-3D Printing of objects with complex shape could be achieved with all the considered formulations, even the ones completely based on PILs.

5.5.2 Absorption and Desorption Capacities

5.5.2.1 Basic Considerations on Permeability

The gas absorption capacities of these polymeric materials may be considered as a part of the phenomenon of gas permeation through a polymeric membrane: the efficiency of this process is defined as the permeability (P) of the considered gas in a specific polymeric material.

This parameter is defined by two contributions (equation 5.1): the first one is the diffusion of the gas into the material (represented by the diffusion coefficient D), while the second one is the solubility of the gas in the polymer (given by the coefficient S). Both depend on the temperature by an Arrhenius relationship, as reported in equation 5.2 and 5.3: the permeation of a gas into a polymer is favored by the increase of temperature. E_d is the activation energy for diffusion, while ΔH_{sol} is the enthalpy of solubilization of the gas into the polymer.

$$P = D * S$$

Equation 5.12.

$$D = D_0\, e^{\left(\frac{-E_d}{RT}\right)}$$

Equation 5.13.

$$S = S_0\, e^{\left(\frac{-\Delta H_{sol}}{RT}\right)}$$

Equation 5.14.

The absorption of a gas into a polymer refers specifically to its solubilization in the organic matrix, so for this work, only the contribution given by S is considered, as permeation or diffusion tests have not been carried out for the materials.

In general, the solubility of a gas may be influenced by the chemical characteristics of the polymer, for instance, the polarity of its functional groups; and by its physical properties, like the amount of crystalline phase, its density, the free volume located between the polymer chains constituting the polymeric structure. This last feature of the polymers is strongly influenced by their glass transition temperature: in fact, if they are subjected to temperature which is higher than their T_g, their behavior will be plastic and less rigid, the macromolecules will be more prone to movement, thus the free volume between them will be increased [7].

The DSC and DMTA analyses were useful to identify the approximate glass transition temperature of all the materials studied in this work. The T_g obtained for the materials based completely on PILs (nr. 5 and 6) were close to the temperature at which the absorption tests were carried out: this means that the behavior of these materials may be influenced by their physical state, that permitted to increase the amount of free volume presented by the polymeric structure. At the same time, the materials based on PEGDA Mn 575 (nr. 2 and 4) presented T_g lower than 40°C, so during the absorption tests they showed higher free volume in their own polymeric structure, as they were characterized prevalently by plastic behavior. For the same phenomenon, PEGDA Mn 250 provided, in general, lower absorption capacity, as its T_g is higher than the temperature at which the absorption tests were carried out, meaning that the free volume in the rigid polymeric structure is minimized.

5.5.2.2 Thermodynamics of Solubilization

The solubility of a gas into a polymer is mainly influenced by thermodynamical contributions: the solubility of Volatile Organic Compounds in Room Temperature Ionic Liquids (RTILs) has been studied by Gonzalez-Miquel M. *et al.* [8]. The lack in literature of similar analysis carried out for systems based on Poly (Ionic Liquid)s, makes it necessary to rely on those that consider Room Temperature Ionic Liquids, taking into account the possible limits of the parallelism.

Nevertheless, this could be considered somehow reasonable as the ionic spots in PILs are similar to the ones of RTILs, despite they are included in a polymeric structure.

In the paper mentioned before, the study of the thermodynamics of these systems was provided by COSMO-RS simulation technology, through which some parameters were defined for describing the interactions between RTILs and VOCs. These are:

- *Henry's constant* (K_h), that defines the proportionality between the pressure applied by a gas on a liquid and the molar fraction of the diluted gas into the liquid itself at the equilibrium. The higher this constant, the lower the solubility of the gas into the liquid.

- *Activity coefficient at infinite dilution* (γ^{∞}), that represents the deviations in the Raoult's law, connected to the real interactions occurring between the gaseous solute and the solvent, when the solute concentration tends to zero. If this coefficient is smaller than 1, then the deviation to the Raoult's law will be negative, as the solute-IL system will be favored, because their attractive forces are greater than the one of solute-solute and solvent-solvent systems. This means that the solubilization process will be exothermic, thus convenient from an energetical point of view. On the contrary, if this coefficient is higher than 1, the deviation to the Raoult's law will be positive, so the solubilization will not be favored, as it will provide an endothermic behavior.

According to these parameters, some of the VOCs that have been considered in this work are characterized by favorable interactions with RTILs, due to their polarity or their capacity to generate hydrogen bonds (such as acetone, chloroform, acetonitrile) and to their thermodynamic parameters (γ^{∞}<1, very low K_h); while others may present moderate to insufficient interactions with RTILs, as they manifest higher γ^{∞} and higher K_h (as aromatic solvents or apolar ones).

5.5.2.3 Influence of VOCs' Polarity (Dielectric Constant)

In general, the experimental data collected in this work, make it clear that it is not sufficient to consider the polarity of the VOCs (represented by their dielectric constant), to understand how they interact with ionic liquids.

In fact, it was observed that acetone and acetonitrile (which have the highest dielectric constant) were absorbed excellently by PILs-based materials, but also that isopropyl alcohol (ε=18) was captured by PILs with very low absorption capacities; while, on the contrary, the ones referred to chloroform (ε =4,89) and di-chlorobenzene (ε =10) were higher, despite their different dielectric constants.

Nevertheless, it was confirmed by the study of Hu Xingbang *et al.* [9] that the dielectric constant of organic solvents has an influence in their solubility in ionic liquids: it was demonstrated that solvents with higher dielectric constant could provide the decrease of the interaction's strength between the cation and the anion of [C_2Mim][BF_4], which is similar to the ionic structure of PILs considered in this work, making it possible to form stronger interactions between the VOC and the ions and thus, permitting their solubilization.

5.5.2.4 Other Aspects influencing VOCs' Absorption

It is important to state that the strength of electrostatic forces is not sufficient to explain the solubility of VOCs in ionic liquid structures: for instance, it could be influenced also by steric effects, and by the way through which the molecules of solvent approach the ions, as reported in the work of Valsecchi C. *et al.* [10]. It was demonstrated, in fact, that the spatial position of the solvent in relation to the ions may be decisive in the way it diminishes the strength of the ionic interaction to permit its solubilization.

Furthermore, the ability of the molecules to form hydrogen bonds may be an important parameter to determine the efficiency of the solubilization process [8, 10, 11, 12].

The data presented by Poole C.F. *et al.* [13], deriving from solvatochromism technique and from mathematical models that aim to define the partition coefficient for gas-liquid systems, are useful to understand qualitatively the tendency of different ionic liquids and VOCs to create hydrogen bonds.

In particular, they may present two different behaviors: they may be hydrogen bond bases, and so proton acceptors, or they may be more likely to donate protons, being hydrogen bonds acids.

The anion of Poly (Ionic Liquid)s that have been considered in this work is able to accept protons, as it is characterized by fluorine and oxygen atoms; while the cation acts more likely like a proton donor.

This may explain the high absorption capacities revealed by PILs-based materials for some VOCs (such as acetone, acetonitrile and chloroform), as are able to interact efficiently with them through hydrogen bonds [8,11].

In conclusion, it is important to state that also the volatility of the VOCs may have a strong impact on the amount of organic vapor absorbed by the materials.

Furthermore, the designable structure of ionic liquid monomers makes it possible to improve the absorption capacity of PILs, by changing their cation or their anion: in particular, the selection of the anion may be decisive in order to enhance the formation of hydrogen bonds, and thus the solubilization of VOCs in the polymeric structure. As an example, it was reported that the solubilization of chloroform is not favored by big anions with dispersed charge (like *bis(trifluoromethylsulfonyl) imide* anion), but it is increased by anions that behave like stronger basis in hydrogen bonding, as $[CH_3CO_2]^-$ [8].

The capability of PEGDA (especially the one with higher molecular weight) to absorb VOCs is effective: Scordo G. *et al.* [14] studied sensors based on PEGDA matrix with PEDOT:PSS fillers, that permitted to evaluate the concentration of VOCs surrounding them, according to the amount of vapor absorbed by this polymeric structure.

5.5.2.5 Discussion of Results: Absorption and Desorption of VOCs

Acetone and acetonitrile are characterized by molecules with strong polarity (represented by their high dielectric constant), and with the capability of creating hydrogen bonds: the oxygen atom of acetone may interact more likely with the PILs' cation [15], while acetonitrile may interact with *bis(trifluoromethylsulfonyl)imide* anion (donating a proton to it) or with the cation, as the nitrile group would accept its hydrogen [16].

The fact that chloroform and di-chlorobenzene were absorbed more efficiently by PEGDA Mn 575 could be explained by considering that this polymer presented the lowest T_g, thus the highest free volume at the absorption temperature conditions, that enhanced its permeability, even for bigger molecules like aromatics. Then, the presence of carbonyls and oxygen atoms in PEGDA structure, makes it prone to accept protons during the formation of hydrogen bonds with these molecules that are likely to be involved in these interactions.

These hypotheses may be supported by what Zheng Yan-Zhen *et al.* [17] reported: the way chloroform approaches the ions is decisive for the efficiency of the solubilization process.

Moreover, its hydrogen atom forms hydrogen bonds with the fluorine atoms of *bis(trifluoromethylsulfonyl)imide* anion. Furthermore, also the chlorine atoms may provide hydrogen bonds as they may interact with other atoms like oxygen (presented by PEGDA, for instance).

Regarding ortho-dichlorobenzene, the considerations made in many articles on the miscibility of halogenated aromatics in ILs [18, 19, 20], show that this aromatic compound provides exothermic solvation enthalpies, and a better miscibility in ILs compared to the one of benzene.

This is mainly due to the higher polarity of the halogenated molecule. Furthermore, its main interactions with imidazolium-based ionic liquids with *bis(trifluoromethylsulfonyl)imide* anions are stronger than the ones provided by benzene: not only $\pi - \pi$ interactions are possible, but also hydrogen bonds with the anion and Van der Waals forces acting between this VOC and the cation's alkyl chains, are provided. These interactions may be presented as well with PEGDA functional groups: this material gives the advantage of having a more open molecular structure (for the consideration made about its T_g), thus permitting a better absorption of this big molecule.

The behavior of isopropyl alcohol is different from the one of the other considered VOCs: in fact, the absorption capacity of all the polymeric materials is way lower than the ones revealed for the other solvents. This has been unexpected, considering the polarity of the molecule and the presence of a hydroxyl group, prone to hydrogen bonding.

Even though Liu W. *et al.* [21] demonstrated that isopropyl alcohol is miscible in *1-alkyl-3 methylimidazolium bis(trifluoromethylsulfonyl)imide* (a structure which is similar to the ones considered in this work), its solubility in these ionic liquids is inhibited by the shortening of the alkyl functional groups presented by the cation.

In this case, the monofunctional ionic liquid monomers, which are prevalent in the studied formulations, are characterized by the presence of ethyl groups, that are not long alkyl chains. This could be a hypothesis to explain the unexpected behavior of the materials in the absorption of 2-propanol.

Having considered that 2-propanol is capable of creating hydrogen bonds and dipole-dipole interactions (due to its polarity), it may interact better with the oxygen atoms provided by PEGDA: this may be the reason why PEGDA Mn 575 turned out to be the one that absorbed this VOC most successfully.

The good results given by the desorption tests may be connected to the weak strength of the secondary interactions occurring between VOCs and the absorbents: for this reason, the increase of temperature is sufficient to break these interactions and to release completely the volatile organic compounds from the polymeric structure.

5.5 References

[1] ASIGA®COMPOSER

[2] https://www.sigmaaldrich.com/IT/en/technical-documents/technical-article/analytical-chemistry/photometry-and-reflectometry/ir-spectrum-table

[3] Lemus J. *et al.*; 2015; UV Polymerization of room temperature ionic liquids for high temperature PEMs: Study of ionic moieties and crosslinking effects; International Journal of Hydrogen Energy; 40, 5416-5424.

[4] 3shape®software (https://www.3shape.com/en)

[5] Wang *et al.*; 2017; Study on absorbability, regeneration characteristics and thermal stability of ionic liquids for VOCs removal; Chemichal Engineering Journal; 328, 353-359.

[6] https://webbook.nist.gov/cgi/cbook.cgi?ID=C67663&Type=IR-SPEC&Index=1

[7] Slides from "Polymer Science" lessons by M. Sangermano, 2018.

[8] Gonzalez-Miquel M. *et al.*; 2013; Selection of Ionic Liquids for Enhancing the Gas Solubility of Volatile Organic Compounds; Journal of Physical Chemistry; 117, 296-306.

[9] Hu Xingbang *et al.*; 2011; Anion-cation and ion-solvent interaction of some typical ionic liquids in solvents with different dielectric constant; Chemical Physics Letters; 516, 35-39.

[10] Valsecchi C. *et al.*; 2020; Solvent influence on imidazolium based ionic liquid contact pairs; Journal of Molecular Liquids; 315, 113615.

[11] Khachatrian A. A. *et al.*; 2021; Effect of cation structure on the formation of hydrogen bond between ionic liquids and solute molecules; Journal of Molecular Liquids; 334, 116089.

[12] Zhou Yu *et al.;* 2020; The interactions between polar solvents (methanol, acetonitrile, dimethylsulfoxide) and the ionic liquid 1-ethyl-3-methylimidazolium bis(fluorosulfonyl)imide; Journal of Molecular Liquids; 199, 112159.

[13] Poole C.F., Poole S.K.; 2010; Extraction of organic compounds with room temperature ionic liquids; Journal of Chromatography A; 1217, 2268-2286.

[14] Scordo G. *et al.*; 2021; Effect of Volatile Organic Compounds Adsorption on 3D-Printed PEGDA:PEDOT for Long-Term Monitoring Devices; Nanomaterials; 11, 94.

[15] Indra S. *et al.*; 2021; Interaction of volatile organic compounds acetone and toluene with room temperature ionic liquid at the bulk and the liquid-vaccum interface; Journal of Molecular Liquids; 331, 115608.

[16] Zheng Yan-Zhen *et al.*; 2020; The structure and interaction properties of two task-specific ionic liquids and acetonitrile mixturesL: A combined FTIR and DFT study; Spectrochimica Acta Part A: Molecular and Biomolecular Spectroscopy; 226, 117641.

[17] Zheng Yan-Zhen *et al.*; 2021; Structures and non-covalent interaction behaviours of binary systems containing the ionic liquid 1-(2'-hydroxylethyl)-3-methylimidazolium bis(trifluoromethylsulfonyl)imide and chloroform; Spectrochimica Acta Part A: Molecular and Biomolecular Spectroscopy; 244, 118843.

[18] Siporska A., Szydłowski J.; 2015; Phase behavior of ionic liquids 1-alkyl-3-methylimidazolium bis(trifluoromethylsulfonyl)imides with halogenated benzenes; J. Chem. Thermodynamics; 88, 22-29.

[19] Khachatrian A.A. *et al.*; 2019; Solvation thermochemistry of aromatic hydrocarbons and their halogen derivatives in imidazolium-based ionic liquids; Journal of Molecular Liquids; 289, 111105.

[20] Khachatrian A.A. *et al.*; 2016; Enthalpies of solution and enthalpies of solvation of chloro- and nitro- substituted benzenes in 1-butyl-3-methyl imidazolium based ionic liquids at 298.15 K: Additivity of group contributions; Thermochimica Acta; 645, 1-6.

[21] Liu Wei *et al.*; 2016; Liquid-liquid equilibria for ternary mixtures of water + 2-propanol + 1-alkyl-3-methylimidazolium bis(trifluoromethylsulfonyl)imide ionic liquids at 298.15 K; Fluid Phase Equilibria; 412, 205-210.

Chapter 6: Conclusions

In the present work, six materials have been studied, characterized by different concentrations of Poly (Ionic Liquid)s (*3-Ethyl-1-vinylimidazolium bis(trifluoromethanesulfonyl) imide ; 1,4-Butandyl-3,3'-[bis-(1-vinyl)-imidazolium]di-bis(trifluoromethanesulphonyl)imide*) in some matrices made by PEGDA with different molecular weight. This has been made in order to observe the influence of different amount of PILs on the VOCs' absorption capacities of these materials.

It has been demonstrated that all these solid materials can be obtained through DLP-3D Printing, even providing the realization of complex structures. This was attested thanks to photo-rheological tests made on the starting formulations, and by the results given by the analysis of FTIR spectra, that revealed conversion percentages around 50-90%, according to the composition of each polymeric material.

Furthermore, the influence of different amount of ionic liquid monomers in the starting formulation on the rheological properties and on the physical characteristics of the solid materials, have been investigated. In particular, the photopolymerization of these formulations is not inhibited nor variated by the increase in ionic liquid monomers' concentration; even though the photocuring of the formulation only based on ionic liquids presented lower polymerization rate and a delayed initiation of the process. In general, the presence of PEGDA in the formulations improves a lot their photopolymerization processes, increasing their rate and efficiency.

The glass transition temperature of each polymeric material has been defined, through DSC and DMTA analysis: they are influenced by the concentration of PILs in the PEGDA matrix, which may provoke an increase or decrease of this parameter, depending on the T_g of the relative PEGDA matrix. This could be due to the variation of intermolecular interactions and of the density of the polymeric structures, occurring because of the presence of a certain amount of PILs in the materials. The material only based on PILs presented a T_g around 40°C.

The ability of these materials to absorb acetone, isopropyl alcohol, ortho-dichlorobenzene, acetonitrile and chloroform has been investigated, at the constant temperature of 40°C for 24 hours.

The presence of PILs turned out to be decisive to enhance the absorption of acetone and acetonitrile; as for chloroform and ortho-dichlorobenzene, the absorption capacities of PILs-based materials were intermediate. In fact, these two VOCs, together with isopropyl alcohol, were better absorbed by PEGDA Mn 575.

The desorption tests, carried out in the same conditions, revealed that all the materials provided good regeneration from the absorbed VOCs.

These results are not only connected to the polarity of the Volatile Organic Compounds, but they may be influenced also by other parameters: the thermodynamic of VOCs' solubilization in PILs, the spatial position that the solvent's molecules adopt in relation to PILs' structure, the capability of these organic solvents to create hydrogen bonds and the other secondary interactions occurring between VOCs, the cations and anions of PILs. Furthermore, the temperature and the polymers' molecular weight may influence the permeability of the gas into the material.

Considering these results, the studied materials based on PILs may ideally be suitable for the realization of regenerable 3D Printed polymeric filters to absorb some Volatile Organic Compounds, as acetone or acetonitrile. The absorption of VOCs with different characteristics may be enhanced by other types of PILs, with variable cations or anions, whose behavior may be investigated in future works.

Bibliography

3shape®software (https://www.3shape.com/en)

Allen N.S.; 1996; Photoinitiators for UV and visible curing of coatings: mechanisms and properties; Journal of Photochemistry and Photobiology A: Chemistry; 100, 101-107.

Andrzejewska E.; 2016; Free Radical Photopolimerization of Multifunctional Monomers in "Three-Dimensional Microfabrication Using Two-Photon Polymerization, Fundamentals, Technology and Applications; Baldacchini T. Ed.; Elsevier.

Ann j.; 2014; Mitigation of Oxygen Inhibition in UV LED, UVA and Low Intensity UV Cure; Allnex USA Inc., Allnex Belgium SA.

Aparicio S. *et al.;* 2010; Thermophysical Properties of Pure Ionic Liquids: Review of Present Situation; Ind. Eng. Chem. Res.; 49, 9580-9595.

Armand M. *et al.*; 2009; Ionic-liquid materials for the electrochemical challenges of the future; Nature Materials; DOI: 10.1038/NMAT2448

ASIGA®COMPOSER

Avci D., Nur Eren T.; 2018; Monomeric and Polymeric Photoinitiators in "Photopolymerization Initiating Systems"; Lalevée J., Fouassier J.P Eds.; Royal Society of Chemistry.

Berenjian A., Chan N., Malmiri H.J.; 2012; Volatile Organic Compounds Removal Methods: A Review; American Journal of Biochemistry and Biotechnology; 8(4); 220-229.

Chang-wei Xu; 2021; Determination of Acidic Dissociation Constant of Methyl Red by Multi-Peaks Gaussian Fitting Method Based on UV-Visible Absorption Spectrum; Acta Physica Sinica-Chinese Edition; 28, 1030-1036.

Chiappe C. *et al.;* 2009; Ionic Liquids: Solvation ability and polarity; Pure Appl. Chem.; 81(4), 767-776.

Control of Odors and Emissions from Wastewater Treatment Plants Task Force of the Water Environment Federation; 2004; Chemical and Physical treatment of Odors in "Control of

Odors and Emissions from Wastewater Treatment Plants"; Chapter 13; Water Environment Federation; Alexandria, USA.

Copolovici L., Popitanu A.C., Copolovici D.M.; 2021; Volatile Organic Compound emission and residual substances from plants in light of the globally increasing CO_2 levels; Aleya L., Uddin S., Bungau S. G. Eds; Environmental Health: Interdisciplinary medical research in the field of public and environmental health; 19: 100216.

Davis H., James Jr.; 2004; Task-Specific Ionic Liquids; Chemistry Letters, 33 (9); 1072-1077.

Deflorian F., Fedel M.; 2014; UV-curable organic polymer coatings for corrosion protection of steel in "Handbook of Smart Coatings for Materials Protection"; Chapter 20; Makhlouf A.S.H. Ed.; Woodhead Publishing, Elsevier.

Derwent R.D.; 1995; Sources, Distributions and Fates of VOCs in the Atmosphere; in "Volatile Organic Compounds in the Atmosphere"; Hester R.E., Harrison R.M. Eds; Royal Society of Chemistry.

Dietlin C. *et al.*; 2020; New Phosphine Oxides as High Peformance Near-UV Type I Photoinitiators of Radical Polymerization; Molecules; 25, 1671.

Do-Thanh C.L. *et al.*; 2020; Ionic Liquid-Based Membranes in "Materials for Carbon Capture"; Jiang D., Mahurin S.M., Dai S. Eds.; Wiley.

Dunne S.R.; 2010; Industrial has Phase Adsorptive Separations in "Zeolites in Industrial Separation and Catalysis"; Chapter 9; Kulprathipanja S. Ed.; Wiley-VHC; Des Plaines, USA.

European Union Council Directive 1999/13/EC on the limitation of emissions of volatile organic compounds due to the use of organic solvents in certain activities and installations, 11th March 1999; Official Journal of the European Communities.

Gebhardt A., Kessler J., Thurn L.; 2019; Additive Manufacturing Processes/3D Printing in "3D Printing, Understanding Additive Manufacturing, 2nd Edition"; Chapter 2; Hanser Publishers, Munich.

Gebhardt A., Kessler J., Thurn L.; 2019; Basics of 3D Printing Technology in "3D Printing, Understanding Additive Manufacturing, 2nd Edition"; Chapter 1; Hanser Publishers, Munich.

Gillono M. *et al.*; 2019; Study on the Printability through Digital Light Processing Technique of Ionic Liquids for CO_2 Capture; Polymers; 11, 1932.

GoetheLab, University of Applied Science, Aachen.

Goldberg E., Min M.K.; 1997; Environmental Concerns in "Fermentation and Biochemical Engineering Handbook-Principles, Process Design, Equipment, 2nd Edition"; Chapter 15; Vogel H.C., Todaro C.L. Eds.; Noyes Publications; Westwood, USA.

Gonzalez-Miquel M. *et al.*; 2013; Selection of Ionic Liquids for Enhancing the Gas Solubility of Volatile Organic Compounds; Journal of Physical Chemistry; 117, 296-306.

Guan W. *et al.*, 2017; Determination and Prediction for the Polarity of Ionic Liquids; Journal of Chemical and Engineering Data; 62, 2610-2616.

Guterman R., Smith C. A.; 2019; Photopolymerization of Ionic Liquids – A Mutually Beneficial Approach for Materials Fabrication; Isr. J. Chem.; 59, 803-812.

Hu Xingbang *et al.*; 2011; Anion-cation and ion-solvent interaction of some typical ionic liquids in solvents with different dielectric constant; Chemical Physics Letters; 516, 35-39.

Hutten I.M.; 2016; Federal Law and Regulatory Activity That May Relate to Nonwoven Filter Media in "Handbook of Nonwoven Filter Media"; Chapter 10; Butterworth-Heinemann (Elsevier).

Indra S. *et al.;* 2021; Interaction of volatile organic compounds acetone and toluene with room temperature ionic liquid at bulk and the liquid-vacuum interface; Journal of Molecular Liquids; 331, 115608.

Jing M. *et al.*; 2019; Construction of multifunctional electrochemical sensor based on electroactivity-adjustable poly(ionic liquids)/reduced graphene oxide; 197, 277-283.

Khachatrian A. A. *et al.*; 2021; Effect of cation structure on the formation of hydrogen bond between ionic liquids and solute molecules; Journal of Molecular Liquids; 334, 116089.

Khachatrian A.A. *et al.*; 2016; Enthalpies of solution and enthalpies of solvation of chloro- and nitro- substituted benzenes in 1-butyl-3-methyl imidazolium based ionic liquids at 298.15 K: Additivity of group contributions; Thermochimica Acta; 645, 1-6.

Khachatrian A.A. *et al.*; 2019; Solvation thermochemistry of aromatic hydrocarbons and their halogen derivatives in imidazolium-based ionic liquids; Journal of Molecular Liquids; 289, 111105.

Khan F.I., Ghoshal A.K.; 2000; Removal of Volatile Organic Compounds from polluted air; Journal of Loss Prevention in the Process Industries; 13, 527-545.

Kocovic P.; 2017; 3D Printing Technologies in “3D Printing and its Impact on the Production of Fully Functional Components: Emerging Research and Opportunities”; IGI Global; USA.

Kohl A.L., Nielsen R.B.; 1997; Thermal and Catalytic Conversion of Gas Impurities in “Gas Purification. 5th Edition”; Chapter 13; Gulf Publishing Company; Houston.

Kohli R.; 2013; Removal of Surface Contaminants Using Ionic Liquids in “Developments in Surface Contamination and Cleaning, Volume 6”; Kohli R., Mittal K.L. Eds.; Chapter 1; Elsevier; USA.

Kumar T.P., Kumar R.M.A.; Chandrajit B.; 2011; Biofiltration of Volatile Organic Compounds (VOCs)-An Overview; Research Journal of Chemical Sciences; 1(8); 83-92.

Lee J. *et al.*; 2017; Effect of degree of crosslinking and polymerization of 3D printable polymer/ionic liquid composites on performance of stretchable piezoresistive sensors; Smart Mater. Struct.; 26, 35043.

Lemus J. *et al.*; 2015; UV Polymerization of room temperature ionic liquids for high temperature PEMs: Study of ionic moieties and crosslinking effects; International Journal of Hydrogen Energy; 40, 5416-5424.

Li X. *et al.*; 2020; Adsorption materials for volatile organic compounds (VOCs) and the key factors for VOCs adsorption process: A review; Separation and Purification Technology; 235, 116213.

Lin Y., Egeghy P., Rappaport S.; 2008; Relationships between levels of volatile organic compounds in air and blood from the general population; Journal of Exposure Science and Environmental Epidemiology; 18, 421-429.

Liu F. *et al.*; 2021; Multifunctional poly(ionic liquid)s cross-linked polybenzimidazole membrane with excellent long-term stability for high temperature-proton exchange membranes fuel cells; Journal of Power Sources; 494, 229732.

Liu Wei *et al.*; 2016; Liquid-liquid equilibria for ternary mixtures of water + 2-propanol + 1-alkyl-3-methylimidazolium bis(trifluoromethylsulfonyl)imide ionic liquids at 298.15 K; Fluid Phase Equilibria; 412, 205-210.

Marcinkowski L. *et al.*; 2019; Nanoconfined Ionic Liquids, Properties and Analytical Applications in “Handbook of Smart Materials is Analytical Chemistry, Volume I”; de la Guardia M. Ed.; Chapter 2; Wiley.

Markstedt K. *et al.*; 2014; 3D Bioprinting of Cellulose Structures from an Ionic Liquid; 3D Printing and Additive Manufacturing, 1(3).

Mecerreyes D. *et al.*; 2020; Innovative Polymers for Next-Generation Batteries; Macromolecular Chemistry and Physics; 221, 1900490.

Mecerreyes D.; 2011; Polymeric ionic liquids: Broadening the properties and applications of polyelectrolytes; Progress in Polymer Science; 36, 1629-1648.

Miller S.L.; 2018; Indoor Air Pollution in “Handbook of Environmental Engineering”; Kuts M. Ed; Wiley; chapter 17.

Mølhave L.; 2009; Volatile Organic Compounds and Sick Building Syndrome in “Environmental Toxicants: Human Exposures and their Health Effects, 3rd Edition”; Chapter 8; Lippmann M. Ed.; Van Nostrand Reinhold; New York.

Morton S.A., Morton L.A.; 2010; Ionic Liquids for the Utilization of Lignocellulosics in “Thermochemical Conversion of Biomass to Liquid Fuels and Chemicals”; Crocker M. Es.; Chapter 12; RSC Publishing; Cambridge.

Nancarrow P. *et al.;* 2021; Comprehensive analysis and correlation of ionic liquid conductivity data for energy applications; Energy; 220, 119761.

Noorhisham N. A., Amri D., Mohamed A. H., Yahaya N., Ahmad N. M., Mohamad S., Kamaruzaman S., Osman H.; 2021; Characterization techniques for analysis of imidazolium-based ionic liquids and application in polymer preparation: A review; Journal of Molecular Liquids, 326, 115340.

Nulwala H. *et al.*; 2018; Ionic liquids and poly(ionic liquid)s for 3D printing – A focused mini-review; European Polymer Journal; 108, 390-398.

Ozokwelu D., Zhang S., Cheng W., Litombe N.; 2017; Properties of Ionic Liquids in “Novel Catalytic and Separation Processes Based on Ionic Liquids”; Chapter 3; Elsevier.

Ozturk B., Yilmaz D.; 2006; Absorptive Removal of Volatile Organic Compounds from Flue Gas Streams; Process Safety and Environmental Protection; 84(B5), 391-398.

Pappas S.P.; 2013; Radiation Curing: A Personal Perspective in “Radiation Curing: Science and Technology”; Chapter 1; Springer Science & Business Media.

Poole C.F., Poole S.K.; 2010; Extraction of organic compounds with room temperature ionic liquids; Journal of Chromatography A; 1217, 2268-2286.

Prado R., Weber C.C.; 2016; Applications of Ionic Liquids in “Application, Purification and Recovery of Ionic Liquids”; Kuzmina O., Hallett J.P. Eds.; Chapter 1; Elsevier.

Rashid T.U.; 2021; Ionic liquids: Innovative fluids for sustainable gas separation from industrial waste stream; Journal of Molecular Liquids; 321, 114916.

Roy W. R.; 2019; Environmental Impact of Solvents in “Handbook of Solvents, 3rd Edition. Volume2. Use, Health and Environment”; Wypych G. Ed.; Chapter 16; ChemTech Publishing; Toronto.

Salar-Garcia M.J. *et al.*; 2016; Ionic liquid technology to recover volatile organic compounds (VOCs); Journal of Hazardous Materials; 321, 484-499.

Sangermano M.; Slides from “Polymer Science” lessons, 2018.

Sangermano M.; “Polymer Science” lessons, 2018.

Sangermano M. ; Slides from“Materiali Nanostrutturati” lessons; 2019.

Sangermano M.; Slides: “Scienza dei materiali polimerici” lessons; 2018.

Schultz A. R. *et al*.; 2014; 3D Printing Phosphonium Ionic Liquid Networks with Mask Projection Microstereolitography; ACS Macro Letters; 3, 1205-1209.

Schwalm R.; 2001; Photoinitiators and Photopolymerization in “Encyclopedia of Materials, Vol. 1 A-B”; Jürgen Buschow K. H., Cahn R.W., *et al*. Eds.; pp. 6946-6948.

Scordo G. *et al.*; 2021; Effect of Volatile Organic Compounds Adsorption on 3D-Printed PEGDA:PEDOT for Long-Term Monitoring Devices; Nanomaterials; 11, 94.

Siporska A., Szydłowski J.; 2015; Phase behavior of ionic liquids 1-alkyl-3-methylimidazolium bis(trifluoromethylsulfonyl)imides with halogenated benzenes; J. Chem. Thermodynamics; 88, 22-29.

Teimoori S. *et al.* ; 2020; A Review, Methods for removal and adsorption of volatile organic compounds from environmental matrixes; Analytical Methods in Envirionmental Chemistry Journal; 3 (2), 34-58.

Thomas M., Rajiv S.; 2020; Porous membrane of polyindole and polymeric ionic liquid incorporated PMMA for efficient quasi-solid state dye sensitized solcar cell; Journal of Photochemistry and Photobiology A: Chemistry; 394, 112464.

Tiwana M.; 2020; Future Technology for Metal Extraction from Waste: II. Ionic Liquids in "Sustainable Metal Extraction from Waste Streams"; Chauhan G., Kaur P.J., Pant K.K., Nigam K.D.P. Eds.; Chapter 7; Wiley-VCH; Weinheim (Germany).

Tiwari G.N., Mishra R.K.; 2012; General Introduction in "Advanced Renewable Energy Sources"; chapter 1; RSC Publishing; Cambridge.

Tomè L.C. *et al.*; 2015; Polymeric ionic liquid-based membranes: Influence of polycation variation on gas transport and CO_2 selectivity properties; Journal of Membrane Science; 486, 40-48.

Tran T.S.; 2020; Poly(ionic liquid)-Stabilized Graphene Nanoinks for Scalable 3D Printing of Graphene Aerogels; ACS Applied Nano Materials; 3, 11608-11619.

Truby R.L. *et al.* ; 2018; Soft Somatosensitive Actuators via Embedded 3D Printing; Advanced Materials; 30, 1706383.

Tudor A. *et al.*; 2017; Poly(ionic liquid) thermo-responsive hydrogel microfluidic actuators; Sensors and Actuators B: Chemical; 247, 749-755.

Valsecchi C. *et al.*; 2020; Solvent influence on imidazolium based ionic liquid contact pairs; Journal of Molecular Liquids; 315, 113615.

Vekariya R.L.; 2017; A review of ionic liquids: Applications towards catalytic organic transformations; Journal of Molecular Liquids; 227, 44-60.

Walden P.; Molecular weights and electrical conductivity of several fused salts; Bull. Acad. Imp. Sci. St Petersbg 8 (1914) 405-422.

Wang *et al.*; 2017; Study on absorbability, regeneration characteristics and thermal stability of ionic liquids for VOCs removal; Chemichal Engineering Journal; 328, 353-359.

Wang S. *et al.*; 2014; Enhanced adsorption and desorption of VOCs vapor on novel micro-mesoporous polymeric adsorbents; Journal of Colloid and Interface Science; 428, 185-190.

Wei L. *et al.* ; 2021; Recent advances in VOCs and CO removal via photothermal synergistic catalysis; Chinese Journal of Catalysis; 42, 1078-1095.

Wickliffe J.K., Stock T.H., Howard J.L., Frahm E., Simon-Friedt B.R., Montgomery K., Wilson M.J., Lichtveld M.Y., Harville E.; 2020; Increased long-term health risks attributable to select volatile organic compounds in residential indoor air in southeast Louisiana; Nature; 10:21649.

Wilkes J.S. *et al.* ; 1992; Air and water stable 1-ethyl-3-methylimidazolium based ionic liquids; Journal of Chemical Society; 965-967.

Wilkes J.S. *et al.;* 1982; Dialkylimidazolium chloroaluminate melts: a new class of room-temperature ionic liquids for electrochemistry, spectroscopy and synthesis; Inorg. Chem. 21(3) 1263-1264.

Yan X., et al.; 2021; Toluene removal from gas streams by an ionic liquid membrane: experiment and modeling; Chemical Eng. Journal; 404, 127109.

Yu M. *et al.;* 2021; Ionic liquid-based adsorbents in indoor pollutants removal; Green and Sustainable Chemistry; 27, 100405.

Yuan J. *et al.;* 2013; Poly(ionic liquid)s: An update; Progress in Polymer Science; 38, 1009-1036.

Yuan J., Antonietti M.; 2011; Poly(ionic liquid)s: Polymers expanding classical property profiles; Polymer; 52, 1469-1482.

Zhang M. *et al.*; 2021; 3D Printing for Biological Scaffolds using Poly(Ionic Liquid)/Gelatin/Sodium Alginate Ink; Macromolecular Materials and Engineering; 2100084.

Zheng Yan-Zhen *et al.*; 2020; The structure and interaction properties of two task-specific ionic liquids and acetonitrile mixturesL: A combined FTIR and DFT study; Spectrochimica Acta Part A: Molecular and Biomolecular Spectroscopy; 226, 117641.

Zheng Yan-Zhen *et al.*; 2021; Structures and non-covalent interaction behaviours of binary systems containing the ionic liquid 1-(2’-hydroxylethyl)-3-methylimidazolium bis(trifluoromethylsulfonyl)imide and chloroform; Spectrochimica Acta Part A: Molecular and Biomolecular Spectroscopy; 244, 118843.

Zhou X. *et al.;* 2019; Poly(ionic liquid)s: Platform for CO_2 capture and catalysis; Current Opinion in Green and Sustainable Chemistry; 16: 39-46.

Zhou Yu *et al.;* 2020; The interactions between polar solvents (methanol, acetonitrile, dimethylsulfoxide) and the ionic liquid 1-ethyl-3-methylimidazolium bis(fluorosulfonyl)imide; Journal of Molecular Liquids; 199, 112159.

Zhu L. *et al*.; 2020; A critical review on VOCs adsorption by different porous materials: Species, mechanisms and modification methods; Journal of Hazardous Materials; 389, 122102.

Sitography

https://en.wikipedia.org/wiki/1,2-Dichlorobenzene

https://en.wikipedia.org/wiki/Acetone

https://en.wikipedia.org/wiki/Acetonitrile

https://en.wikipedia.org/wiki/Chloroform

https://en.wikipedia.org/wiki/Isopropyl_alcohol

https://en.wikipedia.org/wiki/Menshutkin_reaction

https://en.wikipedia.org/wiki/Methyl_red

https://en.wikipedia.org/wiki/Photopolymer

https://en.wikipedia.org/wiki/Quantum_yield

https://webbook.nist.gov/cgi/cbook.cgi?ID=C67663&Type=IR-SPEC&Index=1

https://www-scopus-com.ezproxy.biblio.polito.it/search/form.uri?display=basic#basic

https://www.asiga.com/products/printers/pico2/

https://www.carlroth.com/com/en/xylene-alternatives/acetone/p/cp40.5

https://www.epa.gov/indoor-air-quality-iaq/technical-overview-volatile-organic-compounds

https://www.sigmaaldrich.com/IT/en/product/aldrich/437441?context=product

https://www.sigmaaldrich.com/IT/en/product/aldrich/475629 https://www.sigmaaldrich.com/IT/en/product/aldrich/511447

https://www.sigmaaldrich.com/IT/en/technical-documents/technical-article/analytical-chemistry/photometry-and-reflectometry/ir-spectrum-table

https://www.tcichemicals.com/GB/en/p/B5421

https://www.tcichemicals.com/HK/en/p/E1280